Hybrid *P,E* Ligands

Synthesis, Coordination Chemistry and Catalysis

by
Kathryn Mary Allan

Victoria
UNIVERSITY OF WELLINGTON
Te Whare Wānanga
o te Ūpoko o te Ika a Māui

A thesis
submitted to Victoria University of Wellington
in fulfilment of the
requirements for the degree of
Doctor of Philosophy
in Chemistry

Victoria University of Wellington
2014

Abstract

This thesis provides an account of research into a family of novel hybrid *P,E* ligands containing an *o*-xylene backbone. A methodology for the synthesis of these ligands has been developed, and their coordination behaviour with platinum(II) and platinum(0) precursors has been explored, with particular focus on a phosphine-thioether (*P,S*) ligand of this type. The coordination modes of this *P,S* ligand with palladium precursors have also been investigated, and the utility of the ligand in a palladium and copper co-catalysed Sonogashira carbon-carbon bond-forming reaction has been evaluated.

A range of hybrid *P,E* ligands of the type *o*-$C_6H_4(CH_2PBu^t{}_2)(CH_2E)$ (E = PR_2, SR, $S(O)Bu^t$, NR_2, $SiPh_2H$) have been synthesised in two or three steps from the novel substrate, *o*-$C_6H_4\{CH_2PBu^t{}_2(BH_3)\}(CH_2Cl)$. The initial step involved treatment of the substrate with the appropriate nucleophilic reagent, or preparation of a Grignard reagent from *o*-$C_6H_4\{CH_2PBu^t{}_2(BH_3)\}(CH_2Cl)$ and reaction with the appropriate electrophile. In most cases, this versatile strategy produced air-stable crystalline ligand precursors. Phosphine deprotection was achieved *via* one of three methods, dependent upon the properties of the second functional group.

The reactivity of three of these ligands — *o*-$C_6H_4(CH_2PBu^t{}_2)(CH_2SBu^t)$ (**14a**), *o*-$C_6H_4(CH_2PBu^t{}_2)\{CH_2S(O)Bu^t\}$ (**16**) and *o*-$C_6H_4(CH_2PBu^t{}_2)(CH_2NMe_2)$ (**18a**) — with Pt(II) and Pt(0) precursor complexes has been investigated. Chelated $[PtCl_2(P,E)]$ complexes were synthesised with *P,S* ligand **14a** and *P,N* ligand **18a**, but attempts to produce the equivalent species with *P,S=O* ligand **16** were unsuccessful. The X-ray crystal structure of $[PtCl_2(P,S)]$ complex **21** displayed an unexpectedly small ligand bite angle of 86.1°. A series of platinum(II) hydride complexes of the types $[PtHL(P,S)_2]$ and $[PtHL(P,S)_2]CH(SO_2CF_3)_2$ (L = Cl^-, H^-, NCMe, $-CH_2SBu^t$, CO, pta) have been synthesised, where ligand **14a** binds in a monodentate fashion through the phosphorus donor atom. This work has demonstrated the hemilability of ligand **14a**, *via* the facile and reversible conversion between $[PtH(\kappa^1 P\text{-}\mathbf{14a})(\kappa^2 P,S\text{-}\mathbf{14a})]CH(SO_2CF_3)_2$ (**26**) and

$[PtH(NCMe)(\kappa^1 P\text{-}\mathbf{14a})_2]CH(SO_2CF_3)_2$ (**28**). The X-ray crystal structure of $[PtH_2(P,S)_2]$ complex **25** was used to calculate a cone angle of 180° for the phosphine moiety in ligand **14a**.

Reaction of *P,S* ligand **14a** and *P,S=O* ligand **16** with $[Pt(alkene)_3]$ complexes (alkene = ethene, norbornene) gave the chelated $[Pt(alkene)(P,E)]$ complexes **32**–**35**; however, under similar conditions a $[Pt(norbornene)(P,N)]$ complex did not form. A large ligand bite angle of 106.6° was observed in the X-ray crystal structure of $[Pt(norbornene)(P,S)]$ complex **34**. Reaction of two equivalents of each of the *P,E* ligands with $[Pt(norbornene)_3]$ gave the corresponding 14-electron linear complexes $[Pt(P,E)_2]$ (**36**–**38**) with the ligands coordinated through the phosphorus donor atoms only. The reactivity of $[Pt(norbornene)(P,S)]$ complex **34** and $[Pt(P,S)_2]$ complex **36** has been investigated, resulting in the complexes $[PtH\{CH(SO_2CF_3)_2\}(P,S)]$ (**39**), [Pt(norbornyl)(*P,S*)] (**40**), [Pt(ethyne)(*P,S*)] (**41**) and $[Pt(O_2)(P,S)_2]$ (**42**).

The reactivity of *P,S* ligand **14a** was investigated with Pd(II) and Pd(0) precursors, resulting in the identification of five coordination modes of this ligand. Monodentate binding was observed in $[Pd(P,S)_2]$ complex **44**, and chelation in the [Pd(alkene)(*P,S*)] complexes **47** (alkene = norbornene) and **48** (alkene = dba). Reaction of ligand **14a** with $[PdCl_2(NCBu^t)_2]$ at raised temperature resulted in S−C bond cleavage and the formation of palladium dimer **43** with bidentate coordination of the ligand through phosphine and bridging thiolate moieties. Reaction of ligand **14a** with $[Pd(OAc)_2]$ resulted in C−H activation of the aryl backbone and formation of $[Pd(\mu\text{-}OAc)(P,C)]_2$ dimer **46**. In the presence of excess $[Pd(OAc)_2]$, palladium hexamer **45** was formed, with a combination of *P,C* palladacycle and monodentate thioether binding resulting in bridging *P,C,S* coordination of ligand **14a**.

The Sonogashira cross-coupling of 4-bromoanisole and phenylethyne was performed with 3 mol% of a pre-catalyst mixture containing *P,S* ligand **14a**, $[Pd(OAc)_2]$ and CuI, resulting in quantitative conversion to 4-(phenylethynyl)anisole in four hours. Two enyne by-products were also identified from the reaction. Variations to the pre-catalyst mixture and catalyst loading indicated there was a significant ligand dependence on the yield and selectivity of the reactions. Mercury drop tests and dynamic light scattering experiments confirmed the presence of palladium nanoparticles in the reaction solution; however, the active catalytic species in these reactions has not been identified.

Acknowledgements

Firstly, I must acknowledge my supervisor, Prof. John Spencer. John, thank you so much for your knowledge, kindness and sense of humour. Working with you these past 10 years has been a wonderful experience. A big thank you also to my co-supervisor, Dr. Joanne Harvey, whose positivity and passion for chemistry has motivated me on a number of occasions.

Thank you to the members of my research group over the years — Almas Zayya, Brad Anderson, Sarah Hoyte, Teresa Vaughan, Chris Munro, Jacqui Barber, Melanie Nelson, David Koedyk, Rosie Somerville and Lia van den Kerkhof. A special mention must go to my lab mates in LB211 — Sarah, Teresa, Melanie and Rosie — ladies, your support and friendship has made every day working in the lab worthwhile.

A big thank you to all the academic and general staff of SCPS, past and present, for creating such a great working environment. I am particularly grateful to Dr. Rob Keyzers for all the help with GC-MS. I'm also very grateful to Helen Rowley, Jaime-Anne Elliott, Jackie King, Teresa Gen, Rhys Batchelor, John Ryan, Ian Vorster and the workshop guys for responding to my requests with efficiency, patience and humour. I would also like to thank Patricia Stein and Shona De Sain in the Faculty of Science for all their support and kindness over the past year.

To all my lovely chemistry and non-chemistry friends — thank you for your support and patience, especially over the past year while I ignored you completely. I'm really looking forward to spending time with all of you in the near future. A huge thank you to my family — Mum, Dad and Iain — your love and support (financial and otherwise) has meant the world to me. And to my wonderful partner Graham Fairweather — you're my best friend and the love of my life.

I'd also like to acknowledge Victoria University of Wellington, the Freemasons, the Kathleen Stewart Scholarship and the Curtis-Gordon Research Scholarship in Chemistry for funding over the years.

Table of Contents

List of Figures

List of Schemes

List of Tables

Glossary

Ad	1-adamantyl
$BAr^F{}_4^-$	tetrakis3,5-bis(trifluoromethyl)phenylborate
bcp	bicyclopropylidene
bisbi	1,1′-bis(diphenylphosphinomethyl)-2,2′-biphenyl
Cp*	1,2,3,4,5-pentamethylcyclopentadienyl anion
CPCC	3-carboxypyridinium chlorochromate
DABCO	1,4-diazabicyclo[2.2.2]octane
dba	*trans,trans*-dibenzylideneacetone
dbpx	α,α'-bis(di-*t*-butylphosphino)-*o*-xylene
ee	enantiomeric excess
Fc	ferrocene
GC-MS	gas chromatography-mass spectrometry
HMBC	heteronuclear multiple bond correlation
HMPA	hexamethylphosphoramide
HRMS	high resolution mass spectrometry
IR	infrared spectroscopy
Mes	1,3,5-trimethylbenzene
mcp	methylenecyclopropane
nb	norbornene
nbd	norbornadiene
NMR	nuclear magnetic resonance
PCg	6-phospha-2,4,8-trioxa-1,3,5,7-tetramethyladamant-6-yl
pta	1,3,5-triaza-7-phosphaadamantane
RLATT	reciprocal lattice display program produced by Bruker AXS Inc.
tfa	trifluoroacetate
tht	tetrahydrothiophene
tmeda	1,2-bis(dimethylamino)ethane
TOF	turnover frequency (moles of product formed per mole of catalyst per unit time)
TON	turnover number (moles of product formed per mole of catalyst)
VT-NMR	variable temperature nuclear magnetic resonance

Chapter 1

Introduction

Hybrid *P,E* ligands have attracted a great deal of interest in recent years in the field of homogeneous catalysis and a number of other research areas. This attention is based on the ability of these ligands to produce transition metal complexes with unusual and potentially beneficial patterns of reactivity. This thesis provides an account of research into a family of novel hybrid *P,E* ligands with a large bite angle *o*-xylene backbone.

1.1 *P,P* Ligands

Organophosphorus compounds, and tertiary phosphines in particular, are ubiquitous ligands in the field of transition metal coordination chemistry. The combination of σ-donation and π-back bonding ability of these neutral ligands results in stable metal complexes with a large number of metals and over a range of metal oxidation states. The ability to easily tune the steric and electronic features of phosphine ligands (quantified using the Tolman cone angle and electronic parameter respectively[1]) through modification of the substituents on the phosphorus donor atom has led to a huge array of different phosphine ligands reported in the literature.

As each ligand present in a transition metal complex influences the characteristics of the complex, including the physical space around the metal centre and the electron density on the metal itself, these features can be easily tuned *via* the choice of ligand employed. Phosphine ligands are widely utilised for this purpose, particularly as ancillary ligands in transition metal-based catalysts, including a number of examples used in large-scale industrial processes.[2,3]

Diphosphine (*P,P*) ligands are one of the most common types of organophosphorus ligand. In general, these ligands chelate to metal atoms, producing very stable transition metal complexes through the chelate effect (an entropic effect used to explain the increased thermodynamic stability of a bidentate ligand when compared with two similar monodentate ligands).[4] Chelating ligands also tend to create well-defined transition metal complexes, which offer more control of the regio- and stereoselectivity in catalytic reactions employing these ligands. Along with the Tolman cone angle and electronic parameter, chelating diphosphine ligands contain a third tunable parameter, the bite angle, which is dependent upon the properties of the ligand backbone. The bite angle is defined as the P−M−P angle present in metal complexes of chelating diphosphine ligands, and is calculated either from the crystal structure of a complex (or the average of a number of complexes) or by molecular modelling, using a rhodium dummy atom and fixed Rh−P distances of 2.315 Å (the "natural" bite angle).[5,6]

1.1.1 Large bite angle ligands

Diphosphine ligands with large bite angles have been shown to promote reactivity patterns in transition metal catalysts quite unlike those of similar ligands with smaller bite angles. The first example of this phenomenon was with bisbi (Figure 1.1), a diphosphine ligand with a "natural" bite angle of 113° and crystallographically determined bite angles of 124.8 and 117.9°.[7] A pre-catalyst mixture of [Rh(acetylacetonate)$(CO)_2$] and bisbi in a 1:1 ratio was used for the rhodium-catalysed hydroformylation of 1-hexene, performed at 34 °C under six atm of dihydrogen/carbon monoxide. This reaction gave excellent selectivity for the straight-chain isomer (66.5:1 heptanal/2-methylhexanal) with a turnover frequency (TOF) of 29.4 h^{-1}. In contrast, the use of $Ph_2PCH_2CH_2PPh_2$ (with a "natural" bite angle of 84.5°) under the same conditions gave a heptanal/2-methylhexanal ratio of 2.1:1 and a TOF of only 1.1 h^{-1}.

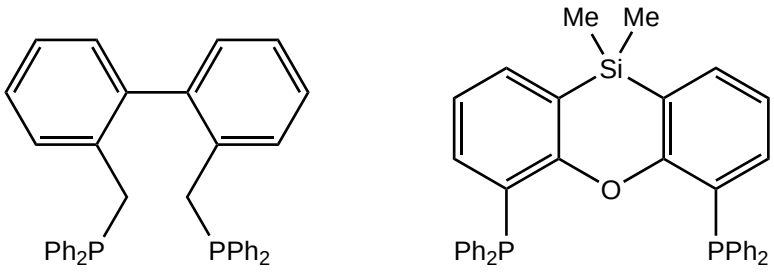

Figure 1.1 Large bite angle *P,P* ligands bisbi (left) and Sixantphos (right).

Another example of a family of large bite angle ligands that has been extensively studied in transition metal-catalysed reactions is the xantphos ligands, diphosphine ligands with phenyl substituents and xanthene-based backbones.[8,9] One of these ligands, Sixantphos, is shown in Figure 1.1 and has a "natural" bite angle of 105°. This ligand (among others) was tested for the nickel-catalysed hydrocyanation of styrene, using a pre-catalyst mixture of [Ni(1,5-cyclooctadiene)$_2$] and Sixantphos in a 1:1.2 ratio.[10] This reaction produced a yield of 94–95% with 97–98% selectivity for the branched nitrile product. Again, $Ph_2PCH_2CH_2PPh_2$ was also tested in this reaction and found to be essentially inactive, producing a yield of <1%. The authors attributed the difference in reactivity to the fact that large bite angle diphosphine ligands enhance the reductive elimination step by supporting a tetrahedral geometry of the catalyst species.

1.1.2 Dbpx

An example of a commercially useful large bite angle ligand is α,α'-bis(di-*t*-butylphosphino)-*o*-xylene (dbpx), a chelating diphosphine ligand with a crystallographically determined bite angle of 104° (in [$PtCl_2$(dbpx)]),[11] first reported by Moulton and Shaw in 1976.[12] The initial investigations focused on the coordination chemistry of dbpx with Group 10 metals.[12–16] In 1996, it was discovered that dbpx forms part of a highly active and selective catalyst for the methoxycarbonylation of ethene, producing methyl propanoate, an industrially important compound.[17,18] This result was significant, as chelating diphosphine ligands usually promote the co-polymerisation of ethene and carbon monoxide to form high molecular weight polyketone under the same reaction conditions,[19] indicating that the bite angle and steric environment present in transition metal complexes of dbpx produce reactivity different to other diphosphine ligands. The catalyst, formed *in situ* from [Pd(dba)(dbpx)] (dba = *trans,trans*-dibenzylideneacetone) and methanesulfonic acid in methanol, produces methyl propanoate with selectivity of 99.98% and a TOF of 50,000 h^{-1} under mild conditions (80 °C and 10 atm pressure of carbon monoxide/ethene).[20] Under steady state conditions, the catalyst gives turnover numbers (TON) in excess of 100,000.[18] In 2000, all the intermediates in the catalytic cycle were identified, establishing that the reaction occurs *via* the hydride cycle shown in Figure 1.2, rather than the alternative methoxycarbonyl cycle.[20,21]

This research was instrumental in the development of the Alpha process, a two step industrial-scale synthesis of methyl methacrylate. The first step of the Alpha process is the synthesis of methyl propanoate, using a homogeneous catalyst based upon the palladium dbpx catalyst shown in Figure 1.2, which has a TON of 1,000,000. The

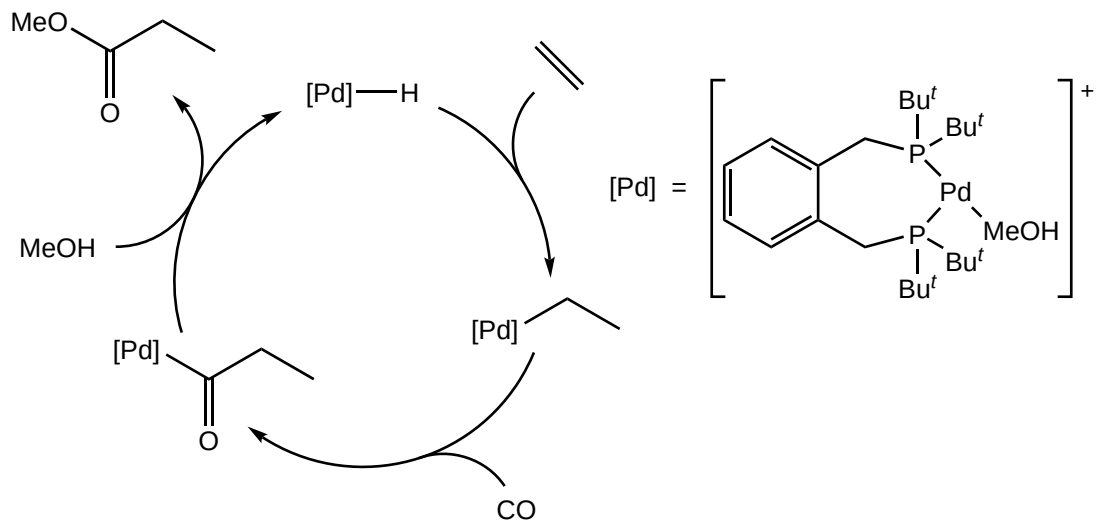

Figure 1.2 Catalytic cycle for the formation of methyl propanoate.

second step is the reaction of methyl propanoate with formaldehyde, employing a heterogeneous caesium silica catalyst. Since 2008, a Lucite International plant in Singapore has used the Alpha process to produce 120,000 tonnes of methyl methacrylate per annum.[22] Lucite International are currently constructing the world's largest methyl methacrylate plant in Saudi Arabia, scheduled to begin production of 250,000 tonnes per annum in late 2014.[23] As a result of this commercial success, a lot of interest has been generated in diphosphine ligands containing *o*-xylene backbones. A number of patents have subsequently been granted for catalytic processes that utilise dbpx,[24–28] and the use of phosphine substituents other than *t*-butyl groups has also been investigated.[29–32]

1.1.3 Unsymmetric *P,P* ligands

Further variations on the dbpx ligand that have generated interest in the past ten years are the unsymmetric analogues of this ligand, where the substituents on each phosphorus atom are different (Figure 1.3). A number of articles have been published,[11,33–37] and patents granted,[38–44] on the use of these unsymmetric ligands in recent years, almost exclusively concerning the synthesis of esters from alkenes, alcohols and carbon monoxide.

In 2012, Pringle and co-workers published a study of structure/activity relationships in the methoxycarbonylation of ethene with a number of these ligands.[37] The investigation of a range of *o*-$C_6H_4(CH_2PBu^t{}_2)(CH_2PAr_2)$ ligands showed that all of the ligands were active and selective for the Pd-catalysed synthesis of methyl propanoate, with subtle differences in activity and rate, and generally suggested that steric influ-

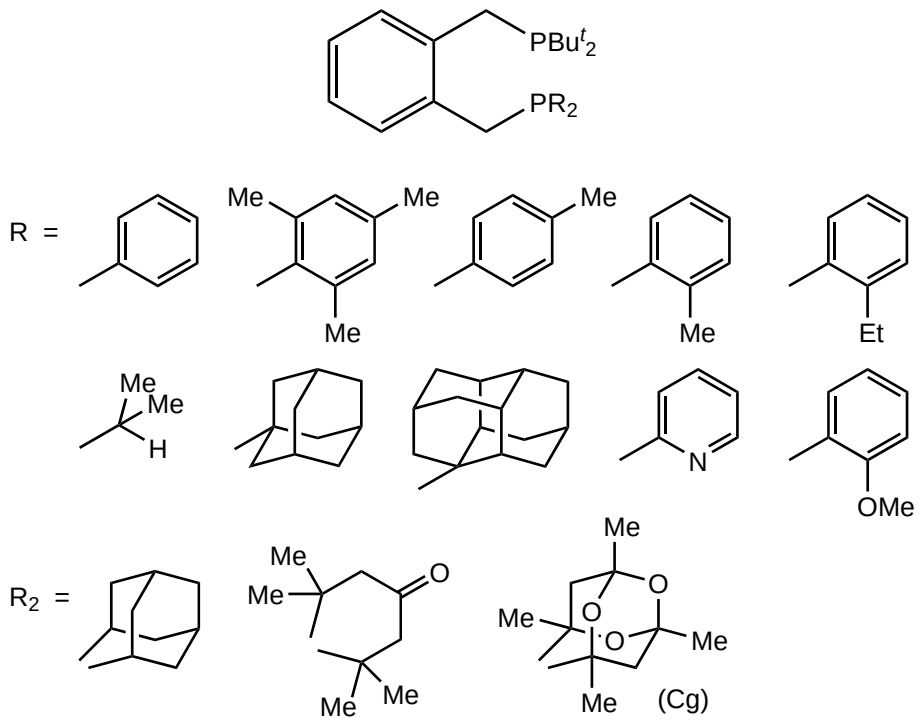

Figure 1.3 Unsymmetric *o*-xylene-based *P,P* ligands.

ences are more important than electronic influences in these catalysts. Interestingly, reactions with the ligand *o*-$C_6H_4(CH_2PBu^t{}_2)(CH_2PCg)$ (PCg = 6-phospha-2,4,8-trioxa-1,3,5,7-tetramethyladamant-6-yl, shown in Figure 1.3) gave higher TONs than either of the symmetric parent ligands, *o*-$C_6H_4(CH_2PCg)_2$ and dbpx. This enhancement in activity was attributed to a mutual perturbation of the PCg and $PBu^t{}_2$ bonding in the active catalyst species, inferred from crystallographic and spectroscopic studies of platinum complexes of *o*-$C_6H_4(CH_2PBu^t{}_2)(CH_2PCg)$. The authors also noted "it has been emphatically demonstrated that only one bulky phosphine donor is required for xylenyl diphosphines to produce a very effective hydromethoxycarbonylation catalyst". This statement suggests that hybrid *P,E* ligands based upon dbpx may also provide interesting and beneficial properties as components of homogeneous catalysts.

1.2 Hybrid Ligands

Hybrid ligands are defined as ligands containing at least two different donor atoms, generally with significantly different binding properties. Ligands of this type are attractive homogeneous catalyst components as they have the potential to influence the reactivity and selectivity of catalysts in a beneficial manner. It is well established that the electronic properties of ligand donor atoms in transition metal complexes have an influence on the environment at the metal centre and affect the other

ligands present in the metal complex. In particular, ligand donor atoms influence the properties (stability and bond length, for example) of the ligands in the *trans* positions on the metal centre (*trans* influence), even to the extent of impacting the lability of those ligands, and therefore the reaction rates associated with the metal complex (*trans* effect).[45] As the electronic properties of each donor atom in a hybrid ligand are different, this creates quite distinct binding sites in the *trans* positions on the metal centre (Figure 1.4) and can, for example, influence the selectivity for particular products in catalytic reactions.

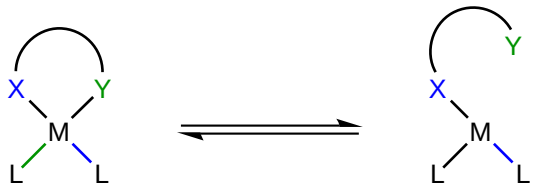

Figure 1.4 Schematic of the features of hybrid ligands.

Another reason hybrid ligands have attracted interest in recent years is their potential for hemilability. The term "hemilability" (coined by Jeffrey and Rauchfuss in 1979[46]) describes the reversible dissociation of one donor atom of a hybrid ligand, while the ligand remains "anchored" to the metal centre by the other donor atom(s) (Figure 1.4). Ligand hemilability is particularly advantageous in the field of homogeneous catalysis as the dissociation of a donor atom creates an empty site in which substrates can bind or metal-directed reactions can take place. Conversely, facile reassociation of the donor atom imparts stability to the catalyst in the resting state. The following sections provide a number of literature examples of hybrid *P,E* ligands, in the field of homogeneous catalysis and in other research areas.

1.2.1 *P,N* ligands

As both phosphorus and nitrogen donor atoms are prevalent in the field of coordination chemistry, *P,N* ligands are by far the most abundant type of hybrid ligand known, based upon the soft (phosphorus) and hard (nitrogen) dichotomy of the donor atoms.[47] Generally in these ligands, the more strongly binding (especially in complexes of low oxidation state metals) phosphorus donor atom anchors the ligand to the metal centre, while the nitrogen donor atom binds reversibly. For example, in a 1992 paper, Werner and co-workers reported the observation of fluxional behaviour in a rhodium(I) complex containing two phosphine-amine ligands.[48] This fluxionality was attributed to the facile exchange of nitrogen donor atoms in solution at room temperature (Figure 1.5). It was also found that the bound amine group could be

displaced by carbon monoxide, ethene or dihydrogen (in the case of dihydrogen, forming a Rh(III) dihydride complex).

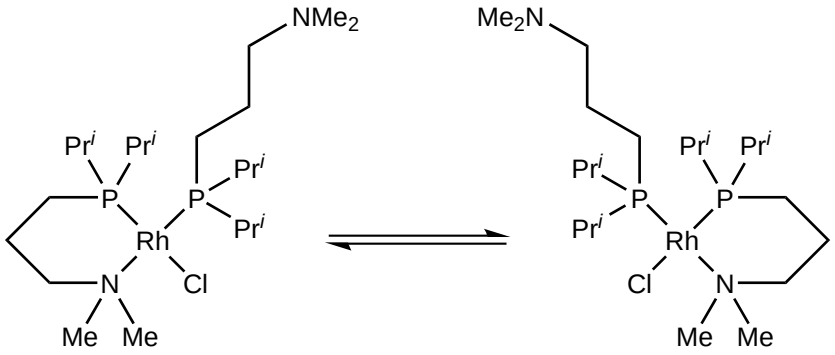

Figure 1.5 Hemilability of *P,N* ligands in a Rh(I) complex.

There are also many instances of *P,N* ligands used successfully for catalytic applications.[47] One example is the chemoselective hydrogenation of imides using the [RuClCp*(*P,N*)] complex shown in Figure 1.6.[49] A 1 mol% loading of this ruthenium complex and potassium *t*-butoxide in *i*-propanol under an H_2 atmosphere (1 MPa) at 80 °C selectively converted *N*-benzylphthalimide to *N*-benzyl 2-hydroxymethylbenzamide in >99% yield after two hours. The equivalent ruthenium complex bearing a similar *N,N* ligand ($Me_2NCH_2CH_2NH_2$) was tested under the same conditions, and resulted in complete recovery of the starting material. The authors attributed the contrast in reactivity with these ligands to the difference in electronic character of the PPh_2 and NMe_2 moieties. They also found that the NH_2 group present in the ligand was imperative to the catalytic process, and postulated that the Brønsted acidity of this group plays a part in the transition state of the reaction.

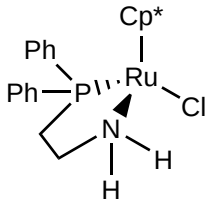

Figure 1.6 A [RuClCp*(*P,N*)] catalyst for the hydrogenation of imides.

1.2.2 *P,S* ligands

Although both phosphorus and sulfur atoms are considered to be soft donors, they display quite different binding strengths to transition metals, producing hybrid ligands with potentially useful properties. In a 1999 review article, Mirkin and

co-workers stated that "most phosphorus-thioether ligands do not exhibit hemilability".[50] Nevertheless, Mirkin has subsequently produced a number of significant examples of research utilising the hemilabile behaviour of phosphine-thioether ligands to various ends.

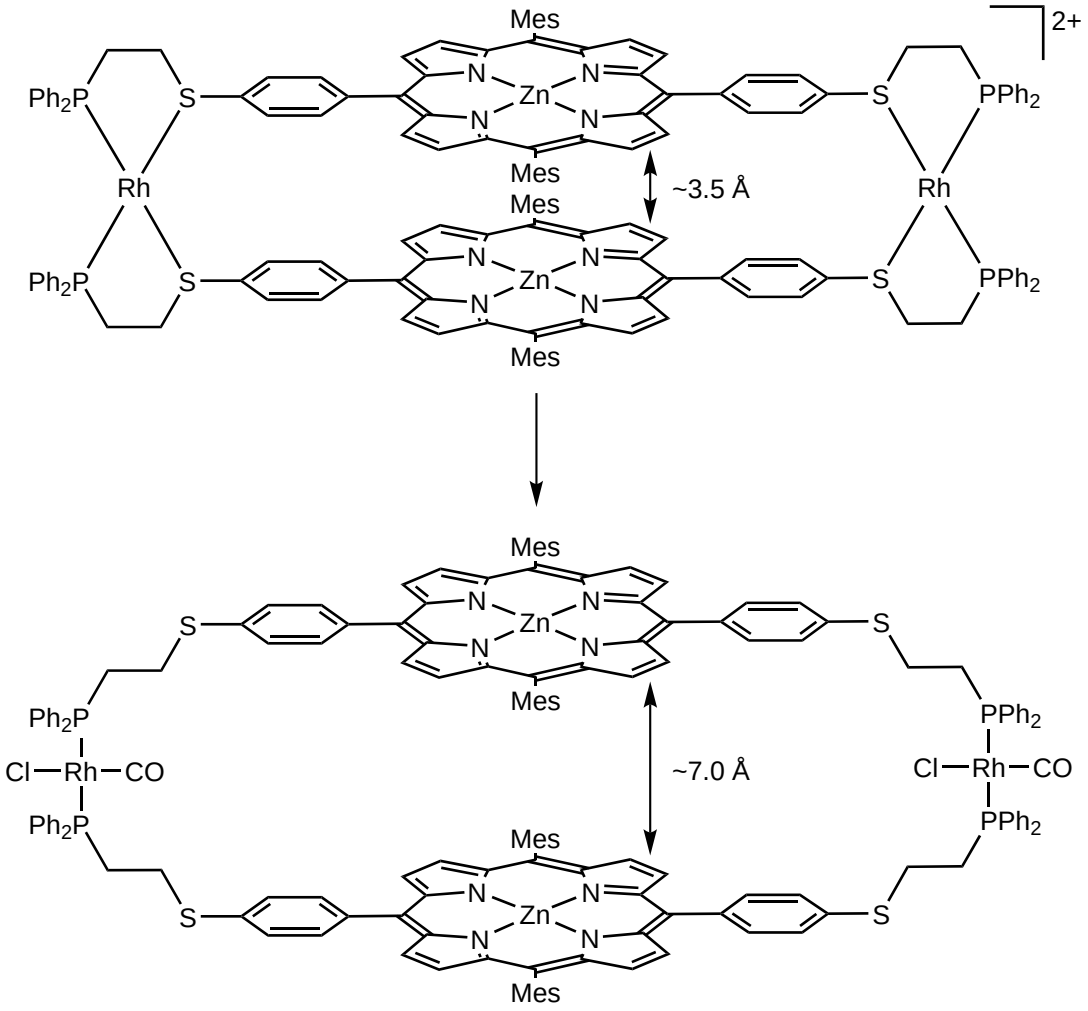

Scheme 1.1 Supramolecular cofacial porphyrin complexes in the "closed" (top) and "open" (bottom) forms.

Using the Weak-Link Approach[51] for the synthesis of inorganic macrocycles, Mirkin and co-workers reported the synthesis of a tetradentate ligand containing a zinc porphyrin core substituted with thioether-phosphine moieties at the 5 and 15 positions.[52] The reaction of two equivalents of this ligand with $[RhCl(nbd)]_2$ (nbd = norbornadiene) and $AgBF_4$ gave the "closed" macrocycle shown in Scheme 1.1. Treatment of this species with carbon monoxide and a source of chloride anions gave the "open" macrocyclic form, through displacement of the sulfur donor atoms from the rhodium centres. In both of these forms, the zinc macrocycles are cofacial, with porphyrin-porphyrin distances of *ca.* 3.5 Å in the "closed" macrocycle and *ca.* 7.0 Å in the "open" macrocycle. These macrocycles were tested as catalysts in acyl transfer reactions, and it was found that the rate of reaction with the

"open" macrocycle was twice that of the "closed" macrocycle, and 14 times that of a mixture of the zinc(II) and rhodium(I) monomers. This increase in reaction rate was attributed to the ability of the "open" macrocycle to preorganise the substrates within the cavity more effectively than the "closed" macrocycle, an effect that is easily controlled due to the hemilability of the *P,S* ligand moieties.

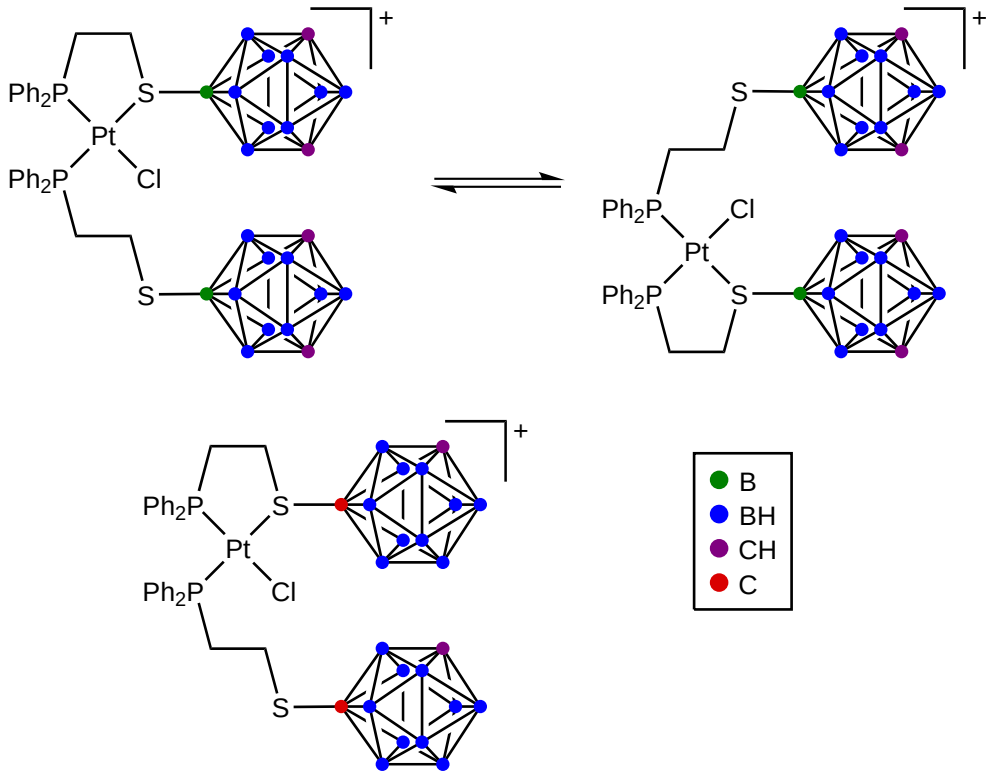

Figure 1.7 Platinum(II) complexes with phosphine-thioether ligands bearing B-linked (top) or C-linked (bottom) icosahedral carborane substituents.

More recently, Mirkin and co-workers utilised the hemilabile behaviour of phosphine-thioether ligands to investigate the electronic properties of icosahedral carborane cages.[53] The authors synthesised $Ph_2PCH_2CH_2SR$ (R = carborane cage) ligands with the carborane cage substituent linked to the sulfur donor atom through either a boron or carbon atom, and combined two equivalents of these *P,S* ligands with [$PtCl_2$(1,5-cyclooctadiene)] and $NaBAr^F{}_4$ to form the platinum complexes shown in Figure 1.7. The ^{31}P NMR spectrum of the complex containing B-linked ligands displayed two broad signals, attributed to the facile exchange of sulfur donor atoms in solution. Conversely, in the ^{31}P NMR spectrum of the complex containing C-linked ligands the signals were sharp, indicating no exchange on the NMR timescale. These results indicated that the nature of the S-carborane linker had an effect on the electronic character of the sulfur donor atom. Analogues of the complexes were synthesised containing carbon-based substituents on the sulfur atoms, and it was established that the B-linked carborane cage is a strongly electron-donating substituent akin to a bulky alkyl moiety, whereas the C-linked carborane

cage is a strongly electron-withdrawing substituent akin to a fluorinated aryl group. Through this work, Mirkin and co-workers have established a method for effectively decoupling electronic effects from steric effects in ligand donor atom substituents.

Examples of the hemilabile behaviour of phosphine-thioether ligands utilised directly in transition metal catalysts (rather than the allosteric effect demonstrated by Mirkin) are still very uncommon; however, phosphine-thioether ligands have been shown to influence the selectivity of catalytic reactions. For example, Consiglio and co-workers studied the effect of a number of ligands, including diphosphine and hybrid phosphine ligands, on the carbonylation of styrene using $[Pd(NCMe)_4](BF_4)_2$ as a pre-catalyst.[54] It was found that of the carbonylation products formed, the ligands $Ph_2PCH_2CH_2PPh_2$, $Ph_2PCH_2CH_2NMe_2$ and $EtSCH_2CH_2SEt$ all gave primarily (>80%) the straight-chain isomer, whereas $Ph_2PCH_2CH_2SEt$ gave 71% conversion to the branched isomer. The authors hypothesised that the phosphine-amine ligand acts as a monodentate phosphine ligand in this system, whereas the phosphine-thioether does not. No explanation was offered for the return to selectivity for the straight-chain isomer in the case of the dithioether ligand.

1.2.3 *P,S=O* ligands

The primary motivation for the study of phosphine-sulfoxide ligands has been their use as chiral ligands for asymmetric catalysis. As the chiral centre in these ligands is the sulfur donor atom, the source of their asymmetry in transition metal complexes is situated very close to the metal centre, which should produce good enantioselectivity. The role of the phosphorus donor atom in these ligands is to provide stability to the M−S bond *via* the chelate effect. Much of the research in this area to date has been performed by Hiroi.[55]

For example, Hiroi and co-workers reported the palladium-catalysed asymmetric allylic alkylation and allylic amination of (±)-1,3-diphenyl-2-propenyl acetate with the methoxynaphthyl-substituted *P,S=O* ligand shown in Figure 1.8.[56] The allylic alkylation of (±)-1,3-diphenyl-2-propenyl acetate with dimethylmalonate was tested under a range of conditions, and resulted in reasonable yields of the product (up to 75%) with ee's of 13–82%. Similar results were obtained for the allylic amination of (±)-1,3-diphenyl-2-propenyl acetate with benzylamine, producing 20–91% yield of the product and ee's between 3 and 85%.

Better results were obtained by Liao and co-workers for the rhodium-catalysed asymmetric 1,4-addition of arylboronic acids to cyclic enones with the *t*-butyl-

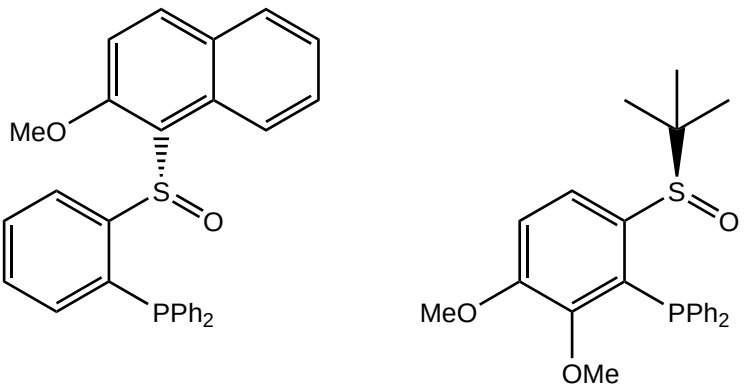

Figure 1.8 Hiroi's (left) and Liao's (right) chiral *P,S=O* ligands for asymmetric catalysis.

substituted *P,S=O* ligand shown in Figure 1.8.[57] Reactions with a range of starting materials were carried out with a pre-catalyst mixture of $[RhCl(ethene)_2]_2$ (1 mol%) and the *P,S=O* ligand (2.4 mol%) at 40 °C for 30 minutes, and resulted in good yields of between 67 and 99% and ee's of 74–98%. The authors proposed a steric repulsion between the *t*-butyl moiety of the *P,S=O* ligand and the enone carbonyl group as the source of the enantioselectivity in these reactions.

1.2.4 *P,Si* ligands

Silyl ligands are of interest in the field of coordination chemistry due to the unusual properties of the silicon donor atom in transition metal complexes. Silicon is an exceptionally strong σ-donor, producing particularly strong Si−M bonds (in one instance calculated to be nearly 100 kJ mol^{-1} higher than an equivalent C−M bond[58]). For this reason, silicon donor atoms have a very high *trans* influence and *trans* effect, and are expected to generate electron-rich metal centres.[59] Unfortunately, metal-silicon bonds are also very reactive, and are easily cleaved *via* reductive elimination, nucleophilic attack at the silicon atom, insertion into the Si−M bond, or σ-bond metathesis. One method employed for reducing the reactivity of metal-silicon bonds is the use of hybrid *P,Si* ligands, which significantly increases the stability of the Si−M bond through the chelate effect.

A number of bidentate *P,Si* ligands have been produced on this basis, and complexes of various transition metals with these ligands have been reported.[59,60] However, very little information on the reactivity of these metal complexes is available, presumably due to their inherent stability. More prevalent in the literature are pincer-type *P,Si,P* ligands, such as $\{o\text{-}(Ph_2P)C_6H_4\}_2MeSi^-$,[61,62] and tripodal *P₃,Si* ligands.

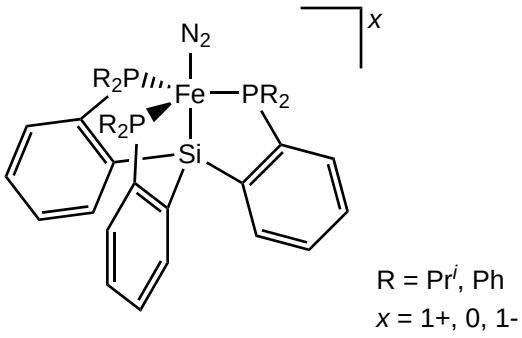

Figure 1.9 Iron dinitrogen complexes containing a tripodal P_3,*Si* ligand.

In 2010, Jones and co-workers reported a number of iron dinitrogen complexes containing a tripodal P_3,*Si* ligand.[63] As part of an investigation into iron-based catalysts for the reduction of dinitrogen to ammonia, the authors produced trigonal bipyramidal complexes of the type shown in Figure 1.9, with dinitrogen occupying the apical site. The neutral iron(I) species was treated with $HBAr^F{}_4$ to produce the equivalent cationic iron(II) species, or reduced with sodium naphthalide and 12-crown-4 to produce the anionic iron(0) species, without loss of the coordinated dinitrogen ligand. Interestingly, the iron(II) species could be treated with a solution of ammonia to produce $[Fe(P_3,Si)(NH_3)]^+$, where the ammonia ligand also inhabits the apical site. Reduction of this complex resulted in quantitative release of ammonia, and regeneration of the iron(I) dinitrogen species (Figure 1.9). The authors noted that this system is a promising lead to an iron-mediated, N_2-fixation catalyst based on three-fold symmetry.

1.3 Research Objectives

There are many examples in the literature of interesting and useful applications of hybrid *P,E* ligands, based upon the weak binding of amine or thioether groups, the chirality of sulfoxide moieties, or the high *trans* influence and *trans* effect of silicon donor atoms. Similarly, unsymmetric diphosphine ligands containing a large bite angle *o*-xylene backbone, based upon the commercially successful dbpx ligand, have shown excellent activity as components of homogeneous catalysts for the synthesis of a range of esters, and structure/activity studies have revealed a significant synergistic effect with one of these *P,P* ligands. However, this area of research has not been extended to the study of heterobidentate ligands with an *o*-xylene backbone, and there are no literature examples of hybrid *P,E* ligands of this type. Based on what is known about the attributes of both hybrid *P,E* ligands and large bite angle diphosphine ligands, the integration of these two aspects promises to produce

compounds with unusual and potentially beneficial reactivity patterns, for use as ligands in the field of homogeneous catalysis and in other research areas.

The initial objective of this research is to produce examples of novel *P,N*, *P,S*, *P,S=O* and *P,Si* ligands containing an *o*-xylene backbone. A route to unsymmetric diphosphine ligands of this type is known; however, this synthetic method is restrictive, and would not be applicable to the synthesis of all the desired *P,E* ligands (specifically phosphine-silane ligands). Ideally, a single methodology will be developed, with the versatility to incorporate a wide range of donor atoms into this ligand framework.

The coordination chemistry of these novel *P,E* ligands with Group 10 metals will then be investigated. Initially, reactions with platinum(II) and platinum(0) precursors will be performed, as the presence of an NMR active platinum isotope (platinum-195) and the high stability of platinum complexes tends to simplify the characterisation and evaluation of complexes with this transition metal when compared with other Group 10 metals. Nuclear magnetic resonance spectroscopy will be used to characterise the products of the reactions, and to assess any hemilabile behaviour or other dynamic processes present in the metal complexes. X-ray crystallography will also be an important tool for this research, and will be used to assess various parameters of the metal complexes, including the bite angles and *trans* influences of the hybrid ligands.

The platinum study should identify any good candidates for use as components of palladium-based homogeneous catalysts, and may also suggest the types of catalytic reactions for which these *P,E* ligands would be appropriate. On this basis, the reactivity of the *P,E* ligands with common palladium precursors will be examined and the resulting metal complexes characterised by NMR spectroscopy, X-ray crystallography and other methods. Palladium-catalysed reactions using these ligands as part of pre-catalyst mixtures and/or in pre-formed palladium complexes will also be performed, and the reaction kinetics evaluated by GC-MS and NMR methods. The combination of these two areas of research should establish whether hybrid *P,E* ligands containing large bite angle *o*-xylene backbones produce homogeneous catalysts with reactivity and/or selectivity different to known catalysts, and assist in the identification of the active catalytic species.

Chapter 2

Ligand Synthesis

2.1 Background

The first synthesis of the diphosphine ligand α,α'-bis(di-*t*-butylphosphino)-*o*-xylene (dbpx) was reported in 1976 by Moulton and Shaw.[12] This synthetic method involved the treatment of α,α'-dibromo-*o*-xylene with di-*t*-butylphosphine and subsequent deprotonation of the diphosphonium cation with a base, resulting in a low yield of dbpx. This remained the sole synthetic methodology[15,64,65] until 1999 when Newman and co-workers patented a different synthesis of dbpx, as part of a catalytic process for the carbonylation of ethene.[66] This method involved the dimetallation of *o*-xylene *via* the *in-situ* formation of a super base (Scheme 2.1).[67] Subsequent addition of two equivalents of chlorodi-*t*-butylphosphine formed the product, dbpx. In 2004, Ooka patented a third method of synthesising dbpx, wherein lithium di-*t*-butylphosphide–borane was combined with α,α'-dichloro-*o*-xylene producing a borane-protected version of the ligand, which was subsequently deprotected by reaction with tetrafluoroboric acid.[68] At present, the most commonly used methodology for the synthesis of dbpx is that of Newman and co-workers.

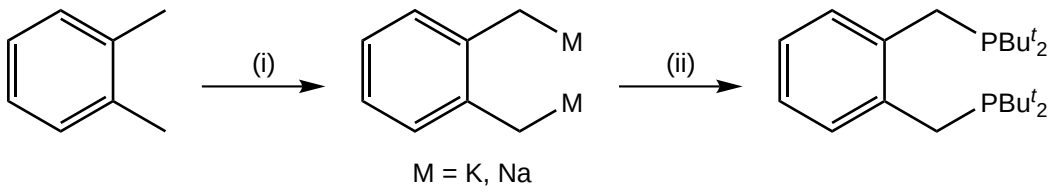

Scheme 2.1 Newman's patented synthesis of dbpx. *Reagents and conditions:* (i) *n*-BuLi, MOBu^t, alkane or ether solvent; (ii) Bu$^t{}_2$PCl.

A large number of α,α'-bis(phosphino)-*o*-xylene ligands with various phosphine substituents have been synthesised using these or similar methods.[31,69,70] However, these methods are only applicable to ligands where the substituents on each phosphorus atom are identical. In order to synthesise unsymmetric ligands of the type *o*-$C_6H_4(CH_2PR_2)(CH_2PR'_2)$, wherein R $\neq$ R$'$, a different approach must be taken. At present, all ligands of this type are synthesised using the 2005 method of Leone and Consiglio.[71] This methodology uses a cyclic sulfate, produced in two steps from α,α'-dihydroxy-*o*-xylene (Scheme 2.2). The addition of a lithium phosphide (or lithium phosphide–borane) to this compound ring-opens the cyclic sulfate, producing a disubstituted *o*-xylene, with phosphine and lithium sulfate substituents at the methyl positions. In the final step of this synthetic procedure, a second lithium phosphide is added, displacing the lithium sulfate substituent to produce the desired *o*-$C_6H_4(CH_2PR_2)(CH_2PR'_2)$ ligand.

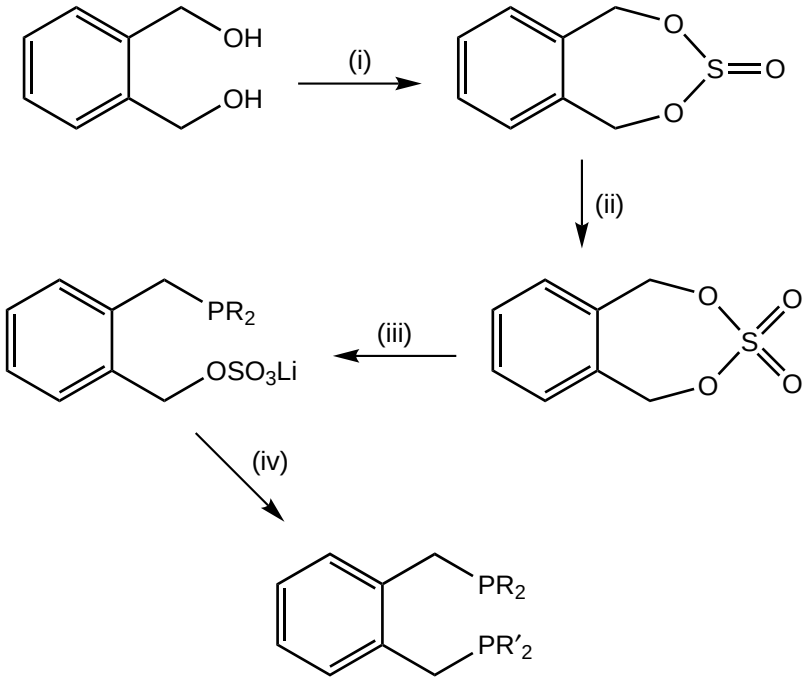

Scheme 2.2 Leone and Consiglio's synthesis of unsymmetric diphosphine ligands. *Reagents and conditions:* (i) $SOCl_2$, CCl_4; (ii) $RuCl_3 \cdot xH_2O$, $NaIO_4$, CCl_4/MeCN/H_2O; (iii) $LiPR_2$, HMPA, THF; (iv) $LiPR'_2$.

This synthetic methodology has been used to produce a wide range of unsymmetric diphosphine ligands,[37,42,43] and while it could be modified to synthesise *o*-xylene-based hybrid *P,E* ligands, it does depend on the availability of two nucleophilic reagents to install the two functional groups. This is restrictive as, for example, secondary silyl anions are generally unstable. The only known examples are $LiSiMes_2H$ and $LiSiPh_2H$ (produced in a low yield),[72] and hence to produce *P,Si* hybrid ligands of this type a different approach is required. This approach would depend upon the formation of an *o*-xylene backbone intermediate species that could

react with an electrophilic precursor of the type R_nEX, to install the non-phosphorus donor atom of the hybrid ligand, ideally with fewer steps than the Leone and Consiglio method.

2.2 Initial Attempts

2.2.1 Dimetallated *o*-xylene

In this study, the first attempts to synthesise hybrid *P,E* ligands with an *o*-xylene backbone used Newman's dimetallated intermediate species shown in Scheme 2.1. The dimetallated *o*-xylene was prepared following the method of Newman and co-workers,[66] the resulting red solid was suspended in diethyl ether and one equivalent each of chlorodi-*t*-butylphosphine and chlorodimethylsilane added sequentially (Scheme 2.3). Unfortunately, analysis of the NMR data associated with the reaction mixture showed these reactions produced the known compounds dbpx[73] and α,α'-bis(dimethylsilyl)-*o*-xylene[74] only. This is a result of the insolubility of the dimetallated *o*-xylene intermediate. Monometallated *o*-xylene is soluble in a number of solvents while the dimetallated species is not (and in fact the two compounds can be separated on this basis), so the first addition of a reagent to the dimetallated *o*-xylene results in a soluble monometallated species, which preferentially reacts with any further reagent in solution, the final result being the two symmetric compounds shown in Scheme 2.3. Even when a mixture of chlorodi-*t*-butylphosphine and chlorodimethylsilane was added in one step, the two symmetric compounds were the major products formed, likely due to a disparity in reaction rate between the two reagents.

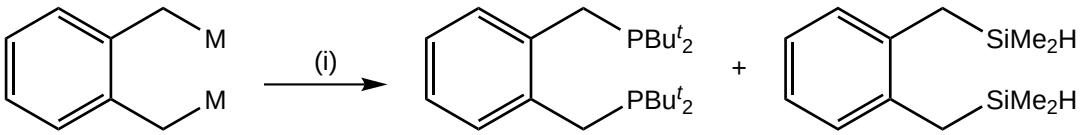

Scheme 2.3 Attempted synthesis of a *P,Si* ligand. *Reagents and conditions:* (i) Bu$^t_2$PCl, Me_2SiHCl, Et_2O.

2.2.2 Cyclic phosphonium salt

As the previous reactions were unsuccessful, alternative synthetic methodologies were investigated. It is known that the synthesis of benzyllithium from benzyl

halides is low yielding, as bibenzyl is readily formed (Wurtz-type coupling),[75] so other methods of producing a substituted benzyllithium intermediate were explored. Initially, it was envisaged that P−C bond cleavage of a cyclic phosphonium ion by lithium metal would give the desired *ortho*-substituted benzyllithium species. The reaction of one equivalent of di-*t*-butylphosphine with α,α'-dibromo-*o*-xylene in acetonitrile in the presence of potassium carbonate formed the cyclic phosphonium bromide **1** in 72% yield (Scheme 2.4). The ^{1}H NMR spectrum of compound **1** in chloroform-*d* displays the expected doublets associated with the PBu^t and CH_2P protons in a 9:2 ratio at 1.54 and 4.07 ppm respectively. The ^{31}P NMR spectrum shows a singlet peak at 71.8 ppm. This compound is similar to known cyclic dimethyl- and diphenyl-substituted phosphonium bromides.[76] Other than the treatment of these compounds with methylenetrimethylphosphorane[76] or potassium *t*-butoxide[77] to form cyclic phosphorus ylides, and P−C bond cleavage with various hydroxides,[78,79] the reactivity of these five-membered cyclic phosphonium salts has not been widely studied.

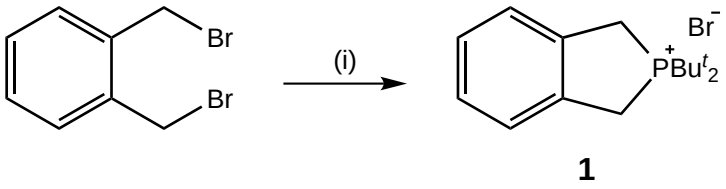

Scheme 2.4 Synthesis of cyclic phosphonium bromide **1**. *Reagents and conditions:* (i) Bu$^t_2$PH, K_2CO_3, MeCN, 72% yield.

The direct reaction of cyclic phosphonium bromide **1** with lithium metal in THF followed by quenching with water resulted largely in the recovery of unchanged starting material (Scheme 2.5). In an attempt to activate the lithium metal, the reaction was repeated with the inclusion of a crystal of naphthalene, followed by addition of one equivalent of chlorodimethylsilane. Unfortunately, an intractable mixture of products resulted, with no evidence of the desired product present in any appreciable amount from the NMR spectra.

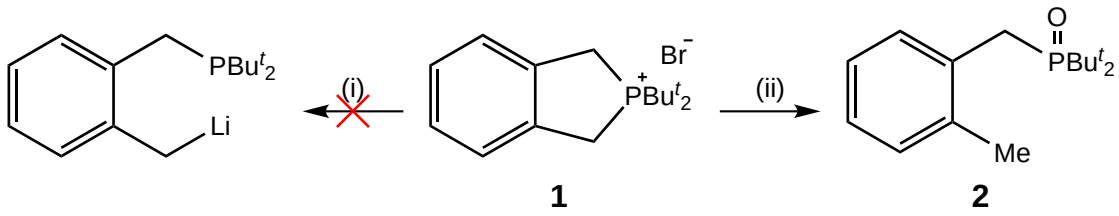

Scheme 2.5 Unsuccessful reactions with cyclic phosphonium bromide **1**. *Reagents and conditions:* (i) Li metal, naphthalene, THF, overnight; (ii) NaOMe, MeOH, 48 h, 45% conversion.

As the direct lithiation of phosphonium bromide **1** did not produce the desired metallated species, other routes to this material were explored. The production of benzyllithiums from benzyl alkyl ether starting materials is a well-established procedure,[75,80] and as such, the synthesis of an *o*-phosphinomethyl-substituted benzyl methyl ether compound was commenced. Compound **1** was combined with sodium methoxide in methanol and the reaction monitored by NMR spectroscopy. After 48 hours, no evidence of the desired ring-opened product was observed. Instead, the starting material slowly converted to *o*-(methyl)benzyldi-*t*-butylphosphine oxide (**2**), resulting in a 45% yield of this compound after 48 hours (Scheme 2.5). The structure of compound **2** was established through ^{1}H, ^{13}C and ^{31}P NMR spectroscopy. The ^{31}P NMR shift of this compound, 60.9 ppm, is consistent with other benzyldi-*t*-butylphosphine oxides (typically 55–70 ppm[81,82]). As mentioned previously, P−C bond cleavage of five-membered cyclic phosphonium salts with various hydroxides,[78,79] producing the corresponding phosphine oxides, is a known reaction type. This suggests that compound **1** did not react with sodium methoxide, but rather slow formation of sodium hydroxide occurred in solution due to the presence of water, which in turn reacted with compound **1**, cleaving one of the benzylic P−C bonds and producing compound **2**.

2.2.3 Phosphine–boranes

Another route to the desired compound α-(di-*t*-butylphosphino)-α'-methoxy-*o*-xylene was through the known starting material, α-chloro-α'-methoxy-*o*-xylene (**3**). This compound was first synthesised in 1936 by Murahashi in crude form[83] and subsequently synthesised and isolated successfully by Mann and Stewart in 1954,[84] requiring at least three reaction steps from a commercially available material. As the previous synthetic methodologies were not ideal, a new synthesis of compound **3** was developed. This method involved the dropwise addition of a methanol solution of sodium methoxide to an excess of α,α'-dichloro-*o*-xylene in methanol at reflux (Scheme 2.6). The reaction of stoichiometric quantities of these reactants would result in a statistical distribution of products, and therefore a theoretical maximum 50% yield of the desired product. However, the use of an excess of the xylene substrate and dropwise addition of the sodium methoxide at reaction temperature ensured the production of the by-product, α,α'-dimethoxy-*o*-xylene, was minimised, and therefore the proportion of desired compound **3** increased. Subsequent separation of the products and remaining α,α'-dichloro-*o*-xylene substrate by column chromatography gave pure desired compound **3** as a clear liquid in 62% yield.[85] This new synthetic methodology gives yields similar to that of Mann and Stewart, and

as only one reaction step is required, is more atom economic and time efficient than previous methods.

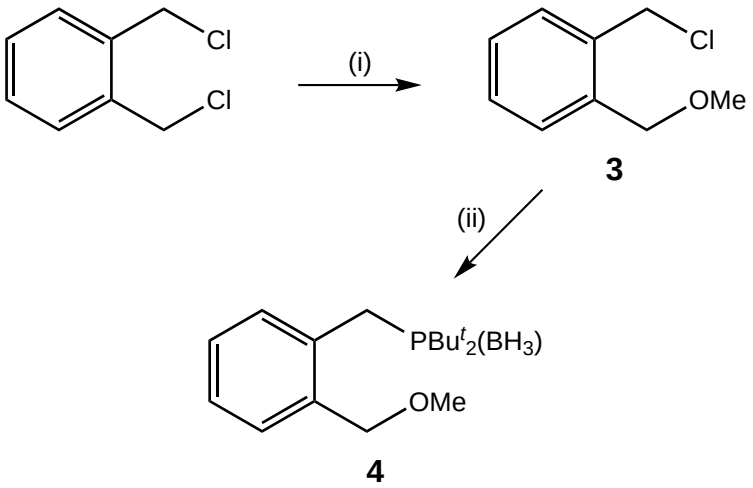

Scheme 2.6 Synthesis of *ortho*-substituted benzyl methyl ethers **3** and **4**. *Reagents and conditions:* (i) 0.5 eq. NaOMe, MeOH, reflux, 1.5 h, 62% yield; (ii) LiPBu$^t_2$(BH$_3$), Et$_2$O, 0 °C $\longrightarrow$ rt, overnight, 51% yield.

Compound **3** was then used to synthesise the desired α-(di-*t*-butylphosphino)-α'-methoxy-*o*-xylene compound **4** (Scheme 2.6). In this instance, lithium di-*t*-butylphosphide–borane was reacted with compound **3** in diethyl ether, and desired compound **4** crystallised in a 51% yield.[85] Borane-protection of the phosphine moiety in compound **4** rendered the product an easily handled air-stable crystalline solid, and protected the phosphorus atom from oxidation or other side reactions in any subsequent reaction steps (for example, cyclisation to the corresponding phosphonium ion has been reported for a compound of this type[86]). The ^{31}P NMR signal associated with compound **4** is a broad multiplet centred at 47.3 ppm, due to coupling to NMR-active boron (primarily boron-11). The presence of borane is also reflected in the ^{1}H NMR spectrum with a very broad peak between 1.0 and 1.8 ppm, which intergrates for three protons. A B−H stretching peak is also seen in the infrared spectrum of compound **4**, at 2380 cm^{-1}.

The lithiation of compound **4** was attempted in a similar fashion to that of the cyclic phosphonium bromide **1**, initially by combining compound **4** and an excess of lithium metal in THF overnight, and subsequently quenching with water. Proton and phosphorus-31 NMR data of the resulting reaction mixture showed unchanged starting material **4** only (Scheme 2.7). Again, the reaction was repeated with the inclusion of naphthalene. Following the method of Azzena and co-workers,[80] lithium metal and 5 mol% naphthalene were combined in THF and heated to 50 °C until a dark green colour was observed. The solution was cooled and compound **4** was added, the mixture stirred overnight, and then quenched with water. The resulting

^{1}H NMR spectrum of the reaction mixture showed no sign of unreacted compound **4**, but also no peaks associated with CH_2P moieties, suggesting that C−P bond cleavage had occurred along with the desired C−O bond cleavage. This is perhaps unsurprising, as C−P bond cleavage with alkali metals in THF is a well established reaction type.[87]

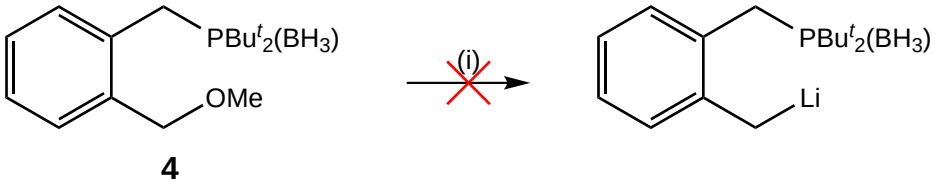

4

Scheme 2.7 Unsuccessful lithiation of compound **4**. *Reagents and conditions:* (i) Li metal, naphthalene, THF, overnight.

As all lithiation reactions undertaken had been unsuccessful, it was decided the use of an *o*-phosphinomethyl-substituted benzyl Grignard reagent may provide a viable route to the desired compounds. To this end, the synthesis of α-(di-*t*-butylphosphino)-α'-chloro-*o*-xylene–borane (**5**) was carried out, *via* reaction of lithium di-*t*-butylphosphide–borane with α,α'-dichloro-*o*-xylene (Scheme 2.8). Again, the reaction of stoichiometric quantities of these reactants would result in a statistical distribution of products, so a three-fold excess of α,α'-dichloro-*o*-xylene was used in order to minimise production of the by-product, α,α'-bis-(di-*t*-butylphosphino)-*o*-xylene–diborane. In this case, borane-protection of the phosphine moiety was imperative to prevent cyclisation of the product to the chloride analogue of compound **1**. After the reaction was complete, the excess starting material was removed from the reaction mixture by vacuum sublimation, and the remaining crude product recrystallised from *n*-hexane to give pure compound **5** as an air-stable crystalline solid in 54% yield.[85]

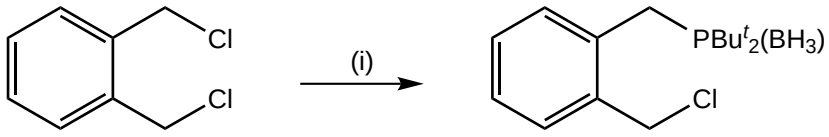

5

Scheme 2.8 Synthesis of *o*-phosphinomethyl-substituted benzyl chloride **5**. *Reagents and conditions:* (i) 0.3 eq. LiPBu$^t_2$(BH$_3$), Et_2O, −78 °C ⟶ rt, 2 h, 54% yield.

The identity of compound **5** was established through NMR and infrared spectroscopy, high resolution mass spectrometry and elemental analysis. The ^{31}P NMR signal is a broad multiplet centred at 47.9 ppm, very similar to that of compound **4**. The ^{1}H NMR spectrum displays a broad peak between 0.6 and 1.5 ppm

corresponding to the borane protons, doublets centred at 1.05 and 3.11 ppm for the PBu^t and CH_2P groups respectively, a singlet at 4.72 ppm corresponding to the CH_2Cl protons, and peaks in the aromatic region of the spectrum integrating for four protons. Again, the infrared spectrum contains a B−H stretching peak, at 2377 cm^{-1}.

Compound **5** is a versatile substrate for the synthesis of a range of hybrid *P,E* ligands with *o*-xylene backbones. Through either direct reaction with nucleophiles or conversion to a Grignard reagent, this compound has been utilised as the precursor to unsymmetric diphosphine, phosphine-thioether, phosphine-sulfoxide, phosphine-amine and phosphine-silane ligands.[88] In most cases, this method has the benefit of providing air-stable, crystalline ligand precursors, which can be easily stored for many months without decomposition.

2.3 Hybrid *P,E* Ligands

2.3.1 *P,P* ligands

Initially, compound **5** was used to synthesise the known ligand, α-(di-*t*-butylphosphino)-α'-(diphenylphosphino)-*o*-xylene (**7**)[36] in two steps. Compound **5** was reacted with freshly prepared lithium diphenylphosphide–borane to give a 57% yield of desired compound **6** after work-up and recrystallisation (Scheme 2.9). The ^{31}P NMR spectrum associated with compound **6** displays broad peaks centred at 18.5 and 47.7 ppm, confirming the presence of benzyldiphenylphosphine–borane and benzyldi-*t*-butylphosphine–borane moieties respectively.[89] Again, the ^1H NMR spectrum shows a very broad peak between 0.2 and 1.2 ppm, this time integrating for six protons, for the borane groups in compound **6**, and B−H stretching peaks are present in the infrared spectrum between 2349 and 2386 cm^{-1}.

The deprotection of phosphine–borane adducts to give the corresponding free phosphines has been achieved *via* various synthetic methodologies,[90,91] and the use of diethylamine, 1,4-diazabicyclo[2.2.2]octane (DABCO), morpholine and tetrafluoroboric acid have been investigated for the deprotection of derivatives of compound **5**. It was found that morpholine was the most effective deprotection reagent for the majority of these hybrid *P,E* ligands. The use of morpholine as both reagent and solvent for these reactions achieved quantitative deprotection of the phosphine–boranes at 100 °C over one hour. Importantly, the by-product of these reactions, morpholine–borane, was easily separated from the desired free phosphine. In the

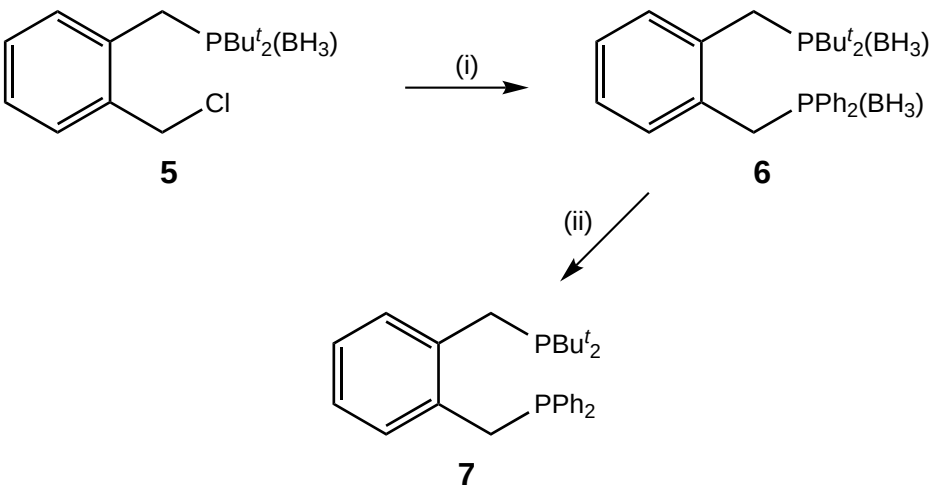

5 **6** **7**

Scheme 2.9 Synthesis of *P,P* ligand **7**. *Reagents and conditions:* (i) $LiPPh_2(BH_3)$, THF, −78 °C ⟶ rt, overnight, 57% yield; (ii) Morpholine, 100 °C, 1 h, 82% yield.

case of compound **6**, reaction with morpholine under these conditions, followed by removal of the remaining morpholine under reduced pressure, extraction into *n*-hexane, and filtration through a plug of alumina gave highly air-sensitive pure compound **7** in 82% yield as a white solid (Scheme 2.9).

Due to the air-sensitivity of compound **7**, characterisation of this material was restricted to NMR methods only. Deprotection of both phosphine moieties was established from the ^{31}P NMR spectrum of compound **7**. Both broad peaks seen in the spectrum of the precursor, compound **6**, had disappeared and were replaced by sharp doublets at −15.6 and 24.5 ppm ($^5J_{PP}$ = 1.4 Hz), corresponding to the deprotected PPh_2 and PBu^t_2 groups respectively. All the NMR data collected for compound **7** are in good agreement with the data published by Fanjul and co-workers in 2010.[36]

As mentioned previously, some hybrid *P,E* ligands containing an *o*-xylene backbone are not able to be synthesised by the previous methods, as the appropriate nucleophilic reagent is unavailable. This is the case for the synthesis of an unsymmetric diphosphine ligand containing a bis(pentafluorophenyl)phosphine group, as the bis(pentafluorophenyl)phosphide anion is known to be unstable even at low temperatures.[92] In these instances, compound **5** can be reacted with magnesium metal to form a substituted benzyl Grignard reagent capable of reacting with appropriate halide precursors to form the desired *P,E* ligands.

In order to synthesise a molecule containing a bis(pentafluorophenyl)phosphine moiety (*i.e.* compound **8**), the *ortho*-substituted benzyl chloride compound **5** was treated with magnesium powder in THF to produce a benzyl Grignard reagent. This solu-

tion was then combined with a THF solution of bis(pentafluorophenyl)bromophosphine to produce borane-protected unsymmetric diphosphine compound **8**, shown in Scheme 2.10. This reaction also resulted in two other products derived from compound **5**; the reduced form, *o*-(methyl)benzyldi-*t*-butylphosphine–borane (**9**), and the bibenzyl dimer resulting from Wurtz-type coupling (**10**). A number of pentafluorophenyl-containing products relating to the bis(pentafluorophenyl)bromophosphine starting material were also present. All the by-products were successfully removed from the reaction mixture by extraction into *n*-hexane and subsequent washing with methanol, giving desired compound **8** in 32% yield. Due to the presence of a bis(pentafluorophenyl)phosphine moiety in this compound, it is mildly air-sensitive. Borane protection of the $P(C_6F_5)_2$ group was attempted; however, the facile reversability of the resulting bis(pentafluorophenyl)phosphine–borane adduct meant this methodology was not worth pursuing.

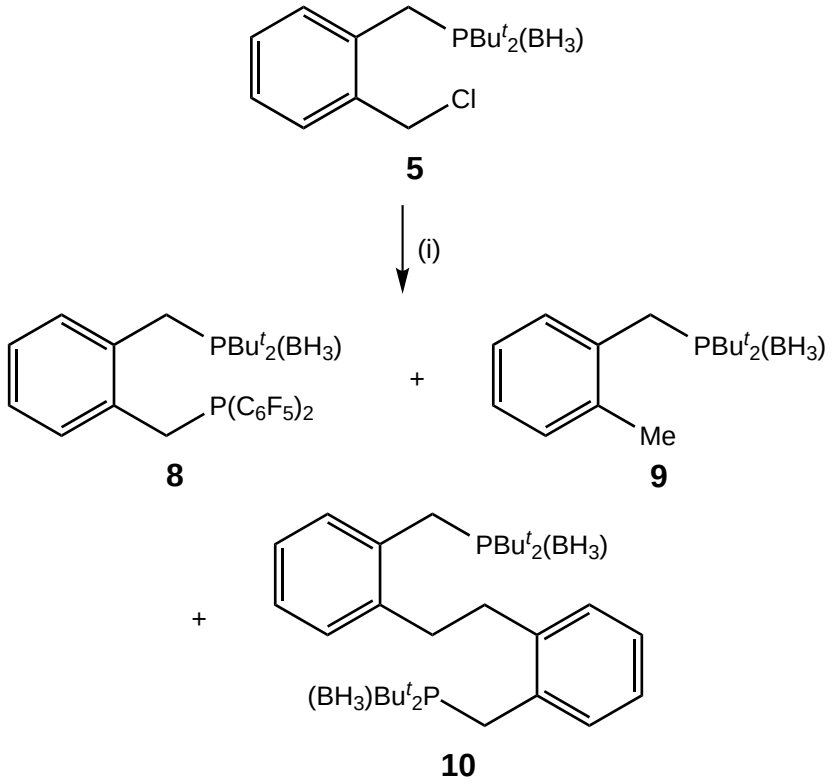

Scheme 2.10 Grignard route to borane-protected *P,P* compound **8**. *Reagents and conditions:* (i) Mg powder, $(C_6F_5)_2PBr$, THF, 32% yield.

Compound **8** was characterised by ^{1}H, ^{31}P, ^{19}F and ^{13}C NMR spectroscopy, and high resolution mass spectrometry. The ^{31}P NMR spectrum of this compound displays the expected broad multiplet centred at 49.4 ppm corresponding to the $PBu^t_2(BH_3)$ moiety, and a quintet ($^3J_{PF} = 22.2$ Hz) centred at -50.5 ppm for the $P(C_6F_5)_2$ group. Both this chemical shift and coupling constant are in good agreement with the only published example of a bis(pentafluorophenyl)benzylphosphine compound.[93] The ^{19}F NMR spectrum of compound **8** shows three complex peaks centred at -160.3,

−149.4 and −130.1 ppm, corresponding to the *meta*, *para* and *ortho* fluorine atoms of the $P(C_6F_5)_2$ moiety respectively.

Deprotection of compound **8** was achieved *via* a different synthetic procedure to the previous *P,P* ligand. In this case, compound **8** was combined with tetrafluoroboric acid diethyl etherate, and after one hour, the mixture quenched with sodium hydrogen carbonate solution (Scheme 2.11). Subsequent work-up gave pure compound **11** in a 51% yield. Again, this highly air-sensitive material was characterised by ^{1}H, ^{31}P, ^{19}F and ^{13}C NMR spectroscopy. Complete deprotection of the PBu^{t}_{2} moiety was established by the disappearance of the broad peak associated with the BH_3 protons in the ^{1}H NMR spectrum, and the replacement of the broad peak in the ^{31}P NMR spectrum of borane-protected compound **8** with a sharp doublet signal centred at 25.2 ppm in the spectrum of compound **11** (shown in Figure 2.1). As in *P,P* ligand **7**, the doublet splitting is due to a $^{5}J_{PP}$ coupling between the phosphorus atoms, in this instance to the quintet of doublets signal at −50.9 ppm, associated with the $P(C_6F_5)_2$ moiety.

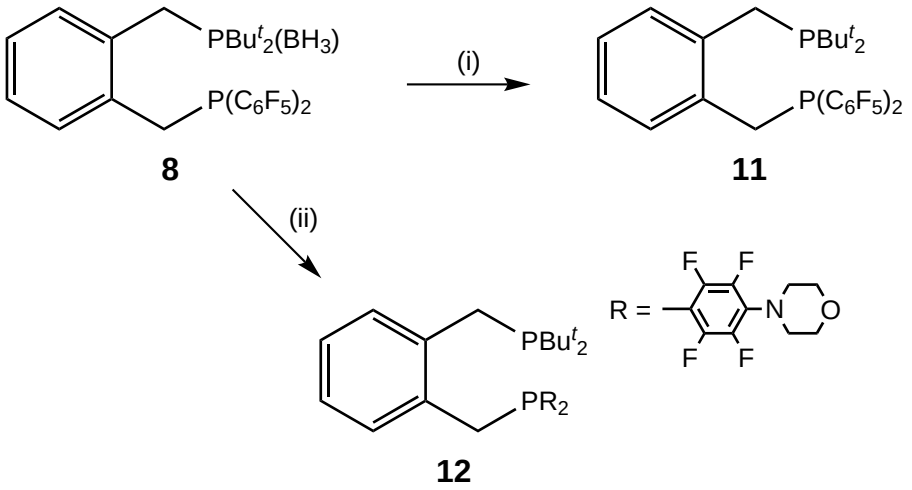

Scheme 2.11 Deprotection of *P,P* compound **8**. *Reagents and conditions:* (i) $HBF_4 \cdot Et_2O$, CH_2Cl_2, 1 h, $NaHCO_3$, H_2O, 30 min, 51% yield; (ii) Morpholine, 100 °C, 1 h, 86% yield.

Deprotection of the phosphine–borane moiety in compound **8** was also attempted with morpholine. Interestingly, along with the desired deprotection reaction, nucleophilic aromatic substitution occurred at the *para* position of each pentafluorophenylphosphine moiety, producing the bis(*p*-*N*-morpholinotetrafluorophenyl)-phosphine compound **12** (Scheme 2.11). The identity of this compound was established by ^{1}H, ^{31}P, ^{19}F and ^{13}C NMR spectroscopy, and high resolution mass spectrometry. Only two signals are observed in the ^{19}F NMR spectrum, in a 1:1 ratio, indicating the loss of the *para* fluorine atoms of the formerly pentafluorophenylphosphine groups. Of note in the ^{13}C NMR spectrum is a triplet peak centred at

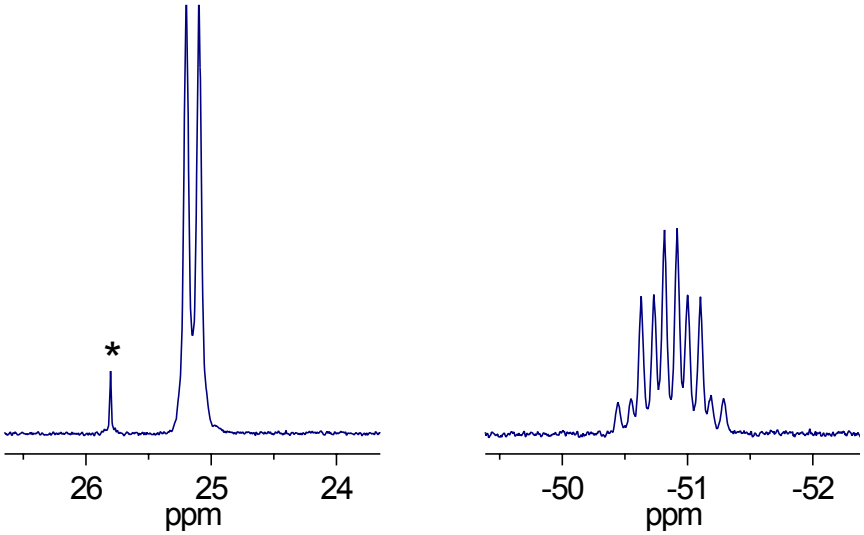

Figure 2.1 ^{31}P NMR spectrum of *P,P* ligand **11** in benzene-d_6. Asterisk denotes a sample impurity.

51.1 ppm corresponding to the CH_2N groups of the morpholino substituents, the 3.4 Hz coupling constant being due to a $^4J_{CF}$ coupling to the two *meta* fluorine atoms. This connectivity is supported by an HMBC correlation between the protons of the CH_2N groups and one of the fluorine-bearing carbon atoms. This reaction type has previously been shown to occur between pentafluorophenyl substituents of various compounds and morpholine,[94–96] and with many other secondary amines. This is, however, the first example of nucleophilic aromatic substitution at the *para* position of a pentafluorophenylphosphine by a secondary amine.

2.3.2 *P,S* ligands

The synthesis of phosphine-thioether ligands with an *o*-xylene backbone from compound **5** was quite straightforward. Compound **5** was treated with an excess of the appropriate sodium thiolate precursor to produce phosphine–borane compounds with either an electron-rich *t*-butyl (**13a**) or electron-poor phenyl (**13b**) thioether moiety in recrystallised yields of 80% and 75% respectively (Scheme 2.12). These compounds are odourless, easy to handle, air-stable white solids. The NMR spectra of compounds **13a** and **13b** contain all the expected features of phosphine–borane species, including broad multiplets in the ^{31}P NMR spectra centred around 48 ppm. The ^{1}H NMR spectra display doublet peaks at *ca.* 3.2 ppm corresponding to the protons of the CH_2P groups, and singlets at 3.99 and 4.40 ppm respectively for the CH_2S groups. Proton decoupled ^{11}B NMR spectra were also collected for these compounds. The spectrum of compound **13a** displays a signal centred at −40.4 ppm with a $^1J_{PB}$ coupling constant of 47.6 Hz. Similarly, the spectrum of compound **13b** displays a signal centred at −40.7 ppm with a $^1J_{PB}$ coupling constant of 48.4 Hz.

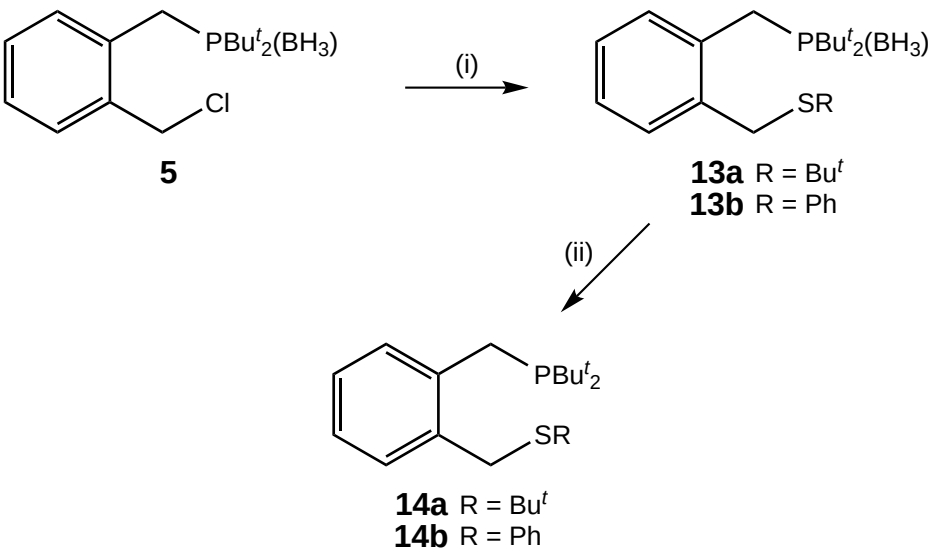

Scheme 2.12 Synthesis of *P,S* ligands **14a** and **14b**. *Reagents and conditions:* (i) NaSR, EtOH, rt, overnight, 75–80% yield; (ii) Morpholine, 100 °C, 1 h, 71–93% yield.

Deprotection of the phosphine–borane adducts was again achieved by heating the compounds in an excess of morpholine for one hour, followed by extraction with *n*-hexane and filtration through alumina (Scheme 2.12). By this method, pure samples of the highly air-sensitive free phosphine compounds **14a** and **14b** were produced in yields of 93% and 71% respectively. Similarly to the previously discussed diphosphine ligands, the complete deprotection of compounds **14a** and **14b** was established through NMR spectroscopy, primarily by the replacement of the broad peaks in the ^{31}P NMR spectra with sharp peaks at 25.0 and 25.9 ppm respectively. The ^{1}H NMR spectra of these compounds show a reduction in the $^2J_{\mathrm{PH}}$ coupling constant of the CH_2P groups, from 12.0 Hz in the phosphine–boranes to 1.2 Hz for compound **14a** and no observed coupling for compound **14b**; however, the ^{1}H NMR peak corresponding to the CH_2S protons of compound **14b** did display a long-range $^5J_{\mathrm{PH}}$ coupling of 2.2 Hz. The ^{1}H NMR spectrum of ligand **14a** is shown in Figure 2.2.

2.3.3 *P,S=O* ligand

The second *P,S* target in this study was a phosphine-sulfoxide ligand. As it is known that standard peroxide-based sulfur oxidising agents deprotect and oxidise trialkylphosphine–boranes,[97,98] it was important to select an oxidising agent for the synthesis of a phosphine-sulfoxide ligand from compound **13a** that not only selectively produced the sulfoxide (rather than further oxidation to the sulfone), but also had no effect on the phosphine–borane moiety. In 2005, Mohammadpoor-

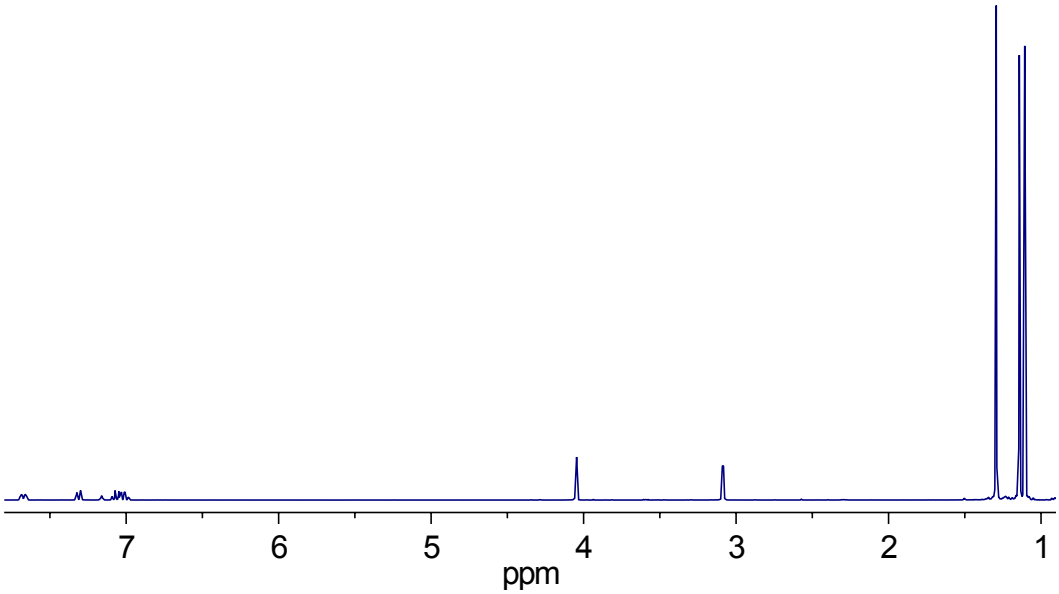

Figure 2.2 ^{1}H NMR spectrum of *P,S* ligand **14a** in benzene-d_6.

Baltork and co-workers published a synthetic procedure that selectively oxidised thioethers to sulfoxides in good yield, and was tolerant of a number of functional groups.[99] Their method used one equivalent each of 3-carboxypyridinium chlorochromate (CPCC) and aluminium trichloride, and gave sulfoxide yields greater than 73% either in refluxing acetonitrile solution or under microwave irradiation. In this case, the CPCC/$AlCl_3$ system oxidised compound **13a** to the racemic borane-protected *P,S=O* compound **15** in 58% recrystallised yield (Scheme 2.13). It is possible that a single enantiomer of compound **15** could be synthesised *via* formation of a benzyl Grignard reagent from compound **5** and reaction with an enantiomerically pure *t*-butylsulfinate ester or *t*-butylthiosulfinate ester;[100] however, this methodology has not been investigated.

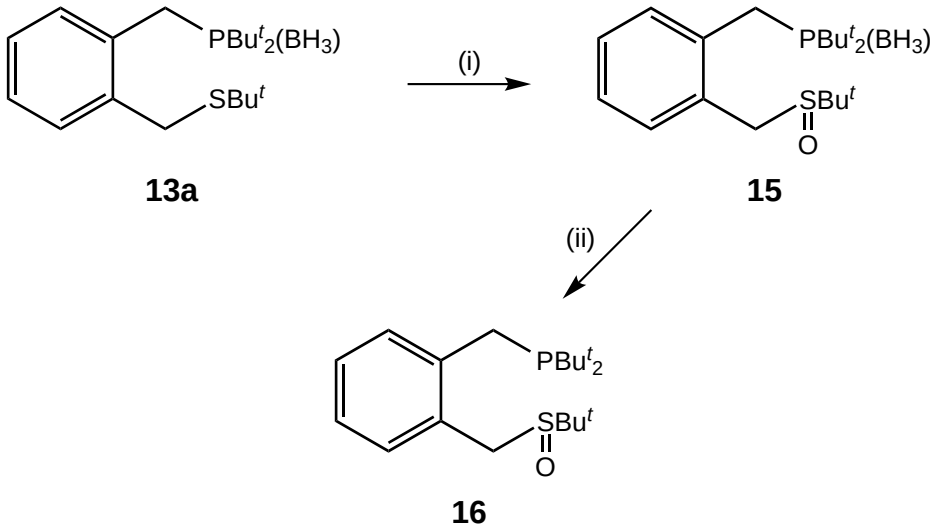

Scheme 2.13 Synthesis of *P,S=O* ligand **16**. *Reagents and conditions:* (i) CPCC, $AlCl_3$, MeCN, reflux, 2 h, 58% yield; (ii) Morpholine, 100 °C, 1 h, 79% yield.

As the sulfur atom in compound **15** is a chiral centre, the methylene protons and phosphine *t*-butyl groups are rendered diastereotopic, which is reflected in the doubling of ^{1}H and ^{13}C NMR signals corresponding to these atoms. The ^{1}H NMR spectrum of compound **15** displays AB systems associated with the protons of the CH_2P group (at 3.04 and 4.07 ppm, $^{2}J_{HH}$ = 15.0 Hz) and CH_2S group (at 3.63 and 4.61 ppm, $^{2}J_{HH}$ = 13.5 Hz), and distinct signals for the protons of each PBu^{t} group (Figure 2.3). The infrared spectrum of this compound was collected, and displays both a B−H stretching peak (2391 cm^{-1}) and a S=O stretching peak (1028 cm^{-1}).

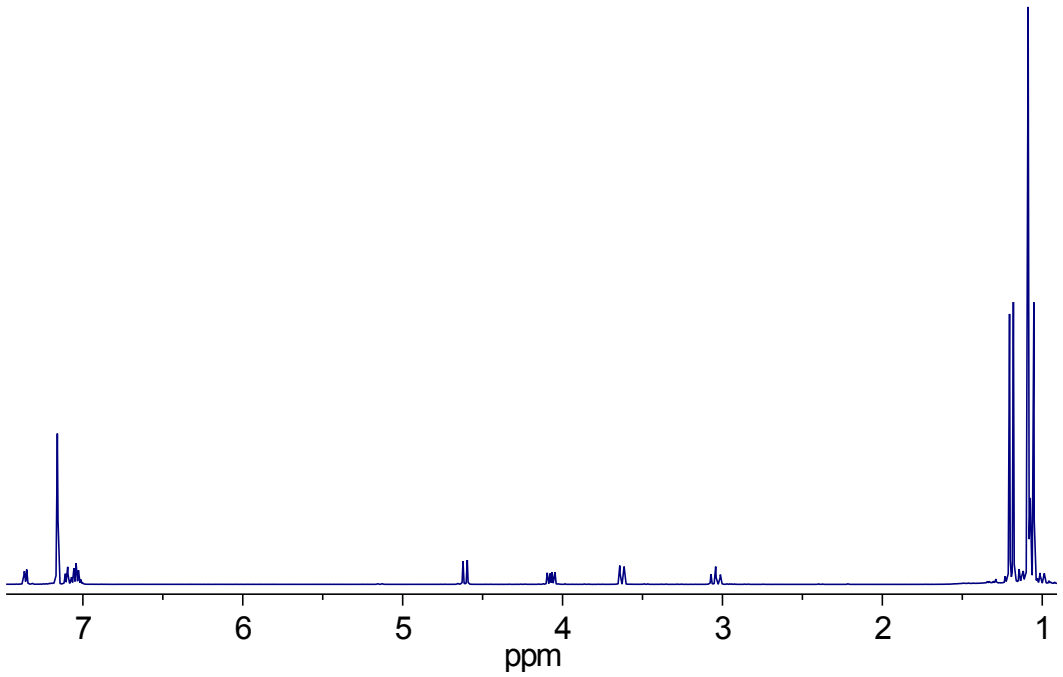

Figure 2.3 ^{1}H NMR spectrum of borane-protected *P,S=O* compound **15** in benzene-d_6.

Again, compound **15** was easily deprotected by heating to 100 °C for one hour in excess morpholine, giving 79% yield of the highly air-sensitive white solid ligand **16** after work up (Scheme 2.13). As in the borane-protected precursor, the chirality of this ligand is reflected in the NMR spectra, with AB systems again evident for the ^{1}H NMR peaks associated with the methylene protons in compound **16**, and distinct signals for the PBu^{t} groups. Interestingly, the ^{1}H NMR peaks corresponding to the CH_2S protons also display long-range $^{5}J_{PH}$ coupling constants of 1.4 and 3.5 Hz.

2.3.4 *P,N* ligands

The synthesis of phosphine-amine ligands from compound **5** was problematic in comparison to the synthesis of the phosphine-thioether compounds for two reasons. Firstly, lithium dialkylamide reagents are known to reduce alkyl and aryl halides,[101]

and secondly, the reagent or resulting benzyl dialkylamine compound would likely deprotect the phosphine–borane moiety producing an air-sensitive compound.[90,91] As was the case for the synthesis of diphosphine compound **6**, it was necessary to borane-protect the amine source prior to use in these reactions, in order to prevent scrambling of the borane protecting group. Lithium *N,N*-dialkylaminoborohydride (LAB) reagents are also well-known reducing agents when utilised at room temperature or above; however, at or below 0 °C, it has been shown that LAB reagents react with benzyl halides to produce tertiary amine–boranes.[102] Using this methodology, compounds **17a–c** were synthesised in good yield, even when the LAB reagent contained bulkier ethyl substituents (Scheme 2.14). Very minor amounts of the reduced by-product, *o*-(methyl)benzyldi-*t*-butylphosphine–borane (**9**), were seen in the reaction mixtures of compounds **17b** and **17c**, but this was not present in the reaction mixture of benzyldimethylamine compound **17a**.

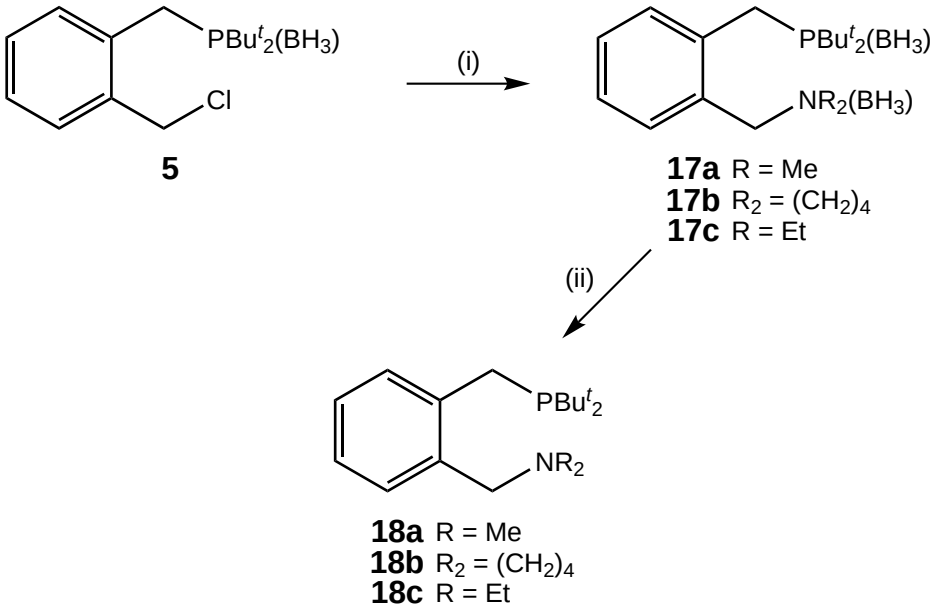

Scheme 2.14 Synthesis of *P,N* ligands **18a–c**. *Reagents and conditions:* (i) $LiNR_2(BH_3)$, THF, −5 °C, 1 h, 80–89% yield; (ii) $HBF_4 \cdot Et_2O$, CH_2Cl_2, rt, 1 h, $NaHCO_3$, H_2O, rt, 30 min, 60–85% yield.

These phosphine-amine–diborane compounds were fully characterised by NMR and infrared spectroscopy, high resolution mass spectrometry and elemental analysis. The ^{1}H NMR spectra of these compounds display very broad peaks centred around 1.2 and 2.2 ppm, corresponding to the phosphine–borane and amine–borane protons respectively, along with all the other expected features. Proton-decoupled ^{11}B NMR spectra of these compounds were also collected. These spectra all display two peaks, a doublet for the phosphine–borane moiety centred around −40.9 ppm ($J \approx 50$ Hz), and a singlet for the amine–borane moiety. The chemical shifts of the amine–borane

peaks are more varied due to the differing amine substituents, from −8.8 ppm for compound **17a** to −12.9 ppm for compound **17c**.

These phosphine-amine ligands also required a different deprotection strategy, as heating in an excess of morpholine did not entirely deprotect the amine–borane moiety. An effective deprotection strategy for compounds **17a–c** involved treatment with tetrafluoroboric acid diethyl etherate, followed by sodium hydrogen carbonate, to give novel ligands **18a–c** in moderate to good yield with high purity (Scheme 2.14). Again, due to the particularly high air-sensitivity of **18a–c**, characterisation was performed by NMR methods only. Complete removal of the borane protecting groups was established by the absence of both broad peaks associated with the BH_3 moieties in the ^{1}H NMR spectra. The ^{31}P NMR spectra of these compounds also display the expected sharp singlets at *ca.* 24 ppm for the free phosphines.

2.3.5 *P,Si* ligands

As discussed previously, the synthesis of phosphine-silane ligands with an *o*-xylene backbone requires a different strategy than previously published methods, due to the instability of secondary silyl anions.[72] For this reason, an appropriate route to phosphine-silane compounds of this type is *via* an *in situ* benzyl Grignard reagent. Compound **5** was combined with excess magnesium turnings, a crystal of iodine, and chlorodiphenylsilane in THF under anhydrous conditions and stirred overnight, to give the borane-protected phosphine-silane compound **19a**, as shown in Scheme 2.15. This reaction also produced a number of by-products, including the reduced form, *o*-(methyl)benzyldi-*t*-butylphosphine–borane (**9**). The desired compound **19a** was isolated by column chromatography using an alumina stationary phase, resulting in a yield of 34%. This material was characterised by NMR spectroscopy, high resolution mass spectrometry and elemental analysis. The ^{1}H NMR spectrum of compound **19a** displays all the expected features, including a triplet peak associated with the Si−H moiety at 5.10 ppm with silicon satellites ($^1J_{\mathrm{SiH}} = 197.3$ Hz).

A similar methodology was used to synthesise the dimethylsilane analogue, compound **19b**. Again, compound **5** was combined with excess magnesium turnings, a crystal of iodine, and chlorodimethylsilane in THF under anhydrous conditions, but in this case the mixture was heated to reflux for one hour, followed by extraction into toluene (Scheme 2.15). ^{1}H NMR spectroscopy of the reaction mixture showed 85% conversion to desired compound **19b**, with *o*-(methyl)benzyldi-*t*-butylphosphine–

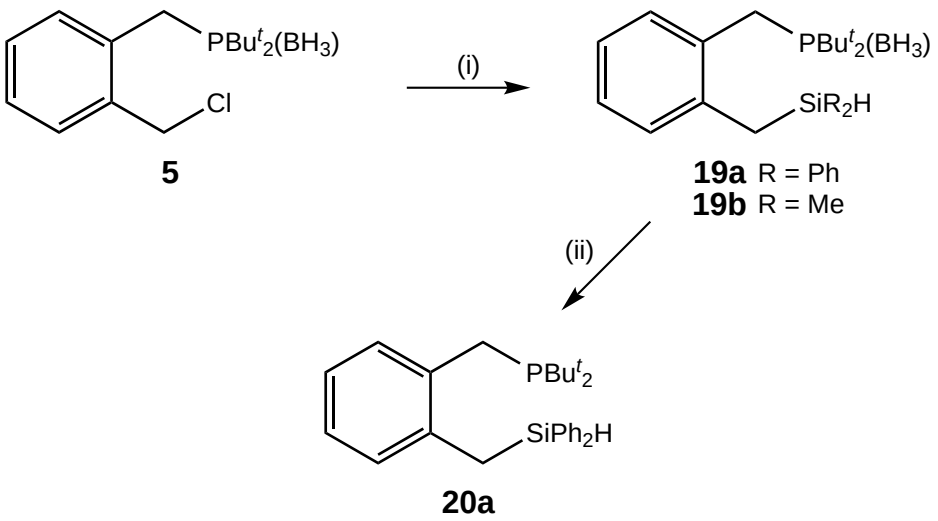

5 **19a** R = Ph **19b** R = Me **20a**

Scheme 2.15 Grignard route to *P,Si* compounds **19a**, **19b** and **20a**. *Reagents and conditions:* (i) Mg turnings, I_2, R_2SiHCl, THF; (ii) DABCO, toluene-d_8, 60 °C, overnight, 69% yield.

borane (**9**) the only by-product. Unfortunately, all attempts to separate these two compounds by crystallisation and column chromatography were unsuccessful.

Deprotection of isolated compound **19a** was attempted a number of times by heating in excess morpholine; however, in all instances this methodology led to a mixture of products. Unfortunately, the tetrafluoroboric acid deprotection route used previously for the *P,N* ligands was also not appropriate for the deprotection of phosphine-silane compound **19a**, as Si−H bonds are known to undergo acid-catalysed solvolysis;[103] and hence, a third deprotection strategy was required. Compound **19a** and 1,4-diazabicyclo[2.2.2]octane (DABCO) were dissolved in toluene-d_8, and the solution heated to 60 °C overnight (Scheme 2.15). The reaction was monitored by ^{1}H and ^{31}P NMR spectroscopy, and showed clean transformation of the starting materials into compound **20a** and DABCO–borane. Subsequent solvent removal under reduced pressure, extraction into *n*-hexane and filtration through a plug of alumina gave pure compound **20a** as a highly air-sensitive white solid in 69% yield. The NMR spectra of this ligand show all the expected features, including a sharp singlet at 25.2 ppm in the ^{31}P NMR spectrum, and the intact Si−H moiety at 5.22 ppm with silicon satellites ($^1J_{SiH}$ = 197.5 Hz) in the ^{1}H NMR spectrum.

2.4 NMR Comparison

Common ^{1}H and ^{31}P NMR data for the novel *o*-$C_6H_4\{CH_2PBu^t{}_2(BH_3)\}(CH_2E)$ compounds are shown in Table 2.1. The signals corresponding to the $PBu^t{}_2(BH_3)$

moieties show little variation, for example the broad ^{31}P NMR signals range from 47.3 ppm (E = OMe) to 49.8 ppm (E = $NMe_2(BH_3)$, $NEt_2(BH_3)$), and the *t*-butyl ^{1}H NMR signals vary by only 0.20 ppm over the twelve compounds. The protons of the CH_2P moieties are somewhat more influenced by the identity of substituent E, with chemical shifts of 2.69 ppm in compound **19a** (E = $SiPh_2H$) to 4.07 ppm in compound **15** (E = $S(O)Bu^t$). The AB system associated with the CH_2P protons of compound **15** is also the outlier in terms of the $^2J_{PH}$ coupling constants, with values of 9.0 and 15.0 Hz, as compared to $J \approx 12.0$ Hz for all the other borane-protected *P,E* compounds. As would be expected, the ^{1}H NMR chemical shifts of the signals associated with the CH_2E protons are highly dependent upon the identity of E, varying from 2.32 ppm in compound **19b** (E = $SiMe_2H$) to 4.72 ppm in compound **5** (E = Cl). These values are consistent with those of benzyldimethylsilane[104] and benzyl chloride respectively.

Table 2.1 Selected ^{31}P and ^{1}H NMR shifts (in ppm) and coupling constants (in Hz) of borane-protected *P,E* compounds in benzene-d_6.

		PBu^t			CH_2P		CH_2E
Compound	**E**	δ_P [a]	δ_H	$^3J_{PH}$	δ_H	$^2J_{PH}$	δ_H
4	OMe	47.3	1.08	12.5	3.16	12.5	4.44
5	Cl	47.9	1.05	12.3	3.11	12.0	4.72
6[b]	$PPh_2(BH_3)$	47.7	1.23	12.3	3.11	11.8	3.93
8	$P(C_6F_5)_2$	49.4	1.09	12.2	3.29	11.9	4.23
13a	SBu^t	47.9	1.12	12.5	3.27	12.0	3.99
13b	SPh	48.0	1.05	12.0	3.20	12.0	4.40
15	$S(O)Bu^t$	48.0	1.06	12.5	3.04	15.0	3.63
			1.19	12.5	4.07	9.0	4.61
17a	$NMe_2(BH_3)$	49.8	1.08	12.0	3.55	12.0	3.98
17b	$N(CH_2)_4(BH_3)$	49.6	1.13	12.5	3.69	12.0	4.10
17c	$NEt_2(BH_3)$	49.8	1.12	12.5	3.82	12.0	4.02
19a	$SiPh_2H$	48.6	1.03	12.2	2.69	12.0	2.93
19b	$SiMe_2H$	48.1	1.10	12.2	3.07	11.9	2.32

[a] Broad multiplet coupling.
[b] Spectra recorded in chloroform-*d*.

A number of dissimilarities in the ^{1}H and ^{31}P NMR data are observed upon removal of the borane protecting groups to give the *o*-$C_6H_4(CH_2PBu^t_2)(CH_2E)$ (*P,E*) ligands (Table 2.2). The greatest difference is seen in the ^{31}P NMR spectra, where the broad signals of the formerly $PBu^t_2(BH_3)$ moieties (*ca.* 49 ppm) are replaced by sharp singlets at *ca.* 25 ppm, corresponding to the free di-*t*-butylphosphine groups. Deprotection of the phosphine also has a significant effect on the $^2J_{PH}$ coupling constants of the signals associated with the CH_2P protons. These coupling constants are reduced from *ca.* 12 Hz in the phosphine–borane compounds, to <3 Hz in the free phosphines. In fact, in many cases no $^2J_{PH}$ coupling is observed. However, in a number of the deprotected *P,E* ligands a long-range $^5J_{PH}$ coupling of up to 3.5 Hz

is seen between the CH_2E protons and the di-*t*-butylphosphine. This feature is not present in the ^1H NMR spectra of any of the borane-protected compounds.

Table 2.2 Selected ^{31}P and ^1H NMR shifts (in ppm) and coupling constants (in Hz) of *P,E* ligands in benzene-d_6.

		PBu^t			CH_2P		CH_2E	
Ligand	**E**	δ_P	δ_H	$^3J_{PH}$	δ_H	$^2J_{PH}$	δ_H	$^5J_{PH}$
7	PPh_2	24.5	1.09	10.5	3.09	–	3.92	–
11	$P(C_6F_5)_2$	25.2	1.07	10.8	3.07	–	4.27	–
12	$P\{(C_6F_4)N(CH_2CH_2)_2O\}_2$	25.4	1.12	10.7	3.20	–	4.53	–
14a	SBu^t	25.0	1.13	10.6	3.09	1.2	4.05	–
14b	SPh	25.9	1.07	10.8	3.06	–	4.51	2.2
16	$S(O)Bu^t$	25.2	1.06	10.9	2.99	2.0	3.85	1.4
			1.14	10.8	3.37	–	4.25	3.5
18a	NMe_2	24.5	1.13	10.7	3.16	2.4	3.60	–
18b	$N(CH_2)_4$	24.6	1.14	10.5	3.16	2.7	3.82	–
18c	NEt_2	23.8	1.14	10.8	3.12	2.7	3.69	–
20a	$SiPh_2H$	25.2	1.05	10.5	2.65	1.5	3.10	1.5

2.5 Concluding Remarks

A number of methodologies for the synthesis of a family of hybrid *P,E* ligands containing *o*-xylene backbones have been investigated, resulting in the development of the versatile substrate *o*-$C_6H_4\{CH_2PBu^t{}_2(BH_3)\}(CH_2Cl)$ (**5**). Compound **5** was treated with the appropriate nucleophilic reagents to produce the novel air-stable phosphine–borane compounds *o*-$C_6H_4\{CH_2PBu^t{}_2(BH_3)\}(CH_2E)$, where E = PPh_2 (**6**), SR (**13**) or $NR_2(BH_3)$ (**17**). Oxidation of phosphine-thioether compound **13a** gave borane-protected phosphine-sulfoxide compound **15**, where E = $S(O)Bu^t$. When the appropriate nucleophilic reagent was not available, compound **5** was converted to a Grignard reagent and treated with an appropriate electrophile to give phosphine–borane compounds *o*-$C_6H_4\{CH_2PBu^t{}_2(BH_3)\}(CH_2E)$, where E = $P(C_6F_5)_2$ (**8**) or SiR_2H (**19**).

Deprotection of the phosphine (and amine) moieties of the compounds was achieved *via* one of three methods, namely reaction with morpholine, DABCO or HBF_4, dependent upon the properties of the second functional group present. In this manner, a range of novel *P,E* ligands of the type *o*-$C_6H_4(CH_2PBu^t{}_2)(CH_2E)$ have been synthesised, where E = PR_2 (**7** and **11**), SR (**14**), $S(O)Bu^t$ (**16**), NR_2 (**18**) or $SiPh_2H$ (**20a**). All of the borane-protected compounds have been fully characterised using a combination of NMR spectroscopy, infrared spectroscopy, high resolution mass spectrometry and elemental analysis. Due to the high air-sensitivity of the

deprotected *P,E* ligands, the characterisation of these species was restricted to NMR methods only.

This synthetic methodology has been used to produce the first examples of hybrid *P,E* ligands containing an *o*-xylene backbone. The versatile procedure enables the incorporation of a wide range of donor atoms, from either nucleophilic or electrophilic reagents. In most cases, this route also has the benefit of providing air-stable, crystalline ligand precursors, which can be easily stored for many months without decomposition.

Chapter 3

Platinum Complexes

Platinum coordination complexes are often used as models for the more catalytically active complexes of palladium. This is due to the presence of an NMR active isotope of platinum (^{195}Pt, 34% abundant) and the tendency of platinum complexes to be more inert than their corresponding palladium analogues (to processes such as ligand exchange and redox changes at the metal, and catalytically). For these reasons, platinum complexes are often easier to characterise, and can offer insight into the behaviour of the same ligands with palladium. This chapter focuses on Pt(II) and Pt(0) complexes of primarily phosphine-thioether ligand **14a**, with some complexes of phosphine-sulfoxide ligand **16** and phosphine-amine ligand **18a** included for comparison.

3.1 [$PtCl_2$(*P,E*)] Complexes

The reaction of [$PtCl_2$(1,5-hexadiene)] with one equivalent of *P,S* ligand **14a** in acetone at room temperature rapidly produced the chelated complex **21** (Scheme 3.1). The appearance of platinum satellites associated with the ^{31}P NMR signal (27.7 ppm, $^1J_{PtP}$ = 3447 Hz) and the CH_2S peak in the ^{1}H NMR spectrum (4.92 ppm, $^3J_{PtH}$ = 74.7 Hz) of this complex in acetone-d_6 confirmed binding of both donor atoms to the platinum centre.

Crystals suitable for single crystal X-ray diffraction were grown by inwards diffusion of *n*-hexane into a dichloromethane solution of complex **21**. The X-ray crystal structure (Figure 3.1) confirms the chelating behaviour of ligand **14a**. Crystallographic data are given in Table 3.1 and Table 3.2. The structure also demonstrates

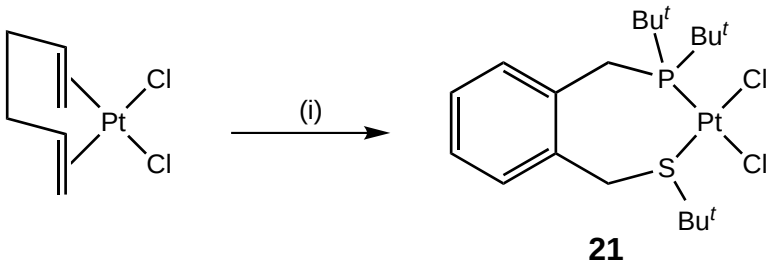

21

Scheme 3.1 Synthesis of $[PtCl_2(P,S)]$ complex **21**. *Reagents and conditions:* (i) 1 eq. ligand **14a**, acetone, overnight, 84% yield.

the different *trans* influences of the phosphorus and sulfur donor atoms. The Pt−Cl bond length *trans* to phosphorus is 2.369(1) Å, whereas the Pt−Cl bond length *trans* to sulfur is 2.324(1) Å (a difference of *ca.* 0.05 Å), consistent with the phosphorus donor atom binding more strongly to the platinum centre than the sulfur. These bond lengths are similar to those of a number of other platinum dichloride complexes of chelating phosphine-thioether ligands.[105–108]

Somewhat unexpectedly, the bite angle of ligand **14a** in this complex is 86.11(2)°, lower than would be expected for a chelating ligand with an *o*-xylene backbone. For comparison, the crystallographically determined bite angle of the diphosphine analogue of **14a**, dbpx, in $[PtCl_2(dbpx)]$ is 104.06(10)°.[11] A result of the constriction of ligand **14a** to near-ideal square planar geometry is the buckling of the ligand backbone (shown in Figure 3.2). The aryl ring plane of the ligand lies at an angle of 98.38(7)° from the P−Pt−S plane of the complex (the Pt−Cl bonds lie 2.74(3)° and −3.41(3)° off this plane). The angle between the P−Pt−S and aryl ring planes in complex **21** is significantly smaller than the equivalent angle in $[PtCl_2(dbpx)]$ (137.9(3)°),[11] a result of the greater buckling of *P,S* ligand **14a** compared to dbpx in these complexes.

Apparent from the ^{1}H NMR spectrum of complex **21** at room temperature is the presence of a dynamic process taking place on the NMR timescale, as the signals corresponding to the CH_2S, CH_2P and PBu^t protons are very broad (all methylene protons are almost undetectable in dichloromethane-d_2 at room temperature). This fluxionality has been encountered before in similar complexes; for example, in the chelated diphosphine complex $[PtCl_2\{o\text{-}C_6H_4(CH_2PBu^t{}_2)(CH_2PPh_2)\}]$, the diphosphine ligand backbone adopts an envelope conformation, which readily inverts at room temperature.[36] This dynamic process causes the phosphine substituents to be inequivalent on the NMR timescale, and thus the ^{1}H NMR spectrum displays the characteristic broad humps of near-coalescence. In the case of complex **21**, however, there is a second dynamic process occurring, as indicated by the sharpness of the SBu^t peak in the ^{1}H NMR spectrum.

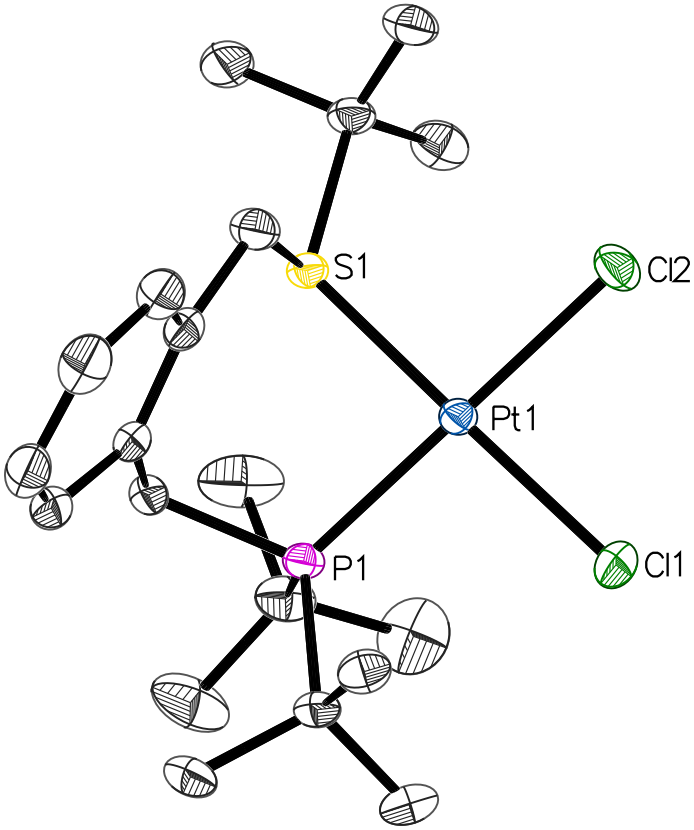

Figure 3.1 ORTEP diagram of [$PtCl_2$(*P,S*)] complex **21** (50% probability thermal ellipsoids). Dichloromethane solvate and hydrogen atoms omitted for clarity.

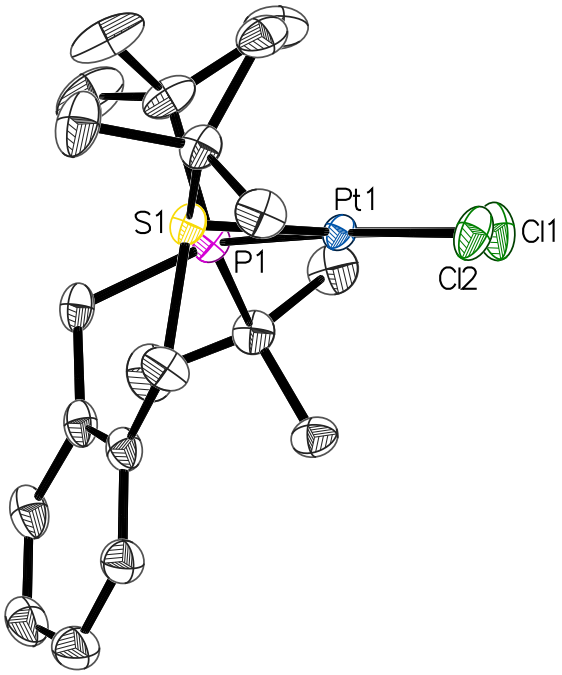

Figure 3.2 ORTEP diagram of [$PtCl_2$(*P,S*)] complex **21** showing buckling of *P,S* ligand backbone (50% probability thermal ellipsoids). Dichloromethane solvate and hydrogen atoms omitted for clarity.

Table 3.1 Crystallographic data of [$PtCl_2$(*P*,*S*)] complex **21**.

Empirical formula	**$C_{20}H_{35}Cl_2PPtS.CH_2Cl_2$**
Formula weight	689.43
Crystal system	Monoclinic
Space group	$P2_1/n$
a/Å	13.7589(4)
b/Å	10.5734(3)
c/Å	18.6757(5)
α/°	90.00
β/°	105.442(1)
γ/°	90.00
V/Å^3	2618.83(13)
Z	4
Cell determination reflections	9795
Cell determination range, $\theta_{min} \longrightarrow \theta_{max}$/°	2.5 $\longrightarrow$ 32.5
Temperature/K	113
Radiation type	Mo Kα
Radiation (λ)/Å	0.71073
Crystal size/ mm	0.32 × 0.30 × 0.12
D_{calc}/g m^{-3}	1.749
F(000)	1360
μ/mm^{-1}	5.91
Experimental absorption correction type	Multi-scan (SADABS)
T_{max}, T_{min}	0.746, 0.527
Reflections collected	76190, R_{equiv} = 0.040
Index range *h*	$-20 \longrightarrow 20$
Index range *k*	$-15 \longrightarrow 15$
Index range *l*	$-28 \longrightarrow 28$
θ range/°	2.2 $\longrightarrow$ 32.7
Independent reflections	9367
Reflections [$I > 2\sigma(I)$]	7982
Restraints/parameters	0/262
GOF	1.04
R_1 [$I > 2\sigma(I)$]	0.0274
wR_2 [$I > 2\sigma(I)$]	0.0653
R_1 [all data]	0.0376
wR_2 [all data]	0.0709
Residual density/e Å^{-3}	$-2.10<3.53$

Table 3.2 Selected bond distances and angles of [$PtCl_2$(*P*,*S*)] complex **21**.

Bond distances (Å)		**Bond angles (°)**	
Pt1−P1	2.2767(7)	P1−Pt1−S1	86.11(2)
Pt1−S1	2.2681(7)	P1−Pt1−Cl1	94.51(3)
Pt1−Cl1	2.3246(7)	S1−Pt1−Cl2	94.27(3)
Pt1−Cl2	2.3692(7)	Cl1−P1−Cl2	85.28(3)
		P1−Pt1−S1 plane $\cdots$ C_6H_4 plane	98.38(7)
		P1−Pt1−S1 plane $\cdots$ Pt1−Cl1	2.74(3)
		P1−Pt1−S1 plane $\cdots$ Pt1−Cl2	3.41(3)

As the sulfur atom in thioether compounds contains two lone pairs of electrons, a simplistic model of the binding of these compounds to transition metals would involve only one pair of electrons, and in cases where the thioether substituents are different (such as in ligand **14a**), the sulfur atom would become a chiral centre. At low temperatures this is the case; however, NMR studies have shown that on increasing the temperature, the time-averaged symmetry of complexes containing thioether ligands is increased, through an inversion process centred at the sulfur atom. This process was first demonstrated by Abel and co-workers in 1966,[109,110] who showed that the ^{1}H NMR spectrum of $[PtCl_2(MeSC_2H_4SMe)]$ below 95 °C displays non-equivalent signals for the methyl groups of the chelating dithioether ligand, attributed to distinct isomers, where the methyl groups are either on the same or opposite faces of the complex. Upon heating these signals converge, and above 95 °C only one signal is seen.

Many subsequent studies[111,112] have explored this inversion process, and although the mechanism is still controversial, it is generally thought to be an associative process *via* a planar intermediate (Figure 3.3),[110] rather than a dissociation-recombination mechanism. For Pt(II) complexes specifically, the major piece of evidence for an associative mechanism is the retention of $^3J_{PtH}$ NMR coupling on the protons surrounding the sulfur atom[111] (this is also the case for complex **21**). The coalescence temperature for the inversion process is heavily dependent upon the nature of the ligand positioned *trans* to the sulfur atom. For instance, the coalescence temperature for the complex $[PtPh_2(EtSC_2H_4SEt)]$ is −70 °C compared with 85 °C for $[PtCl_2(EtSC_2H_4SEt)]$,[113] which reflects the much greater *trans* influence of phenyl ligands when compared to halides.

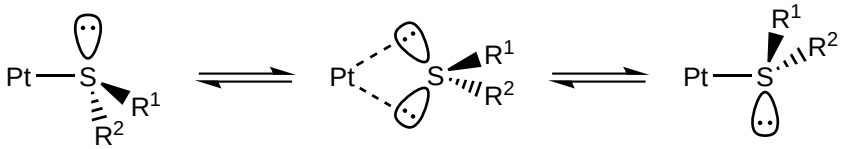

Figure 3.3 Associative mechanism for the inversion of thioether ligands.

In terms of the fluxional behaviour of complex **21**, the ^{1}H NMR data and crystal structure support the argument that both the buckling and inversion processes are occurring. The crystal structure shows that the constraints of the chelate ring force the *P,S* ligand backbone to buckle, and hence there is an asymmetry across the plane of the complex. If the only dynamic process occurring were sulfur inversion, the SBu^t protons would inhabit two chemical environments, and hence the ^{1}H NMR peak for these protons would at least broaden. Similarly, if only inversion of the ligand backbone were occurring, the ^{1}H NMR peak for the SBu^t protons would either be broad, or two distinct peaks. The sharpness of the SBu^t ^{1}H NMR peak

indicates that both of these inversion processes are occurring simultaneously, and hence the SBu^t group remains in the same chemical environment (Figure 3.4).

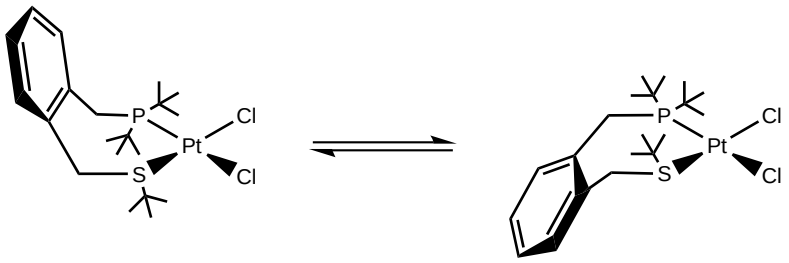

Figure 3.4 Fluxional behaviour of $[PtCl_2(P,S)]$ complex **21**.

VT-NMR spectra of complex **21** were recorded at 20 °C intervals between 50 and −70 °C in a 1:1 mixture of dichloromethane-d_2 and chloroform-d. The ^{1}H NMR spectra (between 0.0 and 7.5 ppm) are shown in Figure 3.5. Over the entire temperature range there is very little change to either the singlet peak associated with the SBu^t protons (at 1.7–1.8 ppm) or the multiplet signal associated with the aromatic protons. However, significant variation is seen in the signals associated with the PBu^t protons. At 50 °C, one doublet is observed for all the PBu^t protons, indicating that they inhabit a single time-averaged chemical environment, and hence both of the previously discussed dynamic processes are rapid on the NMR timescale. At 10 °C, the doublet peak has collapsed into a broad signal, as this temperature is near the coalescence point. Below 10 °C, the doublet peaks associated with the two PBu^t groups separate out, and below −30 °C one of the doublets collapses. At −70 °C, a broad peak integrating for three protons (one methyl group) is observed below 1 ppm. Integration of the SBu^t and remaining PBu^t signals confirms the peaks associated with the other two methyl groups of the relevant PBu^t moiety are obscured by these signals. These data indicate that below 10 °C the two PBu^t groups inhabit different chemical environments, and at lower temperatures one of these is subject to restricted rotation.

An expansion of the methylene region (between 2.4 and 5.2 ppm) of the ^{1}H NMR spectra is shown in Figure 3.6. At 50 °C, the spectrum displays one peak for both CH_2S protons at 4.87 ppm with platinum satellites ($^3J_{PtH}$ = 75.6 Hz). Similarly, one peak is observed for both CH_2P protons centred at 3.82 ppm, although this peak is very broad. Again, the broadness of the methylene peaks in both the 30 °C and 10 °C spectra confirms that coalescence of the fluxional behaviour associated with complex **21** is close to room temperature. Below this temperature, the signals associated with each methylene proton are distinct. For example, at −30 °C an AB system associated with the CH_2S protons is observed at 4.58 and 5.04 ppm ($^2J_{HH}$ = 15.2 Hz), with $^3J_{PtH}$ coupling constants of 90.5 and 61.4 Hz respectively.

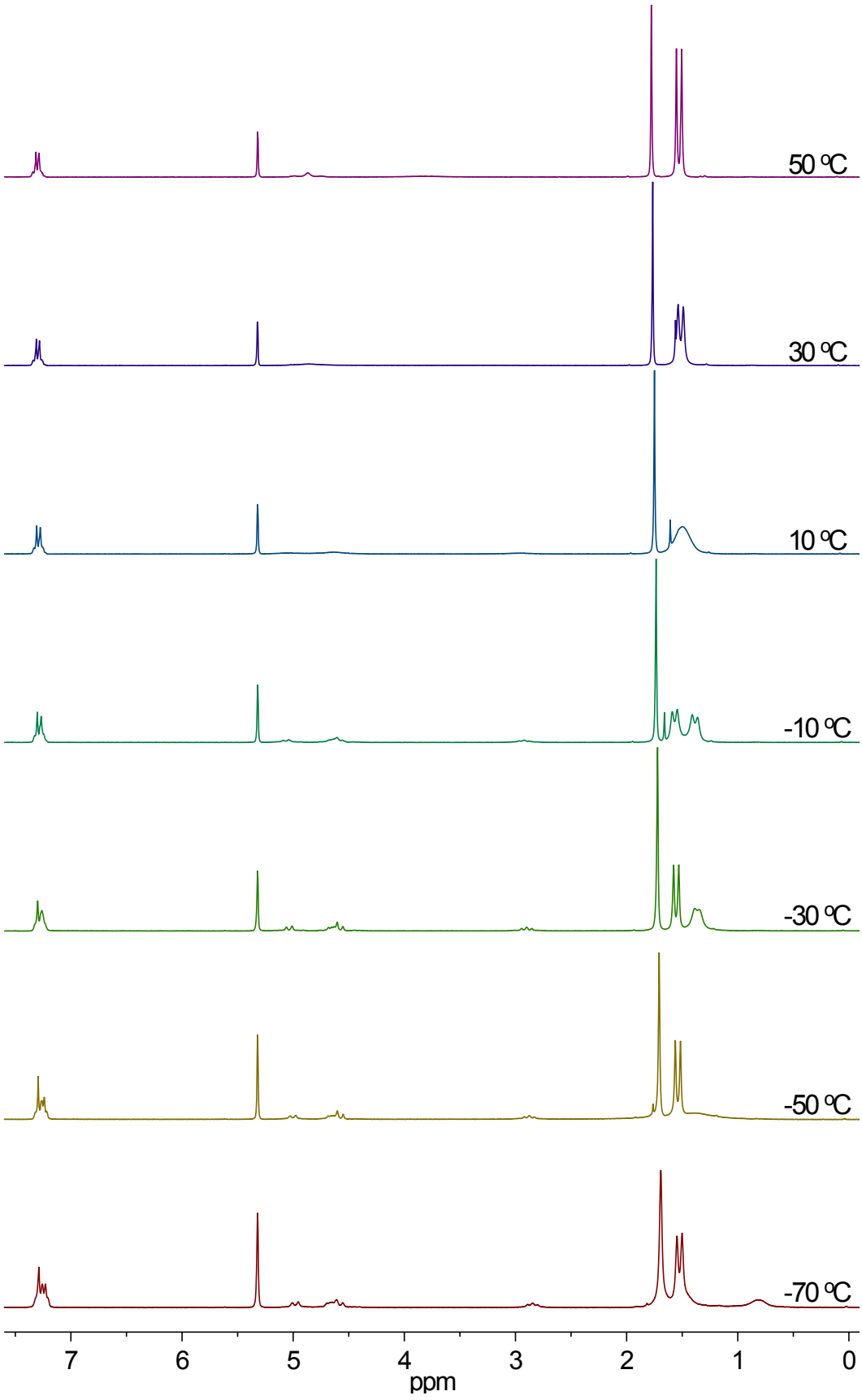

Figure 3.5 ^{1}H NMR spectra of [$PtCl_2$(*P*,*S*)] complex **21** collected between 50 and −70 °C in CD_2Cl_2/$CDCl_3$.

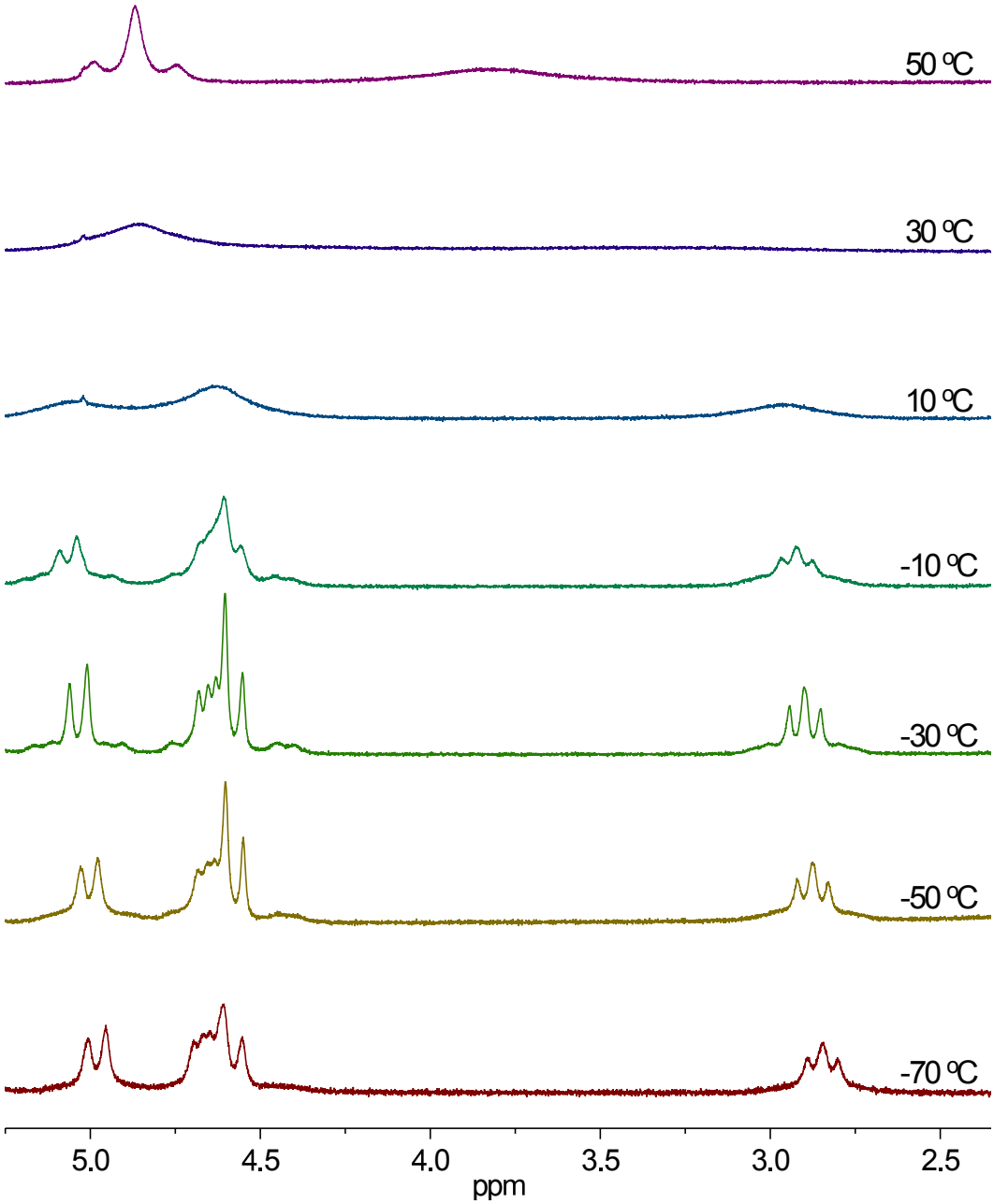

Figure 3.6 Methylene region of the [$PtCl_2(P,S)$] complex **21** ^{1}H NMR spectra collected between 50 and −70 °C in CD_2Cl_2/$CDCl_3$.

The peaks associated with the CH_2P protons have an even larger separation, with an apparent triplet centred at 2.90 ppm ($^3J_{PtH} = 62.0$ Hz) and a doublet of doublets at 4.64 ppm partially obscured by one of the CH_2S signals.

The VT-NMR data presented in Figure 3.5 and Figure 3.6 show there is only one coalescence point for the dynamic processes occurring in complex **21** (disregarding the restricted rotation of one *t*-butyl group at low temperature), and the broadening and/or separation of the SBu^t peak that would be associated with one of the two processes occurring independently is not seen. Consequently, these data confirm that the inversion processes of both the sulfur atom and the ligand backbone occur

on the same timescale over the entire temperature range studied. It should also be noted that there is no change to the ^{31}P NMR spectrum of complex **21** over this temperature range.

The reaction of [$PtCl_2$(1,5-hexadiene)] with one equivalent of *P,N* ligand **18a** gave an entirely different product. When [$PtCl_2$(1,5-hexadiene)] and **18a** were combined in acetone-d_6, a complex with a broad ^{31}P NMR peak at 29.0 ppm and platinum coupling of 3109 Hz formed immediately. This material was tentatively assigned as [$PtCl_2$(η^2-1,5-hexadiene)(κ^1*P*-**18a**)], wherein the phosphine had displaced one half of the 1,5-hexadiene ligand (Scheme 3.2). This assignment was based upon the appearance of peaks centred at 4.96 and 5.78 ppm in the ^{1}H NMR spectrum, which resemble free 1,5-hexadiene but integrate for only two and one protons respectively, and very little change to the ^{1}H NMR shifts of the CH_2NMe_2 moiety.

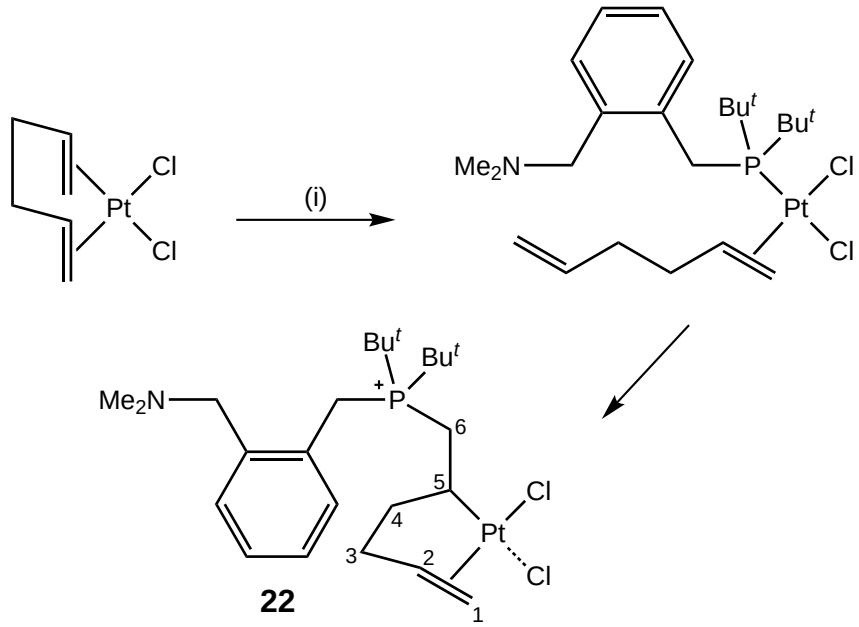

Scheme 3.2 Synthesis of proposed phosphonium complex **22**. *Reagents and conditions:* (i) 1 eq. ligand **18a**, acetone-d_6, 24 h.

Within five minutes, this complex started converting to a different material, with a characteristic sharp peak in the ^{31}P NMR spectrum at 40.4 ppm and a significantly lower platinum coupling constant of 355 Hz. The appearance of a number of new proton peaks in the ^{1}H NMR spectrum suggested the 1,5-hexadiene formed part of this complex, but in a different arrangement. Analysis of the ^{13}C NMR spectrum showed six distinct peaks for the formerly 1,5-hexadiene, and the high-field shifts of four out of six implied the loss of one of the double bonds. Carbon 5 (shown in Scheme 3.2) in particular shows a very high platinum coupling constant of 738 Hz, which would be consistent with this carbon having a σ-bond to platinum. The associated 2D NMR data show correlations between C6 of the former diene and

the CH_2P and PBu^t groups of **18a**, indicating the coupling of these two ligands to form a phosphonium ion adduct. Conversion to this species was complete within 24 hours.

This type of reactivity has been seen previously between platinum complexes of 1,5-hexadiene and secondary amines,[114–116] forming σ:η^2-bound ammonium ions; and between platinum complexes of 1,5-cyclooctadiene and tertiary phosphines,[117–120] forming σ:η^2-bound phosphonium ions. Unfortunately, the NMR data given for these complexes is sparse; however, when $^3J_{\mathrm{PtP}}$ coupling was reported it is in the range 156–223 Hz, similar to the 355 Hz coupling for complex **22**. There are two reports of $^1J_{\mathrm{PtC}}$ coupling constants for the σ-bonded carbon atom, 430[119] and 622 Hz,[117] both of which are *trans* to phosphorus donor atoms, and so expected to be lower than the 738 Hz coupling in complex **22**.

Unfortunately, complex **22** degraded over a number of days into an insoluble oily white solid, so all attempts to grow crystals were unsuccessful and the connectivity of the chlorides was not unequivocally established. It seems likely that one of the chlorides is a non-coordinating counterion. The high resolution mass spectrum of complex **22** displays two peaks, corresponding to $[M-Cl]^+$ and $[M-Cl-HCl]^+$. The absence of a peak corresponding to intact complex **22** suggests one of the chlorides is weakly coordinating or non-coordinating. This would be consistent with the high *trans* influence of the σ-bound alkyl ligand (C5). If one of the chloride ions were non-coordinating, there would be the potential for the nitrogen atom to coordinate; however, there is little evidence for this. The ^{1}H and ^{13}C NMR peaks associated with the CH_2N and NMe groups, although broadened, are very similar in shift to the free ligand and do not display any platinum coupling. It is also unknown whether complex **22** exists in monomeric or dimeric form. Precedent suggests that complex **22** may be a chloride-bridged dimer, as similar organometallic platinum complexes bearing chloride and σ:η^2-bound ligands (formed by reaction of the corresponding $[PtCl_2(\mathrm{diene})]$ species with an alcohol and a weak base) adopt this form.[121,122]

The same reactivity pattern was seen in the reaction of phosphine-sulfoxide ligand **16** with $[PtCl_2(1,5\text{-hexadiene})]$. Initially, a broad ^{31}P NMR peak at 29.3 ppm with platinum coupling of 3100 Hz formed, which was slowly replaced by two peaks at 39.8 and 41.2 ppm, with platinum couplings of 363 and 358 Hz respectively. As the platinum centre in complex **22** is in the +2 oxidation state, the alkene ligand sits perpendicular to the plane of the complex, leading to planar chirality (rendering the PBu^t groups NMR inequivalent in both cases). For this reason, *rac*-**16** produced diastereomers, as indicated by the two separate ^{31}P NMR shifts.

Also, the phosphine-thioether analogue of complex **22** was sometimes observed as a minor product in the synthesis of **21** (at 39.9 ppm, $^3J_{\mathrm{PtP}} = 360$ Hz).

It seems that the nature of the non-phosphorus donor atom in the ligand is fundamental in determining the product of these reactions. It is generally accepted that the bonding ability of sulfur and nitrogen atoms in chelating phosphine-sulfur and phosphine-nitrogen ligands is similar (and slightly higher than alkenes),[50] although exceptions occur when ligand steric considerations or metallacycle strain are involved. Other studies suggest that the *trans* influence of sulfoxide ligands is comparable to primary amines, and slightly less than ethene.[123] There is conflicting evidence regarding the relative bond strengths of sulfoxide and thioether ligands, as $^3J_{\mathrm{PtH}}$ NMR coupling constants tend to be larger for platinum complexes of thioethers (suggesting higher bond strength), but crystallographic data indicate shorter M−S bond lengths in sulfoxide complexes.[123] As ligands **14a**, **18a** and **16** all contain different degrees of steric bulk and, as evidenced by the buckling of the *P,S* ligand backbone in complex **21**, there is significant strain associated with the metallacycle, it is difficult to ascribe the difference in reactivity to any one factor. Suffice it to say that in this specific example, *P,E* chelation rather than phosphonium ion adduct formation is only favourable in the case of thioether ligand **14a**.

In a similar fashion to the reaction with [$PtCl_2$(1,5-hexadiene)], when *P,N* ligand **18a** and *cis*-[$PtCl_2(NCBu^t)_2$] were combined in acetone-d_6, a complex with a broad ^{31}P NMR signal at 21.0 ppm and platinum coupling of 3385 Hz formed immediately. The appearance of a peak corresponding to one equivalent of free Bu^tCN in the ^{1}H NMR spectrum suggested that this material was [$PtCl_2(NCBu^t)(\kappa^1 P$-**18a**)], wherein the phosphorus donor atom of ligand **18a** had displaced one Bu^tCN ligand, but chelation had not occurred (Scheme 3.3).

The solution was then heated to 40 °C for 24 hours and this complex converted to a new species, with a sharp peak in the ^{31}P NMR spectrum at 17.2 ppm and platinum coupling of 3967 Hz. The identity of this species was determined by NMR spectroscopy and high resolution mass spectrometry to be the desired [$PtCl_2$(*P,N*)] complex **23** (Scheme 3.3). The room temperature ^{1}H NMR spectrum of the reaction mixture (shown in Figure 3.7) displays the expected broad signals associated with inversion of the *P,N* ligand backbone. Upon cooling to −20 °C, the signals are much sharper. Clearly visible in this spectrum are signals associated with two inequivalent PBu^t groups (at 1.54 and 1.64 ppm), two NMe groups at 3.14 and 3.35 ppm with platinum coupling constants of 27.0 and 26.3 Hz respectively (confirming the presence of a Pt−N bond), and AB systems corresponding to the CH_2P (3.59 and 3.83 ppm) and CH_2N (3.85 and 4.48 ppm) methylene protons.

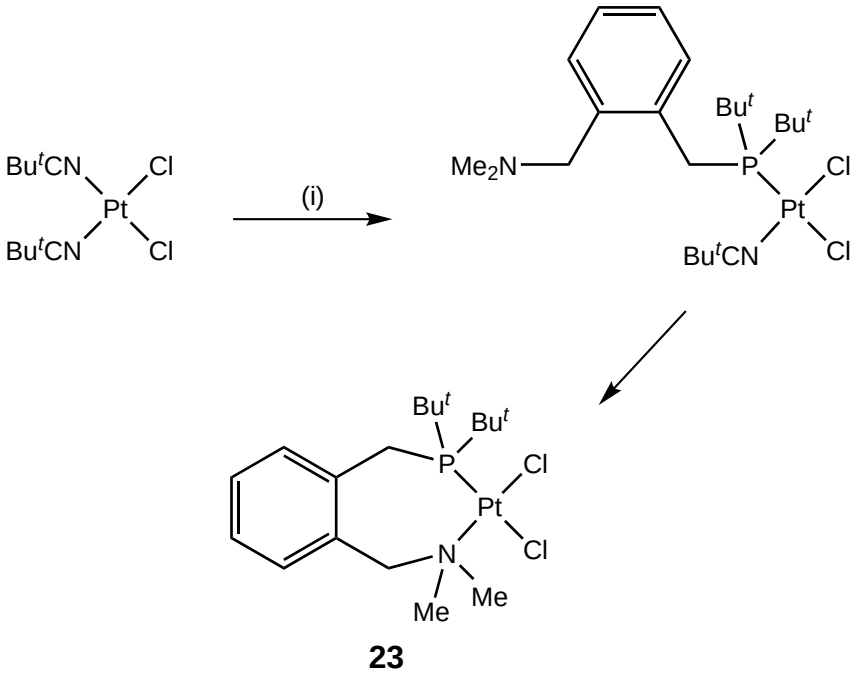

Scheme 3.3 Synthesis of [$PtCl_2(P,N)$] complex **23**. *Reagents and conditions:* (i) 1 eq. ligand **18a**, acetone-d_6, 40 °C, 24 h, >95% conversion.

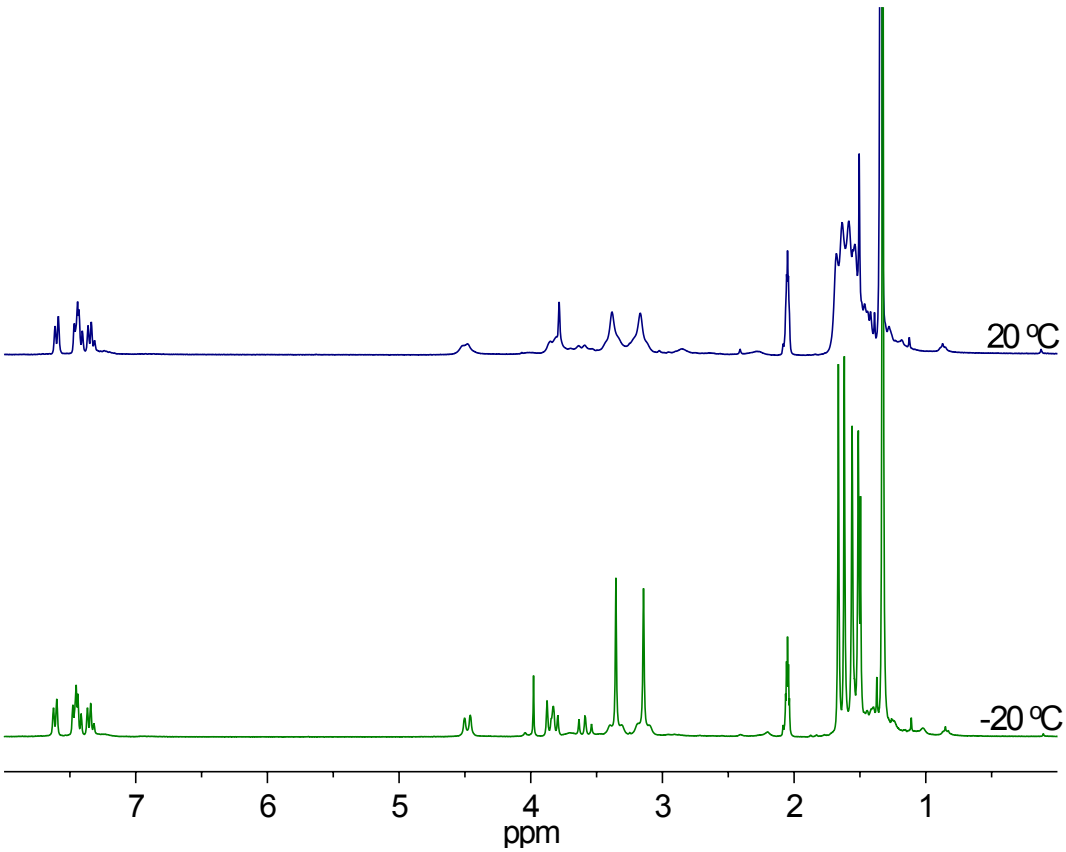

Figure 3.7 ^{1}H NMR spectra of [$PtCl_2(P,N)$] complex **23** collected at 20 and −20 °C in acetone-d_6.

The same synthetic methodology as shown in Scheme 3.3 was used in an attempt to form a chelated $[PtCl_2(P,S{=}O)]$ complex. Phosphine-sulfoxide ligand **16** was combined with *cis*-$[PtCl_2(NCBu^t)_2]$ in acetone-d_6 and the reaction followed by ^{1}H and ^{31}P NMR methods. Again, a complex with a broad ^{31}P NMR signal at 22.1 ppm and platinum coupling of 3395 Hz formed immediately, and was tentatively assigned as $[PtCl_2(NCBu^t)(\kappa^1 P\text{-}\mathbf{16})]$. However, in this case heating the solution to 40 °C for 24 hours produced no change to the complex. As the binding ability of sulfoxide ligands in platinum(II) complexes is considered to be similar to that of thioethers and amines, it is likely that steric considerations play a large part in the failure of phosphine-sulfoxide ligand **16** to form a chelated platinum(II) dichloride species.

3.2 $[PtHL(P,S)_2]$ Complexes

There was no reaction when complex **21** was combined with a second equivalent of ligand **14a**. This is perhaps unsurprising as neither the *cis* nor *trans* isomers of $[PtCl_2(PBu^t{}_3)_2]$[124] or $[PtCl_2(PBnBu^t{}_2)_2]$ are known in the literature, both of which would contain phosphine ligands with a steric bulk comparable to **14a**. However, if one equivalent of a hydride source, such as diethylamine–borane, was included in the reaction, monohydride complex **24** was formed (Scheme 3.4).

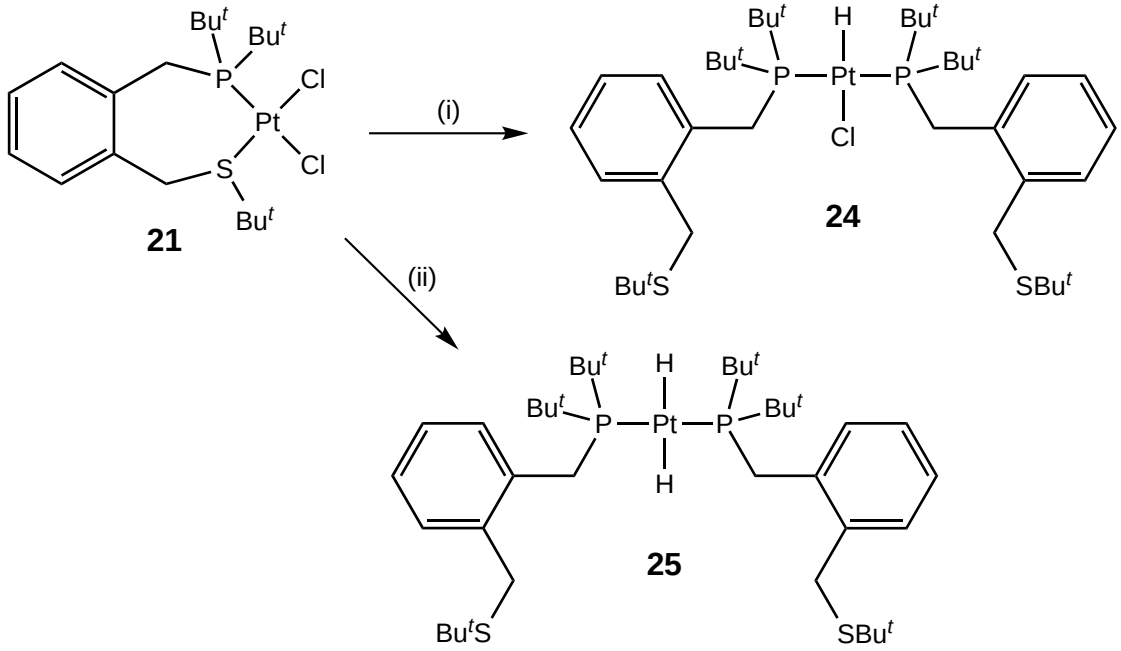

Scheme 3.4 Synthesis of hydride complexes **24** and **25**. *Reagents and conditions:* (i) 1 eq. ligand **14a**, 1 eq. $Et_2NH(BH_3)$, acetone-d_6, overnight, 87% conversion; (ii) 1 eq. ligand **14a**, 10 eq. $NaBH_4$, ethanol, 24 h, 33% yield.

The structure of complex **24** was determined by analysis of the associated NMR data. The ^{1}H NMR spectrum contains a diagnostic hydride peak at −17.38 ppm; the large upfield shift and platinum coupling of this peak ($^1J_{\mathrm{PtH}} = 1248$ Hz) indicating that this hydride lies *trans* to a ligand with a low *trans* influence (chloride in this case).[125] This peak is a triplet with a small coupling constant ($^2J_{\mathrm{PH}} = 12.2$ Hz), confirming the presence of two equivalent phosphorus atoms in mutually *trans* positions. The ^{1}H NMR peaks corresponding to the CH_2P and PBu^t groups of ligand **14a** display virtual triplet coupling, indicative of a second-order $X_nAA'X_n'$ system,[126] in this case $^2J_{\mathrm{PH}} + {}^4J_{\mathrm{PH}}$ and $^3J_{\mathrm{PH}} + {}^5J_{\mathrm{PH}}$ couplings respectively. This is consistent with two mutually *trans* ligand **14a** molecules bound to the platinum through phosphorus only. A number of the ^{13}C NMR peaks for this complex also display this second-order phosphorus coupling. The shifts corresponding to the CH_2S and SBu^t groups of ligand **14a** in both the ^{1}H and ^{13}C NMR spectra are very close to those of the free ligand, consistent with the thioether moiety being removed from the metal centre.

If a large excess of sodium borohydride was added to the reaction mixture, the product formed over 24 hours was dihydride complex **25** (Scheme 3.4). This reactivity type has been reported previously, exclusively with sterically bulky tertiary phosphine ligands, including $PBnBu^t{}_2$.[127] Decomposition was observed with smaller phosphine ligands such as PPh_3 and PMe_2Ph. The ^{1}H NMR spectrum of complex **25** displays a significantly different hydride peak to the precursor. While still a triplet, the peak has shifted downfield from that of complex **24** to −2.83 ppm, and the platinum coupling constant has reduced to 799 Hz, both consistent with the hydride now being located *trans* to a ligand with a much larger *trans* influence (*i.e.* a second hydride).[125] The ^{1}H and ^{13}C NMR spectra of dihydride complex **25** show the same pattern of virtual triplet peaks as complex **24**, indicating no other changes to the molecule.

Recrystallisation from ethanol/toluene yielded crystals of complex **25** suitable for X-ray diffraction. The structure is shown in Figure 3.8, displaying the expected *trans* arrangements of the phosphine ligands and hydride ligands. Crystallographic data are given in Table 3.3 and Table 3.4. The observed cone angle[128] has been calculated for ligand **14a** in this complex, using the angles ascribed by P1, Pt1 and hydrogen atoms H4, H11a and H16b respectively. The extension of these angles to take into account the van der Waals radii of the hydrogen atoms (1.0 Å for H4, 1.2 Å for H11a and H16b[129]) gave the substituent half angles $\theta_i/2$. Application of the equation $\theta_{\mathrm{O}} = 2/3 \sum \theta_i/2$ gave the observed cone angle for **14a**, $\theta_{\mathrm{O}} = 180°$. The observed cone angle differs from the Tolman cone angle (θ_{T}) in that the actual Pt−P bond length is used, rather than an arbitrary M−P bond length of 2.28 Å. However, as the Pt1−P1 bond in this case is less than 0.01 Å shorter than 2.28 Å, θ_{O} should

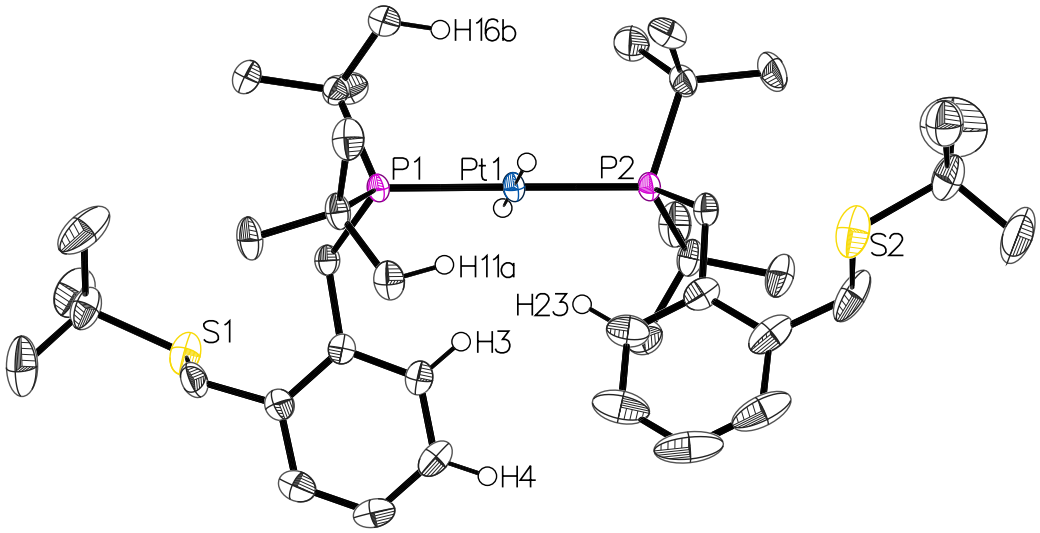

Figure 3.8 ORTEP diagram of $[PtH_2(P,S)_2]$ complex **25** (50% probability thermal ellipsoids). Selected hydrogen atoms omitted for clarity.

be roughly equal to θ_T. By this reckoning, the Tolman cone angle of ligand **14a**, when bound through the phosphorus only, resembles that of $PBu^t{}_3$ and PCy_3.[130] The P−Pt−P bond of complex **25** is not quite linear, at 178.58(1)°, which is likely to be a result of the constraints imposed by the sterically bulky phosphine ligands. The complex exists in an eclipsed conformation, with torsion angles of 0.34(12)° and 1.51(11)° between each xylene group and the proximate Bu^t group (Figure 3.9). The torsion angle between the remaining two Bu^t groups is larger, at 14.06(12)°.

A feature of note in the ^{1}H NMR spectrum of complex **25** is the downfield shift of the peak corresponding to one of the aryl backbone protons. Through analysis of the 2D NMR data, this peak was determined to be associated with the aryl proton *ortho* to the phosphorus arm of ligand **14a**, shifted 1.35 ppm downfield upon complexation. The close proximity of ligand protons to the metal in transition metal complexes has long been known to cause downfield ^{1}H NMR peak shifts,[131–133] and in this case the proposal is supported by the X-ray crystal structure. Protons H3 and H23 (shown in Figure 3.8) are located only 2.771(1) and 2.847(1) Å from the platinum centre respectively, and as evidenced by the ^{1}H NMR spectrum, it is likely that in solution the ligands adopt a similar conformation. This feature is also seen in a number of other complexes of **14a**, in instances where the ligand is bound to the metal through the phosphorus donor atom in a monodentate fashion.

There are two existing publications concerning the protonation of $[PtH_2(PR_3)_2]$-type complexes. In 1994, Gusev and co-workers reported the reaction of *trans*-$[PtH_2(PBu^t{}_3)_2]$ with CF_3SO_3D at −80 °C,[134] and four years later the protonation of *trans*-$[PtH_2(PCy_3)_2]$ by $HBAr^F{}_4$ at −95 °C was reported by Stahl *et al.*[135]

Table 3.3 Crystallographic data of $[PtH_2(P,S)_2]$ complex **25**.

Empirical formula	$\mathbf{C_{40}H_{72}P_2PtS_2}$
Formula weight	874.13
Crystal system	Monoclinic
Space group	$P2_1/c$
a/Å	18.5216(5)
b/Å	21.6736(6)
c/Å	11.1174(3)
$\alpha/^\circ$	90.00
$\beta/^\circ$	100.628(2)
$\gamma/^\circ$	90.00
V/Å^3	4386.3(2)
Z	4
Cell determination reflections	9784
Cell determination range, $\theta_{min} \longrightarrow \theta_{max}/^\circ$	$2.2 \longrightarrow 28.7$
Temperature/K	113
Radiation type	Mo Kα
Radiation (λ)/Å	0.71073
Crystal size/ mm	$0.60 \times 0.45 \times 0.38$
D_{calc}/g m^{-3}	1.324
F(000)	1808
μ/mm^{-1}	3.39
Experimental absorption correction type	Multi-scan (SADABS)
T_{max}, T_{min}	0.746, 0.584
Reflections collected	101973, $R_{equiv} = 0.041$
Index range h	$-25 \longrightarrow 25$
Index range k	$-29 \longrightarrow 29$
Index range l	$-15 \longrightarrow 15$
θ range/$^\circ$	$2.2 \longrightarrow 28.8$
Independent reflections	11344
Reflections [$I > 2\sigma(I)$]	9849
Restraints/parameters	0/432
GOF	1.14
R_1 [$I > 2\sigma(I)$]	0.0224
wR_2 [$I > 2\sigma(I)$]	0.0419
R_1 [all data]	0.0319
wR_2 [all data]	0.0452
Residual density/e Å^{-3}	$-0.59<0.64$

Table 3.4 Selected bond distances and angles of $[PtH_2(P,S)_2]$ complex **25**.

Bond distances (Å)		**Bond angles (°)**	
Pt1−P1	2.2719(5)	P1−Pt1−P2	178.584(19)
Pt1−P2	2.2746(5)	P1−Pt1 · · · H4	84.694(14)
Pt1 · · · H3	2.77091(8)	P1−Pt1 · · · H11a	63.370(13)
Pt1 · · · H23	2.84763(7)	P1−Pt1 · · · H16b	65.481(14)
Pt1 · · · H4	4.86224(13)	C9−P1 · · · P2−C21	0.34(12)
Pt1 · · · H11a	3.01575(13)	C1−P1 · · · P2−C33	1.51(11)
Pt1 · · · H16b	2.90354(6)	C13−P1 · · · P2−C29	14.06(12)

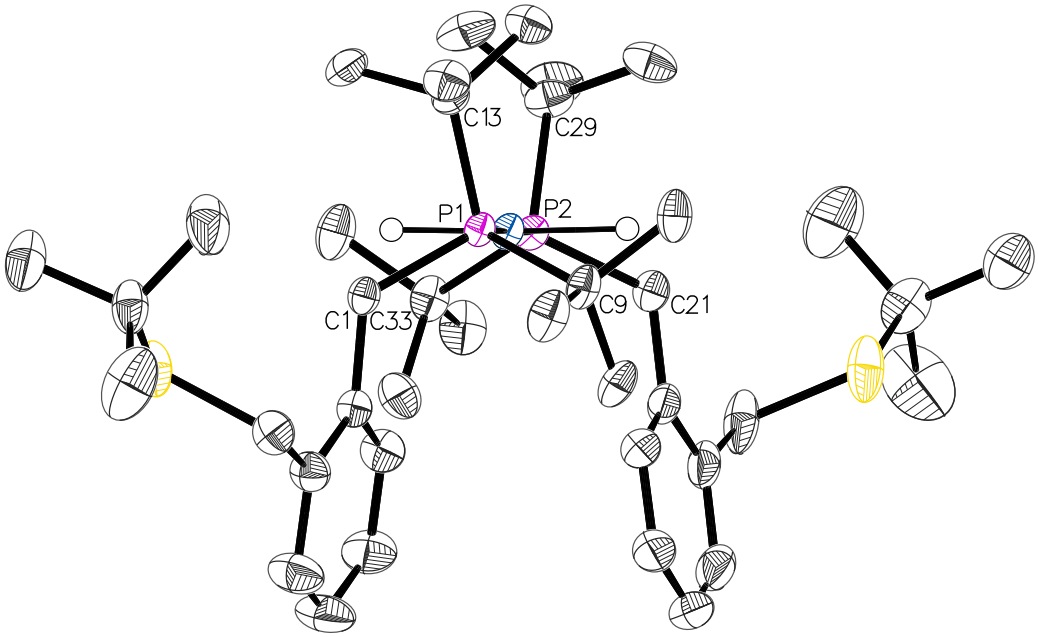

Figure 3.9 ORTEP diagram of $[PtH_2(P,S)_2]$ complex **25** showing the eclipsed conformation (50% probability thermal ellipsoids). Selected hydrogen atoms omitted for clarity.

Both procedures generated the dihydrogen adducts, *trans*-$[PtH(H_2)(PR_3)_2]^+$ (or deuterated analogues), existing in equilibrium with the solvento species, *trans*-$[PtH(solv)(PR_3)_2]^+$. These solvento species have also been synthesised by other methods,[136,137] and react readily to form haloarene, aquo, ammonia, nitrile and carbon monoxide complexes upon treatment with the appropriate ligand. Although it has been noted that treatment of $[PtH(PBu^t{}_3)_2]ClO_4$ with excess dimethylsulfide in acetone led to deprotonation of the complex to form $[Pt(PBu^t{}_3)_2]$,[136] it was anticipated that protonation of dihydride complex **25** would result in chelation of one of the *P,S* ligands.

The addition of one equivalent of the strong fluorocarbon acid, $CH_2(SO_2CF_3)_2$ ($pK_a = 2.4$ in DMSO,[138] and estimated to be -1 in water[139]), to a solution of dihydride complex **25** in acetone-d_6 resulted in the immediate evolution of hydrogen gas (Scheme 3.5). Analysis of the NMR data showed one product had formed, with lower symmetry than complex **25**. For example, the ^{31}P NMR spectrum displays two doublets centred at 44.4 and 54.5 ppm, with $^2J_{PP}$ coupling of 324 Hz, and $^1J_{PtP}$ couplings of 2740 and 2770 Hz respectively. All virtual triplet peaks seen in the starting material have been replaced by two sets of similar peaks with doublet couplings, confirming the differentiation of the two ligand **14a** molecules. A ^1H NMR peak at 3.75 ppm and ^{19}F NMR peak at -81.9 ppm confirmed the presence of the non-coordinating counterion, $^-CH(SO_2CF_3)_2$.[140] Coordination of the sulfur donor atom of one of the *P,S* ligands was verified by the appearance in the ^1H

NMR spectrum of a peak at 4.82 ppm with platinum satellites ($^3J_{\mathrm{PtH}}$ = 27.6 Hz), corresponding to one CH_2S group. This peak resembles the ^{1}H NMR peak of the CH_2S moiety in chelated [$PtCl_2$(*P,S*)] complex **21**, although the platinum coupling constant is lower due to the larger *trans* influence of the ligand located *trans* to the sulfur in complex **26** (*i.e.* H^- rather than Cl^-). The hydride NMR peak in this complex has returned to higher field (−14.88 ppm) and the platinum coupling constant increased ($^1J_{\mathrm{PtH}}$ = 1050 Hz), both similar to hydride-chloride complex **24**, and reflecting the smaller *trans* influence of sulfur as compared to the hydride ligand in complex **25**.

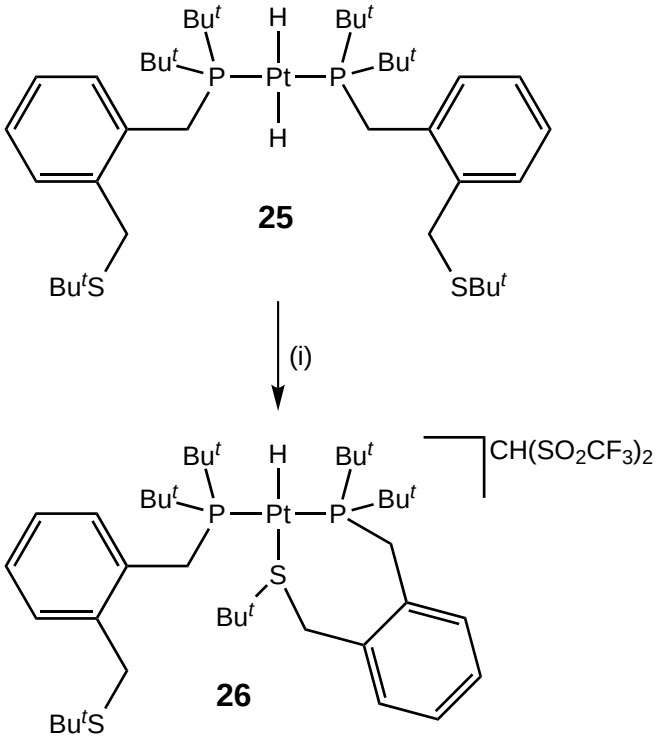

Scheme 3.5 Synthesis of hydride complex **26**. *Reagents and conditions:* (i) $CH_2(SO_2CF_3)_2$, acetone-d_6, 10 min, quantitative conversion.

Interestingly, the two *P,S* ligands are quite distinct in the NMR spectra, indicating no displacement of one sulfur atom from the platinum centre by the other on the NMR timescale at ambient temperature. The fact that the ^{1}H NMR peak of the coordinated CH_2S moiety is a singlet confirms that the inversion process at sulfur is rapid, as were the sulfur atom static, the methylene protons would be rendered diastereotopic and inequivalent in the ^{1}H NMR spectrum. Variable temperature NMR studies confirmed the coalescence temperature for this process is between −20 and −40 °C, and below this temperature the methylene protons appear as an AB system ($^2J_{\mathrm{HH}}$ = 10.9 Hz) at 4.44 and 4.59 ppm. Thus, the lack of interconversion supports the proposal that inversion at sulfur is an associative, rather than dissociative, process.

Complex **26** presented an excellent opportunity to investigate the potential for displacement of the coordinated sulfur atom by other ligands. Initially, carbon monoxide was bubbled through an acetone-d_6 solution of complex **26**. The resulting NMR data closely resemble that of the known carbon monoxide complexes, $[PtH(CO)(PBu^t{}_3)_2]X$[136] and $[PtH(CO)(PBn_3)_2]BPh_4$.[141] The ^{31}P NMR spectrum of complex **27** displays a singlet peak at 68.4 ppm, with a platinum coupling constant of 2415 Hz. This, and the return of virtual triplet couplings in the ^1H NMR spectrum, confirmed the displacement of the sulfur atom from the metal centre (Scheme 3.6). The reaction was repeated with ^{13}C-labelled carbon monoxide, giving a ^{13}C NMR shift corresponding to coordinated carbon monoxide at 184.5 ppm. This peak couples to two identical phosphines ($^2J_{PC} = 7.0$ Hz) and to platinum ($^1J_{PtC} = 1015$ Hz), consistent with the proposed structure. An infrared spectrum of complex **27** was also collected, displaying a CO stretching frequency of 2070 cm^{-1}. Unfortunately, little information regarding the electronic character of the metal centre can be drawn from this frequency, due to the potential for coupling with the PtH stretching frequency.[142,143] Isotopic studies of the related complex, $[PtH(CO)(PBu^t{}_3)_2]PF_6$, indicate that the perturbation of ν(CO) by ν(PtH) is *ca.* 20 cm^{-1}.[125]

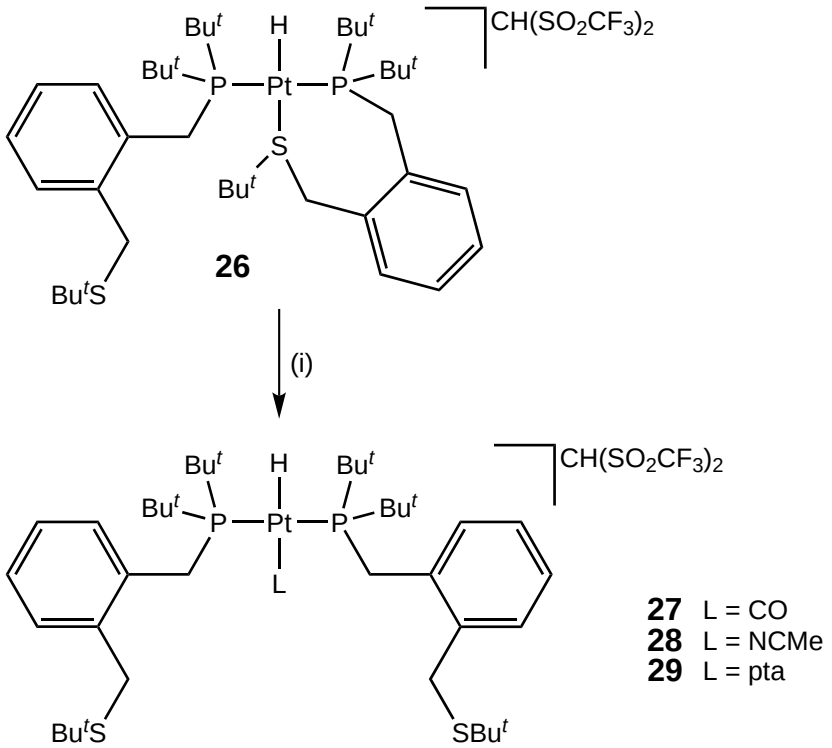

Scheme 3.6 Synthesis of $[PtHL(P,S)_2]CH(SO_2CF_3)_2$ complexes **27**, **28** and **29**. *Reagents and conditions:* (i) CO, NCMe or 1 eq. pta; acetone-d_6, 10 min, quantitative conversion.

Addition of excess acetonitrile to complex **26** in acetone-d_6 produced the very similar complex **28** (Scheme 3.6). Again, $PBu^t{}_3$[136] and PBn_3[141] analogues of this species

have previously been reported, and the NMR data of complex **28** are in good agreement with these. Peaks corresponding to the carbon atom and protons of the methyl group in the coordinated acetonitrile are visible in the NMR spectra at 3.2 ppm and 1.90 ppm ($^4J_{\mathrm{PtH}} = 4.9$ Hz) respectively; however, the ^{13}C NMR peak for the acetonitrile quaternary carbon has not been located. As noted previously with the carbon monoxide ligand of **27**, this carbon would be expected to couple to platinum and two identical phosphorus atoms, and due to the reduced peak height may not be discernible from the noise of the spectrum.

As demonstrating hemilability of the novel *P,E* ligands in metal complexes was one of the goals of this work, complexes **27** and **28** were subjected to high vacuum to investigate the reversibility of the addition reactions that formed them. No change was observed in carbon monoxide complex **27**; however, when acetonitrile complex **28** was left under reduced pressure overnight, approximately 50% of the material reverted to chelated complex **26**. Heating to 40 °C under vacuum overnight resulted in 90% conversion of complex **28** to complex **26**, and addition of acetonitrile reconverted the sample to complex **28** (Figure 3.10).

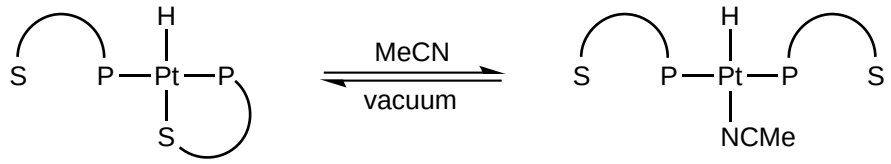

Figure 3.10 Schematic of the hemilabile behaviour of *P,S* ligand **14a** with MeCN.

A comparison of the Pt−H coupling constants for the hydride ligands in these two complexes showed that in chelated complex **26** $^1J_{\mathrm{PtH}} = 1050$ Hz, whereas in the acetonitrile complex **28** it is 120 Hz higher. This indicates the sulfur donor atom has a somewhat larger *trans* influence than the nitrogen in acetonitrile (similar results have been obtained with nitrile and thioether hydride complexes of PBn_3[141]). In light of this result, and when the advantage of the chelate effect is considered, it may be a little counterintuitive that acetonitrile can displace the sulfur ligand in this system. However, in a similar fashion to [$PtCl_2$(*P,S*)] complex **21** discussed previously, there must be considerable strain associated with the 7-membered ring in such a sterically demanding environment, and it is likely that the energy of the system is reduced with the dissociation of the sulfur atom.

The displacement of the sulfur donor atom in complex **26** was also attempted with ethene and ethyne; however, no reaction was observed upon introduction of either gas to acetone-d_6 solutions of the complex. This is unsurprising, as it has been shown previously that ethene does not react with the solvento complexes

$[PtH\{(CD_3)_2CO\}(PBu^t{}_3)_2]X$ and $[PtH(CD_2Cl_2)(PBu^t{}_3)_2]X$.[136] Ethyne does react with $[PtH(CD_2Cl_2)(PBu^t{}_3)_2]ClO_4$, forming what was proposed, using infrared spectral data and changes to the hydride NMR peak, to be $[PtH(HC{\equiv}CH)(PBu^t{}_3)_2]ClO_4$ in solution.[136] However, no ^{1}H NMR shifts for coordinated ethyne were reported, and removal of volatiles under reduced pressure recovered starting material only.

Finally, the reaction of complex **26** with phosphines was tested. No reaction was observed upon addition of one equivalent of triphenylphosphine to an acetone-d_6 solution of the complex, even at elevated temperature. This is most likely a steric effect as, for example, the reaction of $[PtHCl(PBn_3)_2]$ with PPh_3 and $NaBPh_4$ produced the trisphosphine complex $[PtH(PPh_3)(PBn_3)_2]BPh_4$.[141] With this in mind, the reaction with 1,3,5-triaza-7-phosphaadamantane (pta) was investigated. The pta ligand is a sterically unencumbered phosphine, with crystallographically determined cone angles of 102° and 114–117°, in molybdenum carbonyl[144] and palladium iodide[145] complexes respectively (the Tolman cone angle of triphenylphosphine was calculated to be 145°[130]).

Complex **26** and one equivalent of pta were combined in acetone-d_6 and the solution sonicated until all crystals had dissolved (Scheme 3.6). The subsequent NMR data show complete absence of starting material, and the presence of one new complex with two peaks in the ^{31}P NMR spectrum, centred at 47.3 and −89.8 ppm. The peak at 47.3 ppm presents as a doublet with 18 Hz coupling, and platinum satellites with 2553 Hz coupling. The peak at −89.8 ppm presents as a triplet, also with coupling of 18 Hz, and platinum satellites with 1942 Hz coupling. These correspond to two molecules of ligand **14a** in identical environments and one pta ligand respectively, confirming the *trans* arrangement of **29**. The hydride peak in the ^{1}H NMR spectrum, a large doublet ($^2J_{PH}$ = 153.6 Hz) of triplets ($^2J_{PH}$ = 15.0 Hz) with $^1J_{PtH}$ coupling of 728 Hz, supports this assignment. This is the first example of a Group 10 metal complex containing both a pta and hydride ligand.

The hydride NMR shifts and $^1J_{PtH}$ coupling constants of complexes **24**–**29** are shown in Table 3.5. As the $^1J_{PtH}$ values for the hydrides are inversely proportional to the *trans* influence of ligand L in each complex, these values give the *trans* influence series $Cl^- <$ NCMe $< -CH_2SBu^t <$ CO $< H^- <$ pta. This series is in agreement with that deduced from a large number of platinum hydride complexes of PBn_3.[141] The NMR chemical shift of the hydride ligands generally follows the same trend, although pta complex **29** is an outlier. It has been noted previously that hydride NMR shift does not really indicate variations in the Pt−H bond itself but rather variations at the platinum atom, and that anisotropic effects from aromatic rings of

other ligands may also influence the shift,[45] and as such, it cannot be taken as an indicator of *trans* influence.

Table 3.5 ^{1}H NMR data of [PtHL(*P,S*)$_2$] and [PtHL(*P,S*)$_2$]CH(SO$_2$CF$_3$)$_2$ hydride ligands in acetone-d_6.

Complex	Identity of L	Hydride NMR shift (ppm)	$^{1}J_{\mathrm{PtH}}$ coupling (Hz)
24	Cl^-	−17.43	1247.7
28	NCMe	−17.94	1169.5
26	$-CH_2SBu^t$	−14.88	1049.6
27	CO	−5.36	843.3
25	H^-	−3.29	801.0
29	pta	−7.97	728.0

The successful sulfur displacement reactions were repeated with [PtCl$_2$(*P,S*)] complex **21**. As the Pt−S bond in this complex was considered to be stronger than that of hydride complex **26** (as evidenced by the difference in magnitude of the $^{3}J_{\mathrm{PtH}}$ coupling constants of the protons in the CH$_2$S moieties), it was envisaged that the sulfur atom in complex **21** would be more difficult to displace. The addition of an excess of acetonitrile or carbon monoxide to an acetone-d_6 solution of complex **21** (identical conditions to those shown in Scheme 3.6) resulted in no change to the starting material; however, the addition of one equivalent of pta to a chloroform-d (or acetone-d_6) solution of complex **21** rapidly produced a reaction (Scheme 3.7).

The ^{1}H and ^{31}P NMR spectra associated with the reaction mixture after 10 minutes showed a mixture of products including four phosphorus-containing species. Three of these were identified as unreacted complex **21**, entirely displaced *P,S* ligand **14a**, and the known complex [PtCl$_2$(pta)$_2$].[146] The fourth complex (**30**) was identified by two large doublets with a ratio of 1:1 in the ^{31}P NMR spectrum, centred at −62.3 and 35.3 ppm. The chemical shifts of these doublets indicated that they were associated with a pta molecule and a PBu$^t{}_2$ moiety respectively, and the large $^{2}J_{\mathrm{PP}}$ coupling constant of 439 Hz established the mutually *trans* arrangement of these ligands. The $^{1}J_{\mathrm{PtP}}$ coupling constants of these signals, 2294 and 2578 Hz respectively, are consistent with phosphines in *trans* positions. This evidence, along with a low-field doublet centred at 8.37 ppm in the ^{1}H NMR spectrum, allowed the assignment of complex **30** as *trans*-[PtCl$_2$(κ^1*P*-**14a**)(pta)].

After 19 hours, white crystals had appeared in the reaction mixture, which were confirmed by ^{1}H and ^{31}P NMR data to be [PtCl$_2$(pta)$_2$]. The ^{1}H and ^{31}P NMR spectra associated with the reaction solution showed no remaining [PtCl$_2$(pta)$_2$]; however, along with the expected species complex **21**, ligand **14a** and complex **30**, a new phosphorus-containing species (**31**) was identified, at around one quarter of the abundance of complex **30**. The new complex also displays two doublets with a

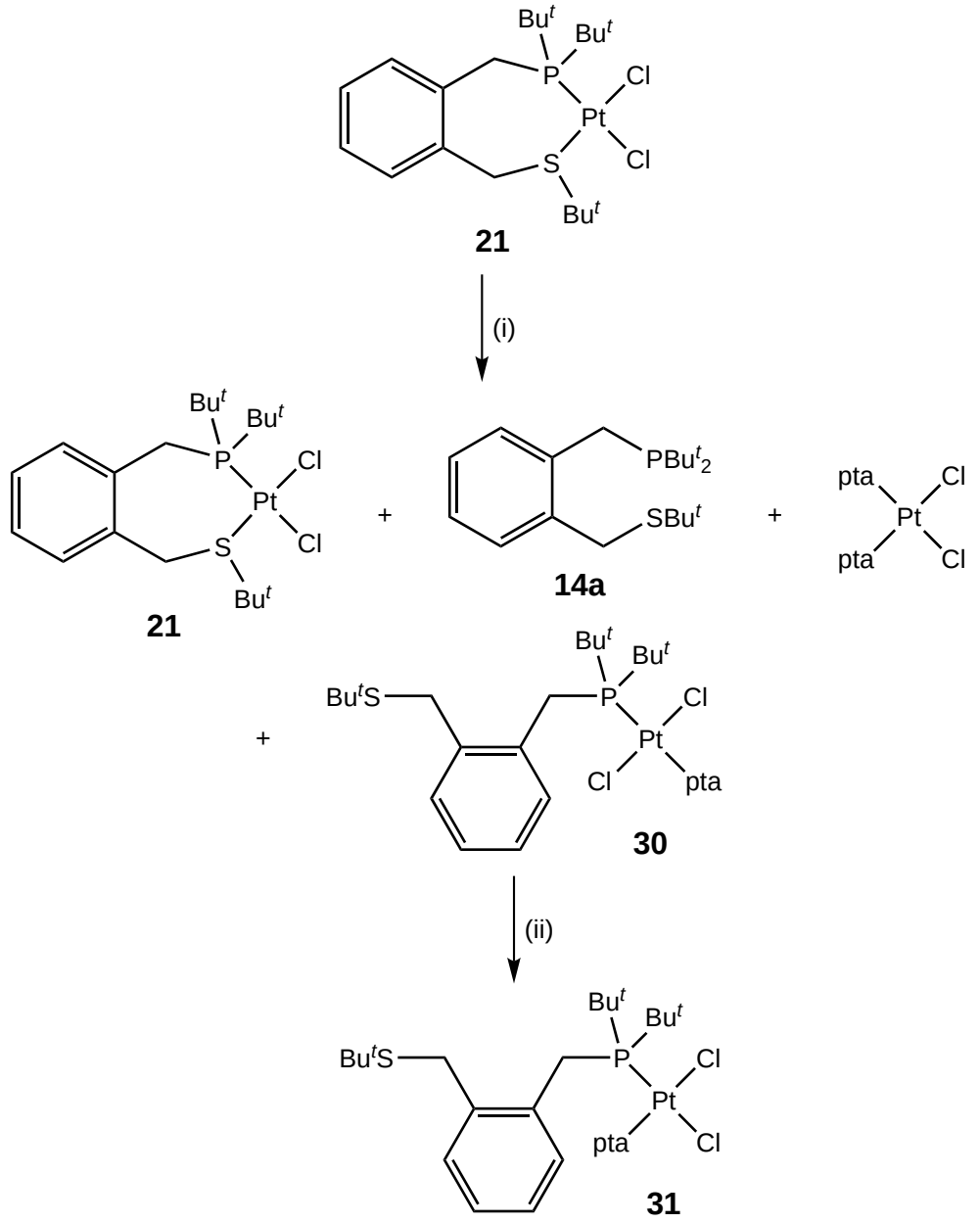

Scheme 3.7 Reaction of $[PtCl_2(P,S)]$ complex **21** with pta. *Reagents and conditions:* (i) 1 eq. pta, chloroform-*d*, 10 min; (ii) Overnight.

ratio of 1:1 in the ^{31}P NMR spectrum, centred at −65.6 and 27.0 ppm, indicating a pta molecule and a PBu$^t_2$ moiety respectively. However, the $^2J_{PP}$ coupling constant of 12 Hz is much smaller than that of complex **30**, and the $^1J_{PtP}$ coupling constants larger at 3359 and 3578 Hz respectively. Again this evidence, along with a new low-field doublet in the ^{1}H NMR spectrum centred at 8.78 ppm, allowed the assignment of complex **31** as *cis*-$[PtCl_2(\kappa^1P$-**14a**$)$(pta)]. Further ^{1}H and ^{31}P NMR spectra collected showed no subsequent changes to the reaction mixture.

As would be expected, the sulfur atom in dichloride complex **21** required a stronger competing ligand to displace than that of hydride complex **26** (due to the larger *trans* effect of the hydride ligand when compared with the chloride ligand). However,

where the sulfur atom was displaced, a more complicated reaction was observed. A reasonable amount of phosphine-thioether ligand **14a** was completely displaced, forming the known complex $[PtCl_2(pta)_2]$, and where only the sulfur atom was displaced, a rearrangement occurred to form the *trans* mixed phosphine complex **30**. Only after 19 hours was the expected *cis* mixed phosphine product **31** observed, and even then only in a minor amount.

3.3 Reaction of *P,E* Ligands with $[Pt(alkene)_3]$

3.3.1 1:1 Complexes

The reaction of one equivalent of either phosphine-thioether ligand **14a** or phosphine-sulfoxide ligand **16** with $[Pt(ethene)_3]$ immediately resulted in the η^2-ethene complexes **32** (Scheme 3.8) and **33** (Scheme 3.9). These are two of the first examples of platinum(0) alkene complexes containing chelating phosphorus-sulfur ligands (η^2-bicyclopropylidene (bcp) and η^2-methylenecyclopropane (mcp) complexes of ligand **14a** have also been prepared recently[147]).

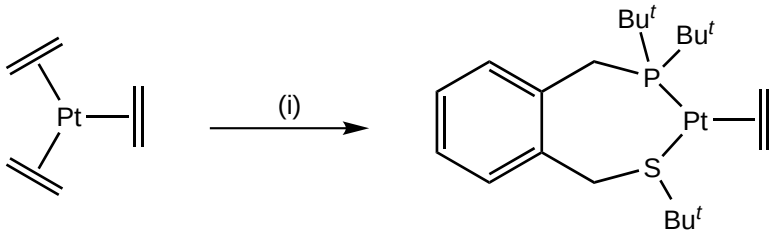

32

Scheme 3.8 Synthesis of [Pt(ethene)(*P,S*)] complex **32**. *Reagents and conditions:* (i) 1 eq. ligand **14a**, benzene-d_6, 10 min, >90% conversion.

The structures of complexes **32** and **33** were determined by analysis of the associated ^{1}H, ^{13}C and ^{31}P NMR data. Integration of the ^{1}H NMR spectra confirmed 1:1 ratios of ligand **14a** or **16** with ethene. Two peaks are observed for the ethene protons in the ^{1}H NMR spectrum of phosphine-thioether complex **32**, centred at 2.04 and 2.49 ppm. Both of these present as triplets of doublets with platinum satellites, indicating that the ethene ligand is static on the NMR timescale at room temperature. Chelation of ligand **14a** in complex **32** was determined by the presence of platinum satellites associated with the ^{31}P NMR signal ($^1J_{PtP}$ = 4067 Hz), and with most of the ^{1}H and ^{13}C NMR signals of both the $CH_2PBu^t{}_2$ and CH_2SBu^t moieties of the complex.

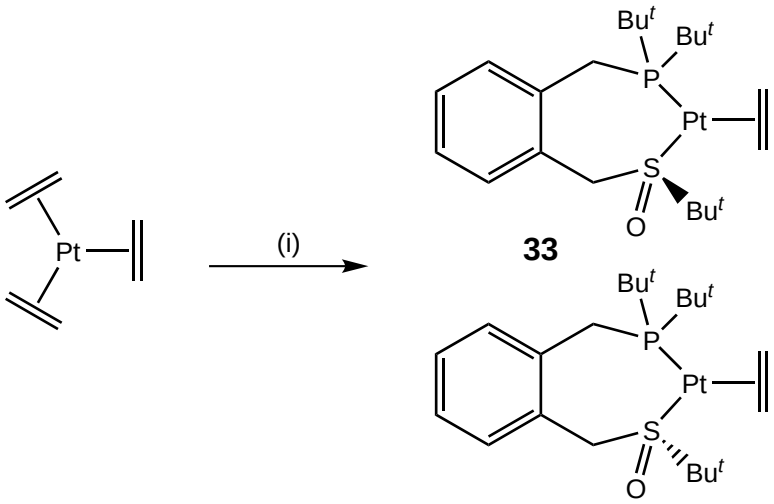

Scheme 3.9 Synthesis of [Pt(ethene)(*P,S=O*)] complex **33**. *Reagents and conditions:* (i) 1 eq. ligand **16**, benzene-d_6, 10 min, >95% conversion.

A feature of note in the ^{1}H NMR spectrum of complex **32** is the single signal associated with the CH_2S methylene protons at 4.29 ppm. As noted previously, when inversion at sulfur is rapid on the NMR timescale, one signal for both methylene protons is seen, and when the sulfur atom is static, an AB quartet results. In this case, the ^{1}H NMR data confirm inversion at the sulfur atom occurs rapidly at room temperature. There is very little published data to compare this result with, as a recent literature search revealed only a single report of a platinum(0) complex containing both a thioether and alkene ligand.[148] In this report, Canovese *et al.* presented a kinetic study of the mechanism of alkene exchange in platinum(0) complexes of pyridine-thioether ligands, as shown in Figure 3.11. They addressed the topic of sulfur inversion, noting that this was the only fluxional rearrangement behaviour seen in solutions of these complexes. For the complex [Pt(η^2-tetramethylethylenetetracarboxylate)(pyridine-*t*-butylthioether)] they reported an AB system in the ^{1}H NMR spectrum for the CH_2S protons at −60 °C, and a singlet for the same protons at 23 °C, indicating that coalescence is somewhere between these temperatures. They noted the same change in the ^{1}H NMR data for the complex [Pt(η^2-fumaronitrile)(pyridine-*t*-butylthioether)] between −50 and

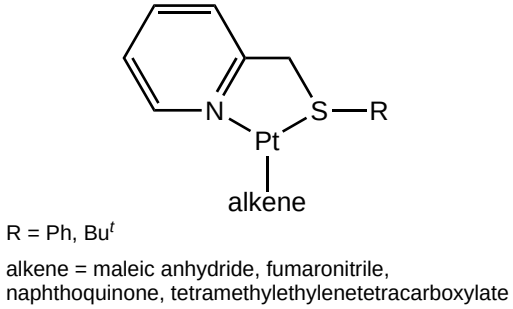

Figure 3.11 Platinum(0) alkene complexes of pyridine-thioether ligands.

23 °C. These data are in agreement with the results obtained for complex **32**, and the cyclopropyl-substituted alkene complexes [Pt(bcp)(κ^2*P,S*-**14a**)] and [Pt(mcp)(κ^2*P,S*-**14a**)],[147] and suggests that in general the coalescence temperature for sulfur inversion in platinum(0) alkene *t*-butylthioether complexes is below room temperature.

As a racemic mixture of phosphine-sulfoxide ligand **16** was used to synthesise complex **33**, this material exists as a pair of enantiomers (as shown in Scheme 3.9), and the presence of the chiral centre results in an asymmetry across the plane of the complex. Again, the ethene ligand is static on the NMR timescale at room temperature, evidenced by the presence of four multiplets in the ^{1}H NMR spectrum between 2.13 and 2.50 ppm associated with the four ethene protons. As in free ligand **16**, the phosphine *t*-butyl groups and methylene protons are diastereotopic, and therefore the ^{1}H and ^{13}C NMR signals corresponding to these atoms are distinct. The ^{1}H NMR spectrum of complex **33** displays the expected AB quartets associated with the protons of the CH_2P group (at 3.23 and 3.41 ppm, $^2J_{HH}$ = 14.0 Hz) and CH_2S group (at 4.20 and 4.39 ppm, $^2J_{HH}$ = 11.6 Hz). Interestingly, only one doublet of each of these AB systems displays platinum coupling. The CH_2P proton signal centred at 3.41 ppm has $^3J_{PtH}$ coupling of 48.0 Hz, and the CH_2S proton signal centred at 4.39 ppm has $^3J_{PtH}$ coupling of 22.0 Hz. This is due to the dihedral angle dependence of ^3J coupling constants. The conformation of chelated *P,S=O* ligand **16** in complex **33** must produce Pt−E−C−H (E = P or S) dihedral angles of close to 90° for one proton of each methylene group (associated with the ^{1}H NMR signals at 3.23 and 4.20 ppm displaying no platinum coupling), and Pt−E−C−H dihedral angles of closer to 0 or 180° for the two remaining methylene protons.[149]

The ^{31}P and η^2-ethene ligand ^{1}H and ^{13}C NMR data of complexes **32** and **33**, and the diphosphine analogue [Pt(ethene)(dbpx)],[16] are shown in Table 3.6. The phosphorus-platinum coupling constants of both hybrid ligands are significantly higher than the equivalent value for [Pt(ethene)(dbpx)] (by over 300 Hz), indicating a weaker Pt−P interaction in the diphosphine complex. This is most likely a combined result of the presence of a more weakly binding donor atom in ligands **14a** and **16**, as compared with the second phosphine in dbpx, and the larger steric bulk of dbpx. This trend is reflected in the $^2J_{PC}$ coupling constants associated with the carbon atoms located *trans* to the phosphorus donor atoms (36.5 and 32.1 Hz respectively for complexes **32** and **33**, as compared to 28 Hz for [Pt(ethene)(dbpx)]).

Of note in Table 3.6 is the difference in magnitude of the $^1J_{PtC}$ and $^2J_{PtH}$ coupling constants associated with the ethene carbon and hydrogen atoms located *trans* to the sulfur donor atoms in complexes **32** and **33** (331.1 and 81.6 Hz *vs.* 284.5 and

Table 3.6 ^{31}P and selected ^{1}H NMR shifts (in ppm) and coupling constants (in Hz) of [Pt(ethene)(*P,E*)] complexes in benzene-d_6.

		P		**H_2C=CH_2**				
Complex	**E**	δ_P	$^1J_{PtP}$	δ_H	$^2J_{PtH}$	δ_C	$^1J_{PtC}$	$^2J_{PC}$
32	SBu^t	59.4	4067	2.04	53.5	27.4	205.9	36.5[a]
				2.49	81.6	29.1	331.1	6.2[b]
33	$S(O)Bu^t$	54.8	3861	2.13	55.2	30.5	199.1	32.1[a]
				2.32	*c*			
				2.42	*c*	32.5	284.5	7.2[b]
				2.50	74.8			
[Pt(ethene)(dbpx)][d]	$PBu^t{}_2$	49.6	3551	2.18	57	27.2	217	28

[a]Located *trans* to the phosphorus donor atom.
[b]Located *cis* to the phosphorus donor atom.
[c]Unable to determine from spectra.
[d]Literature data,[16] spectra recorded in dichloromethane-d_2.

74.8 Hz respectively). In both cases, these values are lower in *P,S=O* complex **33**, suggesting that the Pt−C interaction *trans* to sulfur is weaker (and hence the Pt−S interaction is stronger) in the phosphine-sulfoxide complex than in the phosphine-thioether complex. However, it is difficult to determine how much influence the steric bulk of the chelating ligand has on these values.

The reaction of one equivalent of phosphine-thioether ligand **14a** with [Pt(nb)$_3$] (nb = norbornene) immediately resulted in the η^2-norbornene complex **34** (Scheme 3.10). The structure of this complex was determined by analysis of the ^{1}H and ^{31}P NMR data. Again, integration of the ^{1}H NMR spectrum confirmed a 1:1 ratio of ligands **14a** and norbornene. Coordination of both the phosphorus and sulfur donor atoms of **14a** was determined by the presence of platinum satellites associated with the ^{1}H NMR peaks of both the CH_2P and CH_2S groups, with coupling constants of 22.0 and 29.4 Hz respectively. The ^{31}P NMR signal (at 58.3 ppm) displays a large $^1J_{PtP}$ coupling constant of 3868 Hz. Similarly to the previously discussed phosphine-thioether ethene complex **32**, this value is over 500 Hz greater than that of the diphosphine analogue of complex **34**, [Pt(nb)(dbpx)].[15] Again, this is likely a combined result of the presence of a more weakly binding donor atom in **14a** as compared with the second phosphine in dbpx, and the larger steric bulk of dbpx. The ^{1}H NMR shifts of the norbornene ligand alkene protons are centred at 2.05 and 2.56 ppm, both with triplet coupling, and platinum satellites of 62.3 and 75.6 Hz respectively, confirming η^2 binding of this ligand.

Crystals of complex **34** suitable for single crystal X-ray diffraction were grown from a benzene-d_6 solution at 4 °C. The X-ray crystal structure is shown in Figure 3.12, and crystallographic data given in Table 3.7 and Table 3.8.* This crystal contained some

*Crystal structure solved by Dr. Bradley Anderson, Victoria University of Wellington.

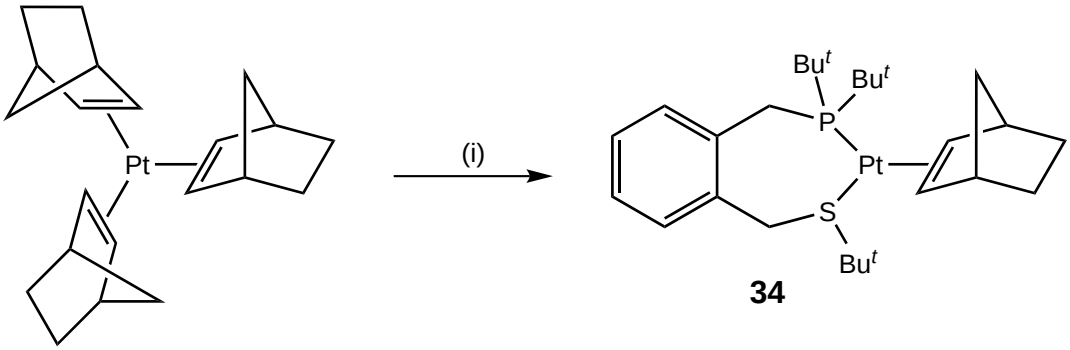

Scheme 3.10 Synthesis of [Pt(nb)(*P,S*)] complex **34**. *Reagents and conditions:* (i) 1 eq. ligand **14a**, toluene, 2.5 h, 92% yield.

disorder, which was modelled with the SHELX program using various restraints. As shown in Figure 3.12, two components were detected, the major part constituting 89% of the crystal and the minor part 11%. These components share the phosphorus and sulfur atoms and one PBu^t group (C3–C6), with the remainder of the molecules reversed along the *b* axis, the norbornene of the major component overlapping the *P,S* ligand backbone of the minor component and *vice versa*. As the sulfur atom in this complex is a chiral centre, these two components comprise enantiomers of complex **34**, with the SBu^t and norbornene bridge-CH_2 groups occupying opposite faces of the complex in both cases.

As would be expected for a platinum(0) complex, the η^2-bound norbornene double bond lies almost parallel with the trigonal plane of the complex, although it is offset from the P−Pt−S plane by 12.3(5)°. This is likely a result of the bulky *t*-butyl groups in close proximity to the norbornene ligand. In a similar fashion to platinum(II) dichloride complex **21**, the aryl ring plane of the ligand lies at an angle of 114.74(9)° from the P−Pt−S plane, and occupies the opposite face from the SBu^t group. The bite angle of ligand **14a** in this complex is 106.63(7)°, over 20° larger than that in complex **21**. This bite angle is similar to those seen in Pt(0) and Pd(0) alkene,[150,151] alkyne[152] and thioketone[153,154] complexes containing *o*-$C_6H_4(CH_2PR_2)_2$-type ligands, and demonstrates the flexibility of the *o*-xylene backbone in *P,S* ligand **14a**.

This is the first crystal structure of a platinum(0) norbornene complex containing a chelating hybrid ligand, and there are only two published examples of crystal structures of platinum(0) norbornene complexes with phosphine ligands. These two structures both contain chelating diphosphine ligands, namely 1,2-bis(di-*t*-butyl-phosphino)ethane[15] and 1,8-bis(diphenylphosphino)naphthalene.[155] Many of the bond lengths in complex **34** are in good agreement with these structures, including the norbornene C=C bond length of 1.459(11) Å (compared with 1.460(11) and 1.469(8) Å respectively for the published structures). The Pt−P bond

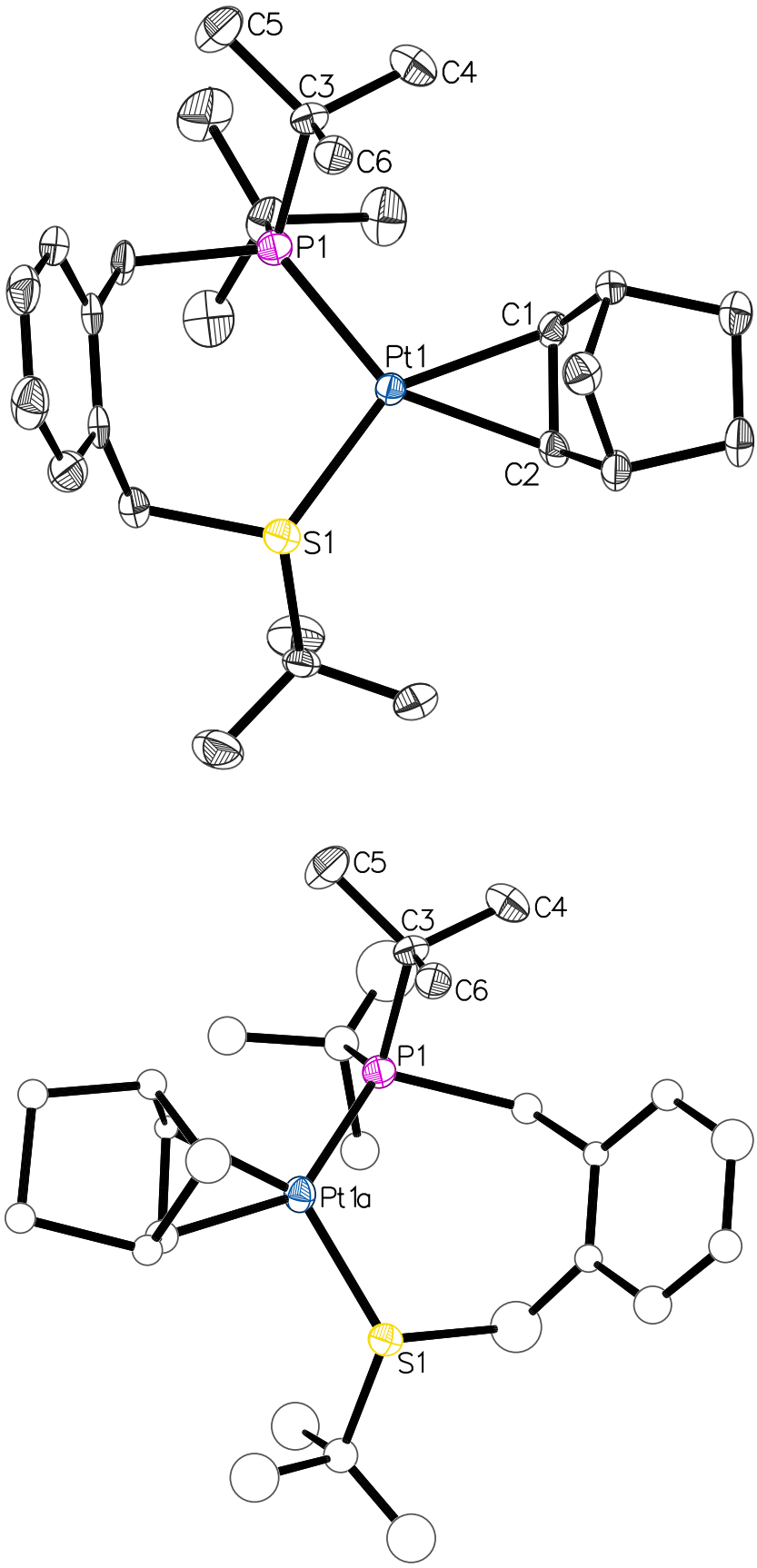

Figure 3.12 ORTEP diagram of the major (89%, top) and minor (11%, bottom) components of the crystal structure of [Pt(nb)(*P,S*)] complex **34** (50% probability thermal ellipsoids). Hydrogen atoms omitted for clarity.

Table 3.7 Crystallographic data of [Pt(nb)(*P*,*S*)] complex **34**.

Empirical formula	**$C_{27}H_{45}PPtS$**
Formula weight	627.75
Crystal system	Monoclinic
Space group	$P2_1/n$
a/Å	8.9787(2)
b/Å	12.5591(4)
c/Å	23.3341(7)
α/°	90.00
β/°	96.212(2)
γ/°	90.00
V/Å^3	2615.81(13)
Z	4
Cell determination reflections	9944
Cell determination range, $\theta_{min} \longrightarrow \theta_{max}$/°	2.4 $\longrightarrow$ 26.1
Temperature/K	113
Radiation type	Mo Kα
Radiation (λ)/Å	0.71073
Crystal size/ mm	0.36 × 0.20 × 0.11
D_{calc}/g m^{-3}	1.594
F(000)	1264
μ/mm^{-1}	5.52
Experimental absorption correction type	Multi-scan (SADABS)
T_{max}, T_{min}	0.745, 0.496
Reflections collected	52570, R_{equiv} = 0.052
Index range h	$-11 \longrightarrow 11$
Index range k	$-15 \longrightarrow 15$
Index range l	$-29 \longrightarrow 28$
θ range/°	2.8 $\longrightarrow$ 26.3
Independent reflections	5226
Reflections [$I > 2\sigma(I)$]	4628
Restraints/parameters	80/356
GOF	1.32
R_1 [$I > 2\sigma(I)$]	0.0384
wR_2 [$I > 2\sigma(I)$]	0.1053
R_1 [all data]	0.0447
wR_2 [all data]	0.1076
Residual density/e Å^{-3}	$-4.04<2.84$

Table 3.8 Selected bond distances and angles of [Pt(nb)(*P*,*S*)] complex **34**.

Bond distances (Å)		**Bond angles (°)**	
Pt1−P1	2.2710(19)	P1−Pt1−S1	106.63(7)
Pt1−S1	2.3250(18)	P1−Pt1−C1	107.8(2)
Pt1−C1	2.109(10)	S1−Pt1−C2	106.0(2)
Pt1−C2	2.118(8)	P1−Pt1−S1 plane $\cdots$ C_6H_4 plane	114.74(9)
C1−C2	1.459(11)	P1−Pt1−S1 plane $\cdots$ C1−Pt1−C2 plane	12.3(5)

length in complex **34** is 2.271(2) Å, essentially identical to those in [Pt(nb){1,2-bis(di-*t*-butylphosphino)ethane}], and *ca.* 0.02 Å longer than those in [Pt(nb){1,8-bis(diphenylphosphino)naphthalene}]. In this case, the different *trans* influences of the phosphorus and sulfur donor atoms have very little effect on the two Pt−C distances. The Pt−C distances in complex **34** are also virtually identical to those seen in the chelating diphosphine complexes.

There are two potential dynamic processes associated with complex **34**, namely inversion of the sulfur donor atom and rotation of the norbornene ligand. If both of these processes were rapid on the NMR timescale, only one signal would be observed for the alkene protons, which is not the case for complex **34** at room temperature. Conversely, if both the sulfur atom and norbornene ligand were static on the NMR timescale, it is likely diastereomers would result and the NMR spectra would reflect this. Again, this is not the case for complex **34** at room temperature. In fact, the NMR data suggest that one of the dynamic processes is rapid at room temperature and the other is not. It is impossible to establish with any certainty from the NMR spectra which of these processes is occurring rapidly; however, the evidence gathered from [Pt(ethene)(*P,S*)] complex **32** along with the pyridine-thioether work of Canovese and co-workers[148] strongly suggests that the norbornene ligand in complex **34** is static, while the sulfur inversion process is rapid at room temperature.

Phosphorus-31 VT-NMR spectra of complex **34** were recorded at 20 °C intervals between 40 and −60 °C in toluene-d_8 (Figure 3.13). These data clearly show the sharp singlet peak with platinum satellites associated with the phosphorus donor atom collapsing to a broad signal at −20 °C, and at lower temperatures separation into two very similar species. These two complexes are the diastereomers of complex **34** that result from both the sulfur atom and norbornene ligand being static on the NMR timescale, producing forms of the complex wherein the SBu^t and norbornene bridge-CH_2 occupy either the same or opposite faces of the molecule. The −40 and −60 °C spectra suggest there is a slight selectivity for one of these forms. Again, these data are consistent with the VT-NMR data reported by Canovese *et al.* for the pyridine-thioether complexes shown in Figure 3.11.

The reaction of one equivalent of phosphine-sulfoxide ligand **16** with [$Pt(nb)_3$] was carried out in an NMR tube and the products characterised *in situ*. After five minutes reaction time, the ^{31}P NMR spectrum contained two related peaks at 53.7 and 54.4 ppm, with platinum coupling constants of 3668 and 3708 Hz respectively, in a ratio of almost 1:1. The ^{1}H NMR spectrum is quite complicated, but a number of signals are closely related to peaks in the previously characterised [Pt(nb)(*P,S*)] complex **34**. Two high-field doublets associated with norbornene bridge-CH_2 groups

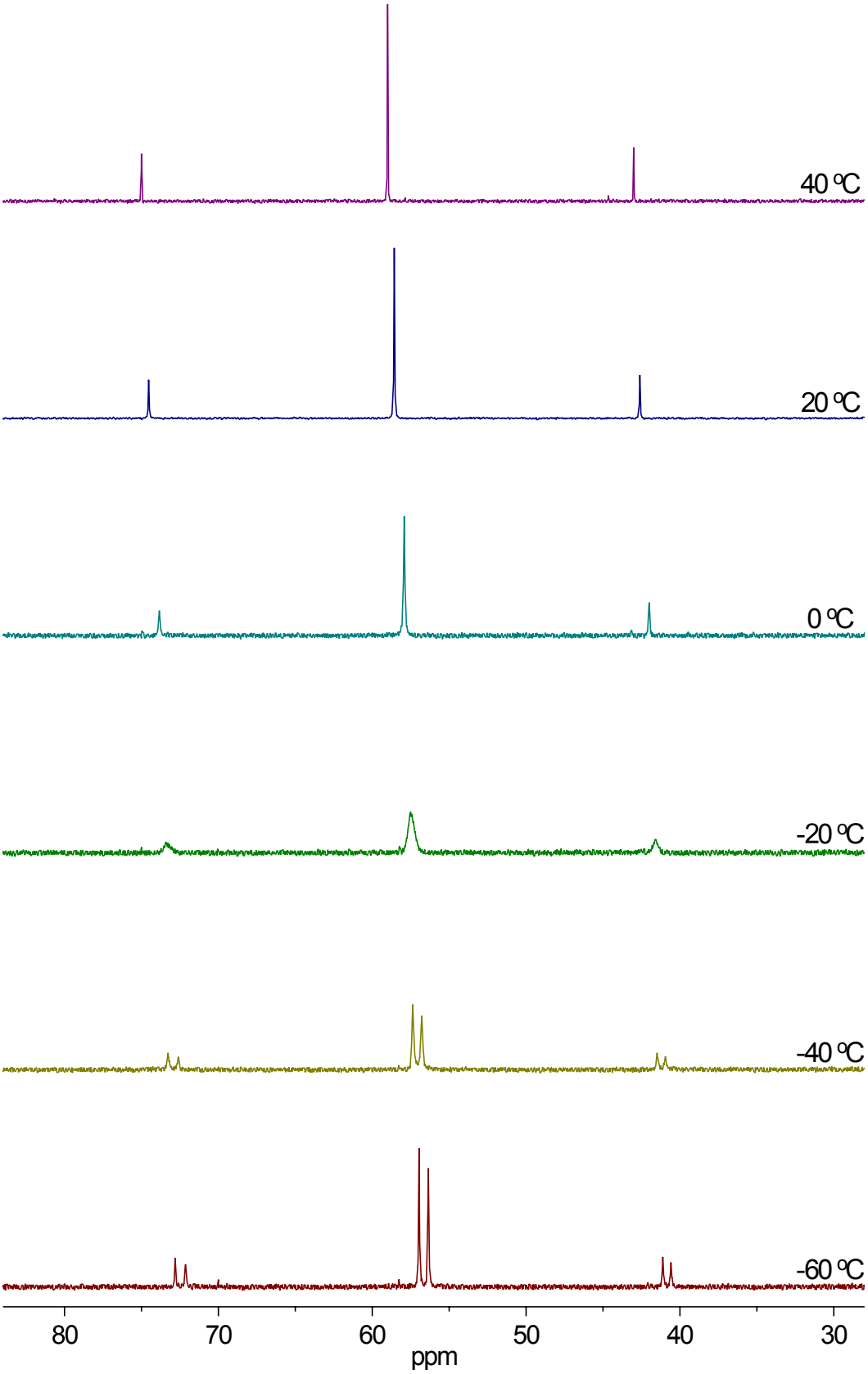

Figure 3.13 ^{31}P NMR spectra of [Pt(nb)(*P*,*S*)] complex **34** collected between 40 and −60 °C in toluene-d_8.

are seen at 0.38 and 0.56 ppm, with J values of 8.5 and 8.0 Hz respectively (*cf.* 0.50 ppm, J = 7.5 Hz in complex **34**). Also apparent are two triplets with large platinum coupling constants at 2.52 ppm (J = 6.5 Hz, $^2J_{\mathrm{PtH}}$ = 77.0 Hz) and 2.63 ppm (J = 6.5 Hz, $^2J_{\mathrm{PtH}}$ = 72.0 Hz) associated with coordinated norbornene alkene protons (*cf.* 2.56 ppm, J = 6.0 Hz, $^2J_{\mathrm{PtH}}$ = 75.6 Hz in complex **34**). Two singlet peaks at 1.38 and 1.40 ppm corresponding to S(O)Bu^t groups are also present (*cf.* 1.42 ppm for SBu^t in complex **34**).

The two closely related sets of peaks visible in the NMR spectra of this reaction indicates that two similar products had formed, both with the formula [Pt(nb)(**16**)]. As only one molecule of racemic ligand **16** was present in the complex, it was determined that the position of the norbornene ligand was inducing planar chirality in the complex to produce two enantiomeric pairs of diastereomers of complex **35**, as shown in Scheme 3.11. As noted previously in complex **34**, the norbornene ligand is static on the NMR timescale at room temperature, thus producing two forms of the complex wherein the SBu^t and norbornene bridge-CH_2 groups occupy either the same or opposite faces of the complex. Interestingly, as the two forms are produced in an almost 1:1 ratio, there seems to be no selectivity for either form.

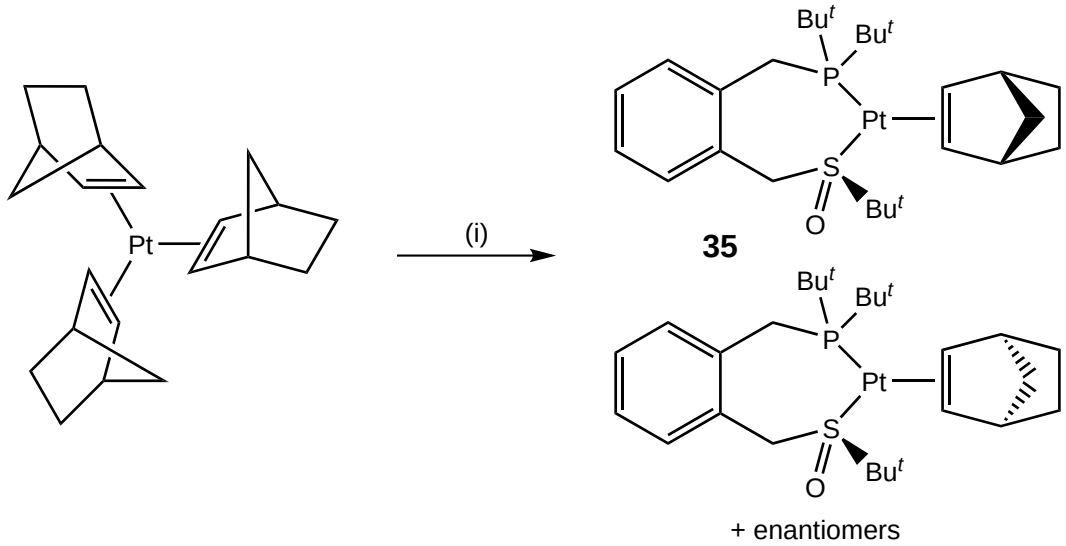

Scheme 3.11 Synthesis of [Pt(nb)(*P,S=O*)] complex **35**. *Reagents and conditions:* (i) 1 eq. ligand **16**, benzene-d_6, 5 min, quantitative conversion.

3.3.2 2:1 Complexes

The reaction of [Pt(nb)$_3$] with two equivalents of phosphine-thioether ligand **14a** initially resulted in a 1:1 mixture of norbornene complex **34** and free ligand. However, over a period of 24 hours, the remaining norbornene ligand and the

coordinated sulfur atom were displaced by the second molecule of ligand **14a**, resulting in the linear, 14-electron complex **36** (Scheme 3.12). The structure of this complex was determined by analysis of the NMR data. Virtual triplet coupling of the peaks associated with the CH_2P and PBu^t protons in the ^1H NMR spectrum indicated a second-order $X_nAA'X_n'$ system,[126] confirming that the coordinated phosphorus atoms were in mutually *trans* positions. The similarity of the ^1H NMR shifts of the CH_2S and SBu^t protons to those of the free ligand indicated that the sulfur atoms were not coordinated to the platinum centre. Monodentate coordination of the ligands through phosphorus only was supported by the large downfield shift (9.06 ppm) of the peak corresponding to one of the aryl backbone protons in the ^1H NMR spectrum. This feature has been seen previously in the platinum dihydride complex **25** and other Pt(II) complexes with similar geometries to complex **36**.

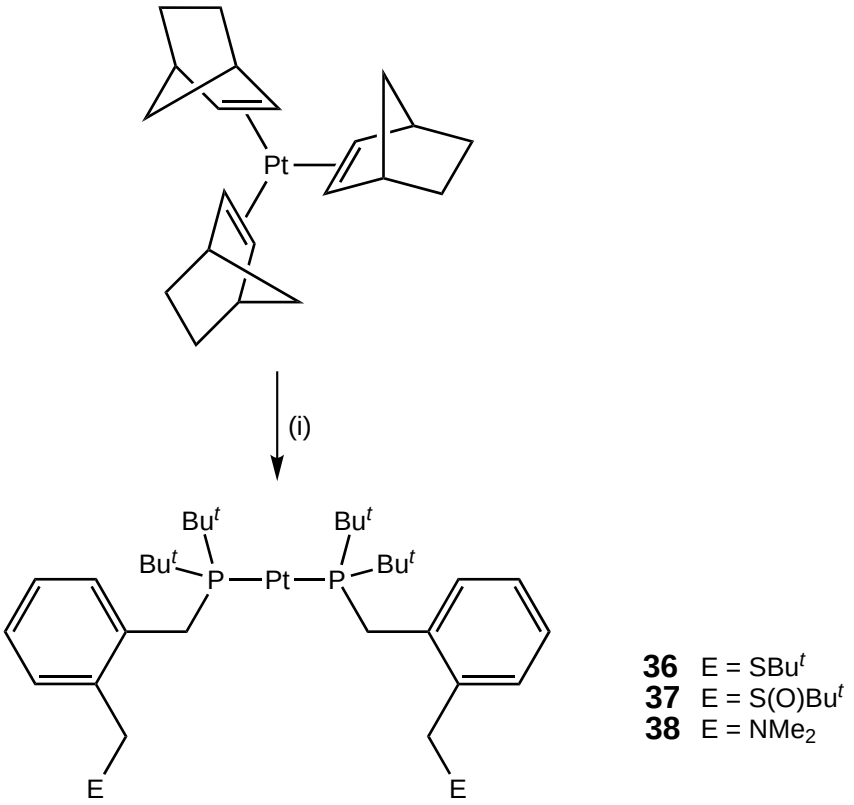

Scheme 3.12 Synthesis of $[Pt(P,E)_2]$ complexes **36**, **37** and **38**. *Reagents and conditions:* (i) 2 eq. ligand **14a** or **16**, or 1–2 eq. ligand **18a**; benzene-d_6, up to 24 h.

This type of platinum complex was first reported in 1966, with the isolation of $[Pt(PPh_3)_2]$ by several different methods (although very little supporting characterisation data were provided).[156] A number of years later, studies containing the complexes $[Pt(PCy_3)_2]$,[157] $[Pt(PBu^t{}_3)_2]$, $[Pt(PBu^t{}_2Ph)_2]$ and $[Pt(PPr^i{}_3)_2]$[158] were published. In 1980, a ^{31}P NMR investigation of this complex type was reported,

including some of the aforementioned complexes.[159] All the linear, 14-electron complexes display $^{1}J_{\mathrm{PtP}}$ coupling constants greater than 4000 Hz, and downfield shifts of the phosphine peaks upon coordination of between 48 and 58 ppm. Trigonal [$\mathrm{Pt(PR_3)_3}$] complexes were also seen for $\mathrm{PPr^{\textit{i}}{}_3}$ and $\mathrm{PCy_3}$ (which do not show virtual triplet couplings in the ^{1}H NMR spectra), but not for $\mathrm{PBu^{\textit{t}}{}_2Ph}$. The ^{31}P NMR spectrum of 14-electron complex **36** displays a singlet peak at 76.1 ppm, a downfield shift of 51.1 ppm from the free ligand, with a large $^{1}J_{\mathrm{PtP}}$ coupling of 4397 Hz. These results are consistent with other complexes of this type.

Similar reactivity was seen when [$\mathrm{Pt(nb)_3}$] was combined with two equivalents of phosphine-sulfoxide ligand **16** in benzene-d_6. Initially, a 1:1 mixture of free ligand and the diastereomers of complex **35** formed, which slowly converted into the linear, 14-electron complex **37** (Scheme 3.12). However, in this case the reaction stopped at around 70% linear complex **37**, with the rest of the sample remaining as a mixture of norbornene complex **35** and free ligand. This equilibrium behaviour suggests that the sulfoxide moiety binds more strongly to platinum(0) than the corresponding thioether. The reaction was repeated using [$\mathrm{Pt(1,5\text{-}cyclooctadiene)_2}$] rather than [$\mathrm{Pt(nb)_3}$], resulting in quantitative conversion to linear complex **37** within 10 minutes. As the racemic form of ligand **16** was used, complex **37** also formed as diastereomers, a mixture of the *R,R* and *S,S* enantiomeric forms, and the meso *R,S* form. The ^{31}P NMR spectrum of complex **37** displays singlet peaks at 76.5 and 77.0 ppm in a 1:1 ratio, with platinum coupling constants of 4408 and 4424 Hz respectively. The ^{1}H NMR spectrum shows two sets of similar peaks, including virtual triplet couplings for the peaks associated with the $\mathrm{CH_2P}$ and $\mathrm{PBu^{\textit{t}}}$ protons.

The reaction of one equivalent of phosphine-amine ligand **18a** with [$\mathrm{Pt(nb)_3}$] did not produce the same chelated norbornene complex as the previous two examples. After 20 minutes reaction time, the major product of this reaction was the linear, 14-electron species **38** (Scheme 3.12). Again, the ^{31}P NMR spectrum of this complex displays a peak with similar downfield shift to that of other 14-electron complexes, and a $^{1}J_{\mathrm{PtP}}$ coupling over 4000 Hz. The ^{31}P NMR data and selected ^{1}H NMR data of the related complexes **36**, **37** and **38** are collated in Table 3.9, showing that the identity of the second potential donor atom (E) has little effect on the platinum core of these complexes.

In light of previous reports, the absence of a [Pt(nb)(κ^2*P,N*-**18a**)] complex is not terribly surprising. It is generally known that nitrogen donor atoms do not bind to platinum(0) centres,[160] and the only known Pt(0) norbornene complex of a chelating phosphine-amine ligand is that of a bicyclic substituted 3-aza-7-phosphabicyclo[3.3.1]-nonan-9-one reported by Zayya in 2012 (shown in

Table 3.9 ^{31}P and selected ^{1}H NMR shifts (in ppm) and coupling constants (in Hz) of [Pt(*P,E*)$_2$] complexes in benzene-d_6.

		P		**CH_2P**			**PBu^t**	
Complex	**E**	δ_P	$^1J_{PtP}$	δ_H	$^2J_{PH} + {}^4J_{PH}$	$^3J_{PtH}$	δ_H	$^3J_{PH} + {}^5J_{PH}$
36	SBu^t	76.1	4397	3.49	6.1	43.3	1.46	12.4
37	$S(O)Bu^t$	76.5	4408	3.36[a]	6.5	*b*	1.40	13.4
		77.0	4424	3.70	5.8	*b*	1.43	13.0
				3.79	5.9	*b*	1.46[c]	12.5
38	NMe_2	75.4	4373	3.60	6.3	49.8	1.49	12.4

[a]This value corresponds to two CH_2P groups.
[b]Unable to determine from spectra.
[c]This value corresponds to two PBu^t groups.

Figure 3.14).[133] This Pt(0) norbornene complex is fragile in solution, even under inert atmosphere, and is not able to be stored for long periods of time in the solid state. Zayya also reported Pt(0) phosphine-amine complexes of ethene and η^2-1,5-cyclooctadiene, both of which reacted spontaneously with the phosphine-amine ligand framework to form Pt(II) metallated species.

It may be less intuitive that a [Pt(nb)$_2$(κ^1*P*-**18a**)] complex did not form in the 1:1 reaction of phosphine-amine ligand **18a** with [Pt(nb)$_3$], as [Pt(nb)$_2$($PBu^t{}_3$)][161,162] is known (although it is unstable in solution, converting to [Pt($PBu^t{}_3$)$_2$] over a number of days). As $PBnBu^t{}_2$ is a better model for the *P,E* ligands than $PBu^t{}_3$, the 1:1 reaction was repeated with [Pt(nb)$_3$] and $PBnBu^t{}_2$ in benzene-d_6 solution. The ^{1}H and ^{31}P NMR spectra of the reaction mixture showed complete conversion to [Pt($PBnBu^t{}_2$)$_2$][163] after 10 minutes. This result indicates that the rapid conversion of mixtures of [Pt(nb)$_3$] and ligand **18a** to linear, 14-electron complex **38** is not a function of the presence of the amine donor atom, but rather it is due to the instability of the [Pt(nb)$_2$($PBnBu^t{}_2$)]-type species.

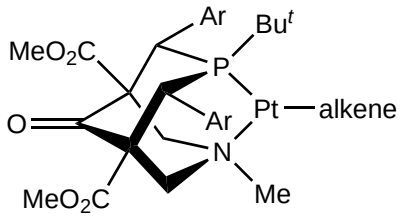

alkene = norbornene, ethene, η^2-1,5-cyclooctadiene

Figure 3.14 Platinum(0) alkene complexes of a phosphine-amine ligand.

3.4 Reactivity of [Pt(nb)(*P,S*)]

Agostic (M · · · H−C) interactions in organometallic complexes have been known for nearly 50 years,[164,165] and have recently become the focus of theoretical investigations,[73,166,167] as they play key roles in a number of industrially important catalytic processes, including their presence in the transition states of chain growth and termination steps of alkene polymerisation reactions. A number of stable agostic complexes have been synthesised *via* protonation of various metal complexes containing η^2-bound alkene ligands.[13,14,73,168,169]

An initial attempt at the protonation of complex **34** was performed using the solid fluorocarbon acid $CH_2(SO_2CF_3)_2$. Although the anion of this acid is nominally non-coordinating, the reaction of complex **34** resulted in displacement of the norbornene ligand and quantitative conversion to platinum(II) hydride complex **39**, shown in Scheme 3.13. The structure of this complex was determined by analysis of the NMR data, and comparison with other complexes of this type.[133,140] The ^{1}H NMR peaks corresponding to the CH_2P and CH_2S groups of ligand **14a** both display platinum satellites (31.8 and 31.7 Hz respectively), confirming that the ligand remains chelated in complex **39**. The hydride NMR signal of this complex is centred at −14.22 ppm, with phosphorus coupling of 16.5 Hz and platinum coupling of 1092.9 Hz. This is in good agreement with the hydride NMR signal associated with [PtH(κ^1*P*-**14a**)(κ^2*P,S*-**14a**)]$^+$ complex **26**, and indicates that the hydride ligand in **39** lies *trans* to the sulfur donor atom. Coordination of the $^-CH(SO_2CF_3)_2$ anion was confirmed by the presence of platinum satellites on both the ^{1}H and ^{13}C NMR signals associated with the CH moiety. The proton NMR peak is centred at 5.84 ppm (quite different to the *ca.* 3.8 ppm shift seen when the anion is non-coordinating[140]), with $^2J_{PtH}$ coupling of 66.0 Hz. The CH carbon NMR signal at 62.3 ppm displays a large $^2J_{PH}$ coupling of 63.8 Hz confirming the *trans* arrangement with the phosphorus donor atom, and a large platinum coupling constant of 492.5 Hz, consistent with this carbon having a σ-bond to platinum.

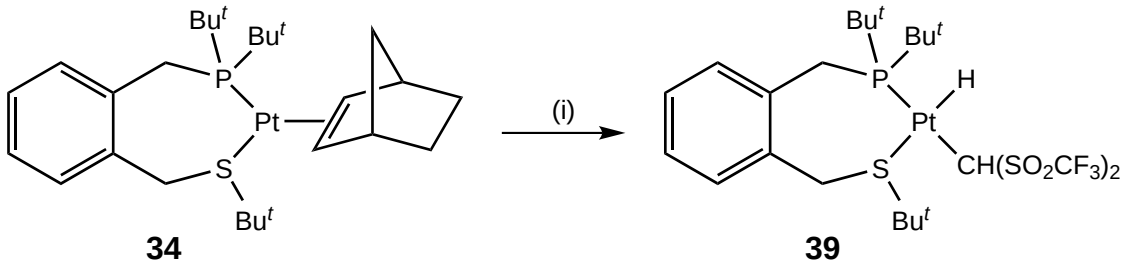

34 **39**

Scheme 3.13 Synthesis of [PtH{$CH(SO_2CF_3)_2$}(*P,S*)] complex **39**. *Reagents and conditions:* (i) 1 eq. $CH_2(SO_2CF_3)_2$, benzene-d_6, 15 min, quantitative conversion.

As this synthetic method did not produce the desired agostic complex, the reaction was repeated with tetrafluoroboric acid diethyl etherate, which has been shown to successfully produce platinum norbornyl complexes with agostic interactions.[15] Analysis of the ^{1}H, ^{31}P and ^{19}F NMR data of the resulting off-white solid confirmed that the desired platinum(II) norbornyl complex **40** had formed almost quantitatively (Scheme 3.14). The ^{31}P NMR spectrum displays a singlet peak with a very large platinum coupling constant of 5791 Hz, indicating the presence of a weakly interacting ligand *trans* to the phosphorus donor atom. The ^{1}H NMR peak corresponding to the CH_2S group of ligand **14a** displays platinum satellites, confirming that the ligand remains chelated in this complex. The existence of a peak in the ^{1}H NMR spectrum with a high-field shift of -1.93 ppm, doublet of doublets coupling with platinum satellites, and integrating for one proton confirmed the presence of a β-agostic interaction in complex **40**. ^{1}H NMR peaks with very similar features have been noted previously for the products of protonation of [Pt(nb)($Bu^t_2PC_2H_4PBu^t_2$)][15] and the [Pt(nb)(*P,N*)] complex[133] shown in Figure 3.14. Both of these complexes were determined crystallographically to contain σ-bound norbornyl ligands with β-agostic interactions.

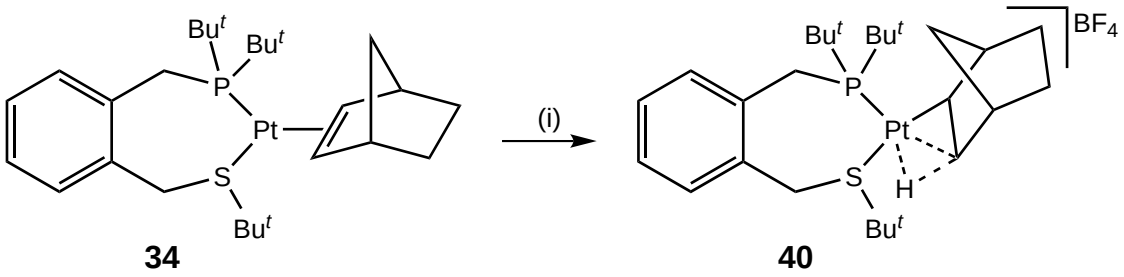

34 **40**

Scheme 3.14 Synthesis of β-agostic complex **40**. *Reagents and conditions:* (i) 1 eq. $HBF_4 \cdot Et_2O$, dichloromethane, 30 min, >95% conversion.

Interestingly, in the ^{1}H NMR spectrum the peaks associated with the CH_2S, CH_2P and PBu^t groups of ligand **14a** appeared as AB systems, indicating asymmetry across the plane of the complex. In other thioether complexes this has been attributed to the sulfur inversion process being slow at room temperature; however, as evidenced previously in this chapter, a sulfur donor atom positioned *trans* to a σ-bound alkyl ligand would be expected to have a coalescence temperature much lower than room temperature, and hence it is very unlikely that this is the cause of the asymmetry. It has been reported in the literature that β-agostic [Pt(norbornyl)(diphosphine)] complexes undergo a rapid intramolecular rearrangement process *via* a mechanism involving transfer of the agostic hydrogen to the metal to give an intermediate alkene-hydride species in which rotation about the metal-alkene bond is facile. The result of this dynamic process is an increase in time-averaged symmetry across the plane of the complex, and a reduction in the number

of proton and carbon shifts in the NMR spectra.[15] Conversely, in complex **40**, the presence of the AB systems indicates that this dynamic process is not occurring on the NMR timescale at room temperature. As it has been noted that the dynamic process also does not occur in the β-agostic [Pt(norbornyl)(*P,N*)] complex,[133] it is likely that the identity of the donor atom *trans* to the σ-bound norbornyl carbon dictates the rapidity of the intramolecular rearrangement. As the *trans* influences of amine and thioether ligands are much lower than those of phosphine ligands, the Pt−C bond strength would be increased in the hybrid ligand complexes, causing the dynamic process to be slowed (or ceased) at room temperature.

Unfortunately, the β-agostic complex **40** immediately began degrading in solution, resulting in an intractable mixture of products after a few hours, which included a large number of hydride signals in the ^{1}H NMR spectrum. The instability of this material precluded any further characterisation of the complex, including the collection of ^{13}C NMR data. The reaction shown in Scheme 3.13 was repeated in dichloromethane-d_2 solution, resulting in a mixture of hydride complex **39** (70%) and the equivalent β-agostic complex (30%), indicating that the choice of solvent has an influence on the coordination behaviour of the $^{-}CH(SO_2CF_3)_2$ anion.

The reaction of complex **34** with ethyne was also studied. There are few literature examples of platinum(0) phosphine complexes containing η^2-ethyne ligands, due to the propensity of these species to react further, producing polyacetylene. However, when ethyne gas was bubbled through a benzene-d_6 solution of **34** for a short time, the η^2-ethyne complex **41** was produced (Scheme 3.15), which existed in solution for a number of hours at room temperature.[†] The ^{1}H and ^{13}C NMR spectra shows that the chemical environment of ligand **14a** in this complex is essentially identical to that in the precursor complex **34**, with very little change to either the chemical shifts or coupling constants of the peaks. Similarly, the ^{31}P NMR spectrum displays a singlet peak at 56.8 ppm, an upfield shift of 1.5 ppm from the precursor, with a $^{1}J_{\mathrm{PtP}}$ coupling of 4018 Hz (150 Hz greater than the precursor). The η^2-ethyne ligand in complex **41** displays two shifts in the ^{13}C NMR spectrum centred at 101.2 and 112.3 ppm, with $^{2}J_{\mathrm{PC}}$ couplings of 8.1 and 68.2 Hz respectively. The much larger phosphorus coupling constant of the peak at 112.3 ppm identified this carbon centre as being positioned *trans* to the phosphorus donor atom. The platinum-carbon coupling constants of these carbon peaks are also quite different, 444.5 and 258.3 Hz respectively. These values reflect the larger *trans* influence of the phosphorus donor atom as compared to the sulfur donor atom in this complex. Two shifts are also seen in the ^{1}H NMR spectrum for the ethyne protons, centred at 6.74 and 7.03 ppm, with similar $^{3}J_{\mathrm{PH}}$ coupling constants of 17.6 and 14.1 Hz respectively.

[†]This work was carried out as part of an undergraduate research project performed with Eva Weatherall.

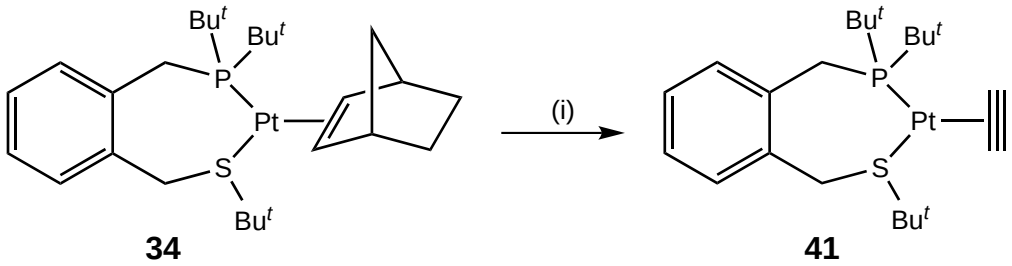

34 **41**

Scheme 3.15 Synthesis of [Pt(ethyne)(*P,S*)] complex **41**. *Reagents and conditions:* (i) Ethyne, benzene-d_6, 1 min, >90% conversion.

The diphosphine analogue of complex **41**, [Pt(ethyne)(dbpx)], has recently been synthesised but not published,[170] and is quite distinct from complex **41** in a number of aspects. Whereas complex **41** formed immediately at room temperature, the synthesis of [Pt(ethyne)(dbpx)] required heating of the precursor, [Pt(norbornene)(dbpx)], to 40 °C overnight in the presence of excess ethyne. The difference in reaction rate of the platinum norbornene complexes can be attributed to the larger steric bulk of dbpx as compared to ligand **14a**. The crystal structure of complex **34**, detailed previously in this chapter, confirmed the bonding of norbornene to platinum(0) in this complex is very similar to that in diphosphine complexes, indicating the reactivity difference is unlikely to be an electronic effect. However, once [Pt(ethyne)(dbpx)] is formed, it is more stable than complex **41**. The ^{1}H NMR shift of the ethyne protons in [Pt(ethyne)(dbpx)] is significantly downfield of that of complex **41**, at 7.78 ppm. This indicates that the ethyne ligand retains more alkyne character in complex **41** than in [Pt(ethyne)(dbpx)], likely contributing to the instability of **41**. The $^1J_{\mathrm{PtP}}$ value in [Pt(ethyne)(dbpx)] is 3463 Hz, over 500 Hz lower than that in **41**, similar to the difference seen in the respective platinum(0) norbornene complexes of these ligands.

Complex **41** is the first example of a platinum(0) ethyne complex containing a chelating hybrid ligand, and the second example of a phosphine-thioether metal complex bearing an η^2-alkyne ligand. In 2008, the X-ray crystal structure of the disubstituted ferrocene (Fc) complex, [Pt(diphenylethyne){κ^2*P,S*-1,2-Fc(PPh_2)(CH_2SPh)}], was published.[106] This complex was synthesised *via* the reduction of the precursor platinum(II) dichloride complex in the presence of diphenylethyne. Unlike complex **41**, in which the sulfur inversion process is rapid at room temperature, the sulfur atom in [Pt(diphenylethyne){κ^2*P,S*-1,2-Fc(PPh_2)(CH_2SPh)}] is static in solution, and in the solid state only one diastereomer is seen. The authors note that this is the case for complexes of all 1,2-Fc(PPh_2)(CH_2SR) ligands, and that the planar chirality of the ferrocene controls the configuration at the sulfur atom. Although not mentioned in the paper, this is most likely a steric effect, and independent of the identity of the ligand *trans* to the sulfur atom in these complexes.

3.5 Reactivity of [Pt(*P*,*S*)$_2$]

The exposure of linear [Pt(*P*,*S*)$_2$] complex **36** to air resulted in the reaction of this species with dioxygen, forming the η^2-dioxygen [Pt(O$_2$)(*P*,*S*)$_2$] complex **42**. This reaction could be controlled by bubbling dioxygen through an *n*-hexane solution of complex **36** and cooling to induce crystallisation, to give a 78% yield of complex **42** as pale brown microcrystals (Scheme 3.16). The identity of complex **42** was determined by ^{1}H, ^{13}C and ^{31}P NMR data, elemental analysis, and comparison with known [Pt(O$_2$)(PR$_3$)$_2$] complexes (where PR$_3$ = PCy$_3$, PBu^{t}Ph$_2$, PBu$^t{}_2$Me, PBu$^t{}_2$Bu^n, PBu$^t{}_2$Ph).[171,172] In contrast to the virtual triplet (X$_n$AA′X$_n$′) couplings seen in the ^{1}H NMR spectrum of precursor complex **36**, the ^{1}H NMR peaks associated with the CH$_2$P and PBu^t groups of **42** display doublet couplings to phosphorus-31, indicating that the ligands not longer inhabit mutually *trans* positions. Similarly, the ^{13}C NMR peaks that had previously displayed virtual triplet couplings, now show complex second-order multiplet couplings to phosphorus-31 and platinum-195. The ^{31}P NMR spectrum of complex **42** displays a singlet peak at 43.5 ppm (a shift of 32.6 ppm upfield from the precursor complex), with a $^1J_{\mathrm{PtP}}$ coupling constant of 4112 Hz, consistent with other complexes of this type.[171]

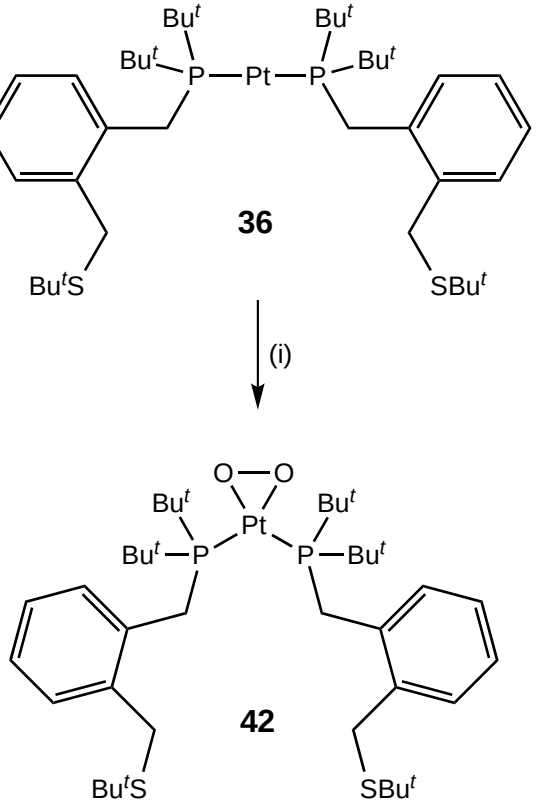

Scheme 3.16 Synthesis of [Pt(O$_2$)(*P*,*S*)$_2$] complex **42**. *Reagents and conditions:* (i) Dioxygen, *n*-hexane, 10 min, 78% yield.

During the synthesis of complex **42** it was discovered that the coordination of dioxygen to the platinum centre was reversible, either by subjecting the material to vacuum, or by passing a stream of another gas through a solution of the complex or over the material in the solid state. For example, when carbon dioxide was bubbled through a solution of the similar complex, $[Pt(O_2)(PBu^t{}_2Bu^n)_2]$, the only product was the peroxycarbonato species, $[Pt(CO_4)(PBu^t{}_2Bu^n)_2]$;[173] however, the same reaction with complex **42** produced a mixture of the desired complex $[Pt(CO_4)(\mathbf{14a})_2]$ and $[Pt(P,S)_2]$ complex **36**.‡ Complete removal of the dioxygen ligand from complex **42** was achieved by heating crystals of the material to 70 °C under high vacuum (∼0.1 mmHg) for 24 hours. This result is significant as it is the first example of reversible binding of dioxygen to a $[Pt(PR_3)_2]$-type complex.

There are only a few examples of reversibility in palladium complexes of this type. For example, the binding of dioxygen in the complex $[Pd(O_2)(PBu^t{}_2Ph)_2]$ is reversible under the same conditions as complex **42**,[174] and the complexes $[Pd(O_2)(PBu^t{}_2Bu^n)_2]$ and $[Pd(O_2)(PAd_2Bu^n)_2]$ (Ad = 1-adamantyl) can be reduced back to their respective palladium(0) linear complexes by reaction with hydrogen under mild conditions.[175] These $[Pd(O_2)(PR_3)_2]$-type complexes have generated interest since their discovery in 1967,[176] including for their potential to separate dioxygen from gaseous mixtures,[177] and their use as stable precursors for formylation and alkoxycarbonylation catalysts.[175] Recently, $[Pd(O_2)(PPh_3)_2]$ was found to play a crucial role in the formation of biaryls as by-products in palladium-catalysed Suzuki-Miyaura reactions when not conducted under oxygen-free atmosphere.[178]

An X-ray crystallographic and computational study has been conducted comparing the dioxygen-reversible palladium complex, $[Pd(O_2)(PBu^t{}_2Ph)_2]$, and the dioxygen-irreversible platinum analogue, $[Pt(O_2)(PBu^t{}_2Ph)_2]$.[172] This study established that the P−M−P angle is *ca.* 2.3° larger in the palladium complex than the platinum analogue, and suggested that the M−O_2 interaction is enhanced for the platinum complex when compared with the palladium analogue. To confirm that the sulfur arm of *P,S* ligand **14a** is not involved in the unprecedented reversible dioxygen binding in complex **42**, the benzyldi-*t*-butylphosphine analogue, $[Pt(O_2)(PBnBu^t{}_2)_2]$, was synthesised.[163] It was found that the dioxygen binding was also reversible under the same conditions as for complex **42**, indicating that the reversible binding of dioxygen to $[Pt(P,S)_2]$ complex **36** is not due to involvement of the thioether moiety of the ligand. Unfortunately, crystals suitable for X-ray diffraction studies were unable to be grown of either of these complexes, so P−Pt−P angles and Pt−O_2 interactions were not able to be determined. However, as $[Pt(PBu^t{}_3)_2]$ does not react with dioxygen and the binding of dioxygen in a number of similar $[Pt(O_2)(PBu^t{}_2R)_2]$

‡This work was carried out as part of an undergraduate research project performed with Eve Martin.

complexes (where R = Me, Bu^n, Ph) is irreversible,[171,172] it follows that the large steric bulk of ligands **14a** and $PBnBu^t{}_2$ is essential in the reversible dioxygen binding in these complexes.

As the isolated yield of dihydride complex **25** from the reaction of ligand **14a** with $[PtCl_2(1,5\text{-hexadiene})]$ and sodium borohydride was only 33%, it was envisaged that linear platinum(0) complex **36** could provide an alternative route to the dihydride species. It is known that the reaction of the similar complex, $[Pt(PCy_3)_2]$, with dihydrogen gas produces the platinum(II) dihydride complex $[PtH_2(PCy_3)_2]$.[157] Unfortunately, the same synthetic method performed with complex **36** produced no reaction. Another synthetic route to $[PtH_2(PR_3)_2]$-type complexes involves the reaction of $[Pt(PR_3)_2]$ with hydrochloric acid to form $[PtHCl(PR_3)_2]$, followed by reduction with sodium borohydride.[125] This reaction type was deemed too similar to the original synthesis of dihydride complex **25** to pursue.

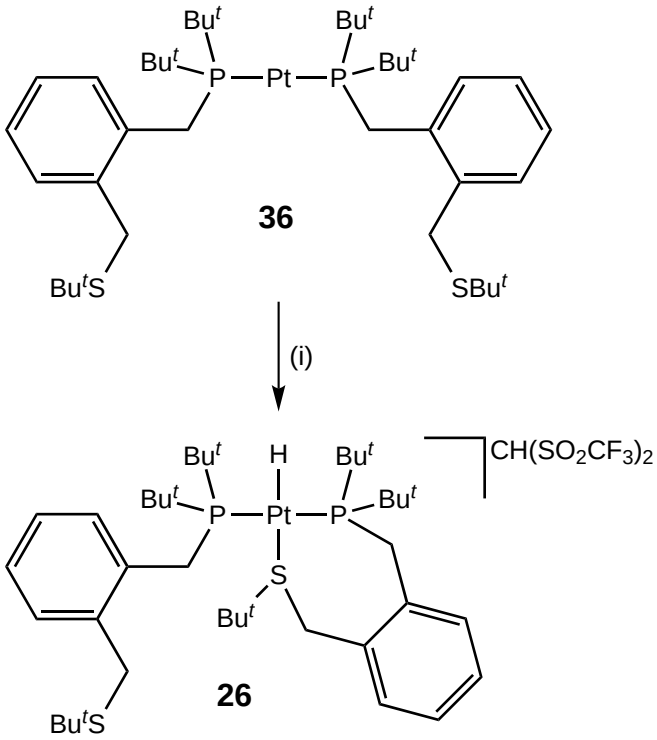

Scheme 3.17 Protonation of $[Pt(P,S)_2]$ complex **36**. *Reagents and conditions:* (i) $CH_2(SO_2CF_3)_2$, acetone, 10 min, 55% yield.

Platinum(0) complex **36** also presented a direct route to cationic complex **26**. As noted above, the reaction of $[Pt(PR_3)_2]$-type complexes with protic acids yield hydride complexes of the type $[PtHX(PR_3)_2]$.[125] It was anticipated that if an acid containing a weakly coordinating counterion was combined with complex **36**, chelation of one of the *P,S* ligands would result, producing complex **26**. To this end, complex **36** and fluorocarbon acid $CH_2(SO_2CF_3)_2$ were combined in acetone and stirred until all solid had dissolved (Scheme 3.17). Analysis of the ^1H and ^{31}P

NMR spectra of the resulting foam confirmed complex **26** was the major product of the reaction. Unfortunately, all attempts at crystallisation were unsuccessful, and trituration of the crude product with toluene was ineffective in completely purifying the material. However, this methodology does constitute a shorter synthetic route to complex **26**.

3.6 Concluding Remarks

The coordination chemistry of *o*-xylene-based phosphine-thioether, phosphine-sulfoxide and phosphine-amine hybrid ligands with platinum(II) and platinum(0) precursors has been investigated. The coordination behaviour of these ligands with the precursor complex [$PtCl_2$(1,5-hexadiene)] varied depending on the identity of the second donor atom, producing a chelated [$PtCl_2$(*P,S*)] complex with phosphine-thioether ligand **14a**, and complexes containing σ:η^2-bound phosphonium ion adducts with *P,S=O* ligand **16** and *P,N* ligand **18a**. A chelated [$PtCl_2$(*P,S=O*)] complex was produced by heating a mixture of [$PtCl_2(NCBu^t)_2$] and ligand **16**, whereas under the equivalent conditions a chelated [$PtCl_2$(*P,N*)] complex did not form. This work highlights the importance of both the electronic and steric characteristics of these large bite angle *P,E* ligands in their coordination chemistry.

Similarly, the reaction of one equivalent of *P,S* ligand **14a** or *P,S=O* ligand **16** with [Pt(alkene)$_3$] gave the corresponding chelated [Pt(alkene)(*P,E*)] complexes, and monodentate [Pt(*P,E*)$_2$] complexes with a 2:1 ratio of the starting materials (*via* displacement of the sulfur donor atoms), whereas *P,N* ligand **18a** gave [Pt(*P,N*)$_2$] in both cases. These results indicate that coordination of the second donor atom to platinum(0) is more favourable with the sulfur-containing ligands than *P,N* ligand **18a**. Further to this, the equilibrium observed in the 2:1 reaction of *P,S=O* ligand **16** and [Pt(nb)$_3$] suggests the sulfoxide moiety binds more strongly to platinum(0) than the equivalent thioether moiety.

The platinum coordination chemistry of phosphine-thioether ligand **14a** was more thoroughly explored. A range of [PtHL(*P,S*)$_2$] and [PtHL(*P,S*)$_2$]$CH(SO_2CF_3)_2$ complexes with monodentate phosphine binding were produced, and it was shown that the removal of ligand L from these complexes resulted in coordination of one of the sulfur donor atoms. In the case where L = MeCN, reversible association of one of the sulfur donor atoms was achieved by removal of the MeCN ligand under reduced pressure, followed by addition of free MeCN to a solution to the resulting [PtH(κ^1*P*-**14a**)(κ^2*P,S*-**14a**)]$CH(SO_2CF_3)_2$ complex.

The reactivity of the platinum(0) complexes [Pt(nb)(*P,S*)] (**34**) and [Pt(*P,S*)$_2$] (**36**) was also investigated. [Pt(nb)(*P,S*)] complex **34** reacted with HBF_4 or ethyne gas to produce unstable β-agostic norbornyl complex **40** and η^2-ethyne complex **41** respectively. This is in contrast to the equivalent platinum(0) β-agostic norbornyl diphosphine and η^2-ethyne diphosphine complexes, which are much more stable. [Pt(*P,S*)$_2$] complex **36** reacted reversibly with dioxygen, forming η^2-dioxygen [Pt(O_2)(*P,S*)$_2$] complex **42**, the first example of reversible binding of dioxygen to a platinum bisphosphine complex of this type. Further investigation showed the reversibility was due to the steric bulk of the phosphine ligands, rather than any involvement of the thioether moieties.

This research has established that phosphine-thioether ligand **14a** displays hemilabile behaviour in complexes of both platinum(II) and platinum(0). The X-ray crystal structure of [$PtCl_2$(*P,S*)] complex **21** demonstrates both the difference in *trans* influence between the phosphorus and sulfur donor atoms of ligand **14a** (based on the disparity in Pt−Cl bond length), and the significantly smaller bite angle of this ligand when compared with the analogous complex of an *o*-xylene-based diphosphine ligand. Conversely, the X-ray crystal structure of [Pt(nb)(*P,S*)] complex **34** exhibits very similar features to the analogous complex of an *o*-xylene-based diphosphine ligand; however, derivatives of this complex proved to be less stable than their diphosphine analogues. Due to the hemilability of *P,S* ligand **14a** and the significant differences between metal complexes of this ligand and the diphosphine analogues, it is likely this ligand would not be suitable for catalytic reactions where large bite angle diphosphine ligands are usually employed (the methoxycarbonylation of ethene, for example). Possibly a more favourable area of research with this ligand would be catalytic reactions where monophosphine ligands are normally used, such as palladium-catalysed C−C bond forming reactions.

In summary, phosphine-thioether ligand **14a** has been shown to adopt chelating, monodentate and hemilabile binding modes in complexes of both platinum(II) and platinum(0), suggesting that this ligand would produce Group 10 metal catalysts with unusual and potentially beneficial patterns of reactivity and selectivity. In contrast, phosphine-amine ligand **18a** showed a greater tendency towards monodentate binding, and hence it is likely this compound would act primarily as a monodentate phosphine ligand in catalytic applications. Phosphine-sulfoxide ligand **16** also adopts chelating and monodentate binding modes with platinum(0); however, characterisation of complexes with this ligand was often hindered by the presence of diastereomers. Continuation of the study of this ligand would benefit from the separation of the two enantiomers or an enantioselective ligand synthesis.

Chapter 4

Palladium Complexes

Palladium coordination complexes bearing phosphine ligands are used extensively as homogeneous catalysts for a wide range of C−C, C−O and C−N bond-forming reactions. These catalysts have revolutionised a number of fields, including medicinal chemistry, materials science and polymer chemistry, from laboratory to industrial scale. As the catalytic cycles for these reactions generally include palladium in both the 0 and +2 oxidation state, this chapter covers the reactivity of phosphine-thioether ligand **14a** with Pd(II) and Pd(0) precursors, with a focus on the palladium complexes commonly used in pre-catalyst mixtures.

4.1 Reactions with Pd(II) Precursors

4.1.1 $[PdCl_2L_2]$

Initially, the synthesis of a chelated $[PdCl_2(P,S)]$ complex was attempted. To this end, one equivalent of *P,S* ligand **14a** was combined with a $[PdCl_2L_2]$ precursor (L = NCMe, $NCBu^t$, NCPh, L_2 = 1,5-cyclooctadiene) in either acetone-d_6, dichloromethane-d_2 or benzene-d_6, and the reaction followed by ^1H and ^{31}P NMR methods (Scheme 4.1). In each case, after 10 minutes reaction time the ^{31}P NMR spectrum of the reaction mixture displayed one broad signal centred between 40 and 45 ppm. The ^1H NMR spectrum showed a set of similarly broad signals including a downfield peak at *ca.* 9 ppm (suggesting monodentate binding of ligand **14a** through the phosphorus donor atom), and in the case of the $[PdCl_2$(1,5-cyclooctadiene)$]$ reaction, a 1:1 ratio of free 1,5-cyclooctadiene

and unreacted [$PdCl_2$(1,5-cyclooctadiene)] was observed. From comparison with the known reactivity of similar phosphine ligands, the product of these reactions was tentatively assigned as *trans*-[$PdCl_2(\kappa^1 P$-**14a**$)_2$]. In contrast to the platinum analogue (discussed in Section 3.2), *trans*-[$PdCl_2(PBnBu^t{}_2)_2$] is known,[179] and the derivative complexes *trans*-[$PdCl_2\{P(CH_2C_6H_3R_2)Bu^t{}_2\}_2$] (R = OMe, $R_2 = OC_2H_4OC_2H_4OC_2H_4OC_2H_4O$) have ^{31}P NMR signals at 43.5 and 43.7 ppm respectively.[180]

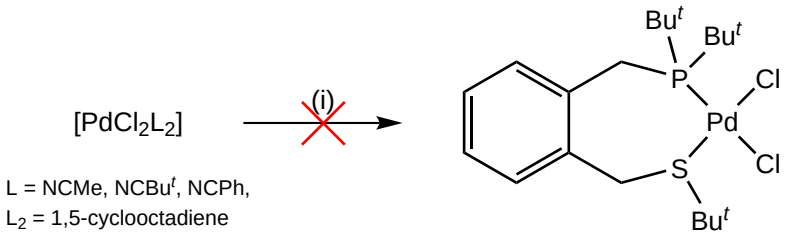

Scheme 4.1 Attempted synthesis of a [$PdCl_2$(*P,S*)] complex. *Reagents and conditions:* (i) 1 eq. ligand **14a**, acetone-d_6, dichloromethane-d_2 or benzene-d_6, 24 h.

Unfortunately, after 24 hours reaction time the NMR spectra showed an intractable mixture of products in every case, with at least three different phosphorus-containing compounds evident from the ^{31}P NMR spectra. These results are in contrast to the usual reactivity of phosphine-thioether ligands; a recent literature survey (March 2014) revealed over 60 examples of chelated [$PdCl_2$(*P,S*)] complexes, many of which were formed from the palladium precursors [$PdCl_2$(1,5-cyclooctadiene)], [$PdCl_2(NCMe)_2$] or [$PdCl_2(NCPh)_2$].

Interestingly, when the orange solution resulting from the [$PdCl_2(NCBu^t)_2$] reaction was heated to 50 °C overnight, orange crystals (complex **43**) formed, leaving a colourless acetone-d_6 solution. Single crystal X-ray diffraction was performed on these crystals, resulting in the structure shown in Figure 4.1. Crystallographic data are given in Table 4.1. Unfortunately, observation of the data in the RLATT program showed that the crystals were extensively twinned with more than one lattice visible, resulting in a data set of low quality. However, it is obvious from the crystal structure that complex **43** is a palladium dimer wherein *P,S* ligand **14a** has dealkylated at the sulfur atom, forming thiolate donor atoms that bridge the two palladium centres. The atoms Pd1, Cl1, P1 and S1 (and associated carbon atoms) form the asymmetric unit of the complex, with the remaining half of the dimer generated through inversion. The ^{1}H NMR spectrum of the colourless acetone-d_6 solution confirmed the presence of 2-chloro-2-methylpropane (Bu^tCl), the by-product of the reaction.

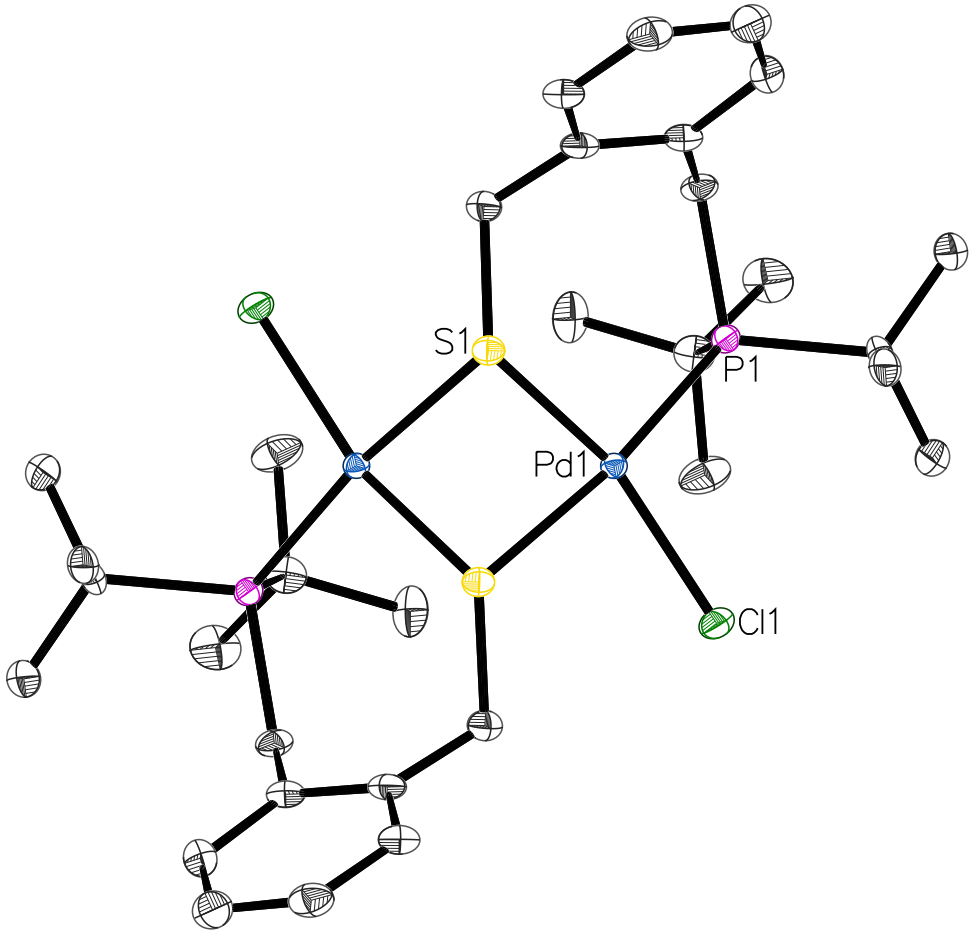

Figure 4.1 ORTEP diagram of palladium dimer **43** (50% probability thermal ellipsoids). Hydrogen atoms omitted for clarity.

The dealkylation of thioethers in hybrid ligands to form bridging thiolate dimers of this type was first published as a Nature communication in 1966.[181] In this note, Lindoy *et al.* reported that when dimethylformamide solutions of the chelated complexes $[PdBr_2(N,S)]$ (*N,S* = 8-(methylthio)quinoline) and $[PdX_2(As,S)]$ (X = Cl or Br, *As,S* = dimethyl{2-(methylthio)phenyl}arsine), amongst others, were heated, the sulfur donor atoms demethylated, forming the corresponding thiolate-bridged palladium dimers. A number of palladium halide dimers containing chelating phosphine-thiolate ligands have since been synthesised *via* dealkylation of phosphine-thioethers, either through an amine-assisted method,[182] with heating[183] or spontaneously,[112] and many others have been synthesised from the corresponding phosphine-thiol ligands.[184–186] However, there are only two related examples of C−S bond cleavage of a *t*-butyl thioether by palladium. In 2006 and 2012, Kersting and co-workers reported the reaction of three similar ligands containing $ArSBu^t$ groups with $[PdCl_2(NCMe)_2]$, resulting in C−S bond cleavage to form dimers in which the thiolate donor atoms of the tridentate *N,S,N* ligands bridged two palladium centres.[187,188]

Table 4.1 Crystallographic data of palladium dimer **43**.

Empirical formula	$\mathbf{C_{32}H_{52}Cl_2P_2Pd_2S_2}$
Formula weight	846.49
Crystal system	Monoclinic
Space group	$C2/c$
a/Å	27.7399(14)
b/Å	8.1262(4)
c/Å	15.7806 (7)
$\alpha/^\circ$	90.00
$\beta/^\circ$	95.703(2)
$\gamma/^\circ$	90.00
V/Å^3	3539.7(3)
Z	4
Cell determination reflections	9816
Cell determination range, $\theta_{\min} \longrightarrow \theta_{\max}/^\circ$	$2.6 \longrightarrow 32.7$
Temperature/K	111
Radiation type	Mo Kα
Radiation (λ)/Å	0.71073
Crystal size/ mm	$0.50 \times 0.36 \times 0.16$
D_{calc}/g m^{-3}	1.588
F(000)	1728
μ/mm^{-1}	1.40
Experimental absorption correction type	Multi-scan (SADABS)
T_{max}, T_{min}	0.747, 0.605
Reflections collected	40365, $R_{\text{equiv}} = 0.041$
Index range h	$-40 \longrightarrow 42$
Index range k	$-11 \longrightarrow 12$
Index range l	$-24 \longrightarrow 23$
θ range/$^\circ$	$2.6 \longrightarrow 32.9$
Independent reflections	5775
Reflections [$I > 2\sigma(I)$]	5463
Restraints/parameters	0/187
GOF	1.13
R_1 [$I > 2\sigma(I)$]	0.0972
wR_2 [$I > 2\sigma(I)$]	0.2719
R_1 [all data]	0.0999
wR_2 [all data]	0.2729
Residual density/e Å^{-3}	$-4.90<5.82$

The ^{1}H, ^{13}C and ^{31}P NMR spectra of a dichloromethane-d_2 solution of complex **43** display a mixture of sharp and broad peaks. For example, the ^{1}H NMR signals corresponding to the PBu^t (1.60 ppm) and CH_2S (3.32 ppm) groups are reasonably sharp; however, the peaks associated with the CH_2P moiety and one of the aromatic backbone protons are almost indistinguishable from the baseline of the spectrum. The ^{31}P NMR signal centred at 51.0 ppm is also very broad at room temperature. By analogy with the behaviour of platinum complexes of *P,S* ligand **14a** (Section 3.1), the fluxional processes responsible for these spectral features are likely to be inversion of the *P,S* ligand backbone and/or inversion at the sulfur donor atom.

The M_2S_2 bis-thiolate cores of complexes of this type are known to adopt either a hinged square-planar structure (where the angle between the two S−M−S planes

is less than 180°) or a flat square-planar structure, dependent upon the relative orientation (*syn* or *anti* respectively) of the thiolate R groups, amongst other factors.[189] Figure 4.2 shows clearly the hinged square-planar structure of the Pd_2S_2 core of complex **43**, and the *syn* arrangement of the *P,S* ligand backbones. However, this structure is not static in solution. It is known that in general the inversion of configuration at the pyramidal sulfur atom in metal complexes containing doubly-bridging thiolate ligands is relatively rapid (*ca.* 100 s^{-1}).[190] One example of this is the VT-NMR study of the diruthenium complex *trans*-$[Ru(CO)(\mu\text{-}SCH_2Ph)(\eta^5\text{-}C_5H_5)]_2$ by Killops and Knox,[191] in which broad ^{1}H NMR signals are seen over a large temperature range and attributed to inversion of the bridging thiolate ligands. This low energy barrier for inversion of the thiolate donor atom suggests that this process, coupled with an inversion of the *P,S* ligand backbone, are occurring in palladium dimer **43** on the NMR timescale.

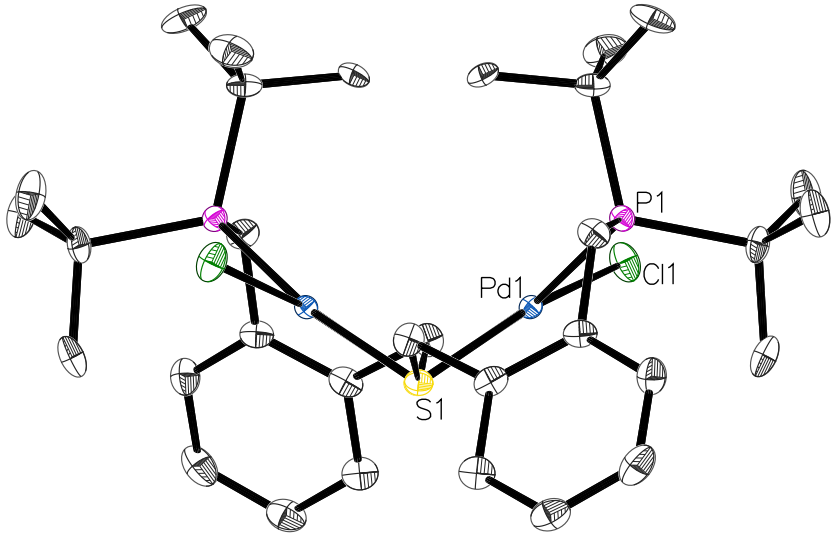

Figure 4.2 ORTEP diagram of palladium dimer **43** viewed along the S · · · S vector, showing the hinged core structure (50% probability thermal ellipsoids). Hydrogen atoms omitted for clarity.

Proton and phosphorus NMR spectra of complex **43** were collected at −60 °C, and are consistent with the presence of both hinged square-planar and flat square-planar isomers of the dimer (shown in Figure 4.3), and therefore *syn* and *anti* arrangements of the *P,S* ligand backbone respectively. The ^{31}P NMR spectrum shows two singlet peaks in an approximately 3:1 ratio, the major peak at 56.2 ppm and the minor at 37.3 ppm, indicating two different phosphorus environments. As would be expected, the ^{1}H NMR spectrum is rather complex at this temperature, due to the presence of AB systems associated with the CH_2P and CH_2S protons of the *P,S* ligand backbone in both *syn* and *anti* arrangements, and also inequivalent PBu^t groups in each form of the complex.

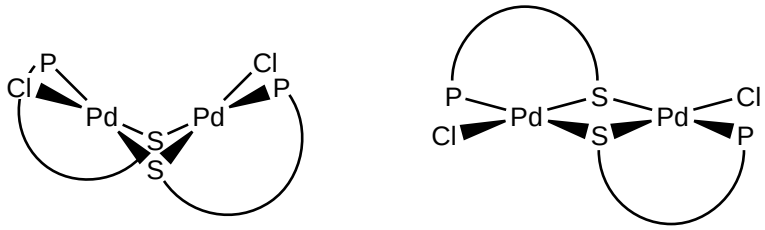

Figure 4.3 Schematic of the hinged square-planar (left) and flat square-planar (right) isomers of palladium dimer **43**.

4.1.2 [$PdMe_2$(tmeda)]

The reactivity of *P,S* ligand **14a** with other palladium(II) precursors was also investigated. Initially, one equivalent of ligand **14a** was combined with [$PdMe_2$(tmeda)] (tmeda = 1,2-bis(dimethylamino)ethane) in benzene-d_6 and the reaction monitored by ^{1}H and ^{31}P NMR spectroscopy. From the ^{31}P NMR spectra, slow conversion of the free ligand (at 25.0 ppm) into a new species with a sharp peak at 54.4 ppm was observed over a few hours. The ^{1}H NMR spectrum associated with the new species displayed virtual triplet peaks centred at 1.41 and 3.29 ppm, corresponding to the PBu^t and CH_2P protons of the new species respectively, and there was very little difference to the peaks associated with the SBu^t and CH_2S protons when compared to those of the free ligand. As seen previously in a number of platinum complexes of ligand **14a**, the observed virtual triplet peaks indicate a second-order $X_nAA'X_n'$ system,[126] and therefore the formation of a complex containing two molecules of ligand **14a** in a mutually *trans* arrangement. This was supported by the presence of unreacted [$PdMe_2$(tmeda)] in the reaction mixture, in a 1:1 ratio with the new species. Also evident in the ^{1}H NMR spectrum was the presence of ethane, indicative of a reductive elimination process to give palladium(0), and allowing the identification of the new species as linear 14-electron [Pd(*P,S*)$_2$] complex **44** (Scheme 4.2). The reaction of two equivalents of ligand **14a** with [$PdMe_2$(tmeda)] in benzene-d_6 gave near-quantitative conversion to complex **44**, ethane and free tmeda in under 24 hours.

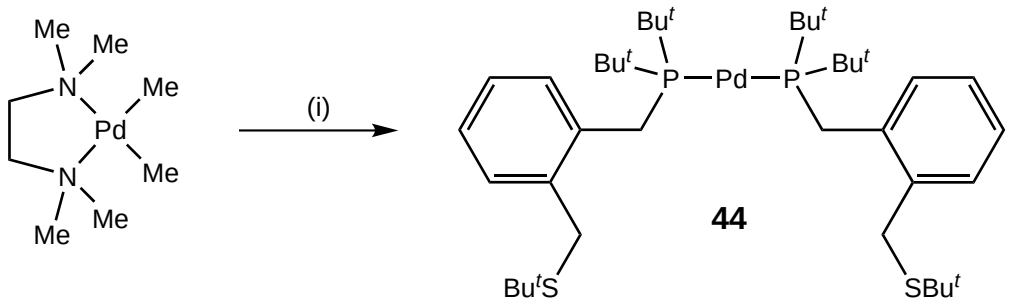

Scheme 4.2 Reaction of *P,S* ligand **14a** with [$PdMe_2$(tmeda)]. *Reagents and conditions:* (i) 1 or 2 eq. ligand **14a**, benzene-d_6, <24 h.

This reaction type has been reported previously by Krause and co-workers,[192] who used the resulting 14-electron $[Pd(PR_3)_2]$ complexes (R = Pr^i, Cy, Ph) as precursors to $[Pd(PR_3)(\eta^4\text{-1,6-diene})]$ complexes. They investigated the synthesis of $[Pd(PPr^i{}_3)_2]$ in detail, showing that at −30 °C $[PdMe_2(tmeda)]$ reacts with two equivalents of $PPr^i{}_3$, displacing tmeda to form *cis*-$[PdMe_2(PPr^i{}_3)_2]$, which eliminates ethane when heated in an inert solvent to >0 °C, forming $[Pd(PPr^i{}_3)_2]$. It is perhaps unsurprising that the desired $[PdMe_2(P,S)]$ complex was not formed from the reaction of $[PdMe_2(tmeda)]$ with ligand **14a**, as to date only one example of a complex of this type has been reported in the literature, and this complex, $[PdMe_2(Ph_2PC_2H_4SMe)]$, was synthesised by reaction of the dichloride analogue with methyllithium.[193] Interestingly, the situation is very similar with the corresponding platinum complexes. Only two examples of these, $[PtMe_2(Ph_2PC_2H_4SMe)]$[194] and $[PtMe_2\{o\text{-}C_6H_4(CH_2PPh_2)(SMe)\}]$,[195] have been reported. Both of these were synthesised by reaction of the appropriate phosphine-thioether ligand with $[PtMe_2(1,5\text{-cyclooctadiene})]$, and in the case of $[PtMe_2(Ph_2PC_2H_4SMe)]$, also by reaction of the dichloride analogue with methyllithium. However, it is noted that $[PtMe_2(Ph_2PC_2H_4SMe)]$ is unstable in acetone-d_6, converting to a solvated mono-methyl derivative over a number of hours.*

4.1.3 $[Pd(OAc)_2]$

The third palladium(II) precursor to be investigated was $[Pd(OAc)_2]$. Although there are no reported $[Pt(OAc)_2(P,S)]$ complexes, palladium diacetate complexes of thioether[196,197] and chelating diphosphine[198,199] ligands are known, and as $[Pd(OAc)_2]$ is widely used as a part of precursor mixtures for homogeneous catalysts, an understanding of the coordination behaviour of phosphine-thioether ligand **14a** with this precursor was considered beneficial to the subsequent catalytic studies.

When $[Pd(OAc)_2]$ was combined with one equivalent of ligand **14a** in benzene-d_6, a yellow solution was produced, and the formation of a small number of benzene-insoluble crystals was observed almost immediately. The single crystal X-ray structure identified these crystals as containing palladium hexamer **45** (shown in Figure 4.4) with a large amount of benzene solvate (nine benzene molecules *per* hexamer). Crystallographic data are given in Table 4.2 and Table 4.3, and Figure 4.5 shows the unit cell viewed along the *b* and *c* axes, showing the layers of benzene solvate molecules present in the crystal. Complex **45** contains six palladium

*The synthesis of a $[PtMe_2(P,S)]$ complex from ligand **14a** was attempted using $[PtMe_2(1,5\text{-hexadiene})]$, and by reaction of $[PtCl_2(P,S)]$ complex **21** with MeLi, Me_2Zn and MeMgBr. All attempts resulted in intractable mixtures of products, including a number of species containing hydride ligands.

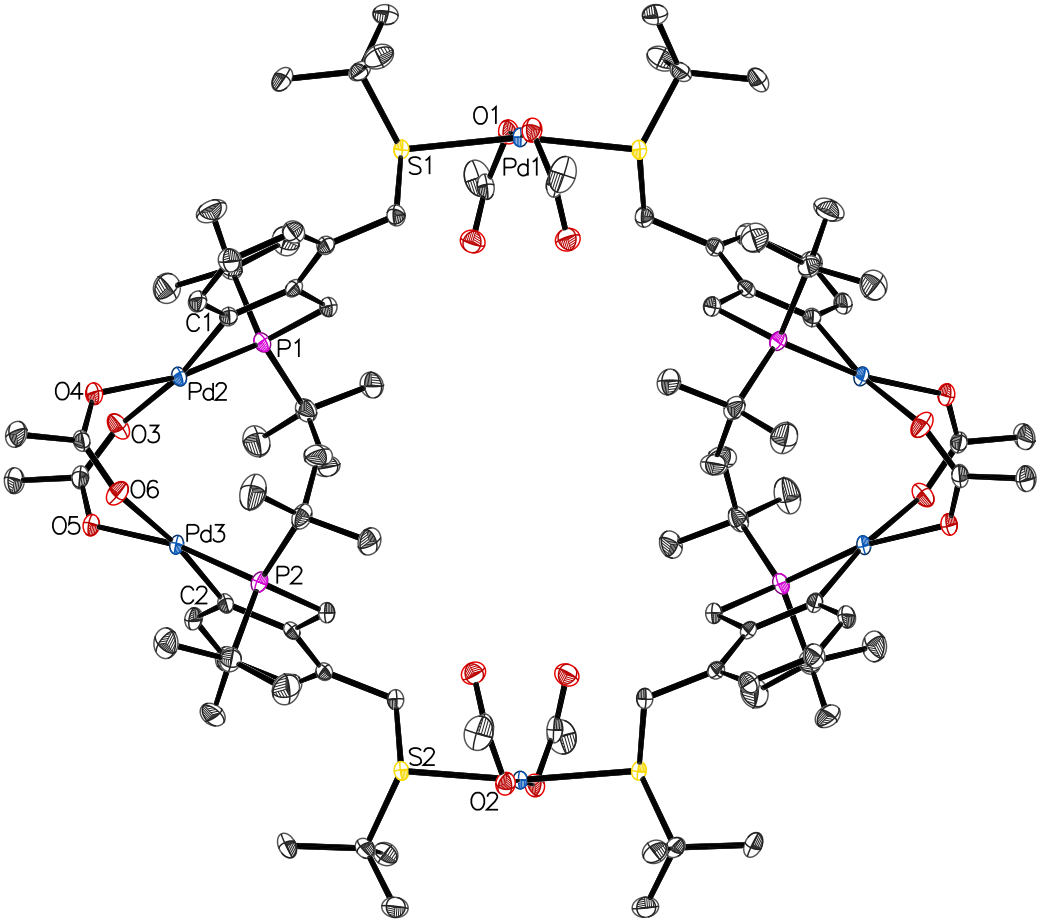

Figure 4.4 ORTEP diagram of palladium hexamer **45** (50% probability thermal ellipsoids). Benzene solvate and hydrogen atoms omitted for clarity.

atoms, four molecules of *P,S* ligand **14a** and eight acetate ligands. The palladium atoms inhabit two different coordination environments: two sites in which the palladium atom is ligated by two sulfur atoms and two terminal acetate ligands in a *trans* arrangement, and four sites in which the palladium atom forms part of a *P,C* metallacycle, with bridging acetate ligands completing the coordination sphere. The atoms between Pd1 and O2 (Figure 4.4) form the asymmetric unit of the complex, with the remaining half of the hexamer generated through inversion.

There are many examples of metallation of the aromatic ring in benzyldialkylphosphines (and similar ligands) in palladium complexes, and complexes of this type are usually synthesised by combining one equivalent of the phosphine with a palladium precursor (including $[Pd(OAc)_2]$) in an inert solvent and stirring at room temperature,[200,201] or with the addition of heat.[202,203] These palladacycles have recently shown good activity as catalysts for a range of transformations including the Heck reaction[202,204] and the amination of aryl chlorides.[200] However, to date

Table 4.2 Crystallographic data of palladium hexamer **45**.

Empirical formula	$\mathbf{C_{96}H_{160}O_{16}P_4Pd_6S_4.9\,C_6H_6}$
Formula weight	3163.72
Crystal system	Orthorhombic
Space group	*Pbcn*
a/Å	28.5619(2)
b/Å	22.6496(3)
c/Å	23.3198(2)
$\alpha/^\circ$	90.00
$\beta/^\circ$	90.00
$\gamma/^\circ$	90.00
V/Å^3	15086.0(3)
Z	4
Cell determination reflections	24873
Cell determination range, $\theta_{\min} \longrightarrow \theta_{\max}/^\circ$	$3.9 \longrightarrow 73.6$
Temperature/K	120
Radiation type	Cu Kα
Radiation (λ)/Å	1.54184
Crystal size/ mm	$0.31 \times 0.25 \times 0.15$
D_{calc}/g m^{-3}	1.393
F(000)	6568
μ/mm^{-1}	7.03
Experimental absorption correction type	Multi-scan (SCALE3 ABSPACK)
$T_{\max}$, $T_{\min}$	1.000, 0.609
Reflections collected	52344, $R_{\text{equiv}} = 0.032$
Index range h	$-24 \longrightarrow 35$
Index range k	$-27 \longrightarrow 26$
Index range l	$-25 \longrightarrow 28$
θ range/$^\circ$	$3.1 \longrightarrow 73.9$
Independent reflections	14880
Reflections [$I > 2\sigma(I)$]	13246
Restraints/parameters	0/834
GOF	1.06
R_1 [$I > 2\sigma(I)$]	0.0278
wR_2 [$I > 2\sigma(I)$]	0.0682
R_1 [all data]	0.0331
wR_2 [all data]	0.0722
Residual density/e Å^{-3}	$-1.19<0.65$

Table 4.3 Selected bond distances and angles of palladium hexamer **45**.

Bond distances (Å)		**Bond angles (°)**	
Pd1−S1	2.3312(6)	S1−Pd1−O1	86.72(4)
Pd1−S2	2.3299(6)	S1−Pd1−O2	94.00(4)
Pd1−O1	2.0158(16)	S1−Pd1−S2	168.21(3)
Pd1−O2	2.0135(16)	O1−Pd1−O2	173.00(9)
Pd2−P1	2.2187(5)	P1−Pd2−C1	82.69(6)
Pd2−C1	2.000(2)	P1−Pd2−O3	97.02(4)
Pd2−O3	2.1165(16)	C1−Pd2−O4	94.00(8)
Pd2−O4	2.1267(15)	O3−Pd2−O4	85.03(6)
Pd3−P2	2.2235(5)	P2−Pd3−C2	82.38(6)
Pd3−C2	1.999(2)	P2−Pd3−O6	97.55(4)
Pd3−O5	2.1402(15)	C2−Pd3−O5	94.14(7)
Pd3−O6	2.1222(15)	O5−Pd3−O6	84.86(6)
Pd2 $\cdots$ Pd3	3.3879(3)		
Pd1 $\cdots$ Pd1′	12.5257(4)		

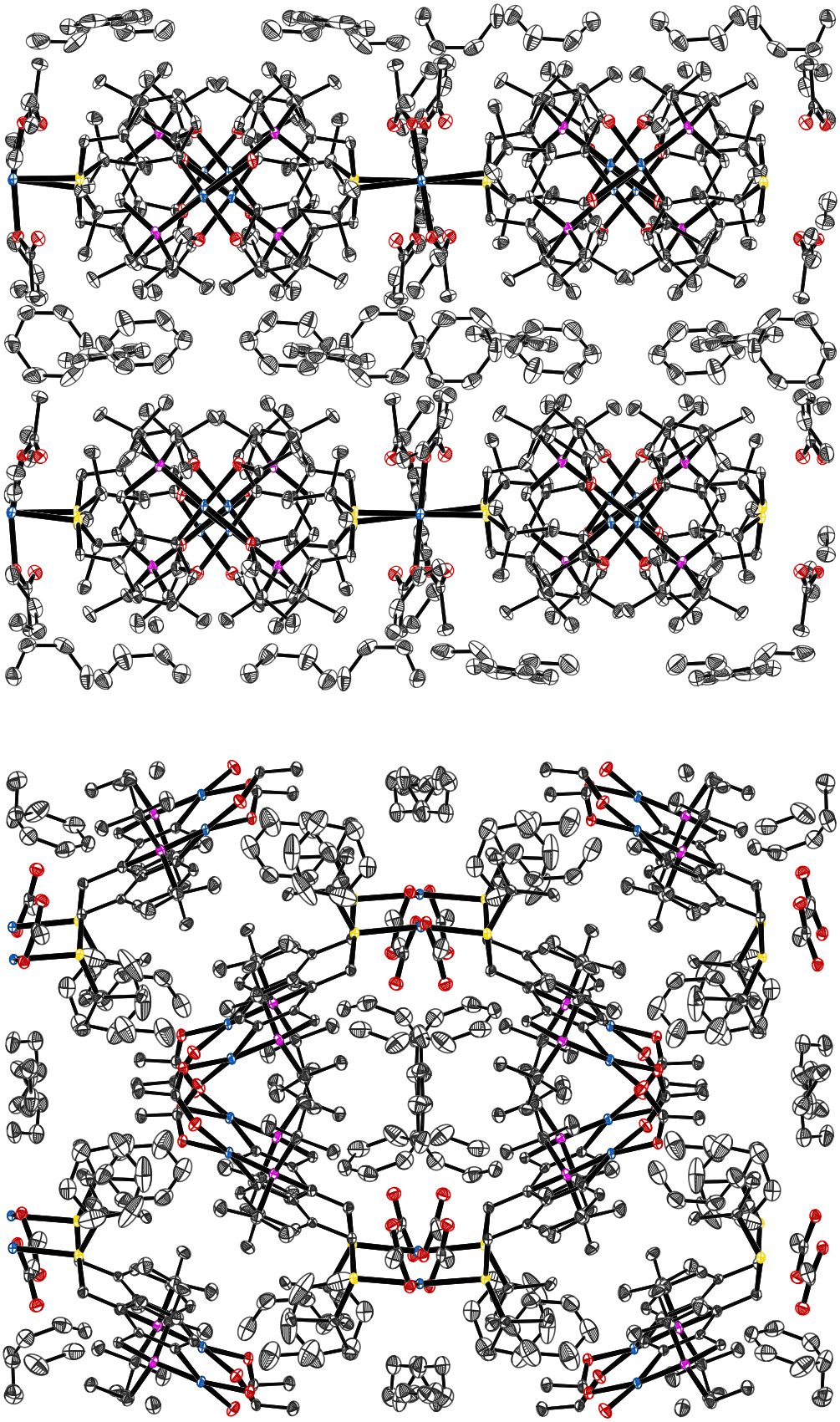

Figure 4.5 ORTEP diagram of palladium hexamer **45** unit cell viewed along the *b* axis (top) and *c* axis (bottom) (50% probability thermal ellipsoids). Hydrogen atoms omitted for clarity.

there are no published crystal structures of palladacycle dimers of this type with bridging acetate ligands.

The crystal structure that most closely resembles the $Pd_2(\mu\text{-}OAc)_2(P,C)_2$ moieties of complex **45** is the palladium dimer $[Pd(\mu\text{-tfa})\{C_6H_4(CH_2PPr^i{}_2)\}]_2$ (tfa = trifluoroacetate), shown in Figure 4.6.[203] The Pd−P, Pd−C and Pd−O distances in this complex are almost identical to those in complex **45**, and the bond angles surrounding each palladium atom are also very similar (the largest divergence is the *cis* P−Pd−O angles: 100.24(10)° and 100.91(11)° in $[Pd(\mu\text{-tfa})\{C_6H_4(CH_2PPr^i{}_2)\}]_2$ *vs.* 97.02(4)° and 97.55(4)° in complex **45**). The biggest difference between the two crystal structures is in the Pd · · · Pd distances, 3.066(8) Å in $[Pd(\mu\text{-tfa})\{C_6H_4(CH_2PPr^i{}_2)\}]_2$ compared with 3.388(1) Å in complex **45**. The larger Pd · · · Pd separation in complex **45** is likely to be primarily due to the greater steric requirements of the *endo* PBu^t groups in the *P,S* ligands when compared with the equivalent Pr^i groups in the benzyldi-*i*-propylphosphine ligands, and may also reflect the requirements of the ring structure of complex **45**.

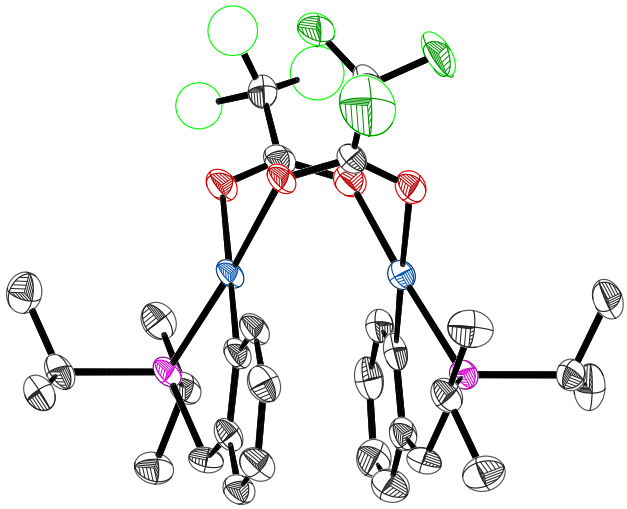

Figure 4.6 ORTEP diagram of $[Pd(\mu\text{-tfa})\{C_6H_4(CH_2PPr^i{}_2)\}]_2$ (50% probability thermal ellipsoids). Hydrogen atoms omitted for clarity.

Similarly, there is only one published crystal structure that resembles the $Pd(OAc)_2(SR_2)_2$ moieties in complex **45**, that of *trans*-$[Pd(OAc)_2(tht)_2]$ (tht = tetrahydrothiophene).[197] The Pd−S and Pd−O bond lengths in *trans*-$[Pd(OAc)_2(tht)_2]$ (2.318(1) Å and 2.015(2) Å respectively) are virtually identical to those in complex **45**, and likewise the S−Pd−O angles are very similar (87.11(7)° and 92.89(7)° in *trans*-$[Pd(OAc)_2(tht)_2]$ *vs.* 86.72(4)° and 94.00(4)° in complex **45**). The only real difference between the two crystal structures is the slight deviation of the Pd−S and Pd−O bonds from the plane in complex **45**. The S−Pd−S and O−Pd−O bond angles in *trans*-$[Pd(OAc)_2(tht)_2]$ are 180.00(12)°, as would be expected for a square

planar complex; however, the S−Pd−S and O−Pd−O bond angles in complex **45** are 11.79(3)° and 7.00(9)° removed from 180° respectively. Again, this is likely due to the requirements of the ring structure of complex **45**.

Metallation of the aromatic backbone of *P,S* ligand **14a** has also been observed in platinum complexes of this ligand. Over time, the [Pt(η^2-alkene)(κ^2*P,S*-**14a**)] complexes (alkene = bcp, mcp) briefly mentioned in Section 3.3 convert to the geometric isomers of the [Pt(allyl)(*P,C*)] complexes shown in Scheme 4.3.[147] Experimental evidence suggests that this conversion proceeds *via* dissociation of the sulfur donor atom, followed by *ortho*-metallation of the *P,S* ligand backbone and transfer of the resulting hydride to the alkene ligand.

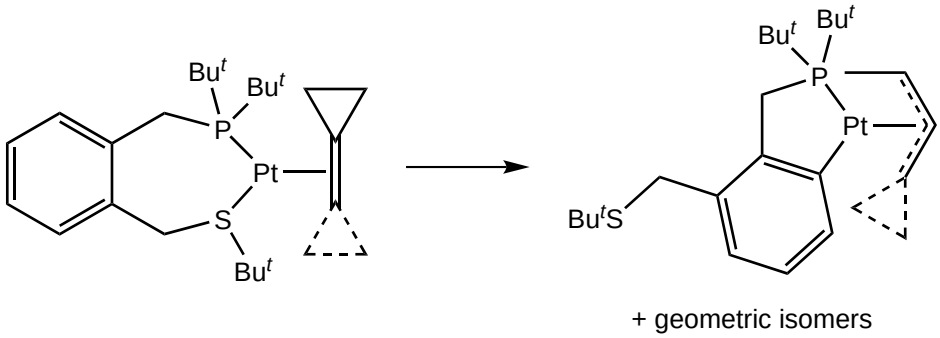

Scheme 4.3 Formation of [Pt(allyl)(*P,C*)] complexes from *P,S* ligand **14a**. Dashed lines denote the second cyclopropyl group present in bcp.

Analysis of the ^{1}H and ^{31}P NMR spectra associated with the mother liquor of palladium hexamer **45** showed a benzene-soluble species (**46**) containing *P,S* ligand **14a** and [Pd(OAc)$_2$] in a 1:1 ratio was present in solution, indicating that the formation of complex **45** was due to the use of a slight excess of [Pd(OAc)$_2$] in the reaction. The ^{1}H NMR spectrum of the initial solution displayed one broad signal centred at 1.84 ppm corresponding to all the acetate ligands in solution (*i.e.* an acetate to ligand **14a** ratio of 2:1, consistent with the ratio of starting materials); however, when the solution was subjected to high vacuum and then redissolved in benzene-d_6, the peak at 1.84 ppm was replaced by a slightly sharper signal centred at 2.15 ppm with half the intensity of the previous peak, indicating that complex **46** actually contains an acetate to ligand **14a** ratio of 1:1. As the ^{1}H NMR chemical shift of acetic acid in benzene-d_6 is 1.52 ppm,[205] these results show that the initial solution in fact contained a 1:1 mixture of acetic acid and acetate ligands exchanging rapidly on the NMR timescale at room temperature.

The presence of acetic acid in solution suggested that metallation of *P,S* ligand **14a** had occurred, and this was confirmed by the associated ^{1}H and ^{13}C NMR data. The ^{1}H NMR spectrum of complex **46** displays only three signals associated

with aryl protons, in a 1:1:1 ratio; and one of these, centred at 7.82 ppm (in toluene-d_8, only a broad singlet is observed in benzene-d_6), shows a 3.9 Hz coupling to phosphorus (established *via* a phosphorus-decoupled ^{1}H NMR experiment), which is not normally observed in complexes of ligand **14a**. Similarly, the ^{13}C NMR spectrum in benzene-d_6 displays a downfield signal at 150.6 ppm, identified through 2D NMR data as the aryl carbon atom situated *ortho* to the $CH_2PBu^t{}_2$ moiety of ligand **14a**, and consistent with the shifts of the equivalent carbon atoms in the *ortho*-metallated platinum complexes shown in Scheme 4.3 (*ca.* 157 ppm[147]) and $[Pd(\mu\text{-tfa})\{C_6H_4(CH_2PPr^i{}_2)\}]_2$ (148.1 ppm[203]).

The bonding mode of the acetate ligands in complex **46** was established through infrared spectroscopy. It is known that the difference between the C−O and C=O infrared stretching frequencies (Δ) in carboxylate complexes is dependent upon the bonding mode of the carboxylate ligand.[206] In general, Δ >200 cm^{-1} for monodentate (terminal) carboxylate ligands, whereas Δ <200 cm^{-1} for bridging carboxylate ligands. The infrared spectrum of complex **46** displays strong bands at 1414 and 1593 cm^{-1} (Δ = 179 cm^{-1}), very similar to the those of the bridging acetate ligands in the related complex $[Pd(OAc)(\mu\text{-OAc})(PPh_3)]_2$ (1411 and 1580 cm^{-1}, Δ = 169 cm^{-1}),[207] and confirms the identity of complex **46** as the $[Pd(\mu\text{-OAc})(P,C)]_2$ dimer shown in Scheme 4.4. The infrared spectrum of palladium hexamer **45** was also collected, and displays very similar bands at 1418 and 1594 cm^{-1} (Δ = 176 cm^{-1}), associated with the bridging acetate ligands. Bands associated with the terminal acetate ligands of complex **45** are also observed in this spectrum, at 1302 and 1638 cm^{-1} (Δ = 336 cm^{-1}). Again, these values are similar to those associated with the terminal acetate ligands in $[Pd(OAc)(\mu\text{-OAc})(PPh_3)]_2$ (1314 and 1629 cm^{-1}, Δ = 315 cm^{-1}).[207]

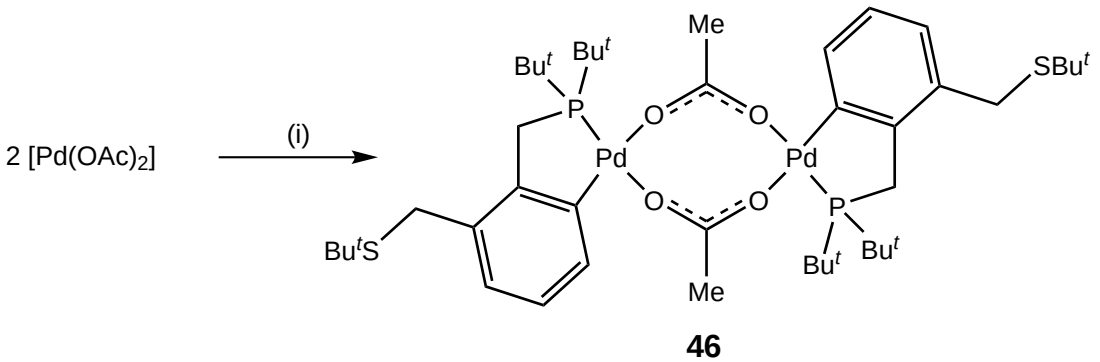

46

Scheme 4.4 Synthesis of palladium dimer **46**. *Reagents and conditions:* (i) 2 eq. ligand **14a**, benzene-d_6, 10 min, >90% conversion.

The *trans* geometry of palladium dimer **46** has been assigned by analogy with the hinged structures observed in $[Pd(\mu\text{-tfa})\{C_6H_4(CH_2PPr^i{}_2)\}]_2$ (Figure 4.6) and

the $Pd_2(\mu\text{-OAc})_2(P,C)_2$ moieties of complex **45** (Figure 4.4); however, this static structure is inconsistent with the NMR spectra at room temperature. The ^{1}H NMR spectrum of complex **46** displays one doublet for all the CH_2P protons (at 3.25 ppm) and also one doublet for all the PBu^t groups (at 1.24 ppm). As the hinged structures shown in Figure 4.4 and Figure 4.6 contain distinct *exo* and *endo* environments for these protons, the NMR data suggest a facile dynamic process that exchanges these proton environments, likely *via* exchange of the bridging acetates. This type of process has been proposed previously for related structures,[202,208] and would be consistent with the broadness of the ^{31}P NMR signal (at 96.8 ppm) and a number of signals in the ^{13}C NMR spectrum (including the acetate carbonyl signal at 179.8 ppm), and the previously mentioned facile exchange of the acetate ligands in complex **46** with acetic acid in solution.

VT-NMR spectra of palladium dimer **46** were collected at 20 °C intervals between 20 and −80 °C in toluene-d_8. The region between 1.0 and 3.5 ppm of the ^{1}H NMR spectra is shown in Figure 4.7 (there is no variation in the aromatic region of the spectra over this temperature range). The 20 °C spectrum shows the doublet signal associated with the CH_2P protons centred at 3.21 ppm and the singlet associated with the CH_2S protons at 3.54 ppm. These signals persist down to −40 °C, and below this temperature broadening and separation of these peaks is observed, indicating the coalescence of the aforementioned dynamic process that exchanges the environments of these protons. The protons of the Bu^t groups (1.0–1.3 ppm) are affected in a similar manner as the solution is cooled. The broad signal corresponding to the acetate ligand protons (2.13 ppm at 20 °C) sharpens and moves to slightly lower field as the solution is cooled (to 2.32 ppm at −80 °C), consistent with the cessation of the exchange process associated with these ligands at low temperature.

4.2 Reactions with Pd(0) Precursors

4.2.1 $[Pd(nb)_3]$

The reaction of one equivalent of phosphine-thioether ligand **14a** with $[Pd(nb)_3]$ immediately resulted in the formation of a new complex with a sharp ^{31}P NMR signal at 56.5 ppm, and a mixture of sharp and broad signals in the ^{1}H and ^{13}C NMR spectra. Analysis of the 2D NMR spectra of the new species identified the sharp peaks as being associated with coordinated ligand **14a**. The downfield shift of the ^{31}P NMR signal (*cf.* 25.0 ppm in the free ligand) and the difference in shift of the peaks associated with the SBu^t and CH_2S protons when compared with

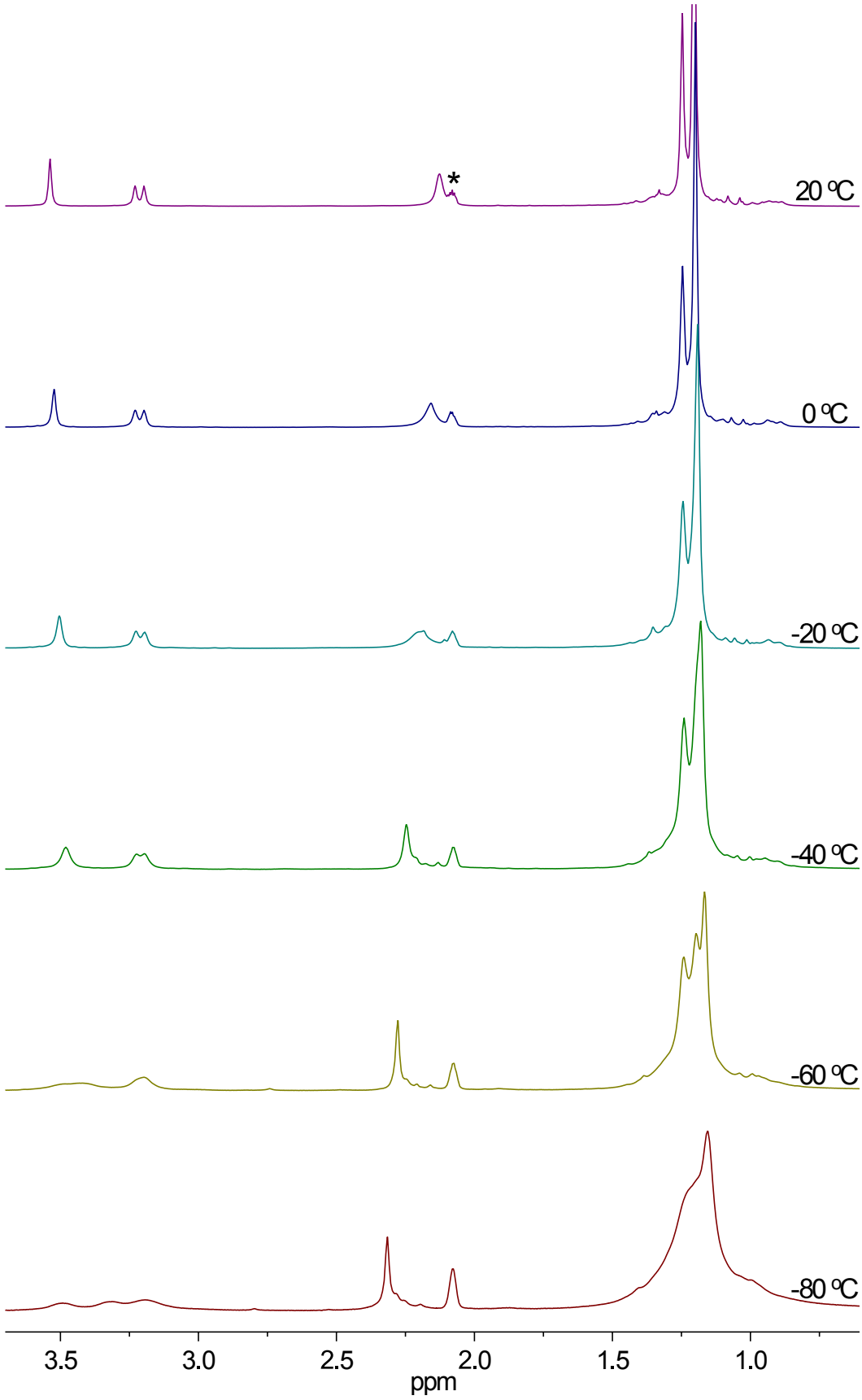

Figure 4.7 ^{1}H NMR spectra of palladium dimer **46** collected between 20 and −80 °C in toluene-d_8. Asterisk denotes solvent peak.

the free ligand (1.44 and 3.88 ppm *vs.* 1.29 and 4.05 ppm in the free ligand) indicated chelation of ligand **14a** to the palladium centre. Comparison of the ^{1}H and ^{13}C NMR spectra of the new complex with those of free norbornene, [Pt(nb)(*P,S*)] complex **34** and the published complex [Pd(nb)(dbpx)][15] allowed identification of the broad signals as free norbornene and an η^2-bound norbornene ligand, and hence the identity of the new species as [Pd(nb)(*P,S*)] complex **47** (shown in Scheme 4.5). Unfortunately, the lack of 2D NMR data and coupling information precluded unequivocal assignment of each peak associated with the norbornene ligand carbons and protons; however, the broad ^{13}C NMR signal at 66.9 ppm is sufficiently similar to that of [Pd(nb)(dbpx)] (65.4 ppm) to identify it as corresponding to the alkene carbon atoms, and indicates that the norbornene ligand binding in these two complexes is comparable. Complex **47** can also be synthesised by combining one equivalent of ligand **14a** with [Pd(C_5H_5)(allyl)] and norbornene in benzene-d_6.

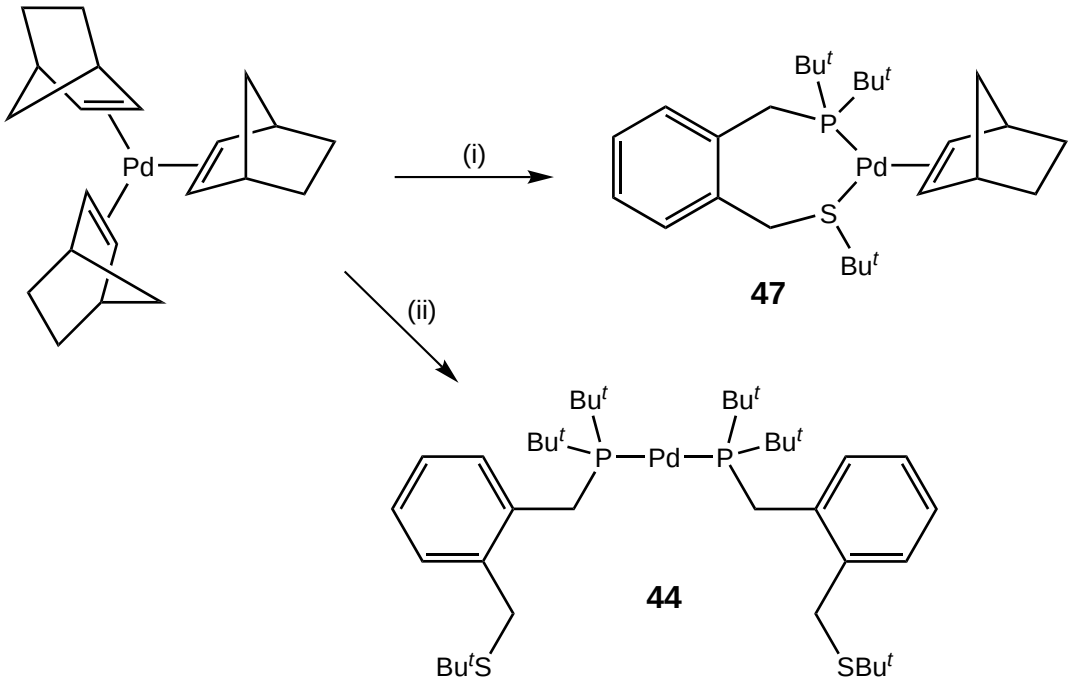

Scheme 4.5 Reactions of *P,S* ligand **14a** with [Pd(nb)$_3$]. *Reagents and conditions:* (i) 1 eq. ligand **14a**, benzene-d_6, 10 min, quantitative conversion; (ii) 2 eq. ligand **14a**, benzene-d_6, 10 min, quantitative conversion.

The ^{1}H NMR data associated with complex **47** show that two dynamic processes are occurring rapidly on the NMR timescale. Firstly, the broad shape of the NMR signals corresponding to the η^2-norbornene ligand and free norbornene in solution indicate that, unlike the static norbornene ligand in the platinum analogue **34**, these norbornene molecules are exchanging rapidly at room temperature. In the presence of free norbornene, solutions of complex **47** are stable over a period of days; however, in the absence of free norbornene, the complex degrades to [Pd(*P,S*)$_2$] complex **44**

and palladium black within a few hours. Also, the signal at 3.88 ppm associated with the CH_2S protons is a singlet, indicating that the sulfur inversion process is rapid on the NMR timescale at room temperature.

The reaction of two equivalents of phosphine-thioether ligand **14a** with $[Pd(nb)_3]$ resulted in the formation of the previously described complex **44** (Scheme 4.5). In contrast to the platinum analogue **36** ($[Pt(P,S)_2]$), in which the second equivalent of ligand **14a** gradually displaced the norbornene ligand and sulfur donor atom from [Pt(nb)(*P,S*)] complex **34** over a number of hours, complex **44** formed immediately. This is consistent with the observed lability of the norbornene ligand in complex **47**, and the generally lessened stability of palladium complexes when compared with their platinum analogues.

4.2.2 $[Pd_2(dba)_3]$

A different reaction pathway was observed for the reaction of *P,S* ligand **14a** with $[Pd_2(dba)_3]$ (dba = *trans,trans*-dibenzylideneacetone). A benzene-d_6 solution of ligand **14a** was combined with a benzene-d_6 solution containing half an equivalent of $[Pd_2(dba)_3]$ (Scheme 4.6), and the reaction followed by ^1H and ^{31}P NMR methods. Initially, the NMR spectra showed complete conversion of ligand **14a** to $[Pd(P,S)_2]$ complex **44**, with free dba and $[Pd_2(dba)_3]$ also present in solution. Over time, a new species formed, identified by a broad signal in the ^{31}P NMR spectrum at 59.1 ppm and a number of broad signals in the ^1H NMR spectrum. Analysis of the ^1H NMR data showed that the protons of the PBu^t groups correlate to two broad signals at 0.91 and 1.27 ppm, and similarly, the CH_2S protons are observed as two broad signals at 3.49 and 3.71 ppm, consistent with binding of both the phosphorus and sulfur donor atoms to the palladium centre. The presence of two further broad peaks in the ^1H NMR spectrum at 4.80 and 4.87 ppm, each integrating for one proton, indicates η^2 binding of one of the dba double bonds to the palladium centre. These shifts are similar to those observed for the η^2-bound double bond protons in [Pd(dba)(dbpx)][65] (at 4.3 and 4.6 ppm) and a [Pd(dba)(*P,N*)] complex[209] (at 4.99 and 5.51 ppm). The high resolution mass spectrum of this complex confirmed the presence of palladium, ligand **14a** and dba in a 1:1:1 ratio. This data allowed identification of the new species as [Pd(dba)(*P,S*)] complex **48**, shown in Scheme 4.6. The reaction pathway observed for the formation of complex **48** from $[Pd_2(dba)_3]$ (*via* $[Pd(P,S)_2]$ complex **44**) has previously been reported for the reaction of $[Pd(dba)_2]$ with dbpx[65] and a number of other diphosphine ligands.[210]

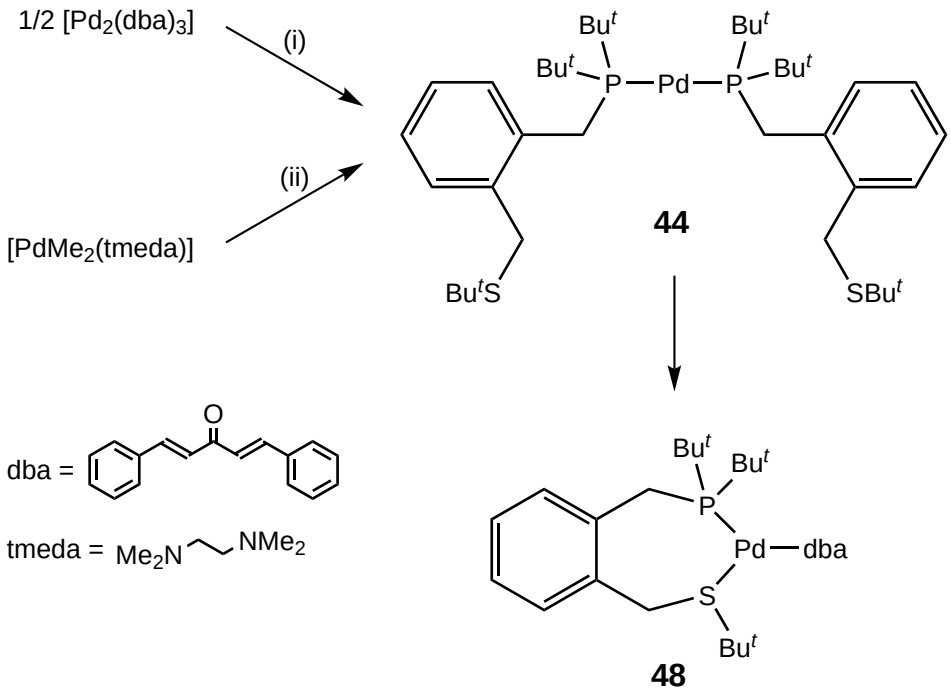

Scheme 4.6 Synthesis of [Pd(dba)(*P,S*)] complex **48**. *Reagents and conditions:* (i) 1 eq. ligand **14a**, benzene-d_6, 24 h, >95% conversion; (ii) 1 eq. ligand **14a**, 1 eq. dba, benzene-d_6, 5 days, >95% conversion.

Unfortunately, all attempts to separate the free dba by-product from complex **48** were unsuccessful, and so a second method for the synthesis of this complex was developed. As the reaction of *P,S* ligand **14a** with [$PdMe_2$(tmeda)] was known to produce [Pd(*P,S*)$_2$] complex **44** (Scheme 4.2), [$PdMe_2$(tmeda)] was combined with ligand **14a** and dba in a 1:1:1 ratio in benzene-d_6, and the reaction monitored by ^{1}H and ^{31}P NMR spectroscopy (Scheme 4.6). Initially, formation of the intermediate complex **44** was observed, followed by slow dissociation of one of the *P,S* ligands from this species to give free ligand **14a** and [Pd(dba)(*P,S*)] complex **48** in a 1:1 ratio. This methodology gave >95% conversion to desired complex **48** over 5 days. The volatiles (tmeda, ethane and benzene-d_6) were removed from the reaction mixture under reduced pressure to give slightly impure complex **48** as a red powder, which was then dissolved in toluene-d_8, and ^{1}H and ^{31}P VT-NMR spectra of the complex collected between 50 and −70 °C (Figure 4.8).

The VT-NMR spectra shown in Figure 4.8 indicate the presence of two dynamic processes in complex **48**, with coalescence temperatures of near room temperature and between −30 and −50 °C respectively. The dynamic process with a coalescence point near room temperature causes no change (other than signal broadening) in the ^{31}P NMR spectrum, but in the ^{1}H NMR spectrum a number of changes are observed. At 50 °C, there is one signal associated with the CH_2S protons (at 3.62 ppm), but below room temperature an AB quartet with chemical shifts of 3.41 and 3.66 ppm is observed for the same protons, indicating a decrease in the

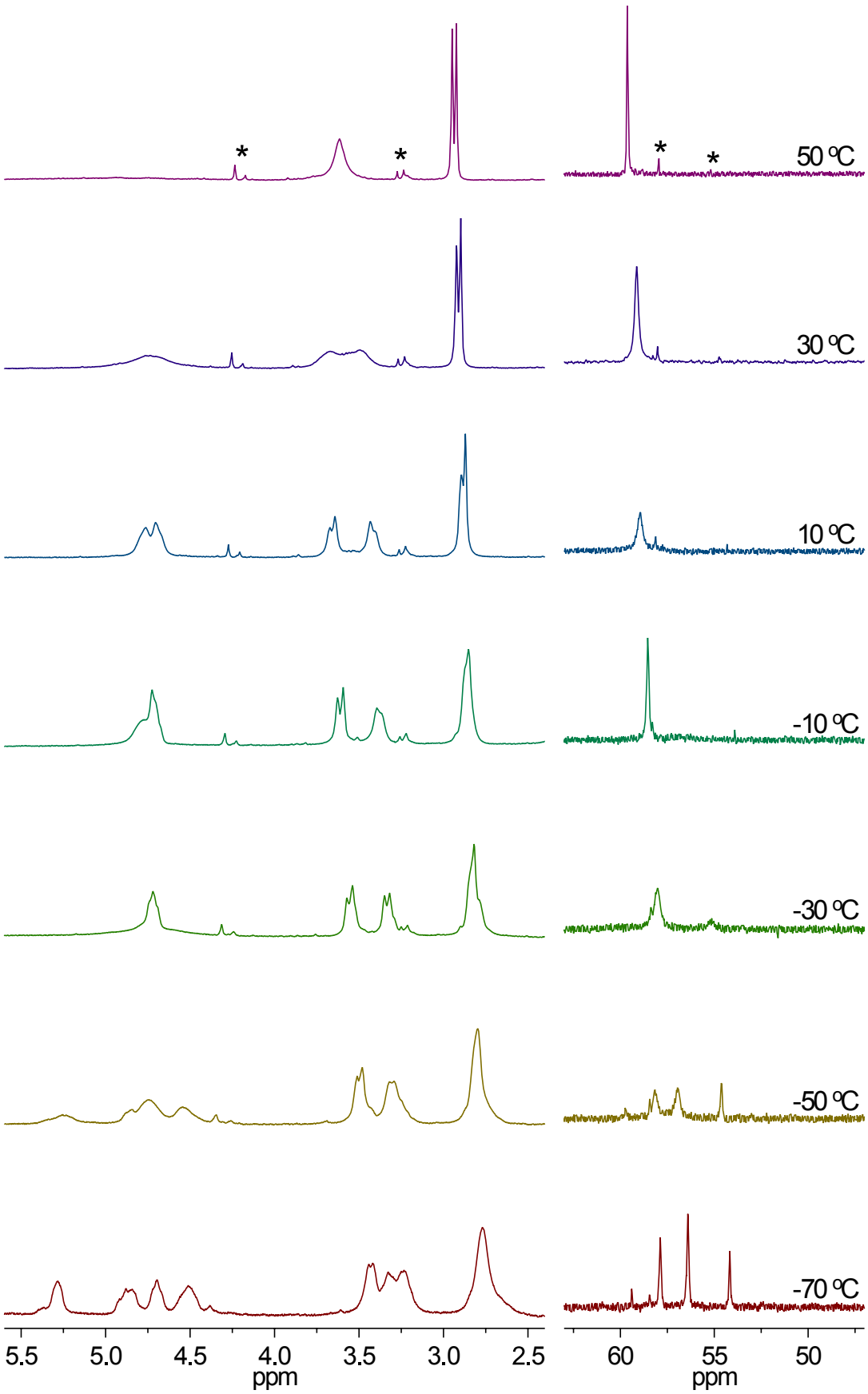

Figure 4.8 ^{1}H (left) and ^{31}P (right) NMR spectra of [Pd(dba)(*P*,*S*)] complex **48** collected between 50 and −70 °C in toluene-d_8. Asterisks denote sample impurities.

time-averaged symmetry of the complex. A similar effect is seen for the signal at 2.94 ppm corresponding to the CH_2P protons, although this doublet peak is observed to collapse rather than split into two, likely due to a coincidental overlap of the AB quartet signals. In thioether complexes, this effect is normally associated with the sulfur inversion process becoming slow on the NMR timescale. However, in the case of [Pd(dba)(*P,S*)] complex **48** this is unlikely to be the cause of the coalescence near room temperature.

It is known that the rate of sulfur inversion in palladium(II) complexes of dithioether ligands is significantly higher than that of the platinum(II) analogues,[110] and in a range of [Pd(alkene)(*N,S*)] (*N,S* = pyridine-thioether) complexes it has been reported that of all the fluxional processes present, sulfur inversion has the lowest coalescence temperature.[211] This literature evidence, and the fact that in the [Pt(alkene)(*P,S*)] complexes of ligand **14a** (**32** and **34**), the coalescence point for the sulfur inversion process is below room temperature (*ca.* −20 °C for norbornene complex **34**), suggests that the sulfur inversion process in complex **48** should be rapid until well below room temperature, and hence a different dynamic process is the cause of the decrease in time-averaged symmetry near room temperature. This is consistent with the single ^{1}H NMR peak observed for the CH_2S protons in [Pd(nb)(*P,S*)] complex **47** at room temperature. A VT-NMR study of a similar dba complex containing a hybrid ligand has been completed by Zayya,[209] on the [Pd(dba)(*P,N*)] analogue of the complexes shown in Figure 3.14. In that system, the ^{1}H NMR spectra showed a time-averaged decrease in symmetry between 80 °C and room temperature, and the change was attributed to an intramolecular alkene exchange between the coordinated and non-coordinated double bonds of the dba ligand. The same exchange process has been reported for another [Pd(dba)(*P,N*)] complex at high temperature,[212] and a [Pd(dba)(*P,P*)] complex, in which coalescence is slightly below room temperature.[213] This intramolecular alkene exchange process is also consistent with the observed VT-NMR data for complex **48**, and hence it is likely to be the cause of the coalescence point near room temperature in the present case.

The coalescence point between −30 and −50 °C shown in Figure 4.8 indicates a further decrease in time-averaged symmetry of [Pd(dba)(*P,S*)] complex **48**. At −70 °C, the ^{31}P NMR spectrum of complex **48** displays three major peaks at 54.2, 56.4 and 57.9 ppm, and a minor peak at 59.4 ppm. Similarly, at this temperature the ^{1}H NMR spectrum is quite complicated, showing a number of signals associated with the η^2-bound double bond protons of the dba ligand between 4.4 and 5.4 ppm. These data are consistent with the presence of four conformational isomers of the complex, with slow interconversion on the NMR timescale. A VT-NMR study of the

diphosphine analogue of complex **48**, [Pd(dba)(dbpx)], was reported by Sabounchei and Karamei in 2001,[65] and showed very similar results at low temperature. At −80 °C, seven sharp peaks were observed in the ^{31}P NMR spectrum, attributed to three major and one minor conformers of [Pd(dba)(dbpx)] (with one of the peaks of the minor isomer obscured). The authors rationalised the data by adapting a schematic representation proposed by Herrmann *et al.* for the conformers of the related complex [Pd(dba)(bisbi)] (bisbi = 1,1′-bis(diphenylphosphinomethyl)-2,2′-biphenyl).[214] The schematic of the four proposed conformers of [Pd(dba)(dbpx)] at low temperature is shown in Figure 4.9. These conformers are based on the two rotamers of free dba (s-*cis*,*cis* and s-*cis*,*trans*) observed in solution at room temperature,[215] and depend upon the ligand backbone inversion process that occurs in metal complexes of dbpx and rotation about the C=C−C=O single bond in the dba ligand being slow on the NMR timescale. A similar schematic could be drawn for [Pd(dba)(*P*,*S*)] complex **48**; however, as *P*,*S* ligand **14a** is less symmetric than dbpx, more conformers are possible for this system. Unfortunately, with the data available at present it is not possible to tell which conformations of the complex relate to the four signals observed in the ^{31}P NMR spectrum of complex **48** at −70 °C.

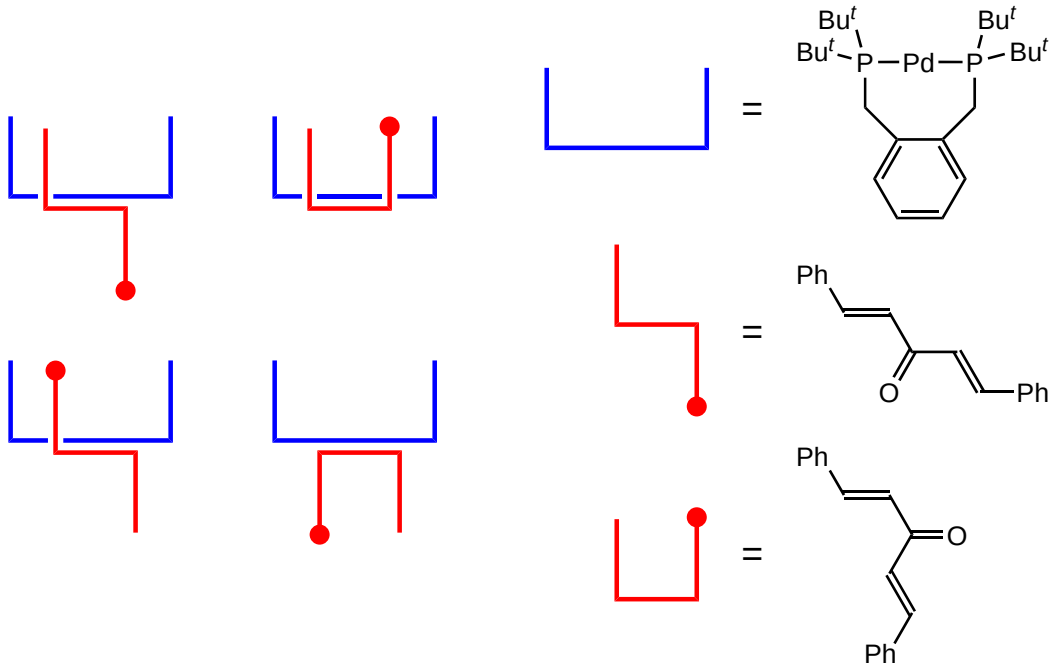

Figure 4.9 Schematic of the four proposed conformers of [Pd(dba)(dbpx)] at −80 °C.

4.3 Concluding Remarks

The coordination chemistry of hybrid *o*-xylene-based phosphine-thioether ligand **14a** with palladium(II) and palladium(0) precursors has been investigated, resulting in the identification of a number of ligand bonding modes. Reaction of *P,S* ligand **14a** with either a palladium(0) or palladium(II) precursor ($[Pd_x(alkene)_y]$ or $[PdMe_2(tmeda)]$) produced the linear 14-electron $[Pd(P,S)_2]$ complex **44**, in which *P,S* ligand **14a** displayed monodentate coordination through the phosphorus donor atom. It is likely monodentate phosphine coordination of ligand **14a** in a palladium(II) complex was also observed in the reaction with $[PdCl_2L_2]$ precursor complexes. The reaction of ligand **14a** with $[Pd_x(alkene)_y]$ also resulted in chelated [Pd(alkene)(*P,S*)] complexes **47** and **48**, either directly in the case of $[Pd(nb)_3]$, or *via* rearrangement of a mixture of $[Pd(P,S)_2]$ complex **44** and free dba.

Two examples of metallation of *P,S* ligand **14a** were observed in reactions of this ligand with palladium(II) precursors. The reaction of $[PdCl_2(NCBu^t)_2]$ with ligand **14a** at raised temperature resulted in S−C bond cleavage of the SBu^t moiety, forming thiolate-bridged palladium dimer **43**. A palladium dimer was also formed in the reaction of ligand **14a** with $[Pd(OAc)_2]$; however, in this case facile C−H activation of the aryl backbone *ortho* to the phosphorus arm of the ligand gave rise to the $[Pd(\mu\text{-OAc})(P,C)]_2$ palladacycle dimer **46**. The presence of a slight excess of $[Pd(OAc)_2]$ in this reaction resulted in another bonding mode of *P,S* ligand **14a**. Coordination of the sulfur donor atoms in two equivalents of $[Pd(\mu\text{-OAc})(P,C)]_2$ dimer **46** to two equivalents of $[Pd(OAc)_2]$ resulted in the formation of palladium hexamer **45**, with ligand **14a** adopting a bridging *P,C,S* coordination mode.

This research has identified five coordination modes of *P,S* ligand **14a** in palladium complexes:

- Monodentate binding through the phosphorus donor atom with both Pd(0) and Pd(II).
- Chelation through the phosphine and thioether moieties in Pd(0) complexes.
- Bidentate coordination through phosphine and bridging thiolate groups.
- Palladacycle formation through chelation of the phosphorus atom and aryl backbone.
- A combination of palladacycle and monodentate thioether binding resulting in bridging *P,C,S* coordination.

The versatile coordination behaviour of ligand **14a** with palladium indicates a number of binding modes could be available in palladium catalysts with this ligand.

This will potentially result in interesting and unusual catalyst behaviour, but may also exacerbate the difficulties involved in identifying and characterising the active catalytic species.

Chapter 5

Sonogashira Catalysis

5.1 Background

The Sonogashira reaction is a homogeneous palladium and copper co-catalysed C−C bond-forming reaction between an aryl or alkenyl halide (or triflate) and a terminal alkyne (or ethyne). It was first reported by Sonogashira, Tohda and Hagihara in 1975.[216] This initial communication detailed the coupling of two equivalents of iodobenzene with ethyne using 1 mol% $[PdCl_2(PPh_3)_2]$ and 0.5 mol% copper(I) iodide in diethylamine solvent. Ethyne gas was bubbled through a solution of the other reactants under a nitrogen atmosphere for six hours at room temperature, to give an 85% recrystallised yield of diphenylethyne. Under similar conditions, a range of aryl and alkenyl halides (bromides and iodides) were coupled with ethyne, phenylethyne and propargyl alcohol, producing the corresponding disubstituted alkynes in generally high yields.

In the intervening four decades, a vast number of variations on the original reaction conditions have been reported,[217–219] with a large number of ligands (including phosphines, nitrogen-based ligands, carbenes and palladacycles), palladium precursors, bases and solvents represented. The choice of substrate has also varied widely, with examples including the less reactive aryl and alkenyl chlorides, sterically hindered substrates, and the presence of a range of functional groups. There are also many examples of not strictly homogeneous catalyst systems, including palladium nanoparticles and solid-supported molecular catalysts. As functionalised arylalkynes and conjugated enynes are recurring building blocks in natural products, agrochemicals, pharmaceuticals and molecular materials for optical and electronic devices, the Sonogashira reaction plays an important role in a number of fields of

chemistry. Recent examples include the synthesis of the benzylisoquinoline alkaloids (+)-(*S*)-laudanosine and (−)-(*S*)-xylopinine,[220] the pharmaceutical Altinicline,[221] and alkynylruthenium complexes that display non-linear optical properties.[222]

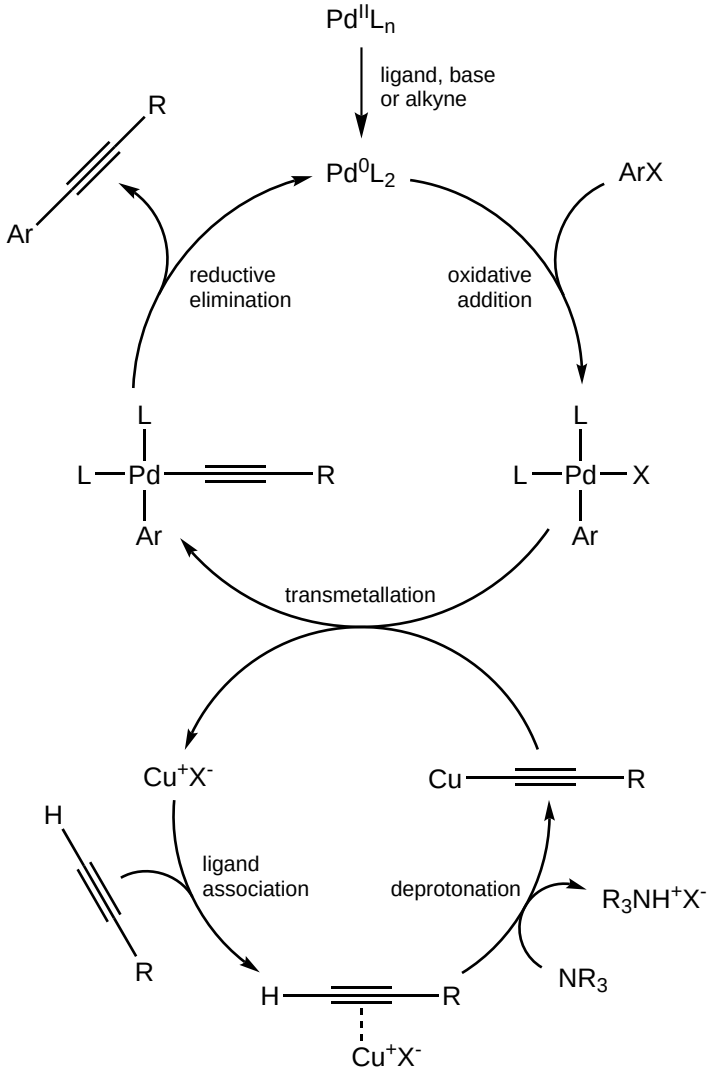

Figure 5.1 Generalised Sonogashira catalytic cycles.

The exact mechanism of the Sonogashira reaction is not well understood, but is generally accepted to take place *via* the two catalytic cycles shown in Figure 5.1.[219] The palladium-cycle is based upon classical palladium-catalysed C−C bond-forming reactions,[223] and begins with the catalytically active species $[Pd^0L_2]$. In cases where a palladium(II) pre-catalyst is used in the reaction, formation of a $[Pd^{II}(C{\equiv}CR)_2L_2]$ species, which then reductively eliminates the corresponding diyne, can yield $[Pd^0L_2]$; or $[Pd^0L_2]$ can be formed *via* the action of ligands or bases present (for example, through the conversion of an amine to an iminium cation). The first step in the palladium-cycle is oxidative addition of the aryl or alkenyl halide, which is considered to be the rate-limiting step of the Sonogashira reaction. The $[PdArXL_2]$ species formed is then converted to $[PdAr(C{\equiv}CR)L_2]$ *via* transmetallation with a

copper acetylide species formed in the copper-cycle, and reductive elimination gives the disubstituted alkyne product and re-forms [Pd^0L_2] (fast *cis-trans* isomerisation may also take place in the palladium(II) species[223]).

The copper-cycle (Figure 5.1) is poorly understood, in part due to the difficulties involved with analysing the combined action of the two metal catalysts. It is believed that the base abstracts the acetylenic proton of the terminal alkyne, forming the copper acetylide species in the presence of a copper(I) salt.[218] It should be noted that the generally employed amines tend not to be basic enough to deprotonate the alkyne, and hence an intermediate π-alkyne copper complex has been proposed, increasing the acidity of the acetylenic proton.[224] However, it has recently been shown that CuI–polyphosphine adducts can be formed in reactions of this type and ligands can be transferred between metals.[225] Therefore, copper–ligand interactions may well influence Sonogashira reactions.

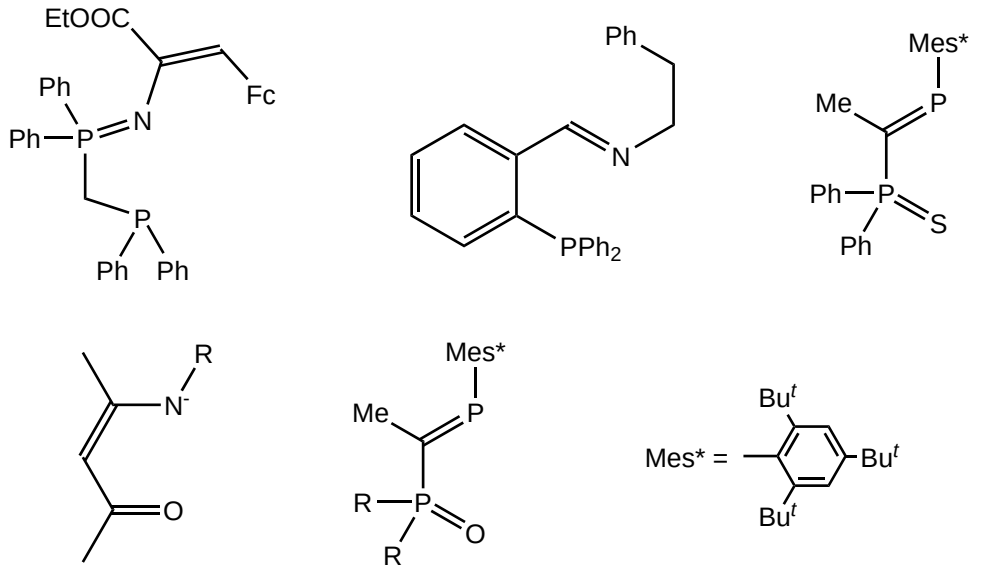

Figure 5.2 Literature hybrid ligands used in Sonogashira reactions.

There are a number of literature examples of Sonogashira coupling reactions utilising hybrid ligands. These *P,N*,[226,227] *P,S*,[228] *P,O*[229] and *N,O*[230] ligands (shown in Figure 5.2) are used in a range of pre-catalyst mixtures under various conditions, and generally display reasonable to good activity in the Sonogashira reactions chosen. However, the primary motivation for investigating the catalytic activity of phosphine-thioether ligand **14a** in the Sonogashira coupling reaction was the excellent results obtained for this type of catalysis using sterically bulky, electron-rich monophosphine ligands. The pioneering work in this area was reported by Buchwald, Fu and co-workers in 2000.[231] They investigated a number of phosphine ligands (PPh_3, P(*o*-tolyl)$_3$, 1,1′-bis(diphenylphosphino)ferrocene, PCy_3, $PBu^t{}_3$) in pre-catalyst mixtures with [$PdCl_2(NCMe)_2$] and CuI for the coupling of 4-bromoanisole

and phenylethyne. It was found that the only ligand displaying any activity was $PBu^t{}_3$ (96% yield of the desired product after two hours at room temperature). A range of alkynes and aryl bromides were also tested under these reaction conditions, and showed good to excellent yields in all cases. Similarly, Plenio and co-workers[232] showed that the bulky monophosphine ligands $PBu^t{}_3$, $PBu^t{}_2Cy$, PBu^tCy_2, $PBnBu^t{}_2$, PAd_2Bu^t and PAd_2Bn all showed good to excellent activity in pre-catalyst mixtures with Na_2PdCl_4 and CuI for the parallel multisubstrate screening of a range of aryl bromides containing different levels of steric bulk with phenylethyne. Critically for the current investigation, $PBnBu^t{}_2$ (the monophosphine analogue of phosphine-thioether ligand **14a**) displayed almost identical activity to $PBu^t{}_3$ in these reactions.

Although the first step of the palladium-cycle in the Sonogashira reaction and other Pd-catalysed C−C bond-forming reactions is generally thought to produce a $[PdArXL_2]$ species, for sterically bulky monophosphine ligands there is strong evidence that the oxidative addition step of the catalytic cycle is preceded by dissociation of one of the phosphine ligands, resulting in 14-electron, three-coordinate palladium complexes of the type $[PdArX(PR_3)]$. Hartwig[233] and Fu and co-workers[234] have provided mechanistic evidence for this, and in 2002, Stambuli, Bühl and Hartwig published the crystal structures of the T-shaped complexes $[PdBrPh(PAdBu^t{}_2)]$ and $[PdI(2,4\text{-xylyl})(PBu^t{}_3)]$ (shown in Figure 5.3).[235] Addition of diphenylamine, sodium *t*-butoxide, 4-methoxyphenylboronic acid or styrene to $[PdBrPh(PAdBu^t{}_2)]$ gave the expected C−N, C−O or C−C coupling products, and reactions of catalytic amounts of $[PdBrPh(PAdBu^t{}_2)]$ with bromobenzene and diphenylamine are kinetically comparable with palladium complexes of $PAdBu^t{}_2$ generated *in situ*. This indicates that these T-shaped complexes are likely intermediates in palladium-catalysed reactions with bulky monophosphine ligands. This study also suggested that rather than $[Pd(PR_3)_2]$, the palladium(0) catalyst may be a $Pd(PR_3)$ species stabilised by other means, for example $[Pd(dba)(PR_3)]$.

Regardless of whether the catalytically active species in Sonogashira reactions with bulky monophosphine ligands is $[Pd(PR_3)_2]$ or a $Pd(PR_3)$ species, it was envisaged that the application of phosphine-thioether ligand **14a** to this type of catalysis in a 1:1 ratio with a palladium precursor may provide a chelated Pd(*P,S*)-type active catalyst. A complex of this type would provide added stabilisation when compared with a $Pd(PR_3)$ species, but also more facile oxidative addition of an aryl halide substrate than a $[Pd(PR_3)_2]$ complex, *via* dissociation of the sulfur donor atom in ligand **14a**. The [Pd(alkene)(κ^2*P,S*-**14a**)] (alkene = nb, dba) complexes detailed in Section 4.2 confirm that chelation is a preferred bonding mode of ligand **14a** with palladium(0), and Chapter 3 provides good evidence of hemilability of ligand **14a**

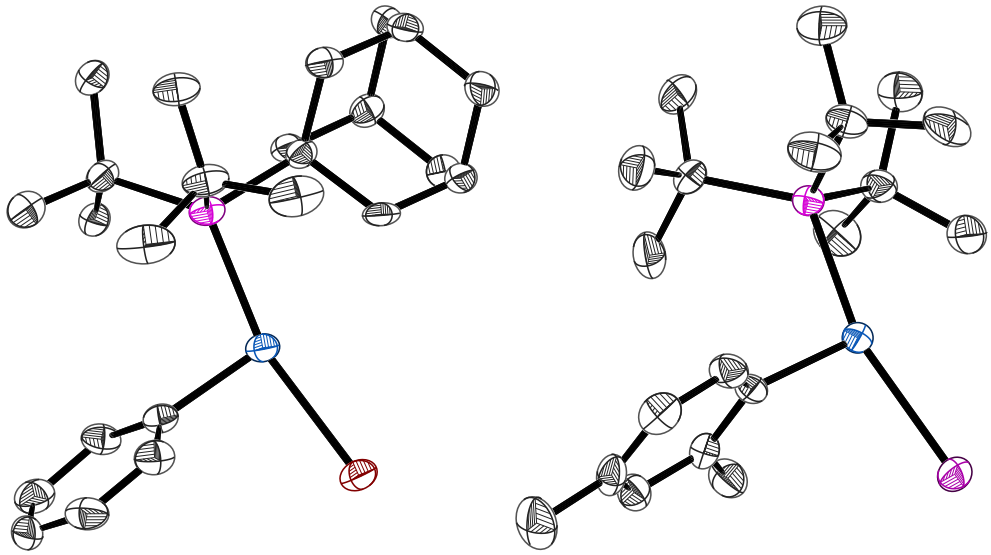

Figure 5.3 ORTEP diagrams of [PdBrPh(PAdBu$^t{}_2$)] (left) and [PdI(2,4-xylyl)(PBu$^t{}_3$)] (right) (50% probability thermal ellipsoids). Hydrogen atoms omitted for clarity.

with both platinum(0) and platinum(II), suggesting that the same reactivity would occur in catalytic reactions with Group 10 metals.

5.2 Kinetic Measurements

One of the major obstacles to the use of electron-rich trialkylphosphine ligands in pre-catalyst mixtures for Sonogashira coupling reactions (and similar) is their high air-sensitivity, rendering them more difficult to handle than triarylphosphine ligands for example. In 2001, Netherton and Fu addressed this problem by replacing the air-sensitive ligands PBu$^t{}_3$ and PBu$^n{}_3$ with the air- and moisture-stable phosphonium salt analogues Bu$^t{}_3$PH$^+$BF$_4^-$ and Bu$^n{}_3$PH$^+$BF$_4^-$.[236] The phosphonium salts were tested in reactions such as the reductions of diphenyl disulfide and *n*-octyl azide, and the palladium-catalysed Suzuki, Stille and Sonogashira coupling reactions. It was found that in all cases the product yields were comparable (within 6%) with the equivalent reactions utilising the free phosphines.

Using the methodology of Netherton and Fu,[236] phosphine-thioether ligand **14a** and PBnBu$^t{}_2$ were converted to the corresponding air-stable phosphonium tetrafluoroborate salts **49** and **50** *via* reaction with excess aqueous tetrafluoroboric acid (Scheme 5.1). Conversion of *P,S* ligand **14a** to phosphonium salt **49** was confirmed by analysis of the associated NMR data and high resolution mass spectrometry. The ^{31}P NMR signal of compound **49** appears at 39.6 ppm in acetone-d_6, a downfield shift of approximately 15 ppm from the free phosphine. In the ^{1}H NMR spectrum

a doublet of triplets signal associated with the PH proton is observed, centred at 6.77 ppm, with a large $^{1}J_{\mathrm{PH}}$ coupling of 466.3 Hz and $^{3}J_{\mathrm{HH}}$ couplings of 6.3 Hz to the CH_2P protons. The ^{19}F NMR spectrum displays a singlet peak at −150.1 ppm, consistent with a non-coordinating tetrafluoroborate anion. The NMR spectra of phosphonium salt **50** display similar features to those associated with phosphonium salt **49**, and are consistent with previously described benzyldi-*t*-butylphosphonium bromide.[237]

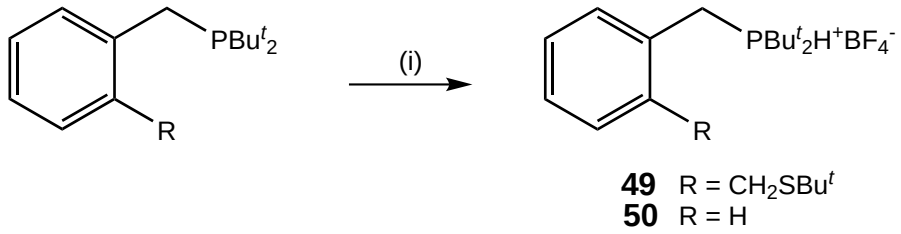

Scheme 5.1 Synthesis of phosphonium tetrafluoroborate salts. *Reagents and conditions:* (i) ∼10 eq. aq. HBF_4, CH_2Cl_2, 10 min.

The reaction conditions used for the kinetic investigation of the Sonogashira coupling of 4-bromoanisole and phenylethyne are shown in Scheme 5.2. In a 2007 review paper, Doucet and Hierso noted that virtually any palladium source is capable of reaching high TONs for facile reactions; however, with less reactive substrates much lower TONs are generally obtained and the ligands have a large influence on the outcome of the reactions.[217] As an electronically deactivated aryl halide, 4-bromoanisole is commonly chosen as a coupling partner for ligand investigations of this type. 4-Bromoanisole also contains a methyl group, the associated ^{1}H NMR shift of which (3.74 ppm in THF-d_8) is situated away from the aryl region, producing a convenient "handle" for NMR-scale studies of this reaction. Similarly, $[Pd(OAc)_2]$ is commonly used in Sonogashira coupling reactions and, of specific importance to this study, $[Pd(OAc)_2]$ is the only easily-handled palladium precursor to initially produce a 1:1 complex with *P,S* ligand **14a** (palladacycle dimer **46**, shown in Scheme 4.4). Di-*i*-propylamine has been shown to be an effective base in reactions of this type,[231,238] and is often used as the solvent as well as the base. However, as the capability to perform NMR-scale studies was desired in this case, an excess of di-*i*-propylamine in THF solvent was used. The palladium precursor loading of 3 mol%, with a slightly lower loading of the copper(I) salt, is a commonly employed catalyst loading for Sonogashira reactions, although usually with a monodentate phosphine ligand loading of 6 mol%.

Two independent runs of the reaction shown in Scheme 5.2 were performed, and the rate of conversion of 4-bromoanisole to 4-(phenylethynyl)anisole monitored by GC-MS. The results of these reactions are shown in Figure 5.4. The data

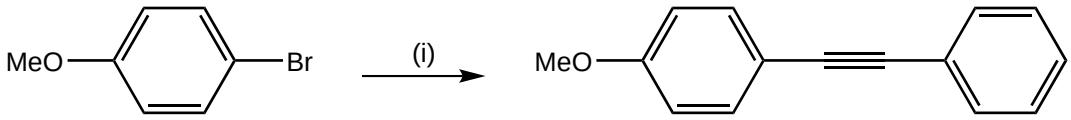

Scheme 5.2 Sonogashira coupling of 4-bromoanisole and phenylethyne. *Reagents and conditions:* (i) 3 mol% $[Pd(OAc)_2]$, 3 mol% *P,S* phosphonium salt **49**, 2 mol% CuI, 5 eq. $Pr^i{}_2NH$, THF, 60 °C, 10 min, 1.3 eq. phenylethyne, 60 °C, 2 h.

show a reproducible kinetic profile for this reaction, with the GC-MS results of the runs consistent within ± 3%. The averaged data from the two experiments show 82% conversion to 4-(phenylethynyl)anisole in 120 minutes, with a turnover frequency (TOF) of 20 h^{-1} (calculated for the 40 to 90 minute time period). This TOF is comparable with that of the synthesis of 4-(phenylethynyl)anisole using a $[PdCl_2(NCPh)_2]/PBu^t{}_3$/CuI pre-catalyst mixture in dioxane solvent at room temperature,[231] but pales in comparison to the same reaction performed with a $Na_2PdCl_4/PBu^t{}_3$/CuI pre-catalyst mixture in di-*i*-propylamine solvent at 80 °C (TOF = 3240 h^{-1}).[238] The data shown in Figure 5.4 also shows an induction period of *ca.* 20 minutes. This induction period is consistent with the conversion of the initial pre-catalyst mixture to the active catalyst species.

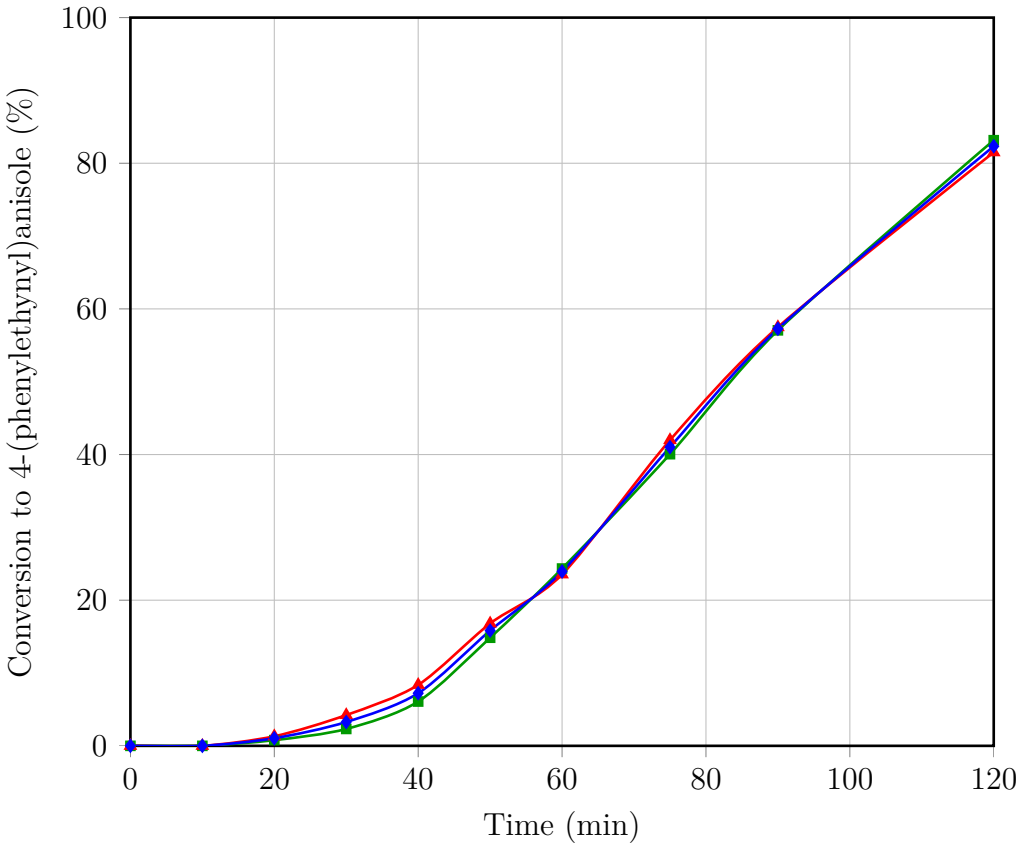

Figure 5.4 Kinetic investigation of the Sonogashira coupling of 4-bromoanisole and phenylethyne. First run, second run, average of two runs.

A preparative run of this reaction was also performed, and monitored by ^{1}H NMR spectroscopy. After two hours, the ^{1}H NMR spectrum of the reaction mixture showed 93% conversion to 4-(phenylethynyl)anisole, broadly consistent with the GC-MS data (it is possible a spuriously high conversion was observed in the ^{1}H NMR spectrum, as the sample was subjected to vacuum in order to remove the solvent, which may also have affected the amount of 4-bromoanisole in the sample). After four hours reaction time, both ^{1}H NMR spectroscopy and GC-MS analysis confirmed quantitative conversion to the desired product. The reaction mixture was then worked up and the crude product purified by column chromatography, resulting in an 86% isolated yield of 4-(phenylethynyl)anisole.

The GC-MS data collected also identified the formation of two by-products in this reaction, both with the empirical formula $C_{16}H_{12}$, indicating that these by-products relate to the dimerisation of phenylethyne. Analysis of the ^{1}H NMR spectrum of the reaction mixture identified these by-products as the enyne compounds (*E*)-1,4-diphenylbut-1-en-3-yne and 2,4-diphenylbut-1-en-3-yne (shown in Figure 5.5). The alkene protons of (*E*)-1,4-diphenylbut-1-en-3-yne appear as doublet peaks centred at 6.39 and 7.05 ppm ($^3J_{HH}$ = 16.3 Hz), and the alkene protons of 2,4-diphenylbut-1-en-3-yne appear as singlet peaks at 5.77 and 5.99 ppm, all consistent with literature data.[239] The transition metal-assisted dimerisation of phenylethyne is well established in the literature, primarily with rhodium and ruthenium complexes, but there are also many examples of palladium-catalysed reactions of this type. Trost and co-workers have published extensively in this area, including on the cross-coupling of terminal alkynes with acceptor alkynes with a [$Pd(OAc)_2$]/tris(2,6-dimethoxyphenyl)phosphine pre-catalyst mixture.[240] The enynes shown in Figure 5.5 have been synthesised as the desired products in a number of palladium-catalysed reactions,[241,242] and as by-products in a number of copper-free Sonogashira reactions.[243,244] In 2012, Jahier and co-workers determined through computational studies that the mechanism of palladium-catalysed formation of (*E*)-1,4-diphenylbut-1-en-3-yne is *via* the hydropalladation catalytic cycle shown in Figure 5.6.[245] Interestingly, the most common by-product of copper co-catalysed Sonogashira reactions performed with phenylethyne, 1,4-diphenylbutadiyne, was not formed in these reactions. 1,4-Diphenylbutadiyne is produced in reactions of this type by the Glaser-Hay reaction, a copper-catalysed homocoupling of terminal alkynes in the presence of an amine base and oxygen,[246] which is the reason Sonogashira reactions must be performed under inert atmosphere.

A number of reactions with variations to the pre-catalyst mixture in Scheme 5.2 were also performed, and monitored by GC-MS. The results of these reactions are shown in Figure 5.7. Initially, 6 mol% phosphonium salt **49** was used, giving a

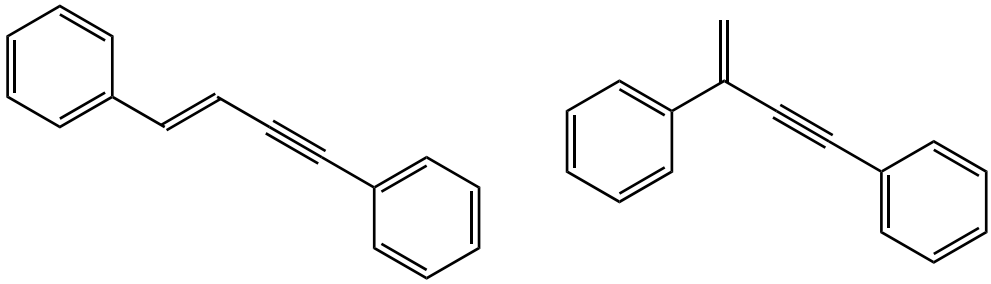

Figure 5.5 Enyne by-products of the Sonogashira coupling of 4-bromoanisole and phenylethyne.

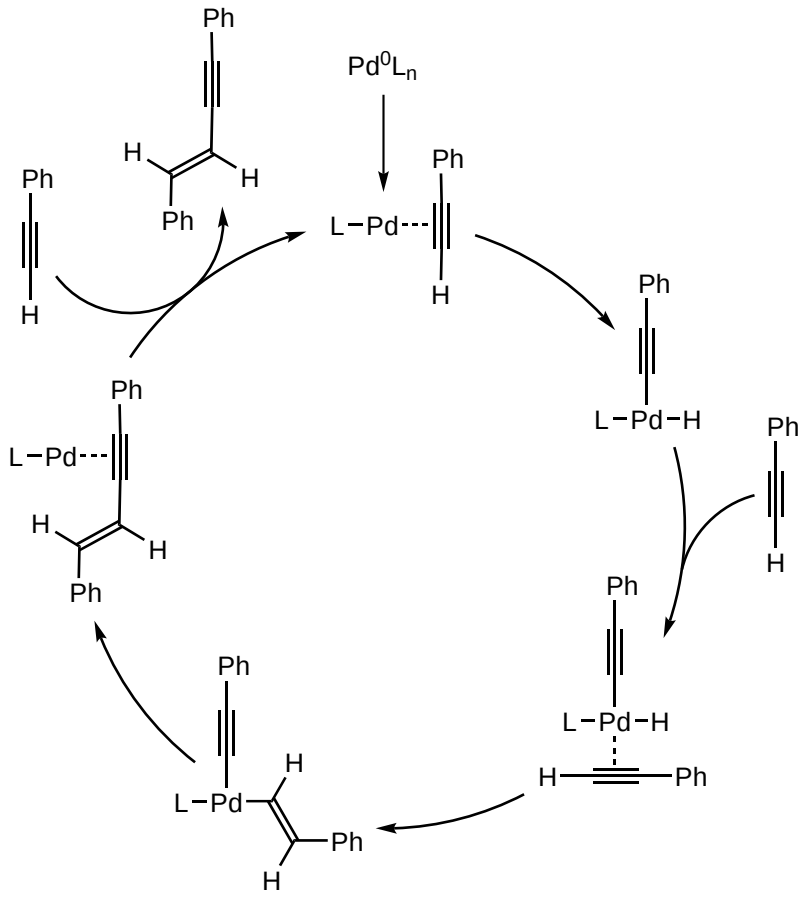

Figure 5.6 Mechanism of the palladium-catalysed formation of (*E*)-1,4-diphenylbut-1-en-3-yne.

ligand/palladium ratio of 2:1. This pre-catalyst mixture resulted in an induction period of over 30 minutes, and a slower reaction rate than the standard reaction conditions (1:1 ligand/palladium ratio). This result indicates that the second equivalent of *P,S* ligand **14a** inhibits the reaction, possibly through the formation of [Pd(*P,S*)$_2$] complex **44**. This is consistent with the observation by Hartwig and co-workers that aryl halides react more slowly with [Pd(PR$_3$)$_2$] complexes of bulky phosphines than with mixtures of [Pd(dba)$_2$] and bulky phosphines, and hence [Pd(PR$_3$)$_2$] cannot be the active catalyst species.[235]

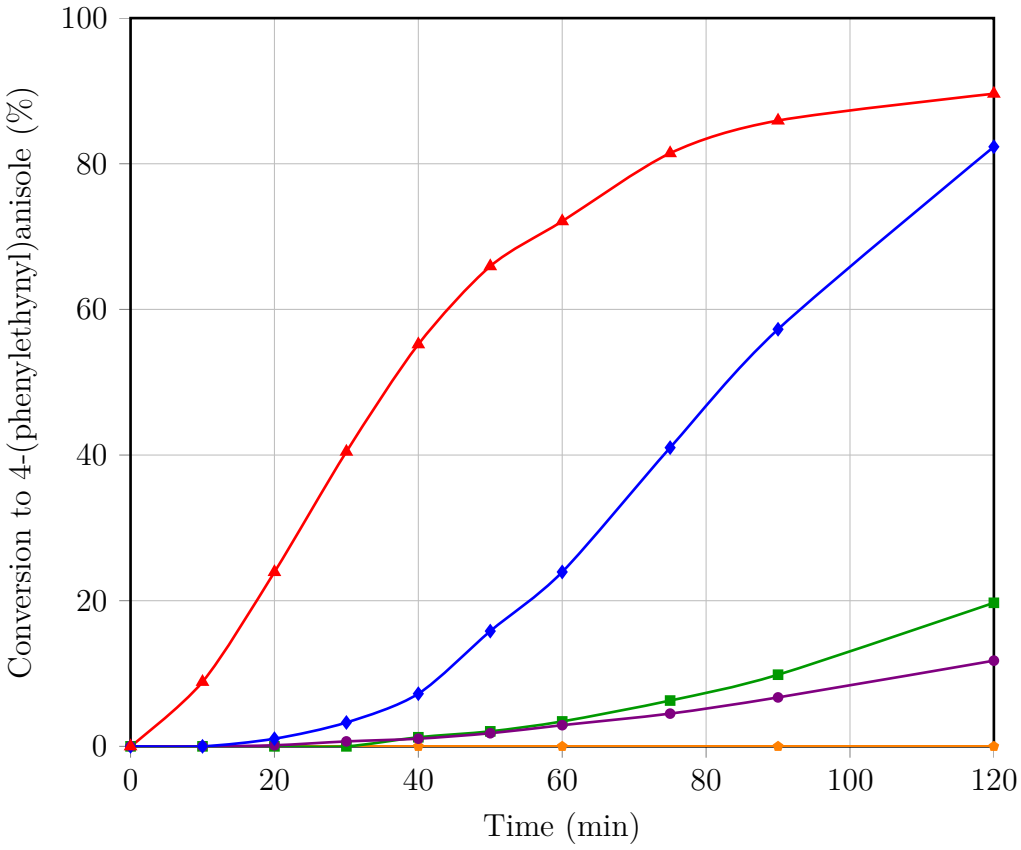

Figure 5.7 Variations of the Sonogashira reaction pre-catalyst mixture. Standard pre-catalyst mixture, 6 mol% phosphonium salt **49**, copper(I) iodide omitted, phosphonium salt omitted, 3 mol% phosphonium salt **50**.

Reactions wherein one of the components of the pre-catalyst mixture was omitted were also performed. When copper(I) iodide was omitted from the reaction, the induction period was not affected; however, the reaction rate was severely decreased (TOF = 3.2 h^{-1} for the 75 to 120 minute time period). This is consistent with the known ability of copper(I) salts to accelerate Sonogashira reactions,[217] likely *via* copper acetylide formation and transmetallation with the palladium catalyst, a more rapid process than direct palladium acetylide formation (although no direct evidence of the transmetallation process has been reported). Reactions were also

performed with the phosphonium salt omitted, and the associated GC-MS data showed no 4-(phenylethynyl)anisole produced over the 120 minute reaction period.

Another variation to the standard reaction conditions investigated was the replacement of *P,S* phosphonium salt **49** with the monodentate analogue, phosphonium salt **50** ($Bu^t_2BnPH^+BF_4^-$). As shown in Figure 5.7, this pre-catalyst mixture produced a more rapid reaction, with the averaged GC-MS data showing 90% conversion to 4-(phenylethynyl)anisole in 120 minutes, and a TOF of 31 h^{-1} (calculated for the 10 to 40 minute time period). This reaction also displayed a much shorter induction period than the reaction using *P,S* phosphonium salt **49**, suggesting that the sulfur donor atom in *P,S* ligand **14a** has a significant effect on the rate of formation of the active catalyst species in these reactions. However, the rate of formation of the enyne by-products shown in Figure 5.5 was also more rapid in reactions using monodentate phosphonium salt **50**. In these reactions, the GC-MS data showed no trace of the phenylethyne starting material after 120 minutes reaction time, although 10% of the 4-bromoanisole had not been converted to 4-(phenylethynyl)anisole (the initial GC-MS phenylethyne/4-bromoanisole ratio observed for all reactions discussed was in the range 1.27–1.52:1). For comparison, the averaged ratio of 4-(phenylethynyl)anisole to enyne by-products at 81% conversion (75 minutes) with $PBnBu^t_2$ is 4.2:1, whereas the averaged ratio of 4-(phenylethynyl)anisole to enyne by-products at 82% conversion (120 minutes) with *P,S* ligand **14a** is 10.5:1 (a ratio of 9:1 was observed in the ^{1}H NMR spectrum of the preparative reaction after four hours reaction time).

As the Sonogashira coupling reactions performed with 3 mol% loadings of $[Pd(OAc)_2]$ and each of the phosphonium salts (**49** and **50**) essentially went to completion, lower catalyst loadings were investigated, with the intention of establishing the maximum turnover number (TON) for each pre-catalyst mixture. The reaction shown in Scheme 5.2 was repeated in duplicate, with pre-catalyst mixtures of 0.3 mol% phosphonium salt **49** or **50**/0.3 mol% $[Pd(OAc)_2]$/0.2 mol% CuI (one tenth of the original pre-catalyst mixture loading). The results of these reactions are shown in Figure 5.8. At this pre-catalyst mixture loading, there is a striking difference between the activities of the catalysts. The averaged GC-MS data for the mixture including phosphonium salt **50** ($Bu^t_2BnPH^+BF_4^-$) show 95% conversion of the starting materials to 4-(phenylethynyl)anisole, a TON of 317; whereas the averaged GC-MS data for the mixture including *P,S* phosphonium salt **49** show only 5% conversion, a TON of only 17.

Of note in these reactions is the increased TOF for the pre-catalyst mixture including phosphonium salt **50** ($Bu^t_2BnPH^+BF_4^-$) with lower catalyst loading, from a TOF

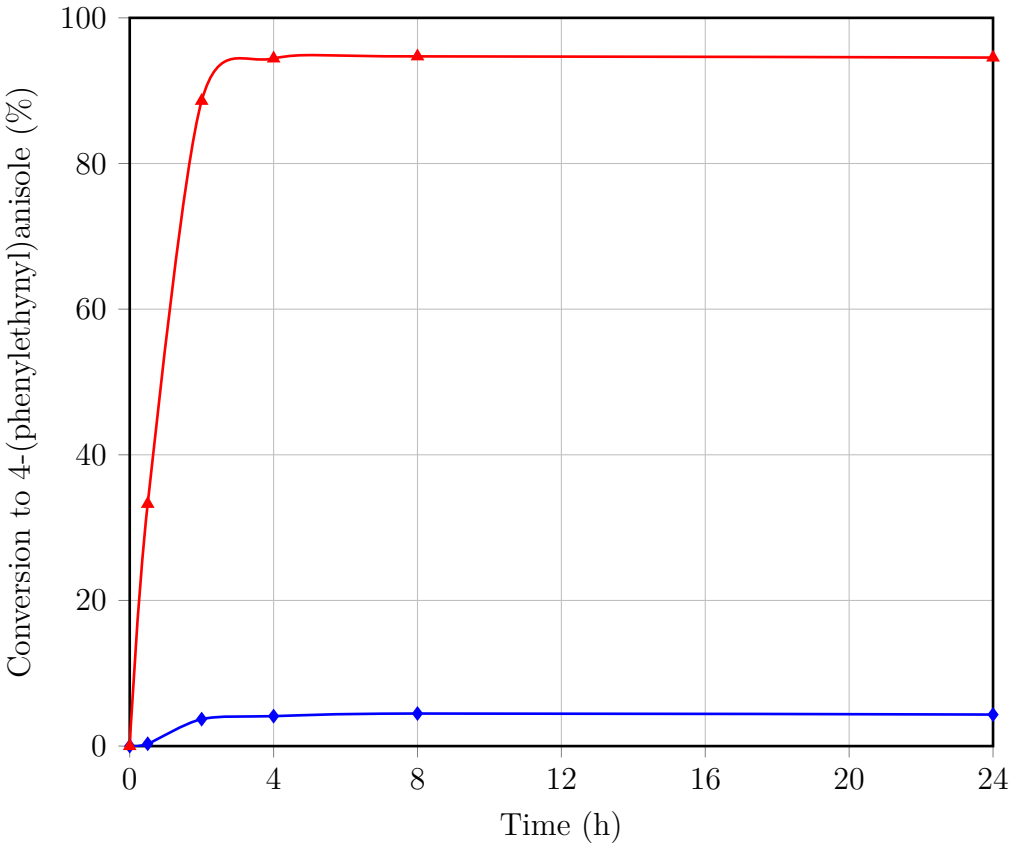

Figure 5.8 Sonogashira coupling of 4-bromoanisole and phenylethyne with a lower catalyst loading. ◆ 0.3 mol% $[Pd(OAc)_2]$/0.3 mol% *P,S* phosphonium salt **49**/0.2 mol% CuI, ▲ 0.3 mol% $[Pd(OAc)_2]$/0.3 mol% phosphonium salt **50**/0.2 mol% CuI.

of 31 h^{-1} at 3 mol% loading to a TOF of 123 h^{-1} (calculated for the 0.5 to two hour time period) with a 0.3 mol% loading. This phenomenon has been reported previously by de Vries and co-workers for the Heck coupling of bromobenzene and butylacrylate with "homeopathic" loadings of ligand-free $[Pd(OAc)_2]$.[247] The authors reported conversions of over 90% at 0.02 and 0.08 mol% catalyst loading; however, when the catalyst loading was increased to 1.28 mol%, the conversion dropped to less than 5% for the same time period. This was attributed to the existence of soluble palladium clusters, from which monomeric Pd(0) species could enter the catalytic cycle, or aggregation of the clusters could occur, withdrawing the palladium from the catalytic cycle. They suggest that while the Heck reaction is first order in palladium concentration, the aggregation process must be higher order, and hence lowering the catalyst-to-substrate ratio reaches a point where the initial oxidative addition step of the Heck cycle outruns the aggregation process. The authors also mention that this phenomenon is generally associated with palladacycles, which by analogy with the synthesis of palladacycle dimer **46**, the reaction of $[Pd(OAc)_2]$ and $PBnBu^t_2$ should produce. In the present study, the aggregation of metastable palladium clusters may also assist in explaining why both of the catalysts operate

for around two hours, suggesting catalyst degradation is a function of time rather than turnover number.

5.3 Suspicious Circumstances

As homogeneous palladium-catalysed carbon-carbon bond-forming reactions have become progressively more important in a number of fields of chemistry, the identification of the nature of the active catalyst species has become a focus of research in this area. It has been found that the catalytic activity present in a number of these systems is not, as previously thought, due to the action of discrete metal complexes, but actually palladium nanoparticles formed by the degradation of the metal complexes during the reaction. Various review papers have been published on this topic, and specifically on the difficulties in distinguishing true homogeneous catalysts from colloidal catalysts, over the past ten years.[248–252] In his 2012 review paper, Crabtree identified a number of "suspicious circumstances" that suggest a supposed homogeneous catalyst may actually be colloidal in nature:[252]

- Unexplained lag time before onset of catalysis.
- Catalyst properties, such as selectivity, closely resemble the properties of the appropriate analogous conventional heterogeneous catalyst.
- Ligand effects are minimal; all active catalysts have similar rates and properties.
- Transmission electron microscopy shows electron-dense particles.
- Catalytic activity is halted by a selective poison for the heterotopic catalyst.
- Kinetic irreproducibility.
- Reaction mixture turns dark in colour.
- Metal-containing deposit or mirror formed.
- Harsh conditions (for example, >150 °C or strong oxidants, acids or bases).

Although the Sonogashira coupling of 4-bromoanisole and phenylethyne with *P,S* phosphonium salt **49** was performed under reasonably mild conditions, proved to be kinetically reproducible and the ligand effects were pronounced, the induction period and solution colour change from yellow to dark brown at the onset of catalysis suggested nanoparticles may play a role in the reaction. For this reason, mercury poisoning reactions were performed on the reaction shown in Scheme 5.2. As the addition of Hg(0) at the beginning of the reaction may have disrupted the formation of the active catalyst species, 150 mol% of Hg(0) (50:1 Hg/Pd) was added after 45 or 65 minutes reaction time, and the high stirring rates (800–1000 rpm) ensured effective mixing of the components. As shown in Figure 5.9, in each case the

addition of mercury caused complete cessation of the reaction. Traditionally, this was considered good evidence that the active catalyst species consisted of Pd(0) nanoparticles; however, in recent years it has become accepted that Hg(0) also poisons relatively naked (*i.e.* sterically unencumbered) mono- or di-nuclear Pd(0) species.[250] In fact, in a 2006 review paper, Phan and co-workers suggested that Hg(0) quenching of catalytic activity can only be interpreted as "catalysis *via* a cycle with a Pd(0) intermediate".[249] An example of this was reported in 1991, where it was found that a number of [Pd^0(alkene)(*N*,*N*)] complexes reacted with Hg(0) under inert atmosphere, with loss of the coordinated alkene, forming an unidentified compound.[253]

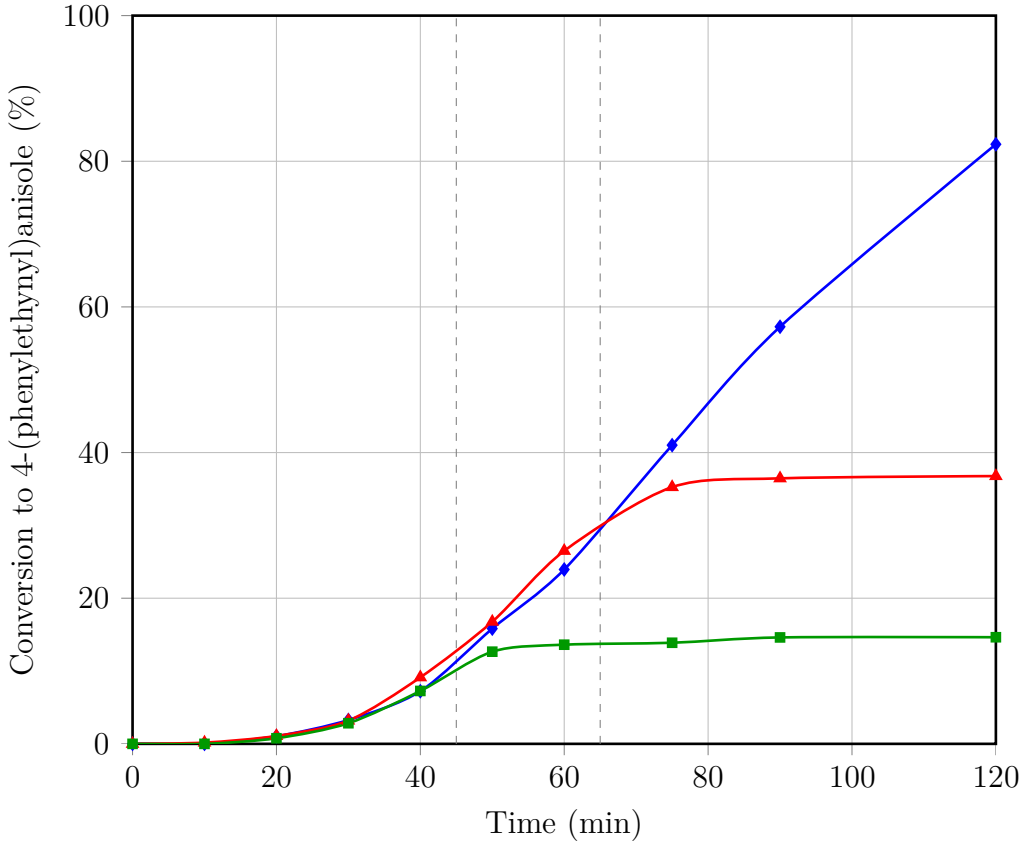

Figure 5.9 Mercury poisoning of Sonogashira coupling of 4-bromoanisole and phenylethyne. —■— Hg(0) added after 45 min, —▲— Hg(0) added after 65 min, —◆— no Hg(0) added.

To confirm the presence of palladium nanoparticles in the reaction mixture, a dynamic light scattering experiment was performed on the reaction solution after low-speed centrifugation (to separate the insoluble di-*i*-propylammonium bromide by-product). This experiment showed a polydisperse colloidal suspension was present, with nanoparticles in the 2–11 nm range. The combination of these two tests confirms the presence of palladium nanoparticles in the reaction solution; however, neither of the tests indicate whether the nanoparticles are the active

catalytic species. There are a number of instances in which it has been reported that palladium nanoparticles (and solid-supported palladium) serve as reservoirs for palladium atoms or ions, which constitute the active catalytic centres.[249] This was demonstrated for the Sonogashira reaction by Rothenberg and co-workers in 2005. The authors used 14.5 nm Pd(0) nanoparticles to catalyse the coupling of 4-bromobenzonitrile and phenylethyne, and using a combination of kinetic analysis and transmission electron microscopy, determined that the reaction proceeds *via* a homogeneously catalysed mechanism with a leached palladium species.[254] In a subsequent paper, Rothenberg and co-workers came to the same conclusion for Suzuki and Heck C−C bond-forming reactions, using a membrane reactor for palladium transfer.[255] In the present case, further study would be required to distinguish between a nanoparticle surface reaction and a mechanism involving the leaching of palladium atoms/ions back into solution. It is generally agreed that a combination of methods is required to unambiguously determine the nature of the active catalytic species, so techniques such as transmission electron microscopy, Rothenberg's membrane reactor experiments,[255] and poisons selective for homogeneous catalysts (*e.g.* carbon disulfide, thiophene, polyvinylpyridine) may prove useful in this case.[248,252]

5.4 NMR Investigation

In an attempt to identify the catalytic species present in this Sonogashira coupling reaction, an NMR-scale reaction with a high catalyst loading was performed and monitored by ^{1}H and ^{31}P NMR spectroscopy. The conditions for this reaction are shown in Scheme 5.3. Initially, a mix of [Pd(OAc)$_2$], *P,S* phosphonium salt **49** and copper(I) iodide was combined with a solution of 4-bromoanisole and di-*i*-propylamine in THF-d_8 and the mixture heated to 60 °C for 10 minutes with stirring. The resulting pale yellow solution was transferred to an NMR tube and ^{1}H and ^{31}P NMR spectra were collected at room temperature. Analysis of the NMR spectra confirmed the presence of the expected [Pd(μ-OAc)(*P,C*)]$_2$ palladacycle dimer **46**. However, the peaks associated with this complex were particularly broad, as was the peak associated with the methine proton of di-*i*-propylamine. The ^{31}P NMR spectrum also contained two broad signals associated with this system, at 97.4 and 106.7 ppm. These data suggested that dimer **46** was in dynamic equilibrium with a [Pd(OAc)(NPr$^{i}_2$H)(*P,C*)] species, an observation that has been made previously by Hartwig and Louie in the reaction of a similar acetate-bridged palladacycle dimer with diethylamine.[256]

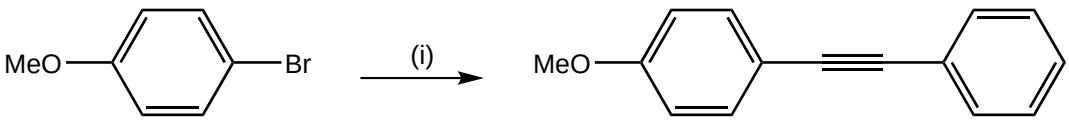

Scheme 5.3 NMR-scale Sonogashira coupling of 4-bromoanisole and phenylethyne. *Reagents and conditions:* (i) 50 mol% [$Pd(OAc)_2$], 50 mol% *P,S* phosphonium salt **49**, 33 mol% CuI, 2.5 eq. $Pr^i{}_2NH$, THF-d_8, 60 °C, 10 min, 1.3 eq. phenylethyne, 60 °C, 1 h.

Also observed in the ^{31}P NMR spectrum was a broad signal centred at 29.1 ppm. This signal correlated with a doublet signal ($^2J_{PH}$ = 7.9 Hz) at 3.41 ppm, a singlet at 4.12 ppm, and a larger singlet at 1.63 ppm in the ^1H NMR spectrum, associated with the CH_2P, CH_2S and SBu^t protons of *P,S* ligand **14a** respectively. The chemical shifts of the phosphorus atom, CH_2P and SBu^t signals, and the CH_2P coupling constant were dissimilar enough to the free ligand to suggest both donor atoms were bound to a metal centre. An NMR-scale test reaction consisting of *P,S* phosphonium salt **49**, copper(I) iodide and di-*i*-propylamine in THF-d_8 showed that this species was a 1:1 *P,S* ligand **14a**/copper(I) iodide complex. A literature search indicated this species may be a $[Cu(\mu\text{-}I)(P,S)]_2$ species, as copper(I) dimers of this type containing phosphine-thioether ligands and bridging iodides[257] or other halides[257,258] are known. The ratio of *P,S* ligand present in the palladacycle dimer **46**/di-*i*-propylamine dynamic system to *P,S* ligand **14a**/copper(I) iodide complex (approximately 1.5:1) indicated neither the entirety of the [$Pd(OAc)_2$] nor copper(I) iodide present in the reaction mixture had reacted with *P,S* ligand **14a**.

A third metal complex was identified in the NMR-scale Sonogashira coupling reaction prior to the addition of phenylethyne. The ^1H NMR spectrum showed two doublets of equal intensity at 1.31 and 1.66 ppm, and a peak with octet coupling centred at 2.79 ppm (in actual fact, two overlapping septet signals). These data are consistent with metal-bound di-*i*-propylamine, as association of the nitrogen donor atom to a metal centre ceases the facile inversion process present in free amines, rendering the methyl and methine protons diastereotopic, and therefore inequivalent in the ^1H NMR spectrum. An NMR-scale test reaction consisting of [$Pd(OAc)_2$] and di-*i*-propylamine in THF-d_8 showed that this species was a [$Pd(OAc)_2$]/di-*i*-propylamine complex, and a signal associated with the acetate protons was identified at 1.68 ppm. The only other signals present in the ^1H NMR spectrum of the NMR-scale Sonogashira coupling reaction prior to the addition of phenylethyne were associated with 4-bromoanisole, and there was no indication that this species had reacted with any of the metal complexes present in solution.

Upon addition of phenylethyne, no physical change to the pale yellow solution was observed; however, the resulting ^{31}P NMR spectrum was significantly different from

the spectrum prior to addition of phenylethyne. A stacked plot of the ^{31}P NMR spectra collected during the reaction is shown in Figure 5.10. The broad peak at *ca.* 30 ppm associated with the *P,S* ligand **14a**/copper(I) iodide complex was unchanged, and in fact remained unchanged throughout the reaction. Conversely, the peaks associated with the palladacycle dimer **46**/di-*i*-propylamine dynamic system had been completely replaced by six sharp peaks in the same region, suggesting that reaction with phenylethyne had occurred, producing a number of species, likely all with the palladacycle moiety intact. The ^{1}H NMR spectrum confirmed that the [$Pd(OAc)_2$]/di-*i*-propylamine complex also remained intact, and a number of new unidentified signals on the baseline of the spectrum were observed, consistent with the six new signals in the ^{31}P NMR spectrum. A signal corresponding to the alkyne proton of phenylethyne was also observed in the ^{1}H NMR spectrum, the associated integral value of which indicated a 1:1 ratio of 4-bromoanisole and free phenylethyne, rather than the expected 1:1.3 ratio (Scheme 5.3).

The NMR tube containing the pale yellow Sonogashira reaction solution was then heated to 60 °C. Almost immediately, the solution turned dark brown in colour. After 10 minutes, the solution was cooled and ^{1}H and ^{31}P NMR spectra collected. As shown in Figure 5.10, more sharp signals were observed in the ^{31}P NMR spectrum between 80 and 110 ppm. The ^{1}H NMR spectrum showed the presence of small amounts of the desired product, 4-(phenylethynyl)anisole, and the enyne by-products shown in Figure 5.5. The solution was heated to 60 °C for a further 20 minutes and ^{1}H and ^{31}P NMR spectra collected again. At this point, the number of peaks in the 80 and 110 ppm region of the ^{31}P NMR spectrum had returned to six, but with different chemical shifts and intensities from the six peaks observed directly after the addition of phenylethyne, and in this instance all very near 100 ppm. No phenylethyne starting material was observed in the ^{1}H NMR spectrum, although only around 50% of the 4-bromoanisole had reacted to form 4-(phenylethynyl)anisole. This was due to the large amount of enyne by-products present in the sample, accounting for the disappearance of the other 50% of the diphenylethyne. This result is interesting, and is consistent with the GCMS data collected in the previous Sonogashira reactions, as the reactions performed with the lower (0.3 mol%) catalyst loading produced a lesser amount of by-product when compared with the reactions containing 3 mol% catalyst. No changes to the reaction mixture were observed upon heating to 60 °C for a further 30 minutes.

Although a number of palladacycle-type pre-catalysts have shown good activity in Sonogashira coupling reactions,[218,219] very few mechanistic investigations of these systems have been performed. Instead, authors have tended to draw parallels between these reactions and the mechanistic investigations of other palladacycle-

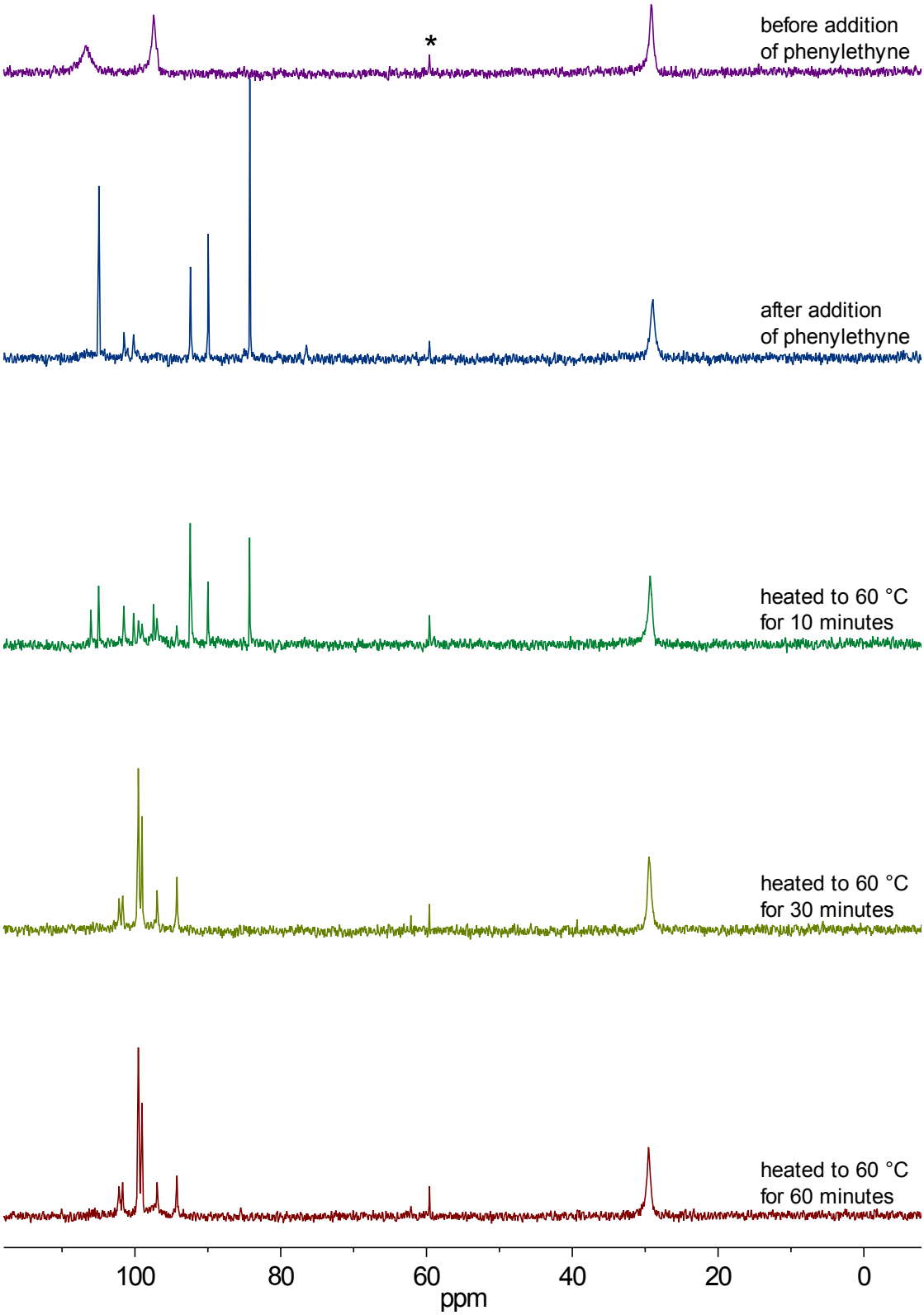

Figure 5.10 ^{31}P NMR spectra of the NMR-scale Sonogashira reaction. Asterisk denotes phosphine oxide of *P,S* ligand **14a**.

catalysed carbon-carbon bond-forming reactions. In the cases of the Stille, Negishi, palladium-catalysed Grignard, and presumably Suzuki cross-coupling reactions, a reduction process for a *P,C* ligand palladacycle has been unequivocally established.[256,259] As shown in route (i) of Scheme 5.4, the reaction of the acetate-bridged palladacycle dimer with $PhSnMe_3$, PhMgBr or PhZnCl resulted in coupling of the carbon donor atom of the *P,C* ligand with the phenyl anion, and hence reduction of the Pd(II) to Pd(0), giving free phosphine, a $[Pd^0P_2]$ complex and unligated Pd(0).

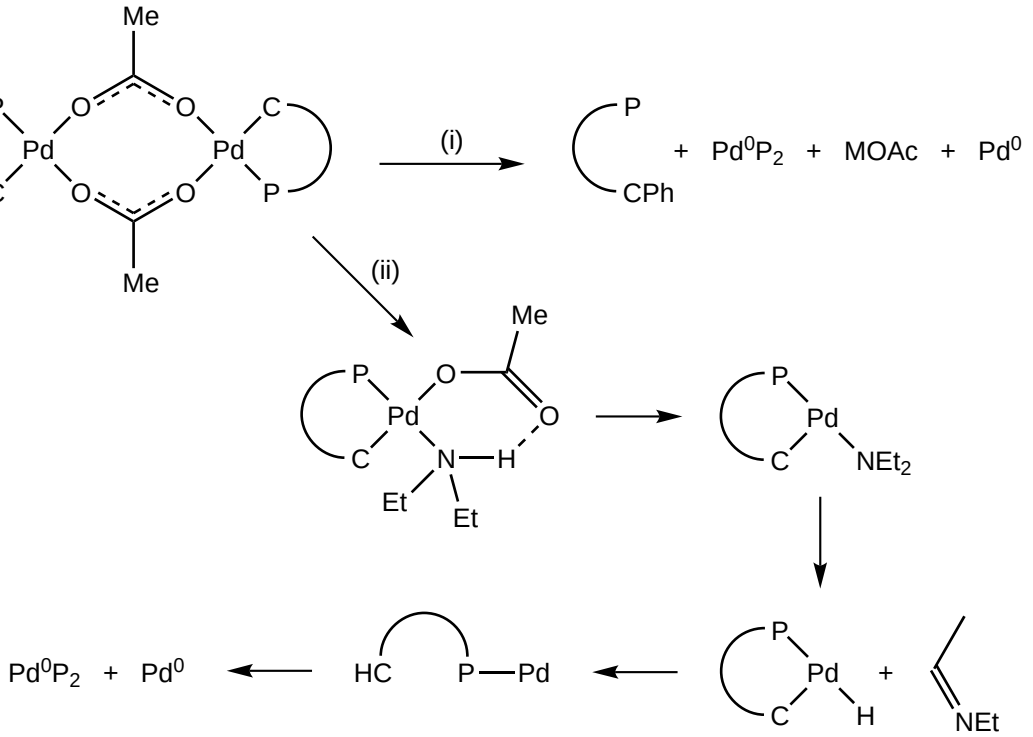

Scheme 5.4 Proposed reactions of palladacycles under catalytic conditions. *Reagents and conditions:* (i) PhM (M = $SnMe_3$, ZnCl, MgBr); (ii) Et_2NH, $NaOBu^t$.

Similarly, Louie and Hartwig investigated the reaction of the same acetate-bridged palladacycle dimer with diethylamine and sodium *t*-butoxide, as part of a study on the palladacycle-catalysed amination of aryl halides.[256] Route (ii) of Scheme 5.4 shows the postulated steps for the formation of $[Pd^0P_2]$ and unligated Pd(0) from these starting materials. Initial reaction of the acetate-bridged palladacycle dimer with diethylamine cleaved the dimer, producing a $[Pd(OAc)(P,C)(NEt_2H)]$ species, which was characterised by NMR spectroscopy and X-ray crystallography. The addition of sodium *t*-butoxide to this species gave nearly quantitative yield of $[Pd^0P_2]$ based on the amount of phosphine in the reaction. The authors proposed this transformation proceeds *via* deprotonation of the amine ligand, β-H elimination to give a palladium hydride species, reductive elimination, and subsequent disproportionation of the resulting $[Pd^0P]$ species. Neither the proposed amide- or hydride-ligated species were observed; however, it was established that the acetate-bridged palladacycle dimer does not catalyse the amination reaction

when the diethylamine was replaced with diphenylamine (which does not possess a β-hydrogen atom).

Other mechanisms have been proposed for palladacycle-catalysed Heck reactions, including a Pd(II)/Pd(IV) catalytic cycle[202,260] and the reduction of Pd(II) to Pd(0) with retention of the palladacycle, to give an active $[Pd^0(P,C)]^-$ catalyst species.[261] However, no experimental evidence for either of these mechanisms has been reported. In their 2006 critical review paper, Phan and co-workers stated that the collected data for *P,C*, *N,C* and *S,C* palladacycle pre-catalysts is consistent with the hypothesis that these complexes are sources of low-ligated, "homeopathic" palladium in a number of palladium-catalysed carbon-carbon bond-forming reactions, and it is widely accepted that the actual catalysts operate *via* traditional Pd(0)/Pd(II) cycles.[249]

In terms of the current investigation of the Sonogashira reaction with acetate-bridged palladacycle dimer **46**, either of the routes to an unligated (or low-ligated) palladium(0) species shown in Scheme 5.4 may be applicable, *via* reaction with a copper(I) acetylide species or with di-*i*-propylamine. However, if either of these processes did occur in the previously discussed NMR-scale Sonogashira coupling reaction, it must have been to a very minor extent, as no evidence of the formation of free *P,S* ligand **14a** or $[Pd(P,S)_2]$ complex **44** (or similar) was observed in the NMR spectra. This is not inconsistent with the idea that in this instance the coupling of 4-bromoanisole and phenylethyne is catalysed by palladium atoms/ions leached from palladium clusters present in solution, as it has previously been noted that it is beneficial to have only very small amounts of these species present.[247] However, the differences in reaction rates and induction periods in the Sonogashira coupling reactions performed with *P,S* ligand **14a** and $PBnBu^t_2$ (discussed in Section 5.2) indicate that the effect of the sulfur donor atom in *P,S* ligand **14a** cannot be discounted, but more investigation would be required to be able to draw any conclusions regarding this matter.

Perhaps the more interesting result of the NMR-scale Sonogashira coupling reaction is the relationship observed between the amount of pre-catalyst mixture employed and the yield of enyne by-products. In both the *P,S* ligand **14a** and $PBnBu^t_2$ ligand systems, it has been demonstrated that increasing the amount of catalyst leads to an increase in the ratio of phenylethyne homocoupling products to desired cross-coupling product, 4-(phenylethynyl)anisole. The palladacycle dimer **46**/di-*i*-propylamine dynamic system has been shown to react directly with phenylethyne (as evidenced by the before and after phenylethyne addition ^{31}P NMR spectra shown in Figure 5.10), likely *via* cleavage of the acetate bridges and/or displacement of

the amine ligand, to form a number of species with ^{31}P NMR shifts suggesting the palladacycle moieties remained intact. It is possible that one or more of these palladium complexes is responsible for the homocoupling of phenylethyne, while the slow conversion of these species to palladium(0) produces the active palladium catalyst for the cross-coupling reaction. Again, this proposition requires further research, including an investigation of the reaction between palladacycle dimer **46** and phenylethyne in the absence of the other starting materials.

5.5 Concluding Remarks

This research has demonstrated that phosphine-thioether ligand **14a** forms part of an active catalyst species for the palladium and copper co-catalysed Sonogashira coupling of 4-bromoanisole and phenylethyne. A 3 mol% loading of a $[Pd(OAc)_2]$/*P,S* phosphonium salt **49**/CuI pre-catalyst mixture gave quantitative conversion to the desired product, 4-(phenylethynyl)anisole, in four hours. Variations to this catalyst mixture showed that significantly slower reactions were produced when two equivalents of *P,S* phosphonium salt **49** were used, or the copper salt was omitted from the reaction. Omission of *P,S* phosphonium salt **49** resulted in complete inactivity of the catalyst. Replacement of *P,S* phosphonium salt **49** with $Bu^t{}_2BnPH^+BF_4^-$ produced a more rapid reaction, and an increase in formation of enyne by-products. Comparison of these two ligands at lower catalyst loading (0.3 mol%) showed an even more significant ligand dependence on the reaction rate and yield.

Investigation of the active catalyst species present in these reactions resulted in the identification of a number of metal complexes in solution. An NMR study showed the initial presence of $[Pd(\mu\text{-OAc})(P,C)]_2$ palladacycle dimer **46**, a *P,S* ligand **14a**/copper(I) iodide complex and a $[Pd(OAc)_2]$/di-*i*-propylamine complex. Upon addition of phenylethyne, palladacycle dimer **46** was replaced by a number of similar species, and subsequent heating caused a dark brown colour to develop in the reaction solution. No change was observed in the *P,S* ligand **14a**/copper(I) iodide or $[Pd(OAc)_2]$/di-*i*-propylamine complexes during the reaction. Mercury drop tests and dynamic light scattering experiments confirmed the presence of 2–11 nm nanoparticles in the reaction solution; however, the nanoparticles are not necessarily the active catalyst species.

The summation of the literature data on the subject of C−C bond-forming reactions catalysed by palladacycles suggests that these species are sources of low-ligated

palladium atoms or ions (*via* a Pd nanoparticle reservoir), and some researchers have asserted that the ligands of the former palladacycles are not involved in the catalytic process. However, a recent literature survey (April 2014) revealed no studies directly comparing palladacycles containing similar ligands under identical conditions. The present investigation does this, and clearly shows that the nature of the phosphine ligand employed in the catalysis affects the rate and selectivity of the reaction. Further study would be required to ascertain the mechanism by which this catalytic reaction proceeds, and specifically the role of phosphine-thioether ligand **14a**. Further investigation of the mechanism by which the enyne by-products are produced would also be of value. Another potentially worthwhile avenue of study in this area is the investigation of catalysis with a pre-formed palladium(0) complex, such as chelated [Pd(dba)(*P,S*)] complex **48**. Reactions with this palladium complex may bypass the complicating factors involved in C−C bond-forming reactions with palladacycle pre-catalysts, and could be employed in Sonogashira reactions or other more widely studied palladium-catalysed cross-coupling reactions, such as the Suzuki cross-coupling of organic halides and boronic acids (or similar).

Chapter 6

Conclusions

Hybrid *P,E* ligands have attracted a great deal of interest in recent years, in the field of homogeneous catalysis and in many other research areas. The combination of a strongly binding phosphorus donor atom and a second donor atom exhibiting quite different binding properties can create transition metal complexes with interesting and unusual characteristics, including hemilability, chirality, and the stabilisation of reactive donor atom types. Other ligand features can be integrated into ligands of this class, creating transition metal complexes with potentially unique patterns of behaviour. For example, unsymmetric diphosphine ligands with a large bite angle *o*-xylene backbone (based on the commercially successful dbpx ligand) have shown excellent catalytic activity and interesting synergistic effects; however, the chemistry of hybrid *P,E* ligands with this backbone type has not previously been explored.

On this basis, a family of novel hybrid *P,E* ligands containing an *o*-xylene backbone has been synthesised from the versatile substrate *o*-$C_6H_4\{CH_2PBu^t{}_2(BH_3)\}(CH_2Cl)$ (**5**). Reaction of this precursor with nucleophilic reagents, or conversion of compound **5** to a Grignard reagent and subsequent reaction with electrophiles produced a number of borane-protected hybrid *P,E* compounds, which in most cases were air-stable and crystalline. Deprotection of these compounds gave novel hybrid *P,E* ligands of the type *o*-$C_6H_4(CH_2PBu^t{}_2)(CH_2E)$, where E = PR_2 (**7** and **11**), SR (**14**), $S(O)Bu^t$ (**16**), NR_2 (**18**) or $SiPh_2H$ (**20a**).

The reactivity of three members of this family of ligands — phosphine-thioether ligand **14a**, phosphine-sulfoxide ligand **16** and phosphine-amine ligand **18a** — has been investigated with platinum(II) and platinum(0) precursor complexes. It was found that *P,S* ligand **14a** adopted chelating, monodentate and hemilabile bonding modes in platinum complexes. The chelated $[PtCl_2(P,S)]$ complex **21**

displayed an unexpectedly small bite angle of 86.1° (18° lower than a diphosphine analogue), whereas [Pt(nb)(*P,S*)] complex **34** displayed a bite angle of 106.6°, demonstrating the flexibility of this ligand. Monodentate [Pt(*P,S*)$_2$], [PtHL(*P,S*)$_2$] and [PtHL(*P,S*)$_2$]CH(SO$_2$CF$_3$)$_2$ complexes wherein ligand **14a** binds through the phosphorus donor atom only were also synthesised. A large observed cone angle of 180° was calculated for the phosphine moiety of ligand **14a** in [PtH$_2$(*P,S*)$_2$] complex **25**, and the large steric bulk of this phosphine ligand was demonstrated in the reversible dioxygen binding of [Pt(O$_2$)(*P,S*)$_2$] complex **42**. The facile and reversible conversion between [PtH(NCMe)(κ^1*P*-**14a**)$_2$]CH(SO$_2$CF$_3$)$_2$ (**28**) and [PtH(κ^1*P*-**14a**)(κ^2*P,S*-**14a**)]CH(SO$_2$CF$_3$)$_2$ (**26**) demonstrated the hemilability of ligand **14a**. The coordination behaviour of this ligand with platinum was found to differ from that of the diphosphine analogue, dbpx, in a number of respects.

A chelated [PtCl$_2$(*P,N*)] complex (**23**) was also synthesised with phosphine-amine ligand **18a**, although this ligand generally favoured binding in a monodentate fashion through the phosphorus donor atom. Chelated [Pt(alkene)(*P,S=O*)] (**33** and **35**) and monodentate [Pt(*P,S=O*)$_2$] (**37**) complexes were produced with phosphine-sulfoxide ligand **16**; however, characterisation of these complexes was often hindered by the presence of diastereomers. Further investigation of this ligand as a potential component of enantioselective catalysts would be valuable, but this would require either separation of the two enantiomers of *P,S=O* ligand **16** or an enantioselective ligand synthesis, neither of which have been attempted.

The coordination chemistry of phosphine-thioether ligand **14a** with palladium(II) and palladium(0) precursor complexes has also been investigated, resulting in the identification of five ligand bonding modes. Monodentate ligand coordination through the phosphorus donor atom was observed in the linear, 14-electron [Pd(*P,S*)$_2$] complex **44**. Chelation of the *P,S* ligand was observed in the palladium(0) alkene complexes [Pd(nb)(*P,S*)] (**47**) and [Pd(dba)(*P,S*)] (**48**). Reaction of ligand **14a** with a palladium(II) dichloride precursor at raised temperature resulted in S−C bond cleavage and the formation of palladium dimer **43** with bidentate coordination of the ligand through phosphine and bridging thiolate moieties. The reaction of *P,S* ligand **14a** with [Pd(OAc)$_2$] identified two further bonding modes of this ligand. Initially, C−H activation of the aryl backbone gave [Pd(μ-OAc)(*P,C*)]$_2$ dimer **46** with ligand **14a** occupying a *P,C* palladacycle bonding mode. In the presence of further [Pd(OAc)$_2$], palladium hexamer **45** was formed, with a combination of palladacycle and monodentate thioether binding resulting in bridging *P,C,S* coordination of ligand **14a**. This rich coordination chemistry indicates a large number of possibilities for active catalyst species in palladium-catalysed reactions with this ligand. Further investigation in this area could include

the synthesis of palladium(II) complexes with ligand **14a** in the monodentate and chelated coordination modes, perhaps *via* oxidation of palladium(0) complexes of this ligand.

The Sonogashira palladium and copper co-catalysed coupling of 4-bromoanisole and phenylethyne was investigated with a 3 mol% loading of a pre-catalyst mixture including phosphine-thioether ligand **14a**. This ligand produced an active catalyst, giving quantitative conversion to the desired product, 4-(phenylethynyl)anisole, in four hours. An NMR-scale study showed that a number of metal complexes (with both palladium and copper) were formed during the reaction, and the reactive pre-catalyst species was $[Pd(\mu\text{-OAc})(P,C)]_2$ dimer **46**. Variations to the pre-catalyst mixture, including the replacement of *P,S* ligand **14a** with $PBnBu^t{}_2$ and omission of the phosphine ligand, showed a definite ligand dependence on the rate and selectivity of the reaction. This result is significant as it is the first example of a direct comparison of similar palladacycles in palladium-catalysed C−C bond-forming reactions under identical conditions. Further investigation showed that polydisperse palladium nanoparticles were formed during the reaction, consistent with the idea that palladacycles are sources of low-ligated palladium atoms or ions, produced *via* a nanoparticle reservoir. Further study would be required to identify the active catalyst species in this system, including the use of techniques such as transmission electron microscopy, membrane reactor experiments, and poisons selective for homogeneous catalysts. Another interesting and potentially valuable avenue of investigation in this area would be the use of a pre-formed palladium(0) complex of phosphine-thioether ligand **14a** in Sonogashira or other palladium-catalysed carbon-carbon bond-forming reactions, or indeed other types of catalysis.

In summary, these novel hybrid *P,E* ligands have shown an interesting and varied coordination chemistry with Group 10 metals. The formation of an active catalyst with *P,S* ligand **14a** for Sonogashira cross-coupling reactions indicates that further investigation of these ligands in homogeneous catalysis could produce unusual and potentially beneficial results.

Chapter 7

Experimental

7.1 General Methods

All reactions were carried out using degassed solvents and standard Schlenk techniques under a nitrogen or argon atmosphere unless stated otherwise. Starting materials were obtained from Sigma-Aldrich or Merck Chemical Companies, and BOC Industrial Gases. DABCO was sublimed under reduced pressure, and other amines and thiols were dried and distilled before use. Di-*t*-butylphosphine,[262] diphenylphosphine–borane,[263] bis(pentafluorophenyl)bromophosphine,[264] 3-carboxypyridinium chlorochromate,[99] pyrrolidine–borane,[265] diethylamine–borane,[266] $[PtCl_2(1,5\text{-hexadiene})]$,[267] *cis*-$[PtCl_2(NCBu^t)_2]$,[268] $CH_2(SO_2CF_3)_2$,[139] 1,3,5-triaza-7-phosphaadamantane,[269] $[Pt(ethene)_3]$,[270] $[Pt(nb)_3]$,[160] $[Pt(1,5\text{-cyclooctadiene})_2]$,[271] $[PdCl_2(NCBu^t)_2]$,[272] $[PdMe_2(tmeda)]$,[273] $[Pd(nb)_3]$,[274] $[Pd(OAc)_2]$,[275] [Pd(Cp)(allyl)][276] and $[Pd_2(dba)_3]$[277] were synthesised using literature methods. Benzyldi-*t*-butylphosphine was synthesised in a manner similar to the syntheses of compound **4** and ligand **7**.[163] Tetrahydrofuran (THF) and diethyl ether (Et_2O) were distilled under a nitrogen or argon atmosphere from sodium benzophenone ketyl immediately prior to use. All other solvents used were of analytical grade, and were degassed and dried over molecular sieves.

Nuclear magnetic resonance (NMR) spectra were recorded using a Varian Unity Inova spectrometer operating at 300, 121 and 282 MHz for ^1H, ^{31}P and ^{19}F spectra respectively, a Varian Unity Inova spectrometer operating at 500, 125 and 96 MHz for ^1H, ^{13}C and ^{11}B spectra respectively, and a Varian DirectDrive spectrometer operating at 600 and 150 MHz for ^1H and ^{13}C spectra respectively. All direct-detected ^1H and ^{13}C chemical shifts, δ (ppm), were referenced to the residual

solvent peak of the deuterated solvent.[278] ^{31}P, ^{19}F and ^{11}B NMR spectra were referenced to H_3PO_4, $CFCl_3$ and $BF_3 \cdot Et_2O$ respectively. ^{13}C, ^{31}P, ^{19}F and ^{11}B NMR spectra were measured with ^{1}H-decoupling. Infrared spectra were obtained using a Perkin-Elmer Spectrum One FT-IR spectrophotometer (resolution 4 cm^{-1}) in absorbance mode. All spectral data were obtained at ambient temperature unless stated otherwise. Electrospray ionisation mass spectrometry was performed using an Agilent 6530 Q-TOF mass spectrometer, or by the Carbohydrate Chemistry Group at Industrial Research Limited, Lower Hutt, using a Waters Q-TOF Premier Tandem mass spectrometer. Gas chromatography-mass spectrometry was performed using a Shimadzu QP2010-Plus GC-MS operating in positive electron impact mode (70 eV). Elemental analysis was performed at the Campbell Microanalytical Laboratory at Otago University, Dunedin. Dynamic light scattering was performed using a Malvern Zetasizer Nano ZS instrument.

X-ray diffraction data were collected on a Bruker SMART APEX-II CCD diffractometer using Mo Kα radiation or an Agilent SuperNova (Dual Source) CCD diffractometer using Cu Kα radiation. Data were reduced using Bruker SAINT or Agilent CrysAlisPro software. Absorption correction was performed using the SADABS or SCALE3 ABSPACK programs. OLEX2 (Version 1.2.5)[279] was used as a front-end for SHELX[280] or Superflip[281] executables during structure solution and refinement. The positions of all hydrogen atoms (other than the hydride ligands in complex **25**) were calculated during refinement.

7.2 Ligands

α,α'-(Di-*t*-butylphosphonium)-*o*-xylene bromide (1)

α,α'-Dibromo-*o*-xylene (0.20 g, 0.76 mmol), di-*t*-butylphosphine (0.14 mL, 0.76 mmol) and potassium carbonate (0.11 g, 0.76 mmol) were combined in acetonitrile (15 mL) and stirred overnight. The solvent was removed under reduced pressure and the resulting white solid extracted into chloroform (25 mL) in the air. Removal of the solvent under reduced pressure and washing with diethyl ether (2 × 5 mL) gave desired compound **1**. Air-stable white powder (0.18 g, 72%). ^{1}H NMR δ (500 MHz, $CDCl_3$): 1.54 (d, J = 16.1 Hz, 18H, PBu^t), 4.07 (d, J = 8.5 Hz, 4H, CH_2P), 7.29 (br s, 2H, Ar), 7.49 (br s, 2H, Ar). ^{13}C NMR δ (125 MHz, $CDCl_3$): 24.97 (d, J = 46.1 Hz, CH_2P), 27.26 (s, $PCMe_3$), 34.02 (d, J = 33.1 Hz, $PCMe_3$), 127.59 (d, J = 13.0 Hz, Ar), 129.11 (s, Ar), 134.51 (d, J = 4.8 Hz, Ar). ^{31}P NMR δ

(121 MHz, $CDCl_3$): 71.75 (s). HRMS calcd for $C_{16}H_{26}P$ $[M-Br]^+$: $m/z = 249.1767$; found: 249.1763.

o-(Methyl)benzyldi-*t*-butylphosphine oxide (2)

Compound **1** (100 mg, 0.3 mmol) and sodium methoxide (16 mg, 0.3 mmol) were dissolved in methanol (3.5 mL) and stirred for 48 h (45% conversion). ^{1}H NMR δ (500 MHz, C_6D_6): 0.97 (d, J = 13.2 Hz, 18H, PBu^t), 2.27 (s, 3H, ArMe), 2.80 (d, J = 11.3 Hz, 2H, CH_2P), 7.01 (m, 2H, Ar), 7.08 (m, 1H, Ar), 7.62 (d, J = 7.3 Hz, 1H, Ar). ^{13}C NMR δ (125 MHz, C_6D_6): 20.68 (s, ArMe), 26.23 (d, J = 52.3 Hz, CH_2P), 26.89 (br, $PCMe_3$), 36.42 (d, J = 58.1 Hz, $PCMe_3$), 126.18 (s, Ar), 127.04 (d, J = 1.9 Hz, Ar), 130.93 (s, Ar), 131.61 (d, J = 3.8 Hz, Ar), 133.01 (d, J = 7.2 Hz, Ar), 136.62 (d, J = 5.2 Hz, Ar). ^{31}P NMR δ (121 MHz, C_6D_6): 60.86 (s).

α-Chloro-α'-methoxy-*o*-xylene (3)

A solution of sodium methoxide (0.59 g, 11 mmol) in methanol (30 mL) was added dropwise in the air to a refluxing solution of α,α'-dichloro-*o*-xylene (3.85 g, 22 mmol) in methanol (30 mL) over 30 min. Reflux was continued for 1 h, and the cooled mixture was reduced to half volume under reduced pressure. Distilled water (40 mL) was added and the mixture extracted with diethyl ether (2 × 40 mL). The combined organic layers were washed with brine (25 mL), dried over magnesium sulfate and the solvent evaporated under reduced pressure to give a yellow liquid containing compound **3**, α,α'-dichloro-*o*-xylene and α,α'-dimethoxy-*o*-xylene. The α,α'-dimethoxy-*o*-xylene by-product was removed by elution through a silica gel column with 5% ethyl acetate in *n*-hexane (R_f = 0.31). Elution through a silica gel column with 10% toluene in *n*-hexane was then used to separate the unreacted α,α'-dichloro-*o*-xylene (R_f = 0.54) and pure compound **3** (R_f = 0.17). Clear liquid (1.16 g, 62%). ^{1}H NMR δ (500 MHz, $CDCl_3$): 3.42 (s, 3H, OMe), 4.60 (s, 2H, CH_2O), 4.71 (s, 2H, CH_2Cl), 7.32 (m, 2H, Ar), 7.38 (m, 2H, Ar). ^{13}C NMR δ (125 MHz, $CDCl_3$): 43.80 (s, CH_2Cl), 58.54 (s, OMe), 72.39 (s, CH_2O), 128.57 (s, Ar), 128.94 (s, Ar), 129.65 (s, Ar), 130.43 (s, Ar), 136.09 (s, Ar), 136.72 (s, Ar). IR (liquid film): 1088 (CO), 2823–3068 cm^{-1} (CH). Anal. calcd for $C_9H_{11}ClO$: C, 63.4; H, 6.5; found: C, 63.8; H, 6.6.

α-(Di-*t*-butylphosphino)-α'-methoxy-*o*-xylene–borane (4)

A mixture of di-*t*-butylphosphine (0.55 mL, 3 mmol) and borane–dimethylsulfide complex (0.3 mL, 10 M, 3 mmol) was stirred in THF (4 mL) for 2 h, and the solvent evaporated under reduced pressure. The resulting white solid was dissolved

in diethyl ether (30 mL) and cooled to 0 °C, and a solution of *n*-butyllithium (1.9 mL, 1.59 M in hexanes, 3 mmol) was added dropwise with stirring. The mixture was stirred at room temperature for 30 min, then cooled to 0 °C and a solution of compound **3** (0.51 g, 3 mmol) in diethyl ether (20 mL) was added. After warming to room temperature, the mixture was stirred overnight. The resulting solution was filtered in the air and the solvent evaporated under reduced pressure, leaving a clear liquid. Desired compound **4** was recrystallised from *n*-hexane. Air-stable white crystals (0.45 g, 51%). ^{1}H NMR δ (500 MHz, C_6D_6): 1.0–1.8 (br, 3H, BH_3), 1.08 (d, J = 12.5 Hz, 18H, PBu^t), 3.09 (s, 3H, OMe), 3.16 (d, J = 12.5 Hz, 2H, CH_2P), 4.44 (s, 2H, CH_2O), 6.99 (t, J = 8.0 Hz, 1H, Ar), 7.11 (d, J = 7.5 Hz, 2H, Ar), 8.10 (d, J = 8.0 Hz, 1H, Ar). ^{13}C NMR δ (125 MHz, C_6D_6): 21.16 (d, J = 24.4 Hz, CH_2P), 28.18 (d, J = 1.0 Hz, PCMe_3), 33.06 (d, J = 24.8 Hz, PCMe$_3$), 57.54 (s, OMe), 74.36 (s, CH_2O), 126.75 (d, J = 1.9 Hz, Ar), 130.66 (d, J = 1.0 Hz, Ar), 131.92 (d, J = 2.9 Hz, Ar), 135.50 (d, J = 2.9 Hz, Ar), 136.55 (d, J = 5.3 Hz, Ar), other Ar obscured by solvent. ^{31}P NMR δ (121 MHz, C_6D_6): 47.30 (m). IR (film from CH_2Cl_2): 1070 (CO), 2380 (BH), 2871–2967 cm^{-1} (CH). HRMS calcd for $C_{17}H_{32}BNaOP$ $[M+Na]^+$: m/z = 317.2182; found: 317.2180. Anal. calcd for $C_{17}H_{32}BOP$: C, 69.4; H, 11.0; found: C, 69.2; H, 11.1.

α-(Di-*t*-butylphosphino)-α'-chloro-*o*-xylene–borane (5)

A mixture of di-*t*-butylphosphine (4.4 mL, 24 mmol) and borane–dimethylsulfide complex (2.8 mL, 10 M, 28 mmol) was stirred in THF (15 mL) for 2 h, and the solvent evaporated under reduced pressure. The resulting white solid was dissolved in diethyl ether (50 mL) and cooled to 0 °C, and a solution of *n*-butyllithium (15.1 mL, 1.59 M in hexanes, 24 mmol) was added dropwise with stirring. The mixture was stirred at room temperature for 15 min, then cooled to −78 °C and a solution of α,α'-dichloro-*o*-xylene (12.3 g, 70 mmol) in ether (50 mL) was added. After warming to room temperature, the mixture was stirred for 2 h. The resulting solution was filtered in the air and the solvent evaporated under reduced pressure, leaving a pale yellow solid. Unreacted α,α'-dichloro-*o*-xylene was sublimed out of the crude material at 50 °C and ∼0.1 mmHg overnight, and the desired product **5** recrystallised from *n*-hexane. Air-stable white crystals (3.87 g, 54%). ^{1}H NMR δ (500 MHz, C_6D_6): 0.6–1.5 (br, 3H, BH_3), 1.05 (d, J = 12.3 Hz, 18H, PBu^t), 3.11 (d, J = 12.0 Hz, 2H, CH_2P), 4.72 (s, 2H, CH_2Cl), 6.89 (m, 1H, Ar), 6.98 (m, 2H, Ar), 7.57 (d, J = 7.5 Hz, 1H, Ar). ^{13}C NMR δ (125 MHz, C_6D_6): 21.91 (d, J = 22.9 Hz, CH_2P), 28.27 (d, J = 1.4 Hz, PCMe_3), 32.98 (d, J = 24.3 Hz, PCMe$_3$), 46.21 (s, CH_2Cl), 127.54 (d, J = 2.3 Hz, Ar), 128.70 (d, J = 1.4 Hz, Ar), 131.39 (d, J = 1.4 Hz, Ar), 132.29 (d, J = 3.3 Hz, Ar), 135.01 (d, J = 3.2 Hz, Ar), 137.24 (d, J = 4.1 Hz, Ar). ^{31}P NMR δ (121 MHz, C_6D_6): 47.90 (m). IR (film

from CH_2Cl_2): 2377 (BH), 2870–2969 cm^{-1} (CH). HRMS calcd for $C_{16}H_{29}BClNaP$ $[M+Na]^+$: $m/z = 321.1686$; found: 321.1685. Anal. calcd for $C_{16}H_{29}BClP$: C, 64.4; H, 9.8; found: C, 64.1; H, 9.9.

α-(Di-*t*-butylphosphino)-α'-(diphenylphosphino)-*o*-xylene–diborane (6)

A solution of freshly prepared diphenylphosphine–borane (0.136 g, 0.68 mmol) in THF (5 mL) was cooled to 0 °C and a solution of *n*-butyllithium (0.35 mL, 2.0 M in cyclohexane, 0.70 mmol) was added dropwise with stirring. The mixture was stirred at room temperature for 2 h, cooled to −78 °C and a solution of compound **5** (0.180 g, 0.60 mmol) in THF (4 mL) added. The mixture was stirred at room temperature overnight, the solvent removed under reduced pressure, and the resulting off-white solid stirred in toluene (25 mL) for 1 h in the air. Filtration and solvent removal under reduced pressure gave crude compound **6**, which was recrystallised from 1:3 toluene/*n*-hexane. Air-stable white crystals (0.158 g, 57%). ^{1}H NMR δ (600 MHz, $CDCl_3$): 0.2–1.2 (br, 6H, 2 × BH_3), 1.23 (d, J = 12.3 Hz, 18H, PBu^t), 3.11 (d, J = 11.8 Hz, 2H, CH_2PBu^t), 3.93 (d, J = 11.8 Hz, 2H, CH_2PPh), 6.51 (d, J = 7.6 Hz, 1H, Ar), 6.90 (t, J = 7.4 Hz, 1H, Ar), 7.10 (t, J = 7.6 Hz, 1H, Ar), 7.42 (m, 5H, Ar & PPh), 7.50 (m, 2H, PPh), 7.59 (m, 4H, Ar). ^{13}C NMR δ (150 MHz, $CDCl_3$): 23.54 (d, J = 23.5 Hz, CH_2PBu^t), 28.55 (s, $PCMe_3$), 31.88 (d, J = 31.1 Hz, CH_2PPh), 33.15 (d, J = 24.8 Hz, $PCMe_3$), 126.50 (t, J = 2.6 Hz, Ar), 126.88 (dd, J = 3.2, 1.9 Hz, Ar), 128.81 (d, J = 10.2 Hz, PPh), 129.10 (d, J = 54.0 Hz, PPh), 131.41 (d, J = 1.9 Hz, PPh), 131.60 (dd, J = 3.8, 1.9 Hz, Ar), 131.78 (t, J = 3.8 Hz, Ar), 132.03 (t, J = 3.2 Hz, Ar), 132.80 (d, J = 8.9 Hz, PPh), 134.66 (t, J = 4.5 Hz, Ar). ^{31}P NMR δ (121 MHz, $CDCl_3$): 18.52 (br, PPh), 47.69 (br, PBu^t). IR (film from CH_2Cl_2): 2349–2386 (BH), 2869–3079 cm^{-1} (CH). HRMS calcd for $C_{28}H_{42}B_2NaP_2$ $[M+Na]^+$: $m/z = 485.2850$; found: 485.2848. Anal. calcd for $C_{28}H_{42}B_2P_2$: C, 72.8; H, 9.2; found: C, 73.0; H, 9.0.

α-(Di-*t*-butylphosphino)-α'-(diphenylphosphino)-*o*-xylene (7)

Compound **6** (50 mg, 0.11 mmol) and morpholine (1 mL) were combined in a sealed tube and heated to 100 °C for 1 h. After cooling, the solvent was evaporated under reduced pressure. The resulting white solid was extracted with *n*-hexane (2 × 2 mL), filtered through a plug of alumina, and the solvent evaporated under reduced pressure, giving desired product **7**. Highly air-sensitive white solid (39 mg, 82%). ^{1}H NMR δ (500 MHz, C_6D_6): 1.09 (d, J = 10.5 Hz, 18H, PBu^t), 3.09 (s, 2H, CH_2PBu^t), 3.92 (d, J = 2.5 Hz, 2H, CH_2PPh), 6.75 (d, J = 7.6 Hz, 1H, Ar), 6.85 (t, J = 7.5 Hz, 1H, Ar), 7.00 (t, J = 7.6 Hz, 1H, Ar), 7.04 (m, 6H, PPh), 7.42 (m, 4H, PPh), 7.50 (d, J = 7.9 Hz, 1H, Ar). ^{13}C NMR δ (125 MHz, C_6D_6):

27.41 (dd, J = 26.9, 6.7 Hz, CH$_2$PBu^t), 30.10 (d, J = 13.4 Hz, PCMe_3), 32.12 (d, J = 24.0 Hz, PCMe$_3$), 34.63 (dd, J = 17.0, 11.8 Hz, CH$_2$PPh), 125.82 (t, J = 1.9 Hz, Ar), 126.28 (d, J = 2.9 Hz, Ar), 128.59 (d, J = 6.2 Hz, PPh), 128.77 (s, PPh), 131.45 (d, J = 7.2 Hz, Ar), 131.74 (dd, J = 10.6, 1.4 Hz, Ar), 133.51 (d, J = 18.2 Hz, PPh), 136.03 (dd, J = 6.5, 2.2 Hz, Ar), 139.28 (d, J = 16.3 Hz, PPh), 139.60 (dd, J = 8.7, 3.9 Hz, Ar). ^{31}P NMR δ (121 MHz, C$_6$D$_6$): −15.61 (d, J = 1.4 Hz, PPh), 24.47 (d, J = 1.4 Hz, PBu^t).

Compounds 8, 9 and 10

Flame-dried magnesium powder (1.20 g, 49 mmol) and THF (5 mL) were combined in a Schlenk tube, 1,2-dibromoethane (0.05 mL) added and the mixture heated until bubbles appeared. After reaction was complete, the solvent was decanted and fresh THF (5 mL) added. A solution of compound **5** (0.40 g, 1.34 mmol) in THF (5 mL) was added and the mixture stirred for 2 h. The resulting green solution was decanted and added dropwise to a solution of bis(pentafluorophenyl)bromophosphine (0.30 mL, 1.34 mmol) in THF (5 mL) at 0 °C. The solution was stirred at room temperature overnight and the solvent removed under reduced pressure giving a mixture of compounds **8**, **9** and **10** as a sticky solid. Compound **10** was removed by trituration with *n*-hexane (40 mL) and filtration through a plug of alumina. The solvent was removed under reduced pressure and the resulting cloudy oil washed with methanol (2 × 5 mL) to remove **9** and other impurities, giving compound **8**. Air-sensitive white powder (0.27 g, 32%).

*α-(Di-t-butylphosphino)-α′-{bis(pentafluorophenyl)phosphino}-o-xylene–borane (**8**)*
^{1}H NMR δ (500 MHz, C$_6$D$_6$): 0.9–1.6 (br, 3H, BH$_3$), 1.09 (d, J = 12.2 Hz, 18H, PBu^t), 3.29 (d, J = 11.9 Hz, 2H, CH_2PBu^t), 4.23 (d, J = 4.6 Hz, 2H, CH_2P(C$_6$F$_5$)), 6.64 (d, J = 7.6 Hz, 1H, Ar), 6.69 (t, J = 7.6 Hz, 1H, Ar), 6.86 (t, J = 7.6 Hz, 1H, Ar), 7.51 (d, J = 7.8 Hz, 1H, Ar). ^{13}C NMR δ (125 MHz, C$_6$D$_6$): 23.22 (dd, J = 22.1, 9.1 Hz, CH$_2$PBu^t), 28.29 (s, PCMe_3), 30.20 (m, CH$_2$P(C$_6$F$_5$)), 33.08 (d, J = 24.0 Hz, PCMe$_3$), 108.60 (m, P(C$_6$F$_5$)), 127.34 (t, J = 2.4 Hz, Ar), 127.45 (dd, J = 3.4, 1.5 Hz, Ar), 130.91 (d, J = 8.6 Hz, Ar), 132.74 (t, J = 2.9 Hz, Ar), 134.02 (dd, J = 5.8, 4.3 Hz, Ar), 134.44 (t, J = 3.8 Hz, Ar), 137.76 (dm, J = 254.3 Hz, P(C$_6$F$_5$)), 142.50 (dm, J = 257.2 Hz, P(C$_6$F$_5$)), 147.96 (dm, J = 246.6 Hz, P(C$_6$F$_5$)). ^{31}P NMR δ (121 MHz, C$_6$D$_6$): −50.47 (quin, J = 22.2 Hz, P(C$_6$F$_5$)), 49.38 (br, PBu^t). ^{19}F NMR δ (282 MHz, C$_6$D$_6$): −160.32 (m, 4F, P(*m*-C$_6$F$_5$)), −149.37 (tt, J = 21.8, 4.0 Hz, 2F, P(*p*-C$_6$F$_5$)), −130.11 (m, 4F, P(*o*-C$_6$F$_5$)). HRMS calcd for C$_{28}$H$_{28}$BF$_{10}$P$_2$ [M−H]$^+$: m/z = 627.1599; found: 627.1597.

*o-(Methyl)benzyldi-t-butylphosphine–borane (**9**)*
^{1}H NMR δ (500 MHz, C_6D_6): 1.0–1.8 (br, 3H, BH_3), 1.05 (d, J = 12.3 Hz, 18H, PBu^t), 2.22 (s, 3H, ArMe), 2.85 (d, J = 12.5 Hz, 2H, CH_2P), 7.00 (m, 2H, Ar), 7.07 (m, 1H, Ar), 7.98 (d, J = 7.9 Hz, 1H, Ar). ^{13}C NMR δ (125 MHz, C_6D_6): 20.86 (s, ArMe), 21.99 (d, J = 24.0 Hz, CH_2P), 28.29 (br s, $PCMe_3$), 33.00 (d, J = 24.5 Hz, $PCMe_3$), 126.19 (d, J = 1.4 Hz, Ar), 127.05 (d, J = 2.4 Hz, Ar), 130.86 (d, J = 1.5 Hz, Ar), 131.64 (d, J = 2.9 Hz, Ar), 134.05 (d, J = 3.4 Hz, Ar), 136.20 (d, J = 4.8 Hz, Ar). ^{31}P NMR δ (121 MHz, C_6D_6): 48.05 (br). HRMS calcd for $C_{16}H_{30}BNaP$ $[M+Na]^+$: m/z = 287.2076; found: 287.2080.

*2,2′-(Di-t-butylphosphinomethyl)bibenzyl–diborane (**10**)*
Selected ^{1}H NMR δ (300 MHz, C_6D_6): 1.0–1.8 (br, 6H, BH_3), 1.03 (d, J = 12.0 Hz, 36H, PBu^t), 2.52 (d, J = 12.0 Hz, 4H, CH_2P), 2.98 (s, 4H, CH_2CH_2), 7.78 (m, 2H, Ar). ^{31}P NMR δ (121 MHz, C_6D_6): 49.07 (br). HRMS calcd for $C_{32}H_{57}B_2P_2$ $[M-H]^+$: m/z = 525.4127; found: 525.4116.

α-(Di-*t*-butylphosphino)-α'-{bis(pentafluorophenyl)phosphino}-*o*-xylene (11)

A solution of compound **8** (60 mg, 0.10 mmol) in dichloromethane (2 mL) was cooled to −10 °C, tetrafluoroboric acid–diethyl ether complex (0.17 mL, 85% solution, 1.0 mmol) added dropwise, and the resulting solution stirred at room temperature for 1 h. Diethyl ether (3 mL) was added, followed by saturated sodium hydrogen carbonate solution (6 mL), and the mixture stirred for 30 min. The resulting layers were separated, the aqueous layer washed with diethyl ether (2 × 3 mL), combined organic fractions washed with distilled water (3 mL) and brine (3 mL), dried over magnesium sulfate, filtered, and the solvent removed under reduced pressure, giving desired compound **11**. Highly air-sensitive white solid (30 mg, 51%). ^{1}H NMR δ (500 MHz, C_6D_6): 1.07 (d, J = 10.8 Hz, 18H, PBu^t), 3.07 (s, 2H, CH_2PBu^t), 4.27 (s, 2H, $CH_2P(C_6F_5)$), 6.69 (d, J = 7.8 Hz, 1H, Ar), 6.74 (t, J = 7.3 Hz, 1H, Ar), 6.91 (t, J = 7.5 Hz, 1H, Ar), 7.41 (d, J = 7.6 Hz, 1H, Ar). ^{13}C NMR δ (125 MHz, C_6D_6): 27.36 (dd, J = 27.8, 6.7 Hz, CH_2PBu^t), 29.29 (m, $CH_2P(C_6F_5)$), 29.87 (d, J = 13.4 Hz, $PCMe_3$), 32.07 (d, J = 24.0 Hz, $PCMe_3$), 109.13 (m, $P(C_6F_5)$), 126.24 (dd, J = 2.4, 1.9 Hz, Ar), 127.63 (d, J = 3.4 Hz, Ar), 130.50 (d, J = 9.6 Hz, Ar), 132.36 (dd, J = 11.1, 2.4 Hz, Ar), 133.21 (dd, J = 7.7, 1.9 Hz, Ar), 137.77 (dm, J = 252.9 Hz, $P(C_6F_5)$), 139.97 (dd, J = 8.6, 4.3 Hz, Ar), 142.46 (dm, J = 257.2 Hz, $P(C_6F_5)$), 148.03 (dm, J = 246.6 Hz, $P(C_6F_5)$). ^{31}P NMR δ (121 MHz, C_6D_6): −50.87 (quind, J = 22.3, 11.9 Hz, $P(C_6F_5)$), 25.15 (d, J = 12.6 Hz, PBu^t). ^{19}F NMR δ (282 MHz, C_6D_6): −160.51 (m, 4F, P(m-C_6F_5)), −149.81 (tt, J = 20.8, 4.0 Hz, 2F, P(p-C_6F_5)), −130.01 (m, 4F, P(o-C_6F_5)).

α-(Di-*t*-butylphosphino)-α'-{bis(*p*-*N*-morpholinotetrafluorophenyl)-phosphino}-*o*-xylene (12)

Compound **8** (61 mg, 0.10 mmol) and morpholine (1 mL) were combined in a sealed tube and heated to 100 °C for 1 h. After cooling, the solvent was evaporated under reduced pressure. The resulting white solid was extracted with *n*-hexane (2 × 2 mL), filtered through a plug of alumina, and the solvent evaporated under reduced pressure, giving compound **12**. Highly air-sensitive white foam (63 mg, 84%). ^{1}H NMR δ (500 MHz, C_6D_6): 1.12 (d, J = 10.7 Hz, 18H, PBu^t), 2.76 (br s, 8H, CH_2N), 3.20 (s, 2H, CH_2PBu^t), 3.36 (br s, 8H, CH_2O), 4.53 (s, 2H, CH_2P(C_6F_4)N), 6.85 (t, J = 7.3 Hz, 1H, Ar), 6.98 (m, 2H, Ar), 7.56 (d, J = 7.0 Hz, 1H, Ar). ^{13}C NMR δ (125 MHz, C_6D_6): 27.11 (dd, J = 27.3, 7.2 Hz, CH$_2$PBu^t), 29.78 (m, CH$_2$P(C_6F_4)N), 30.00 (d, J = 13.4 Hz, PCMe_3), 32.11 (d, J = 24.5 Hz, PCMe$_3$), 51.11 (t, J = 3.4 Hz, CH_2N), 67.05 (s, CH_2O), 106.06 (m, P(C_6F_4)N), 126.13 (s, Ar), 127.24 (d, J = 3.4 Hz, Ar), 130.83 (d, J = 8.7 Hz, Ar), 132.00 (m, P(C_6F_4)N), 132.19 (dd, J = 12.5, 2.4 Hz, Ar), 134.37 (dd, J = 7.8, 2.1 Hz, Ar), 140.12 (dd, J = 9.1, 4.3 Hz, Ar), 142.06 (dm, J = 230.3 Hz, P(C_6F_4)N), 149.04 (dm, J = 234.2 Hz, P(C_6F_4)N). ^{31}P NMR δ (121 MHz, C_6D_6): −51.73 (quind, J = 23.7, 8.1 Hz, P(C_6F_4)N), 25.40 (d, J = 8.1 Hz, PBu^t). ^{19}F NMR δ (282 MHz, C_6D_6): −150.56 (dd, J = 20.9, 7.0 Hz, 4F, P(*m*-C_6F_4)N), −132.47 (td, J = 22.8, 9.9 Hz, 4F, P(*o*-C_6F_4)N). HRMS calcd for $C_{36}H_{43}F_8N_2O_2P_2$ [M+H]$^+$: m/z = 749.2667; found: 749.2659.

α-(Di-*t*-butylphosphino)-α'-(*t*-butylthio)-*o*-xylene–borane (13a)

Sodium metal (0.164 g, 7.1 mmol) and ethanol (50 mL) were combined and after reaction was complete, *t*-butylthiol (0.84 mL, 7.5 mmol) was added and resulting solution stirred for 1 h. Compound **5** (1.05 g, 3.5 mmol) was added and the mixture stirred overnight, followed by solvent evaporation under reduced pressure. The resulting white solid was dissolved in toluene (50 mL) in the air, filtered and the solvent evaporated under reduced pressure leaving crude compound **13a**, which was recrystallised from *n*-hexane. Air-stable white powdery crystals (0.98 g, 80%). ^{1}H NMR δ (500 MHz, C_6D_6): 1.0–1.8 (br, 3H, BH_3), 1.12 (d, J = 12.5 Hz, 18H, PBu^t), 1.29 (s, 9H, SBu^t), 3.27 (d, J = 12.0 Hz, 2H, CH_2P), 3.99 (s, 2H, CH_2S), 6.99 (t, J = 7.5 Hz, 1H, Ar), 7.04 (t, J = 7.5 Hz, 1H, Ar), 7.23 (d, J = 7.0 Hz, 1H, Ar), 7.79 (d, J = 8.0 Hz, 1H, Ar). ^{13}C NMR δ (125 MHz, C_6D_6): 22.43 (d, J = 23.5 Hz, CH_2P), 28.38 (d, J = 1.0 Hz, PCMe_3), 30.98 (s, SCMe_3), 32.93 (s, CH_2S), 33.08 (d, J = 24.8 Hz, PCMe$_3$), 42.67 (s, SCMe$_3$), 127.22 (d, J = 1.5 Hz, Ar), 127.37 (d, J = 1.9 Hz, Ar), 131.69 (d, J = 1.4 Hz, Ar), 132.16 (d, J = 3.3 Hz, Ar), 134.67 (d, J = 3.4 Hz, Ar), 137.17 (d, J = 4.8 Hz, Ar). ^{31}P NMR δ (121 MHz,

C_6D_6): 47.94 (br). ^{11}B NMR δ (96 MHz, C_6D_6): −40.37 (d, J = 47.6 Hz). IR (film from CH_2Cl_2): 2383 (BH), 2902–3051 cm^{-1} (CH). HRMS calcd for $C_{20}H_{38}BNaPS$ $[M+Na]^+$: m/z = 374.2459; found: 374.2462. Anal. calcd for $C_{20}H_{38}BPS$: C, 68.2; H, 10.9; S, 9.1; found: C, 68.0; H, 11.1; S, 9.0.

α-(Di-*t*-butylphosphino)-α'-(phenylthio)-*o*-xylene–borane (13b)

Sodium metal (0.175 g, 7.6 mmol) and ethanol (50 mL) were combined and after reaction was complete, thiophenol (0.82 mL, 8.0 mmol) was added and resulting solution stirred for 1 h. Compound **5** (1.13 g, 3.8 mmol) was added and the mixture stirred overnight, followed by solvent evaporation under reduced pressure. The resulting white solid was dissolved in toluene (50 mL) in the air, filtered and the solvent evaporated under reduced pressure leaving crude compound **13b**, which was recrystallised from *n*-hexane. Air-stable white plate-like crystals (1.05 g, 75%). ^{1}H NMR δ (500 MHz, C_6D_6): 0.9–1.7 (br, 3H, BH_3), 1.05 (d, J = 12.0 Hz, 18H, PBu^t), 3.20 (d, J = 12.0 Hz, 2H, CH_2P), 4.40 (s, 2H, CH_2S), 6.92 (m, 2H, Ar & SPh), 7.01 (m, 4H, Ar & SPh), 7.32 (d, J = 8.5 Hz, 2H, SPh), 7.61 (d, J = 8.0 Hz, 1H, Ar). ^{13}C NMR δ (125 MHz, C_6D_6): 22.31 (d, J = 22.9 Hz, CH_2P), 28.31 (d, J = 1.0 Hz, $PCMe_3$), 32.99 (d, J = 24.4 Hz, $PCMe_3$), 38.50 (s, CH_2S), 126.52 (s, SPh), 127.33 (d, J = 2.0 Hz, Ar), 127.51 (d, J = 1.4 Hz, Ar), 129.17 (s, SPh), 130.11 (s, SPh), 131.57 (d, J = 1.5 Hz, Ar), 132.20 (d, J = 3.4 Hz, Ar), 134.67 (d, J = 3.4 Hz, Ar), 136.61 (d, J = 4.3 Hz, Ar), 137.21 (s, SPh). ^{31}P NMR δ (121 MHz, C_6D_6): 47.97 (br). ^{11}B NMR δ (96 MHz, C_6D_6): −40.65 (d, J = 48.4 Hz). IR (film from CH_2Cl_2): 2381 (BH), 2870–3059 cm^{-1} (CH). HRMS calcd for $C_{22}H_{34}BNaPS$ $[M+Na]^+$: m/z = 395.2110; found: 395.2116. Anal. calcd for $C_{22}H_{34}BPS$: C, 71.0; H, 9.2; S, 8.6; found: C, 71.0; H, 9.4; S, 8.5.

α-(Di-*t*-butylphosphino)-α'-(*t*-butylthio)-*o*-xylene (14a)

Compound **13a** (50 mg, 0.14 mmol) and morpholine (1 mL) were combined in a sealed tube and heated to 100 °C for 1 h. After cooling, the solvent was evaporated under reduced pressure. The resulting white solid was extracted with *n*-hexane (2 × 2 mL), filtered through a plug of alumina, and the solvent evaporated under reduced pressure, giving desired product **14a**. Highly air-sensitive clear oil (44 mg, 93%). ^{1}H NMR δ (600 MHz, C_6D_6): 1.13 (d, J = 10.6 Hz, 18H, PBu^t), 1.29 (s, 9H, SBu^t), 3.09 (d, J = 1.2 Hz, 2H, CH_2P), 4.05 (s, 2H, CH_2S), 7.01 (t, J = 7.3 Hz, 1H, Ar), 7.07 (t, J = 7.7 Hz, 1H, Ar), 7.31 (d, J = 7.3 Hz, 1H, Ar), 7.68 (d, J = 7.3 Hz, 1H, Ar). ^{13}C NMR δ (150 MHz, C_6D_6): 26.21 (d, J = 26.0 Hz, CH_2P), 30.07 (d, J = 13.2 Hz, $PCMe_3$), 31.00 (s, $SCMe_3$), 32.01 (d, J = 24.2 Hz, $PCMe_3$), 32.25 (d, J = 8.7 Hz, CH_2S), 42.57 (s, $SCMe_3$), 126.18 (d, J = 1.8 Hz, Ar), 127.20 (s, Ar),

131.14 (s, Ar), 131.63 (d, J = 14.4 Hz, Ar), 136.58 (d, J = 2.9 Hz, Ar), 140.06 (d, J = 9.2 Hz, Ar). ^{31}P NMR δ (121 MHz, C_6D_6): 24.99 (s).

α-(Di-*t*-butylphosphino)-α'-(phenylthio)-*o*-xylene (14b)

Compound **13b** (50 mg, 0.13 mmol) and morpholine (1 mL) were combined in a sealed tube and heated to 100 °C for 1 h. After cooling, the solvent was evaporated under reduced pressure. The resulting white solid was extracted with n-hexane (2 × 2 mL), filtered through a plug of alumina, and the solvent evaporated under reduced pressure, giving desired product **14b**. Highly air-sensitive white solid (33 mg, 71%). ^{1}H NMR δ (500 MHz, C_6D_6): 1.07 (d, J = 10.8 Hz, 18H, PBu^t), 3.06 (s, 2H, CH_2P), 4.51 (d, J = 2.2 Hz, 2H, CH_2S), 6.93 (m, 2H, Ar & SPh), 6.99 (t, J = 7.6 Hz, 2H, SPh), 7.03 (t, J = 7.3 Hz, 1H, Ar), 7.09 (d, J = 7.5 Hz, 1H, Ar), 7.30 (d, J = 7.0 Hz, 2H, SPh), 7.47 (d, J = 7.5 Hz, 1H, Ar). ^{13}C NMR δ (125 MHz, C_6D_6): 26.79 (d, J = 27.4 Hz, CH_2P), 29.99 (d, J = 13.5 Hz, PCMe_3), 32.04 (d, J = 24.4 Hz, PCMe$_3$), 37.84 (d, J = 12.9 Hz, CH_2S), 126.19 (d, J = 1.4 Hz, Ar), 126.35 (s, SPh), 127.57 (s, Ar), 129.06 (s, SPh), 130.23 (s, SPh), 131.18 (s, Ar), 131.91 (d, J = 10.5 Hz, Ar), 135.65 (d, J = 2.4 Hz, Ar), 137.50 (s, SPh), 140.16 (d, J = 8.6 Hz, Ar). ^{31}P NMR δ (121 MHz, C_6D_6): 25.93 (s).

α-(Di-*t*-butylphosphino)-α'-(*t*-butylsulfinyl)-*o*-xylene–borane (15)

Compound **13a** (1.00 g, 2.84 mmol), 3-carboxypyridinium chlorochromate (0.74 g, 2.84 mmol) and aluminium trichloride (0.38 g, 2.84 mmol) were combined in acetonitrile (50 mL) in the air, and heated to reflux for 2 h. The resulting mixture was separated by centrifugation and the solid washed with acetonitrile (2 × 40 mL). The combined purple solutions were passed through a plug of alumina, which was then washed through with further acetonitrile (30 mL). Solvent evaporation under reduced pressure gave the crude product. Recrystallisation from hot toluene gave desired compound **15**. Air-stable hygroscopic white powder (0.61 g, 58%). ^{1}H NMR δ (500 MHz, C_6D_6): 0.8–1.6 (br, 3H, BH_3), 1.06 (d, J = 12.5 Hz, 9H, PBu^t), 1.09 (s, 9H, SBu^t), 1.19 (d, J = 12.5 Hz, 9H, PBu^t), 3.04 (t, J = 15.0 Hz, 1H, CH_2P), 3.63 (d, J = 13.5 Hz, 1H, CH_2S), 4.07 (dd, J = 15.0, 9.0 Hz, 1H, CH_2P), 4.61 (d, J = 13.5 Hz, 1H, CH_2S), 7.06 (m, 3H, Ar), 7.36 (d, J = 7.5 Hz, 1H, Ar). ^{13}C NMR δ (150 MHz, C_6D_6): 22.95 (s, SCMe_3), 23.33 (d, J = 22.7 Hz, CH_2P), 28.51 (d, J = 0.9 Hz, PCMe_3), 28.53 (d, J = 1.1 Hz, PCMe_3), 32.99 (d, J = 25.0 Hz, PCMe$_3$), 33.01 (d, J = 24.1 Hz, PCMe$_3$), 52.19 (d, J = 1.2 Hz, CH_2S), 53.44 (s, SCMe$_3$), 127.43 (d, J = 2.0 Hz, Ar), 127.55 (d, J = 2.2 Hz, Ar), 132.39 (d, J = 2.0 Hz, Ar), 132.56 (d, J = 3.9 Hz, Ar), 134.34 (d, J = 3.6 Hz, Ar), 136.47 (d, J = 3.9 Hz, Ar). ^{31}P NMR δ (121 MHz, C_6D_6): 47.98 (br). IR (film from CH_2Cl_2): 1028 (SO), 2391 (BH),

2870–3052 cm^{-1} (CH). HRMS calcd for $C_{20}H_{38}BNaOPS$ $[M+Na]^+$: $m/z = 391.2372$; found: 391.2376. Anal. calcd for $C_{20}H_{38}BOPS$: C, 65.2; H, 10.4; S, 8.7; found: C, 65.1; H, 10.6; S, 8.4.

α-(Di-*t*-butylphosphino)-α'-(*t*-butylsulfinyl)-*o*-xylene (16)

Compound **15** (50 mg, 0.14 mmol) and morpholine (1 mL) were combined in a sealed tube and heated to 100 °C for 1 h. After cooling, the solvent was evaporated under reduced pressure. The resulting white solid was extracted with *n*-hexane (2 × 2 mL), filtered through a plug of alumina, and the solvent evaporated under reduced pressure, giving desired product **16**. Highly air-sensitive white solid (39 mg, 79%). ^{1}H NMR δ (500 MHz, C_6D_6): 1.06 (d, J = 10.9 Hz, 9H, PBu^t), 1.08 (s, 9H, SBu^t), 1.14 (d, J = 10.8 Hz, 9H, PBu^t), 2.99 (dd, J = 14.8, 2.0 Hz, 1H, CH_2P), 3.37 (d, J = 14.9 Hz, 1H, CH_2P), 3.85 (dd, J = 13.0, 1.4 Hz, 1H, CH_2S), 4.25 (dd, J = 13.0, 3.5 Hz, 1H, CH_2S), 7.04 (m, 2H, Ar), 7.23 (d, J = 8.1 Hz, 1H, Ar), 7.46 (d, J = 7.1 Hz, 1H, Ar). ^{13}C NMR δ (125 MHz, C_6D_6): 22.99 (s, SCMe_3), 27.59 (d, J = 26.4 Hz, CH_2P), 30.06 (d, J = 13.0 Hz, PCMe_3), 30.13 (d, J = 13.0 Hz, PCMe_3), 32.04 (d, J = 26.9 Hz, PCMe$_3$), 32.22 (d, J = 26.4 Hz, PCMe$_3$), 50.89 (d, J = 13.4 Hz, CH_2S), 53.46 (s, SCMe$_3$), 126.41 (d, J = 1.5 Hz, Ar), 128.00 (s, Ar), 131.79 (d, J = 1.9 Hz, Ar), 132.04 (d, J = 10.5 Hz, Ar), 132.54 (s, Ar), 141.00 (d, J = 7.7 Hz, Ar). ^{31}P NMR δ (121 MHz, C_6D_6): 25.23 (s).

α-(Di-*t*-butylphosphino)-α'-(dimethylamino)-*o*-xylene–diborane (17a)

A solution of dimethylamine–borane (93 mg, 1.6 mmol) in THF (5 mL) was cooled to 0 °C and a solution of *n*-butyllithium (1.0 mL, 1.6 M in hexanes, 1.6 mmol) was added dropwise with stirring. The mixture was stirred at room temperature for 1 h, then added dropwise to a solution of compound **5** (0.42 g, 1.4 mmol) in THF (5 mL) at -5 °C and stirred at this temperature for 1 h. The solvent was evaporated under reduced pressure, and the resulting white solid was stirred in distilled water (10 mL) in the air for 1 h, filtered and desired compound **17a** recrystallised from 1:2 toluene/*n*-hexane. Air-stable white needle-like crystals (0.36 g, 80%). ^{1}H NMR δ (500 MHz, C_6D_6): 0.8–1.6 (br, 3H, PBH_3), 1.08 (d, J = 12.0 Hz, 18H, PBu^t), 1.9–2.8 (br, 3H, NBH_3), 2.09 (s, 3H, NMe), 3.55 (d, J = 12.0 Hz, 2H, CH_2P), 3.98 (s, 2H, CH_2N), 6.74 (d, J = 8.0 Hz, 1H, Ar), 6.93 (t, J = 7.5 Hz, 1H, Ar), 7.09 (t, J = 7.5 Hz, 1H, Ar), 7.69 (d, J = 8.0 Hz, 1H, Ar). ^{13}C NMR δ (125 MHz, C_6D_6): 24.08 (d, J = 22.5 Hz, CH_2P), 28.43 (d, J = 1.0 Hz, PCMe_3), 32.99 (d, J = 24.4 Hz, PCMe$_3$), 51.32 (s, NMe), 64.98 (s, CH_2N), 126.23 (d, J = 2.4 Hz, Ar), 128.62 (d, J = 2.0 Hz, Ar), 132.02 (d, J = 4.3 Hz, Ar), 132.74 (d, J = 3.8 Hz, Ar), 133.51 (d, J = 1.4 Hz, Ar), 137.70 (d, J = 3.8 Hz, Ar). ^{31}P NMR δ (121 MHz, C_6D_6):

49.80 (br). ^{11}B NMR δ (96 MHz, C_6D_6): −40.83 (d, J = 52.5 Hz, PBH_3), −8.78 (s, NBH_3). IR (film from CH_2Cl_2): 2278–2380 (BH), 2871–2988 cm^{-1} (CH). HRMS calcd for $C_{18}H_{38}B_2NNaP$ $[M+Na]^+$: m/z = 344.2832; found: 344.2832. Anal. calcd for $C_{18}H_{38}B_2NP$: C, 67.3; H, 11.9; N, 4.4; found: C, 67.4; H, 12.1; N, 4.4.

α-(Di-*t*-butylphosphino)-α′-pyrrolidino-*o*-xylene–diborane (17b)

A solution of pyrrolidine–borane (68 mg, 0.8 mmol) in THF (3 mL) was cooled to 0 °C and a solution of *n*-butyllithium (0.5 mL, 1.6 M in hexanes, 0.8 mmol) was added dropwise with stirring. The mixture was stirred at room temperature for 1 h, then added dropwise to a solution of compound **5** (0.21 g, 0.7 mmol) in THF (3 mL) at −5 °C and stirred at this temperature for 1 h. The solvent was evaporated under reduced pressure, and the resulting white solid was stirred in distilled water (5 mL) in the air for 1 h, filtered and desired compound **17b** recrystallised from 1:2 toluene/*n*-hexane. Air-stable white crystals (0.22 g, 89%). ^{1}H NMR δ (500 MHz, C_6D_6): 0.8–1.6 (br, 3H, PBH_3), 1.13 (d, J = 12.5 Hz, 18H, PBu^t), 1.8–2.6 (br, 3H, NBH_3), 1.19 (m, 2H, NCH_2CH_2), 1.82 (m, 2H, NCH_2CH_2), 2.31 (m, 2H, NCH_2CH_2), 2.90 (m, 2H, NCH_2CH_2), 3.69 (d, J = 12.0 Hz, 2H, CH_2P), 4.10 (s, 2H, $ArCH_2N$), 6.84 (d, J = 7.5 Hz, 1H, Ar), 6.99 (t, J = 7.5 Hz, 1H, Ar), 7.11 (t, J = 7.5 Hz, 1H, Ar), 7.66 (d, J = 7.5 Hz, 1H, Ar). ^{13}C NMR δ (125 MHz, C_6D_6): 22.15 (s, NCH_2CH_2), 24.36 (d, J = 22.9 Hz, CH_2P), 28.50 (d, J = 1.0 Hz, $PCMe_3$), 33.06 (d, J = 24.4 Hz, $PCMe_3$), 59.93 (s, NCH_2CH_2), 63.18 (s, $ArCH_2N$), 126.39 (d, J = 2.4 Hz, Ar), 132.71 (d, J = 3.4 Hz, Ar), 132.79 (d, J = 1.9 Hz, Ar), 133.28 (d, J = 3.8 Hz, Ar), 138.00 (d, J = 3.9 Hz, Ar), other Ar obscured by solvent. ^{31}P NMR δ (121 MHz, C_6D_6): 49.55 (br). ^{11}B NMR δ (96 MHz, C_6D_6): −40.86 (d, J = 47.8 Hz, PBH_3), −11.44 (s, NBH_3). IR (film from CH_2Cl_2): 2279–2379 (BH), 2904–3052 cm^{-1} (CH). HRMS calcd for $C_{20}H_{40}B_2NNaP$ $[M+Na]^+$: m/z = 370.2990; found: 370.2981. Anal. calcd for $C_{20}H_{40}B_2NP$: C, 69.2; H, 11.6; N, 4.0; found: C, 69.1; H, 11.7; N, 4.0.

α-(Di-*t*-butylphosphino)-α′-(diethylamino)-*o*-xylene–diborane (17c)

A solution of diethylamine–borane (70 mg, 0.8 mmol) in THF (3 mL) was cooled to 0 °C and a solution of *n*-butyllithium (0.5 mL, 1.6 M in hexanes, 0.8 mmol) was added dropwise with stirring. The mixture was stirred at room temperature for 1 h, then added dropwise to a solution of compound **5** (0.21 g, 0.7 mmol) in THF (3 mL) at −5 °C and stirred at this temperature for 1 h. The solvent was evaporated under reduced pressure, and the resulting white solid was stirred in distilled water (5 mL) in the air for 1 h, filtered and desired compound **17c** recrystallised from 1:2 toluene/*n*-hexane. Air-stable white crystals (0.20 g, 80%). ^{1}H NMR δ (500 MHz,

C_6D_6): 0.6–1.6 (br, 3H, PBH_3), 0.88 (t, J = 7.0 Hz, 6H, NCH_2Me), 1.12 (d, J = 12.5 Hz, 18H, PBu^t), 1.6–2.5 (br, 3H, NBH_3), 2.50 (sext, J = 7.0 Hz, 2H, NCH_2Me), 2.62 (sext, J = 7.0 Hz, 2H, NCH_2Me), 3.82 (d, J = 12.0 Hz, 2H, CH_2P), 4.02 (s, 2H, $ArCH_2N$), 6.95 (d, J = 7.5 Hz, 1H, Ar), 7.00 (t, J = 7.5 Hz, 1H, Ar), 7.10 (t, J = 7.5 Hz, 1H, Ar), 7.53 (d, J = 7.5 Hz, 1H, Ar). ^{13}C NMR δ (125 MHz, C_6D_6): 8.75 (s, NCH_2Me), 24.75 (d, J = 22.5 Hz, CH_2P), 28.55 (s, $PCMe_3$), 33.01 (d, J = 24.8 Hz, $PCMe_3$), 52.51 (s, NCH_2Me), 60.35 (s, $ArCH_2N$), 126.08 (d, J = 2.4 Hz, Ar), 132.89 (d, J = 3.8 Hz, Ar), 133.07 (d, J = 3.8 Hz, Ar), 133.18 (d, J = 1.9 Hz, Ar), 138.35 (d, J = 3.8 Hz, Ar), other Ar obscured by solvent. ^{31}P NMR δ (121 MHz, C_6D_6): 49.80 (br). ^{11}B NMR δ (96 MHz, C_6D_6): −40.97 (d, J = 53.7 Hz, PBH_3), −12.93 (s, NBH_3). IR (film from CH_2Cl_2): 2281–2366 (BH), 2872–2998 cm^{-1} (CH). HRMS calcd for $C_{20}H_{42}B_2NNaP$ $[M+Na]^+$: m/z = 372.3146; found: 372.3138. Anal. calcd for $C_{20}H_{42}B_2NP$: C, 68.8; H, 12.1; N, 4.0; found: C, 68.9; H, 12.2; N, 3.9.

α-(Di-*t*-butylphosphino)-α'-(dimethylamino)-*o*-xylene (18a)

A solution of **17a** (0.17 g, 0.53 mmol) in dichloromethane (10 mL) was cooled to -10 °C, tetrafluoroboric acid–diethyl ether complex (0.85 mL, 85% solution, 5.3 mmol) added dropwise, and the resulting solution stirred at room temperature for 1 h. Diethyl ether (15 mL) was added, followed by saturated sodium hydrogen carbonate solution (30 mL), and the mixture stirred for 30 min. The resulting layers were separated, the aqueous layer washed with diethyl ether (2 × 15 mL), combined organic fractions washed with distilled water (15 mL) and brine (15 mL), dried over magnesium sulfate, filtered, and the solvent removed under reduced pressure, giving desired compound **18a**. Highly air-sensitive cloudy oil (0.133 g, 82%). ^{1}H NMR δ (500 MHz, C_6D_6): 1.13 (d, J = 10.7 Hz, 18H, PBu^t), 2.11 (s, 6H, NMe), 3.16 (d, J = 2.4 Hz, 2H, CH_2P), 3.60 (s, 2H, CH_2N), 7.05 (t, J = 7.3 Hz, 1H, Ar), 7.15 (t, J = 7.6 Hz, 1H, Ar), 7.21 (d, J = 7.3 Hz, 1H, Ar), 7.77 (d, J = 7.3 Hz, 1H, Ar). ^{13}C NMR δ (125 MHz, C_6D_6): 25.53 (d, J = 25.5 Hz, CH_2P), 30.02 (d, J = 13.9 Hz, $PCMe_3$), 31.95 (d, J = 24.0 Hz, $PCMe_3$), 45.46 (s, NMe), 63.46 (d, J = 6.2 Hz, CH_2N), 125.56 (d, J = 1.9 Hz, Ar), 127.38 (s, Ar), 131.08 (s, Ar), 131.54 (d, J = 14.8 Hz, Ar), 137.54 (d, J = 2.9 Hz, Ar), 141.20 (d, J = 10.1 Hz, Ar). ^{31}P NMR δ (121 MHz, C_6D_6): 24.53 (s).

α-(Di-*t*-butylphosphino)-α'-pyrrolidino-*o*-xylene (18b)

A solution of **17b** (50 mg, 0.14 mmol) in dichloromethane (3 mL) was cooled to −10 °C, tetrafluoroboric acid–diethyl ether complex (0.24 mL, 85% solution, 1.4 mmol) added dropwise, and the resulting solution stirred at room temperature

for 1 h. Diethyl ether (4 mL) was added, followed by saturated sodium hydrogen carbonate solution (8 mL), and the mixture stirred for 30 min. The resulting layers were separated, the aqueous layer washed with diethyl ether (2 × 4 mL), combined organic fractions washed with distilled water (4 mL) and brine (4 mL), and solvent evaporated under reduced pressure. The resulting material was extracted into *n*-hexane (6 mL), dried over magnesium sulfate and filtered through a plug of alumina. The solvent was evaporated under reduced pressure, giving desired compound **18b**. Highly air-sensitive clear oil (27 mg, 60%). ^{1}H NMR δ (500 MHz, C_6D_6): 1.14 (d, J = 10.5 Hz, 18H, PBu^t), 1.58 (m, 4H, NCH_2CH_2), 2.40 (m, 4H, NCH_2CH_2), 3.16 (d, J = 2.7 Hz, 2H, CH_2P), 3.82 (s, 2H, $ArCH_2N$), 7.07 (t, J = 7.3 Hz, 1H, Ar), 7.16 (t, J = 7.6 Hz, 1H, Ar), 7.27 (d, J = 7.5 Hz, 1H, Ar), 7.81 (dd, J = 7.6, 1.5 Hz, 1H, Ar). ^{13}C NMR δ (125 MHz, C_6D_6): 23.90 (s, NCH_2CH_2), 25.29 (d, J = 25.0 Hz, CH_2P), 30.00 (d, J = 13.4 Hz, $PCMe_3$), 31.95 (d, J = 24.0 Hz, $PCMe_3$), 54.31 (s, NCH_2CH_2), 59.64 (d, J = 5.8 Hz, $ArCH_2N$), 125.60 (d, J = 1.9 Hz, Ar), 127.24 (s, Ar), 130.50 (s, Ar), 131.35 (d, J = 15.4 Hz, Ar), 138.15 (d, J = 2.9 Hz, Ar), 140.87 (d, J = 10.5 Hz, Ar). ^{31}P NMR δ (121 MHz, C_6D_6): 24.56 (s).

α-(Di-*t*-butylphosphino)-α'-(diethylamino)-*o*-xylene (18c)

A solution of **17c** (50 mg, 0.14 mmol) in dichloromethane (3 mL) was cooled to −10 °C, tetrafluoroboric acid–diethyl ether complex (0.24 mL, 85% solution, 1.4 mmol) added dropwise, and the resulting solution stirred at room temperature for 1 h. Diethyl ether (4 mL) was added, followed by saturated sodium hydrogen carbonate solution (8 mL), and the mixture stirred for 30 min. The resulting layers were separated, the aqueous layer washed with diethyl ether (2 × 4 mL), combined organic fractions washed with distilled water (4 mL) and brine (4 mL), and solvent evaporated under reduced pressure. The resulting material was extracted into *n*-hexane (6 mL), dried over magnesium sulfate and filtered through a plug of alumina. The solvent was evaporated under reduced pressure, giving desired compound **18c**. Highly air-sensitive clear oil (33 mg, 73%). ^{1}H NMR δ (500 MHz, C_6D_6): 0.97 (t, J = 7.1 Hz, 6H, NCH_2Me), 1.14 (d, J = 10.8 Hz, 18H, PBu^t), 2.46 (q, J = 7.1 Hz, 4H, NCH_2Me), 3.12 (d, J = 2.7 Hz, 2H, CH_2P), 3.69 (s, 2H, $ArCH_2N$), 7.08 (t, J = 7.3 Hz, 1H, Ar), 7.17 (t, J = 7.4 Hz, 1H, Ar), 7.33 (d, J = 7.3 Hz, 1H, Ar), 7.95 (dd, J = 7.3, 2.9 Hz, 1H, Ar). ^{13}C NMR δ (125 MHz, C_6D_6): 11.81 (s, NCH_2Me), 25.17 (d, J = 24.0 Hz, CH_2P), 30.09 (d, J = 13.5 Hz, $PCMe_3$), 32.00 (d, J = 24.0 Hz, $PCMe_3$), 46.89 (s, NCH_2Me), 57.64 (d, J = 3.9 Hz, $ArCH_2N$), 125.55 (d, J = 1.9 Hz, Ar), 127.16 (s, Ar), 130.88 (s, Ar), 131.26 (d, J = 18.2 Hz, Ar), 138.00 (d, J = 3.3 Hz, Ar), 140.96 (d, J = 11.0 Hz, Ar). ^{31}P NMR δ (121 MHz, C_6D_6): 23.76 (s).

α-(Di-*t*-butylphosphino)-α'-(diphenylsilyl)-*o*-xylene–borane (19a)

Flame-dried magnesium turnings (24 mg, 1.00 mmol), compound **5** (150 mg, 0.50 mmol), chlorodiphenylsilane (0.15 mL, 0.75 mmol), a crystal of iodine and THF (12 mL) were combined and stirred at room temperature overnight. The solvent was removed under reduced pressure, the resulting mixture extracted into toluene (15 mL) in the air, filtered and solvent again removed under reduced pressure. Elution through an alumina column with 1% ethyl acetate in *n*-hexane gave pure compound **19a** ($R_f = 0.33$). Air-stable clear oil (75 mg, 34%). ^{1}H NMR δ (500 MHz, C_6D_6): 1.0–1.8 (br, 3H, PBH_3), 1.03 (d, $J = 12.2$ Hz, 18H, PBu^t), 2.69 (d, $J = 12.0$ Hz, 2H, CH_2P), 2.93 (d, $J = 3.4$ Hz, 2H, CH_2Si), 5.10 (t, $J = 3.1$ Hz, $^1J_{SiH}$ = 197.3 Hz, 1H, SiH), 6.97 (m, 3H, Ar), 7.11 (m, 6H, SiPh), 7.45 (d, $J = 7.6$ Hz, 4H, SiPh), 7.82 (d, $J = 7.8$ Hz, 1H, Ar). ^{13}C NMR δ (125 MHz, C_6D_6): 21.71 (s, CH_2Si), 22.91 (d, $J = 23.1$ Hz, CH_2P), 28.34 (s, PCMe_3), 32.97 (d, $J = 23.9$ Hz, PCMe$_3$), 125.20 (d, $J = 1.9$ Hz, Ar), 127.22 (d, $J = 1.9$ Hz, Ar), 128.39 (s, SiPh), 130.19 (s, SiPh), 130.59 (d, $J = 1.5$ Hz, Ar), 132.12 (d, $J = 2.9$ Hz, Ar), 132.98 (d, $J = 3.3$ Hz, Ar), 133.73 (s, SiPh), 135.67 (s, SiPh), 137.60 (d, $J = 4.8$ Hz, Ar). ^{31}P NMR δ (121 MHz, C_6D_6): 48.57 (br). HRMS calcd for $C_{28}H_{39}BPSi$ $[M-H]^+$: m/z = 445.2652; found: 445.2643. Anal. calcd for $C_{28}H_{40}BPSi$: C, 75.3; H, 9.0; found: C, 75.3; H, 9.2.

α-(Di-*t*-butylphosphino)-α'-(dimethylsilyl)-*o*-xylene–borane (19b)

Flame-dried magnesium turnings (50 mg, 2.06 mmol), compound **5** (200 mg, 0.67 mmol), chlorodimethylsilane (0.24 mL, 2.16 mmol), a crystal of iodine and THF (15 mL) were combined and heated to reflux for 1 h. The solvent was removed under reduced pressure, the resulting mixture extracted into toluene (10 mL) in the air, filtered and solvent again removed under reduced pressure. Attempts to purify this compound by crystallisation or column chromatography were unsuccessful. Air-stable clear oil (85% conversion). ^{1}H NMR δ (500 MHz, C_6D_6): -0.03 (d, $J = 3.7$ Hz, 6H, SiMe), 1.0–1.8 (br, 3H, PBH_3), 1.10 (d, $J = 12.2$ Hz, 18H, PBu^t), 2.32 (d, $J = 3.2$ Hz, 2H, CH_2Si), 3.07 (d, $J = 11.9$ Hz, 2H, CH_2P), 4.14 (non, $J = 3.7$ Hz, $^1J_{SiH}$ = 185.1 Hz, 1H, SiH), 6.89 (m, 1H, Ar), 7.00 (m, 2H, Ar), 7.94 (m, 1H, Ar). ^{13}C NMR δ (125 MHz, C_6D_6): -4.29 (s, $^1J_{SiC}$ = 51.3 Hz, SiMe), 22.93 (d, $J = 23.6$ Hz, CH_2P), 23.10 (d, $J = 1.0$ Hz, CH_2Si), 28.31 (d, $J = 1.0$ Hz, PCMe_3), 33.05 (d, $J = 24.0$ Hz, PCMe$_3$), 124.95 (d, $J = 1.9$ Hz, Ar), 127.14 (d, $J = 1.9$ Hz, Ar), 130.02 (d, $J = 1.5$ Hz, Ar), 132.11 (d, $J = 2.9$ Hz, Ar), 132.28 (d, $J = 3.3$ Hz, Ar), 138.68 (d, $J = 4.8$ Hz, Ar). ^{31}P NMR δ (121 MHz, C_6D_6): 48.05 (br). HRMS calcd for $C_{18}H_{36}BNaPSi$ $[M+Na]^+$: m/z = 345.2315; found: 345.2314.

α-(Di-*t*-butylphosphino)-α'-(diphenylsilyl)-*o*-xylene (20a)

Compound **19a** (15 mg, 0.03 mmol) and DABCO (4 mg, 0.04 mmol) were combined in toluene-d_8 (0.5 mL) and heated to 60 °C overnight. After cooling, the solvent was evaporated under reduced pressure. The resulting white solid was extracted with *n*-hexane (2 × 1 mL), filtered through a plug of alumina, and the solvent evaporated under reduced pressure, giving desired product **20a**. Highly air-sensitive white solid (9 mg, 69%). ^{1}H NMR δ (500 MHz, C_6D_6): 1.05 (d, J = 10.5 Hz, 18H, PBu^t), 2.65 (d, J = 1.5 Hz, 2H, CH_2P), 3.10 (dd, J = 3.4, 1.5 Hz, 2H, CH_2Si), 5.22 (t, J = 3.7 Hz, $^1J_{SiH}$ = 197.5 Hz, 1H, SiH), 6.95 (m, 1H, Ar), 7.01 (m, 2H, Ar), 7.13 (m, 6H, SiPh), 7.51 (dd, J = 7.5, 1.2 Hz, 4H, SiPh), 7.53 (d, J = 7.8 Hz, 1H, Ar). ^{13}C NMR δ (125 MHz, C_6D_6): 20.72 (d, J = 8.6 Hz, CH_2Si), 27.17 (d, J = 26.4 Hz, CH_2P), 30.03 (d, J = 13.5 Hz, PCMe_3), 31.97 (d, J = 25.0 Hz, PCMe$_3$), 125.13 (s, Ar), 126.07 (d, J = 2.0 Hz, Ar), 128.29 (s, SiPh), 130.01 (s, SiPh), 130.44 (s, Ar), 131.71 (d, J = 12.5 Hz, Ar), 134.23 (s, SiPh), 135.76 (s, SiPh), 137.33 (d, J = 2.4 Hz, Ar), 138.45 (d, J = 8.6 Hz, Ar). ^{31}P NMR δ (121 MHz, C_6D_6): 25.22 (s).

7.3 Platinum Complexes

[PtCl$_2${κ^2*P,S*-*o*-C$_6$H$_4$(CH$_2$PBu$^t_2$)(CH$_2$SBu^t)}] (21)

Ligand **14a** (140 mg, 0.4 mmol) was dissolved in acetone (5 mL), and a solution of [PtCl$_2$(1,5-hexadiene)] (140 mg, 0.4 mmol) in acetone (5 mL) added with stirring. After 24 h, the solvent was removed under reduced pressure, and the crude material recrystallised from a minimum of warm dichloromethane at −20 °C giving desired product **21**. Air-stable, pale yellow microcrystals (204 mg, 84%). X-ray diffraction quality crystals were grown by inwards diffusion of *n*-hexane into a dichloromethane solution of complex **21**. ^{1}H NMR δ (500 MHz, CD_2Cl_2): 1.48 (br, 18H, PBu^t), 1.73 (s, 9H, SBu^t), 2.99 (br, 1H, CH_2P), 4.4–5.2 (br, 3H, CH_2S & CH_2P), 7.27 (m, 3H, Ar), 7.33 (d, J = 7.5 Hz, 1H, Ar). ^{13}C NMR δ (125 MHz, CD_2Cl_2): 22.33 (d, J = 27.3 Hz, CH_2P), 29.86 (s, SCMe_3), 30.75 (br, PCMe_3), 38.86 (d, J = 23.9 Hz, PCMe$_3$), 40.60 (s, SCMe$_3$), 54.83 (d, J = 2.8 Hz, CH_2S), 127.73 (s, Ar), 127.88 (d, J = 2.0 Hz, Ar), 131.17 (d, J = 2.4 Hz, Ar), 132.50 (d, J = 4.8 Hz, Ar), 132.56 (d, J = 2.9 Hz, Ar), 134.61 (d, J = 5.8 Hz, Ar). ^{31}P NMR δ (121 MHz, CD_2Cl_2): 28.55 (s, $^1J_{PtP}$ = 3450 Hz). ^{1}H NMR δ (300 MHz, $(CD_3)_2CO$): 1.52 (br, 18H, PBu^t), 1.77 (s, 9H, SBu^t), 3.36 (br, 1H, CH_2P), 4.65 (br, 1H, CH_2P), 4.92 (br, $^3J_{PtH}$ = 74.7 Hz, 2H, CH_2S), 7.30 (m, 2H, Ar), 7.44 (m, 1H, Ar), 7.53 (m, 1H, Ar).

^{31}P NMR δ (121 MHz, $(CD_3)_2CO$): 27.69 (s, $^1J_{PtP}$ = 3447 Hz). HRMS calcd for $C_{20}H_{39}Cl_2NPPtS$ $[M+NH_4]^+$: m/z = 620.1545; found: 620.1539. Anal. calcd for $C_{20}H_{35}Cl_2PPtS$: C, 39.7; H, 5.8; S, 5.3; found: C, 39.5; H, 5.8; S, 5.3.

Reaction of *o*-$C_6H_4(CH_2PBu^t_2)(CH_2NMe_2)$ (18a) with [$PtCl_2$(1,5-hexadiene)]

Ligand **18a** (95 mg, 0.32 mmol) was dissolved in acetone (2 mL), and a solution of [$PtCl_2$(1,5-hexadiene)] (111 mg, 0.32 mmol) in acetone (3 mL) added with stirring. After 24 h, the solvent was removed under reduced pressure giving crude proposed complex **22** as an off-white solid. Attempts at purification were unsuccessful due to degradation of material. ^{1}H NMR δ (500 MHz, $(CD_3)_2CO$): 1.02 (quin, J = 6.1 Hz, $^3J_{PtH}$ = 96 Hz, 1H, H4), 1.43 (d, J = 14.2 Hz, 9H, PBu^t), 1.56 (m, 2H, H3 & H4), 1.64 (d, J = 14.2 Hz, 9H, PBu^t), 2.03 (m, 1H, H3), 2.25 (br, 6H, NMe), 2.75 (ddd, J = 15.1, 12.2, 7.8 Hz, $^3J_{PtH}$ = 95 Hz, 1H, H6), 2.94 (m, $^2J_{PtH}$ = 130 Hz, 1H, H5), 3.55 (d, J = 12.5 Hz, $^2J_{PtH}$ = 70 Hz, 1H, H1), 3.67 (br, 2H, CH_2N), 3.74 (d, J = 7.8 Hz, 1H, H1), 3.84 (t, J = 13.2 Hz, 1H, H6), 4.06 (t, J = 15.4 Hz, 1H, CH_2P), 4.23 (ddd, J = 12.2, 7.6, 4.7 Hz, $^2J_{PtH}$ = 73 Hz, 1H, H2), 4.58 (t, J = 14.4 Hz, 1H, CH_2P), 7.36 (m, 2H, Ar), 7.44 (m, 1H, Ar), 7.80 (d, J = 7.8 Hz, 1H, Ar). ^{13}C NMR δ (125 MHz, $(CD_3)_2CO$): 21.02 (d, J = 13.9 Hz, $^1J_{PtC}$ = 738 Hz, C5), 22.08 (br d, J = 35.5 Hz, CH_2P), 27.49 (d, J = 15.8 Hz, C6), 28.40 (d, J = 21.1 Hz, 2 × PCMe_3), 31.54 (s, C4), 34.23 (s, C3), 36.72 (d, J = 37.0 Hz, PCMe_3), 36.98 (d, J = 38.8 Hz, PCMe_3), 45.40 (br, NMe), 56.86 (s, $^1J_{PtC}$ = 267 Hz, C1), 64.24 (br, CH_2N), 84.70 (s, $^1J_{PtC}$ = 268 Hz, C2), 128.82 (d, J = 1.4 Hz, Ar), 128.88 (br, Ar), 131.65 (d, J = 7.5 Hz, Ar), 132.55 (d, J = 3.4 Hz, Ar), 133.28 (br, Ar), 138.97 (s, Ar). ^{31}P NMR δ (121 MHz, $(CD_3)_2CO$): 40.35 (s, $^3J_{PtP}$ = 355 Hz). HRMS calcd for $C_{24}H_{41}NPPt$ $[M-Cl_2H]^+$: m/z = 568.2603; found: 568.2608. HRMS calcd for $C_{24}H_{42}ClNPPt$ $[M-Cl]^+$: m/z = 604.2370; found: 604.2380.

Reaction of *o*-$C_6H_4(CH_2PBu^t_2)(CH_2SOBu^t)$ (16) with [$PtCl_2$(1,5-hexadiene)]

Ligand **16** (20 mg, 0.06 mmol) was dissolved in acetone-d_6 (0.4 mL) in an NMR tube, and a solution of [$PtCl_2$(1,5-hexadiene)] (20 mg, 0.06 mmol) in acetone-d_6 (0.4 mL) added. Reaction was complete after 24 h (quantitative conversion). ^{31}P NMR δ (121 MHz, $(CD_3)_2CO$): 39.77 (s, $^3J_{PtP}$ = 363 Hz), 41.18 (s, $^3J_{PtP}$ = 358 Hz).

[$PtCl_2\{\kappa^2$***P,N*****-o-**$C_6H_4(CH_2PBu^t_2)(CH_2NMe_2)\}$] (23)

Ligand **18a** (40 mg, 0.14 mmol) was dissolved in acetone-d_6 (0.4 mL) in an NMR tube, and a solution of *cis*-[$PtCl_2(NCBu^t)_2$] (59 mg, 0.14 mmol) in acetone-d_6 (1.0 mL) added. The resulting solution was heated to 40 °C for 24 h (>95% conversion). ^{1}H NMR δ (500 MHz, $(CD_3)_2CO$): 1.56 (br d, J = 11.2 Hz, 9H, PBu^t), 1.64 (br d, J = 10.7 Hz, 9H, PBu^t), 3.17 (br s, 3H, NMe), 3.39 (br s, 3H, NMe), 3.59 (br, 1H, CH_2P), 3.82 (br, 2H, CH_2P & CH_2N), 4.49 (br, 1H, CH_2N), 7.34 (t, J = 7.6 Hz, 1H, Ar), 7.44 (m, 2H, Ar), 7.60 (d, J = 7.8 Hz, 1H, Ar). ^{13}C NMR δ (125 MHz, $(CD_3)_2CO$): 24.66 (d, J = 21.1 Hz, CH_2P), 30.30 (br, PCMe_3), 33.24 (br, PCMe_3), 39.70 (br, 2 × PCMe$_3$), 52.99 (br s, NMe), 56.53 (br s, NMe), 71.23 (s, CH_2N), 127.63 (d, J = 2.4 Hz, Ar), 130.02 (d, J = 2.0 Hz, Ar), 131.58 (d, J = 5.3 Hz, Ar), 133.41 (d, J = 3.9 Hz, Ar), 135.14 (d, J = 2.9 Hz, Ar), 137.63 (d, J = 3.9 Hz, Ar). ^{31}P NMR δ (121 MHz, $(CD_3)_2CO$): 17.16 (s, $^1J_{PtP}$ = 3967 Hz). HRMS calcd for $C_{18}H_{32}ClNPPt$ [M−Cl]$^+$: m/z = 522.1588; found: 522.1588.

[$PtHCl\{\kappa^1$***P*****-o-**$C_6H_4(CH_2PBu^t_2)(CH_2SBu^t)\}_2$] (24)

Ligand **14a** (25 mg, 0.074 mmol) and diethylamine–borane (3 mg, 0.037 mmol) were dissolved in acetone-d_6 (0.4 mL) in an NMR tube. A solution of [$PtCl_2$(1,5-hexadiene)] (13 mg, 0.037 mmol) in acetone-d_6 (0.4 mL) was added, and solution left to react overnight (87% conversion). ^{1}H NMR δ (500 MHz, $(CD_3)_2CO$): −17.43 (t, J = 12.2 Hz, $^1J_{PtH}$ = 1247.7 Hz, 1H, PtH), 1.39 (vt, $^3J_{PH}$ + $^5J_{PH}$ = 12.9 Hz, 36H, PBu^t), 1.43 (s, 18H, SBu^t), 3.99 (s, 4H, CH_2S), 4.02 (vt, $^2J_{PH}$ + $^4J_{PH}$ = 6.7 Hz, $^3J_{PtH}$ = 40.6 Hz, 4H, CH_2P), 7.12 (m, 4H, Ar), 7.31 (m, 2H, Ar), 8.92 (m, 2H, Ar). ^{13}C NMR δ (125 MHz, $(CD_3)_2CO$): 21.74 (vt, $^1J_{PC}$ + $^3J_{PC}$ = 22.1 Hz, CH_2P), 30.34 (vt, $^2J_{PC}$ + $^4J_{PC}$ = 4.4 Hz, PCMe_3), 31.04 (s, SCMe_3), 32.49 (s, CH_2S), 36.86 (vt, $^1J_{PC}$ + $^3J_{PC}$ = 23.5 Hz, PCMe$_3$), 43.19 (s, SCMe$_3$), 126.77 (s, Ar), 126.96 (s, Ar), 131.44 (s, Ar), 133.88 (vt, $^3J_{PC}$ + $^5J_{PC}$ = 5.3 Hz, Ar), 135.94 (s, Ar), 136.48 (vt, $^2J_{PC}$ + $^4J_{PC}$ = 5.3 Hz, Ar). ^{31}P NMR δ (121 MHz, $(CD_3)_2CO$): 59.69 (s, $^1J_{PtP}$ = 2848 Hz). HRMS calcd for $C_{40}H_{71}P_2PtS_2$ [M−Cl]$^+$: m/z = 871.4099; found: 871.4100.

[$PtH_2\{\kappa^1$***P*****-o-**$C_6H_4(CH_2PBu^t_2)(CH_2SBu^t)\}_2$] (25)

Ligand **14a** (163 mg, 0.48 mmol) and [$PtCl_2$(1,5-hexadiene)] (83 mg, 0.24mmol) were dissolved in ethanol (15 mL) and stirred at room temperature for 24 h. Sodium borohydride (91 mg, 2.4 mmol) was added, and stirring continued for another 24 h. Solvent was removed under reduced pressure, and the resulting off-white solid was extracted with toluene (40 mL). The toluene was removed

under reduced pressure, and the crude material recrystallised from a minimum of 10:1 ethanol/toluene at −20 °C giving desired product **25**. Air-stable, X-ray diffraction quality colourless crystals (70 mg, 33%). ^{1}H NMR δ (500 MHz, C_6D_6): −2.83 (t, J = 16.7 Hz, $^{1}J_{PtH}$ = 798.7 Hz, 2H, PtH), 1.28 (s, 18H, SBu^t), 1.46 (vt, $^{3}J_{PH}$ + $^{5}J_{PH}$ = 12.7 Hz, 36H, PBu^t), 3.91 (s, 4H, CH_2S), 3.98 (vt, $^{2}J_{PH}$ + $^{4}J_{PH}$ = 6.5 Hz, $^{3}J_{PtH}$ = 40.6 Hz, 4H, CH_2P), 7.06 (t, J = 7.3 Hz, 2H, Ar), 7.28 (d, J = 7.3 Hz, 2H, Ar), 9.03 (d, J = 7.5 Hz, 2H, Ar), other Ar obscured by solvent. ^{13}C NMR δ (125 MHz, C_6D_6): 29.43 (vt, $^{1}J_{PC}$ + $^{3}J_{PC}$ = 24.2 Hz, CH_2P), 30.28 (vt, $^{2}J_{PC}$ + $^{4}J_{PC}$ = 5.1 Hz, $^{3}J_{PtC}$ = 21.6 Hz, PCMe_3), 30.96 (s, SCMe_3), 32.84 (s, CH_2S), 36.01 (vt, $^{1}J_{PC}$ + $^{3}J_{PC}$ = 24.0 Hz, $^{2}J_{PtC}$ = 33.0 Hz, PCMe$_3$), 42.52 (s, SCMe$_3$), 126.53 (s, Ar), 126.67 (s, Ar), 131.05 (s, Ar), 132.34 (vt, $^{3}J_{PC}$ + $^{5}J_{PC}$ = 6.5 Hz, Ar), 136.51 (vt, $^{2}J_{PC}$ + $^{4}J_{PC}$ = 5.3 Hz, Ar), 137.09 (s, Ar). ^{31}P NMR δ (121 MHz, C_6D_6): 68.26 (s, $^{1}J_{PtP}$ = 2940 Hz). IR (KBr disk): 2384 (PtH), 2895–3022 cm^{-1} (CH). HRMS calcd for $C_{40}H_{71}P_2PtS_2$ $[M-H]^+$: m/z = 871.4099; found: 871.4097. Anal. calcd for $C_{40}H_{72}P_2PtS_2$: C, 54.8; H, 8.5; S, 7.3; found: C, 55.0; H, 8.5; S, 7.1.

[PtH{κ^1*P*-*o*-C_6H_4(CH_2PBu$^t_2$)(CH_2SBu^t)}{κ^2*P,S*-*o*-C_6H_4(CH_2PBu$^t_2$)(CH_2SBu^t)}]CH(SO_2CF_3)$_2$ (26)

Method 1: Complex **25** (40 mg, 0.046 mmol) and $CH_2(SO_2CF_3)_2$ (13 mg, 0.046 mmol) were combined in acetone-d_6 (0.8 mL) in an NMR tube. The tube was shaken until all crystals had dissolved and bubbling had ceased. Removal of solvent under reduced pressure gave desired product **26**. Air-stable off-white powder (quantitative conversion). Method 2: To a suspension of complex **36** (235 mg, 0.27 mmol) in acetone (5 mL) was added a solution of $CH_2(SO_2CF_3)_2$ (78 mg, 0.28 mmol) in acetone (5 mL). Reaction was stirred until all solid had dissolved, and solvent was removed under reduced pressure leaving a foam. Trituration of material in toluene (3 × 1 mL) gave impure desired product **26**. Air-stable pale brown powder (170 mg, 55%). ^{1}H NMR δ (500 MHz, $(CD_3)_2CO$): −14.88 (t, J = 13.9 Hz, $^{1}J_{PtH}$ = 1049.6 Hz, 1H, PtH), 1.32 (d, J = 13.5 Hz, 18H, monodentate PBu^t), 1.40 (s, 9H, monodentate SBu^t), 1.55 (m, 27H, bidentate PBu^t & bidentate SBu^t), 3.75 (s, 1H, $^-$CH), 3.98 (m, 4H, monodentate CH_2P & monodentate CH_2S), 4.12 (d, J = 7.1 Hz, 2H, bidentate CH_2P), 4.82 (s, $^{3}J_{PtH}$ = 27.6 Hz, 2H, bidentate CH_2S), 7.23 (m, 1H, monodentate Ar), 7.26 (m, 1H, monodentate Ar), 7.34 (m, 2H, bidentate Ar), 7.41 (d, J = 7.4 Hz, 1H, monodentate Ar), 7.53 (d, J = 7.1 Hz, 1H, bidentate Ar), 7.56 (d, J = 6.9 Hz, 1H, bidentate Ar), 8.32 (d, J = 6.3 Hz, 1H, monodentate Ar). ^{13}C NMR δ (150 MHz, $(CD_3)_2CO$): 25.18 (d, J = 18.5 Hz, bidentate CH_2P), 26.65 (d, J = 18.4 Hz, monodentate CH_2P), 30.49 (d, J = 20.3 Hz, monodentate PCMe_3 & bidentate PCMe_3), 31.04 (s, monodentate SCMe_3), 31.26

(s, bidentate SCMe_3), 32.35 (s, monodentate CH_2S), 36.83 (s, bidentate CH_2S), 38.87 (d, J = 24.3 Hz, $^2J_{PtC}$ = 49.8 Hz, bidentate PCMe$_3$), 39.53 (d, J = 24.2 Hz, $^2J_{PtC}$ = 48.6 Hz, monodentate PCMe$_3$), 43.53 (s, monodentate SCMe$_3$), 55.09 (s, bidentate SCMe$_3$), 55.30 (sept, J = 2.8 Hz, $^-$CH), 122.25 (q, J = 326.0 Hz, CF_3), 126.88 (s, monodentate Ar), 128.35 (s, monodentate Ar), 128.76 (s, bidentate Ar), 128.98 (s, bidentate Ar), 132.16 (s, monodentate Ar), 132.40 (d, J = 2.5 Hz, bidentate Ar), 133.13 (s, monodentate Ar & bidentate Ar), 133.81 (s, monodentate Ar), 134.12 (d, J = 1.9 Hz, bidentate Ar), 137.06 (s, bidentate Ar), 138.12 (d, J = 4.7 Hz, monodentate Ar). ^{31}P NMR δ (121 MHz, $(CD_3)_2CO$): 44.43 (d, J = 324 Hz, $^1J_{PtP}$ = 2740 Hz, bidentate P), 54.52 (d, J = 324 Hz, $^1J_{PtP}$ = 2770 Hz, monodentate P). ^{19}F NMR δ (282 MHz, $(CD_3)_2CO$): −81.91 (s). HRMS calcd for $C_{40}H_{71}P_2PtS_2$ [M−CH$(SO_2CF_3)_2$]$^+$: m/z = 871.4099; found: 871.4091. Anal. calcd for $C_{43}H_{72}F_6O_4P_2PtS_4$: C, 44.8; H, 6.3; S, 11.1; found: C, 45.1; H, 6.3; S, 11.1.

[PtH(CO){κ^1*P*-*o*-C_6H_4($CH_2PBu^t_2$)(CH_2SBu^t)}$_2$]CH(SO_2CF_3)$_2$ (27)

Complex **26** (20 mg, 0.017 mmol) was dissolved in acetone-d_6 (0.5 mL) in an NMR tube and carbon monoxide gas was bubbled through the solution for 1 min. Removal of solvent under reduced pressure gave desired product **27**. Air-stable yellow oil (quantitative conversion). ^{1}H NMR δ (500 MHz, $(CD_3)_2CO$): −5.36 (t, J = 11.4 Hz, $^1J_{PtH}$ = 843.3 Hz, 1H, PtH), 1.38 (s, 18H, SBu^t), 1.55 (vt, $^3J_{PH}$ + $^5J_{PH}$ = 14.9 Hz, 36H, PBu^t), 3.77 (br, 1H, $^-$CH), 3.93 (s, 4H, CH_2S), 4.00 (vt, $^2J_{PH}$ + $^4J_{PH}$ = 7.1 Hz, $^3J_{PtH}$ = 28.1 Hz, 4H, CH_2P), 7.24 (t, J = 7.4 Hz, 2H, Ar), 7.28 (t, J = 7.4 Hz, 2H, Ar), 7.42 (d, J = 7.4 Hz, 2H, Ar), 7.63 (d, J = 7.6 Hz, 2H, Ar). ^{13}C NMR δ (125 MHz, $(CD_3)_2CO$): 26.64 (vt, $^1J_{PC}$ + $^3J_{PC}$ = 24.0 Hz, $^2J_{PtC}$ = 12.0 Hz, CH_2P), 30.06 (vt, $^2J_{PC}$ + $^4J_{PC}$ = 3.8 Hz, PCMe_3), 31.05 (s, SCMe_3), 32.92 (s, CH_2S), 39.12 (vt, $^1J_{PC}$ + $^3J_{PC}$ = 25.0 Hz, $^2J_{PtC}$ = 34.6 Hz, PCMe$_3$), 43.85 (s, SCMe$_3$), 55.26 (br, $^-$CH), 122.21 (q, J = 325.8 Hz, CF_3), 128.18 (s, Ar), 128.98 (s, Ar), 132.43 (vt, $^3J_{PC}$ + $^5J_{PC}$ = 5.8 Hz, Ar), 132.84 (s, Ar), 135.43 (s, Ar), 138.37 (vt, $^2J_{PC}$ + $^4J_{PC}$ = 5.7 Hz, Ar), 184.50 (t, J = 7.0 Hz, $^1J_{PtC}$ = 1014.6 Hz, CO). ^{31}P NMR δ (121 MHz, $(CD_3)_2CO$): 68.38 (s, $^1J_{PtP}$ = 2415 Hz). ^{19}F NMR δ (282 MHz, $(CD_3)_2CO$): −81.86 (s). IR (film from $(CD_3)_2CO$): 2070 (CO), 2869–3069 cm^{-1} (CH). HRMS calcd for $C_{41}H_{71}OP_2PtS_2$ [M−CH$(SO_2CF_3)_2$]$^+$: m/z = 899.4048; found: 899.4055.

[PtH(NCMe){κ^1*P*-*o*-C_6H_4($CH_2PBu^t_2$)(CH_2SBu^t)}$_2$]CH(SO_2CF_3)$_2$ (28)

Complex **26** (20 mg, 0.017 mmol) was dissolved in acetone-d_6 (0.5 mL) in an NMR tube and acetonitrile (10 μL, 0.19 mmol) was added. Removal of solvent under reduced pressure gave desired product **28**. Air-stable yellow oil (quantitative conver-

sion). ^{1}H NMR δ (500 MHz, $(CD_3)_2CO$): -17.94 (t, $J = 11.9$ Hz, $^{1}J_{PtH} = 1169.5$ Hz, 1H, PtH), 1.43 (s, 18H, SBu^t), 1.49 (vt, $^{3}J_{PH} + {}^{5}J_{PH} = 14.2$ Hz, 36H, PBu^t), 1.90 (s, $^{4}J_{PtH} = 4.9$ Hz, NCMe), 3.78 (s, 1H, $^{-}$CH), 3.89 (vt, $^{2}J_{PH} + {}^{4}J_{PH} = 6.9$ Hz, $^{3}J_{PtH} = 27.0$ Hz, 4H, CH_2P), 4.05 (s, 4H, CH_2S), 7.26 (m, 4H, Ar), 7.42 (m, 2H, Ar), 8.20 (m, 2H, Ar). ^{13}C NMR δ (125 MHz, $(CD_3)_2CO$): 3.23 (s, NC*Me*), 24.45 (vt, $^{1}J_{PC} + {}^{3}J_{PC} = 22.5$ Hz, CH_2P), 30.21 (vt, $^{2}J_{PC} + {}^{4}J_{PC} = 4.3$ Hz, PC*Me*$_3$), 31.01 (s, SC*Me*$_3$), 32.57 (s, CH_2S), 37.85 (vt, $^{1}J_{PC} + {}^{3}J_{PC} = 25.4$ Hz, P*C*Me$_3$), 43.61 (s, S*C*Me$_3$), 55.16 (sept, $J = 2.8$ Hz, $^{-}$CH), 122.17 (q, $J = 325.8$ Hz, CF_3), 127.33 (s, Ar), 128.06 (s, Ar), 132.18 (s, Ar), 132.50 (vt, $^{3}J_{PC} + {}^{5}J_{PC} = 6.7$ Hz, Ar), 135.07 (s, Ar), 137.89 (vt, $^{2}J_{PC} + {}^{4}J_{PC} = 6.3$ Hz, Ar), N*C*Me not seen. ^{31}P NMR δ (121 MHz, $(CD_3)_2CO$): 56.63 (s, $^{1}J_{PtP} = 2732$ Hz). ^{19}F NMR δ (282 MHz, $(CD_3)_2CO$): -81.93 (s). HRMS calcd for $C_{42}H_{74}NP_2PtS_2$ [M$-$CH$(SO_2CF_3)_2$]$^+$: $m/z = 912.4377$; found: 912.4365.

[PtH(pta){κ^1*P*-*o*-C$_6$H$_4$(CH$_2$PBu$^t_2$)(CH$_2$SBu^t)}$_2$]CH(SO$_2$CF$_3$)$_2$ (29)

Complex **26** (27 mg, 0.023 mmol) and 1,3,5-triaza-7-phosphaadamantane (4 mg, 0.023 mmol) were combined in acetone-d_6 (0.8 mL) in an NMR tube, and sonicated until all crystals had dissolved. Removal of solvent under reduced pressure gave desired product **29**. Air-stable clear oil (quantitative conversion). ^{1}H NMR δ (500 MHz, $(CD_3)_2CO$): -7.97 (dt, $J = 153.6$, 15.0 Hz, $^{1}J_{PtH} = 728.0$ Hz, 1H, PtH), 1.44 (s, 18H, SBu^t), 1.54 (vt, $^{3}J_{PH} + {}^{5}J_{PH} = 14.0$ Hz, 36H, PBu^t), 3.75 (s, 1H, $^{-}$CH), 4.01 (s, 6H, PCH_2N), 4.04 (d, $J = 12.5$ Hz, 3H, NCH_2N), 4.10 (s, 4H, CH_2S), 4.24 (br, 4H, $ArCH_2P$), 4.29 (d, $J = 13.0$ Hz, 3H, NCH_2N), 7.35 (m, 4H, Ar), 7.49 (m, 2H, Ar), 8.15 (m, 2H, Ar). ^{13}C NMR δ (125 MHz, $(CD_3)_2CO$): 27.65 (vt, $^{1}J_{PC} + {}^{3}J_{PC} = 23.1$ Hz, $ArCH_2P$), 31.01 (br, PC*Me*$_3$), 31.08 (s, SC*Me*$_3$), 32.22 (s, CH_2S), 39.62 (vtd, $^{1}J_{PC} + {}^{3}J_{PC} = 27.4$ Hz, $J = 1.9$ Hz, $^{2}J_{PtC} = 43.7$ Hz, P*C*Me$_3$), 43.70 (s, S*C*Me$_3$), 53.58 (d, $J = 11.1$ Hz, PCH_2N), 55.33 (sept, $J = 2.9$ Hz, $^{-}$CH), 72.72 (d, $J = 6.7$ Hz, NCH_2N), 122.26 (q, $J = 325.4$ Hz, CF_3), 127.34 (s, Ar), 128.80 (s, Ar), 131.31 (vt, $^{3}J_{PC} + {}^{5}J_{PC} = 9.1$ Hz, Ar), 132.55 (s, Ar), 134.33 (s, Ar), 138.77 (vt, $^{2}J_{PC} + {}^{4}J_{PC} = 7.2$ Hz, Ar). ^{31}P NMR δ (121 MHz, $(CD_3)_2CO$): -89.77 (t, $J = 18$ Hz, $^{1}J_{PtP} = 1942$ Hz, pta), 47.33 (d, $J = 18$ Hz, $^{1}J_{PtP} = 2553$ Hz, PBu^t). ^{19}F NMR δ (282 MHz, $(CD_3)_2CO$): -81.95 (s). HRMS calcd for $C_{46}H_{83}N_3P_3PtS_2$ [M$-$CH$(SO_2CF_3)_2$]$^+$: $m/z = 1028.4877$; found: 1028.4868.

Reaction of [PtCl$_2${κ^2*P,S*-*o*-C$_6$H$_4$(CH$_2$PBu$^t_2$)(CH$_2$SBu^t)}] (21) with pta

Complex **21** (19 mg, 0.03 mmol) was dissolved in chloroform-*d* (0.4 mL) and a solution of 1,3,5-triaza-7-phosphaadamantane (5 mg, 0.03 mmol) in chloroform-*d* (0.4 mL) added, and the reaction was followed by ^{1}H and ^{31}P NMR spectroscopy.

After 10 min, a mixture of complex **21**, ligand **14a**, $[PtCl_2(pta)_2]$ and complex **30** was observed. After 19 h, all $[PtCl_2(pta)_2]$ had crystallised out of solution and complex **31** was also observed.

*trans-[PtCl$_2$(pta){κ^1 P-o-C$_6$H$_4$(CH$_2$PBu$^t_2$)(CH$_2$SBu^t)}](**30**)*
Selected ^{1}H NMR δ (500 MHz, $CDCl_3$): 8.37 (d, J = 8.0 Hz, 1H, Ar). ^{31}P NMR δ (121 MHz, $CDCl_3$): −62.26 (d, J = 439 Hz, $^1J_{PtP}$ = 2294 Hz, pta), 35.30 (d, J = 439 Hz, $^1J_{PtP}$ = 2578 Hz, PBu^t).

*cis-[PtCl$_2$(pta){κ^1 P-o-C$_6$H$_4$(CH$_2$PBu$^t_2$)(CH$_2$SBu^t)}](**31**)*
Selected ^{1}H NMR δ (500 MHz, $CDCl_3$): 8.78 (d, J = 7.0 Hz, 1H, Ar). ^{31}P NMR δ (121 MHz, $CDCl_3$): −65.56 (d, J = 12 Hz, $^1J_{PtP}$ = 3359 Hz, pta), 27.01 (d, J = 12 Hz, $^1J_{PtP}$ = 3578 Hz, PBu^t).

[Pt(ethene){κ^2*P,S*-*o*-C$_6$H$_4$(CH$_2$PBu$^t_2$)(CH$_2$SBu^t)}] (32)

Ligand **14a** (30 mg, 0.09 mmol) was dissolved in benzene-d_6 (0.4 mL) in an NMR tube, and a solution of $[Pt(ethene)_3]$ (25 mg, 0.09 mmol) in benzene-d_6 (0.4 mL) added. Reaction was complete after 10 min (>90% conversion). ^{1}H NMR δ (500 MHz, C_6D_6): 1.23 (d, J = 12.4 Hz, 18H, PBu^t), 1.34 (s, 9H, SBu^t), 2.04 (td, J = 10.5, 8.1 Hz, $^2J_{PtH}$ = 53.5 Hz, 2H, =CH_2), 2.49 (td, J = 10.5, 4.4 Hz, $^2J_{PtH}$ = 81.6 Hz, 2H, =CH_2), 3.32 (d, J = 8.1 Hz, $^3J_{PtH}$ = 21.9 Hz, 2H, CH_2P), 4.29 (s, $^3J_{PtH}$ = 32.0 Hz, 2H, CH_2S), 6.98 (t, J = 7.6 Hz, 1H, Ar), 7.03 (t, J = 7.6 Hz, 1H, Ar), 7.15 (m, 2H, Ar). ^{13}C NMR δ (125 MHz, C_6D_6): 27.37 (d, J = 36.5 Hz, $^1J_{PtC}$ = 205.9 Hz, =CH_2), 29.14 (d, J = 6.2 Hz, $^1J_{PtC}$ = 331.1 Hz, =CH_2), 29.51 (d, J = 3.9 Hz, $^2J_{PtC}$ = 8.6 Hz, CH_2P), 29.74 (s, $^3J_{PtC}$ = 15.8 Hz, SCMe_3), 30.18 (d, J = 6.2 Hz, $^3J_{PtC}$ = 19.2 Hz, PCMe_3), 37.01 (d, J = 13.4 Hz, $^2J_{PtC}$ = 57.1 Hz, PCMe$_3$), 40.07 (d, J = 3.8 Hz, $^2J_{PtC}$ = 32.6 Hz, CH_2S), 49.90 (d, J = 4.3 Hz, $^2J_{PtC}$ = 10.6 Hz, SCMe$_3$), 126.90 (d, J = 2.4 Hz, Ar), 126.95 (d, J = 1.5 Hz, Ar), 131.69 (d, J = 4.3 Hz, Ar), 132.41 (d, J = 1.9 Hz, Ar), 136.69 (d, J = 3.4 Hz, Ar), 139.27 (d, J = 0.9 Hz, Ar). ^{31}P NMR δ (121 MHz, C_6D_6): 59.37 (s, $^1J_{PtP}$ = 4067 Hz).

[Pt(ethene){κ^2*P,S*-*o*-C$_6$H$_4$(CH$_2$PBu$^t_2$)(CH$_2$S(O)Bu^t)}] (33)

Ligand **16** (45 mg, 0.13 mmol) was dissolved in benzene-d_6 (0.5 mL) in an NMR tube, and a solution of $[Pt(ethene)_3]$ (36 mg, 0.13 mmol) in benzene-d_6 (0.5 mL) added. Reaction was complete after 10 min (>95% conversion). ^{1}H NMR δ (500 MHz, C_6D_6): 1.11 (d, J = 12.7 Hz, 9H, PBu^t), 1.13 (d, J = 11.9 Hz, 9H, PBu^t), 1.34 (s, 9H, SBu^t), 2.13 (m, $^2J_{PtH}$ = 55.2 Hz, 1H, =CH_2), 2.32 (m, 1H, =CH_2), 2.42

(m, 1H, =CH_2), 2.50 (m, $^2J_{PtH}$ = 74.8 Hz, 1H, =CH_2), 3.23 (dd, J = 14.0, 6.1 Hz, 1H, CH_2P), 3.41 (dd, J = 14.0, 10.7 Hz, $^3J_{PtH}$ = 48.0 Hz, 1H, CH_2P), 4.20 (br d, J = 11.6 Hz, 1H, CH_2S), 4.39 (d, J = 11.6 Hz, $^3J_{PtH}$ = 22.0 Hz, 1H, CH_2S), 7.04 (m, 2H, Ar), 7.13 (m, 1H, Ar), 7.37 (m, 1H, Ar). ^{13}C NMR δ (125 MHz, C_6D_6): 23.63 (s, SCMe_3), 29.17 (d, J = 7.7 Hz, CH_2P), 29.99 (d, J = 6.2 Hz, $^3J_{PtC}$ = 19.7 Hz, PCMe_3), 30.31 (d, J = 5.7 Hz, $^3J_{PtC}$ = 17.8 Hz, PCMe_3), 30.46 (d, J = 32.1 Hz, $^1J_{PtC}$ = 199.1 Hz, =CH_2), 32.45 (d, J = 7.2 Hz, $^1J_{PtC}$ = 284.5 Hz, =CH_2), 36.58 (d, J = 14.9 Hz, $^2J_{PtC}$ = 48.0 Hz, PCMe$_3$), 37.43 (d, J = 13.4 Hz, $^2J_{PtC}$ = 50.9 Hz, PCMe$_3$), 58.34 (br s, CH_2S), 61.05 (d, J = 6.2 Hz, $^2J_{PtC}$ = 51.8 Hz, SCMe$_3$), 126.56 (d, J = 2.9 Hz, Ar), 127.66 (d, J = 1.9 Hz, Ar), 130.83 (d, J = 2.9 Hz, Ar), 131.58 (d, J = 4.8 Hz, Ar), 135.54 (s, Ar), 138.66 (s, Ar). ^{31}P NMR δ (121 MHz, C_6D_6): 54.79 (s, $^1J_{PtP}$ = 3861 Hz).

[Pt(nb){κ^2*P,S*-*o*-C_6H_4($CH_2PBu^t_2$)(CH_2SBu^t)}] (34)

Ligand **14a** (170 mg, 0.50 mmol) was dissolved in toluene (10 mL), and a solution of [Pt(nb)$_3$] (240 mg, 0.50 mmol) in toluene (10 mL) added with stirring. After 2.5 h, the brown solution was filtered through a plug of alumina, which was washed with further toluene (10 mL). Solvent was removed under reduced pressure and the crude material dissolved in toluene (9 mL). *n*-Hexane (18 mL) was added and solution cooled to −20 °C to crystallise desired product **34**. Air-stable pale brown crystals (221 mg, 92%). X-ray diffraction quality crystals were grown by cooling of a benzene-d_6 solution of complex **34** to 4 °C. ^{1}H NMR δ (600 MHz, C_6D_6): 0.50 (d, J = 7.5 Hz, 1H, bridge-CH_2), 1.26 (d, J = 12.3 Hz, 9H, PBu^t), 1.29 (d, J = 12.5 Hz, 9H, PBu^t), 1.42 (s, 9H, SBu^t), 1.47 (m, 3H, bridge-CH_2 & CH_2), 1.78 (m, 1H, CH_2), 1.84 (m, 1H, CH_2), 2.05 (t, J = 5.1 Hz, $^2J_{PtH}$ = 62.3 Hz, 1H, =CH), 2.56 (t, J = 6.0 Hz, $^2J_{PtH}$ = 75.6 Hz, 1H, =CH), 2.95 (br s, 1H, CH), 2.98 (br s, 1H, CH), 3.29 (dd, J = 7.9, 3.3 Hz, $^3J_{PtH}$ = 22.0 Hz, 2H, CH_2P), 4.25 (d, J = 10.6 Hz, $^3J_{PtH}$ = 29.4 Hz, 2H, CH_2S), 6.98 (m, 2H, Ar), 7.12 (br d, J = 7.5 Hz, 2H, Ar). ^{13}C NMR δ (150 MHz, C_6D_6): 29.66 (s, $^3J_{PtC}$ = 14.6 Hz, SCMe_3 & CH_2P obscured), 30.08 (br s, PCMe_3), 32.39 (s, $^3J_{PtC}$ = 49.7 Hz, CH_2), 32.46 (s, $^3J_{PtC}$ = 50.2 Hz, CH_2), 36.67 (d, J = 12.7 Hz, $^2J_{PtC}$ = 57.8 Hz, PCMe$_3$), 37.11 (d, J = 13.7 Hz, $^2J_{PtC}$ = 61.2 Hz, PCMe$_3$), 39.71 (d, J = 3.7 Hz, $^2J_{PtC}$ = 32.8 Hz, CH_2S), 40.88 (s, $^3J_{PtC}$ = 56.4 Hz, bridge-CH_2), 44.62 (s, $^2J_{PtC}$ = 17.4 Hz, CH), 44.78 (br s, CH), 49.15 (br d, J = 44.1 Hz, $^1J_{PtC}$ = 324.9 Hz, =CH), 49.20 (br d, J = 7.2 Hz, $^1J_{PtC}$ = 469.8 Hz, =CH), 49.59 (d, J = 5.1 Hz, $^2J_{PtC}$ = 35.0 Hz, SCMe$_3$), 126.88 (d, J = 3.4 Hz, Ar), 126.90 (d, J = 2.8 Hz, Ar), 131.60 (d, J = 3.9 Hz, Ar), 132.20 (d, J = 2.0 Hz, Ar), 136.86 (d, J = 3.1 Hz, Ar), 139.21 (d, J = 1.4 Hz, Ar). ^{31}P NMR δ (121 MHz, C_6D_6): 58.33 (s, $^1J_{PtP}$ = 3868 Hz). HRMS calcd for $C_{20}H_{36}$PPtS

$[M-C_7H_9]^+$: m/z = 533.1902; found: 533.1893. Anal. calcd for $C_{27}H_{45}PPtS$: C, 51.7; H, 7.2; S, 5.1; found: C, 51.7; H, 7.4; S, 4.8.

[Pt(nb){κ^2*P,S*-*o*-$C_6H_4(CH_2PBu^t_2)(CH_2S(O)Bu^t)$}] (35)

Ligand **16** (19 mg, 0.05 mmol) was dissolved in benzene-d_6 (0.4 mL) in an NMR tube, and a solution of [Pt(nb)$_3$] (24 mg, 0.05 mmol) in benzene-d_6 (0.4 mL) added. Reaction was complete after 5 min (quantitative conversion). Selected ^{1}H NMR δ (500 MHz, C_6D_6): 0.38 (d, J = 8.0 Hz, 1H, bridge-CH_2), 0.56 (d, J = 8.5 Hz, 1H, bridge-CH_2), 1.38 (s, 9H, S(O)Bu^t), 1.40 (s, 9H, S(O)Bu^t), 2.52 (t, J = 6.5 Hz, $^2J_{PtH}$ = 77.0 Hz, 1H, =CH), 2.63 (t, J = 6.5 Hz, $^2J_{PtH}$ = 72.0 Hz, 1H, =CH). ^{31}P NMR δ (121 MHz, C_6D_6): 53.71 (s, $^1J_{PtP}$ = 3668 Hz), 54.40 (s, $^1J_{PtP}$ = 3708 Hz).

[Pt{κ^1*P*-*o*-$C_6H_4(CH_2PBu^t_2)(CH_2SBu^t)$}$_2$] (36)

Ligand **14a** (0.20 g, 0.58 mmol) was dissolved in toluene (5 mL), a solution of [Pt(nb)$_3$] (0.13 g, 0.27 mmol) in toluene (5 mL) added and the resulting pale brown solution stirred overnight. Removal of solvent under reduced pressure gave complex **36**. Highly air-sensitive off-white solid (quantitative conversion). ^{1}H NMR δ (500 MHz, C_6D_6): 1.28 (s, 18H, SBu^t), 1.46 (vt, $^3J_{PH}$ + $^5J_{PH}$ = 12.4 Hz, 36H, PBu^t), 3.49 (vt, $^2J_{PH}$ + $^4J_{PH}$ = 6.1 Hz, $^3J_{PtH}$ = 43.3 Hz, 4H, CH_2P), 4.32 (s, 4H, CH_2S), 7.07 (t, J = 7.3 Hz, 2H, Ar), 7.11 (t, J = 7.3 Hz, 2H, Ar), 7.27 (d, J = 7.1 Hz, 2H, Ar), 9.06 (d, J = 7.5 Hz, 2H, Ar). ^{13}C NMR δ (125 MHz, C_6D_6): 25.93 (vt, $^1J_{PC}$ + $^3J_{PC}$ = 15.8 Hz, CH_2P), 30.91 (vt, $^2J_{PC}$ + $^4J_{PC}$ = 7.2 Hz, PCMe_3), 31.13 (s, SCMe_3), 33.84 (s, CH_2S), 37.14 (vt, $^1J_{PC}$ + $^3J_{PC}$ = 20.2 Hz, PCMe$_3$), 42.60 (s, SCMe$_3$), 126.20 (s, Ar), 126.67 (s, Ar), 131.01 (s, Ar), 134.26 (vt, $^3J_{PC}$ + $^5J_{PC}$ = 7.6 Hz, Ar), 137.23 (vt, $^2J_{PC}$ + $^4J_{PC}$ = 3.9 Hz, Ar), 138.14 (s, Ar). ^{31}P NMR δ (121 MHz, C_6D_6): 76.13 (s, $^1J_{PtP}$ = 4397 Hz). HRMS calcd for $C_{40}H_{71}P_2PtS_2$ $[M+H]^+$: m/z = 871.4099; found: 871.4092.

[Pt{κ^1*P*-*o*-$C_6H_4(CH_2PBu^t_2)(CH_2S(O)Bu^t)$}$_2$] (37)

Ligand **16** (35 mg, 0.10 mmol) was dissolved in benzene-d_6 (0.4 mL) in an NMR tube, and a solution of [Pt(1,5-cyclooctadiene)$_2$] (21 mg, 0.05 mmol) in benzene-d_6 (0.4 mL) added. Reaction was complete after 10 min (quantitative conversion). ^{1}H NMR δ (500 MHz, C_6D_6): 1.07 (s, 18H, SBu^t), 1.09 (s, 18H, SBu^t), 1.40 (vt, $^3J_{PH}$ + $^5J_{PH}$ = 13.4 Hz, 18H, PBu^t), 1.43 (vt, $^3J_{PH}$ + $^5J_{PH}$ = 13.0 Hz, 18H, PBu^t), 1.46 (vt, $^3J_{PH}$ + $^5J_{PH}$ = 12.5 Hz, 36H, 2 × PBu^t), 3.36 (dvt, J = 14.6 Hz, $^2J_{PH}$ + $^4J_{PH}$ = 6.5 Hz, 4H, 2 × CH_2P), 3.70 (dvt, J = 13.9 Hz, $^2J_{PH}$ + $^4J_{PH}$ = 5.8 Hz, 2H, CH_2P), 3.77 (d, J = 12.9 Hz, 2H, CH_2S), 3.79 (dvt,

J = 12.5 Hz, $^2J_{PH} + {}^4J_{PH}$ = 5.9 Hz, 2H, CH_2P), 4.12 (d, J = 12.9 Hz, 2H, CH_2S), 4.53 (d, J = 13.0 Hz, 2H, CH_2S), 4.73 (d, J = 12.9 Hz, 2H, CH_2S), 7.09 (m, 8H, Ar), 7.18 (m, 2H, Ar), 7.23 (m, 2H, Ar), 8.48 (m, 2H, Ar), 8.52 (m, 2H, Ar). ^{31}P NMR δ (121 MHz, C_6D_6): 76.45 (s, $^1J_{PtP}$ = 4408 Hz), 76.97 (s, $^1J_{PtP}$ = 4424 Hz).

[Pt{κ^1*P*-*o*-C_6H_4($CH_2PBu^t_2$)(CH_2NMe_2)}$_2$] (38)

Ligand **18a** (23 mg, 0.08 mmol) was dissolved in benzene-d_6 (0.4 mL) in an NMR tube, and a solution of [Pt(nb)$_3$] (19 mg, 0.04 mmol) in benzene-d_6 (0.4 mL) added. Reaction was complete after 20 min (quantitative conversion). ^{1}H NMR δ (500 MHz, C_6D_6): 1.49 (vt, $^3J_{PH} + {}^5J_{PH}$ = 12.4 Hz, 36H, PBu^t), 2.11 (s, 12H, NMe), 3.60 (vt, $^2J_{PH} + {}^4J_{PH}$ = 6.3 Hz, $^3J_{PtH}$ = 49.8 Hz, 4H, CH_2P), 3.74 (s, 4H, CH_2N), 7.12 (m, 4H, Ar), 7.23 (m, 2H, Ar), 9.64 (d, J = 7.8 Hz, 2H, Ar). ^{13}C NMR δ (125 MHz, C_6D_6): 24.71 (vt, $^1J_{PC} + {}^3J_{PC}$ = 17.3 Hz, CH_2P), 30.80 (vt, $^2J_{PC} + {}^4J_{PC}$ = 7.1 Hz, PCMe_3), 37.08 (vt, $^1J_{PC} + {}^3J_{PC}$ = 20.7 Hz, PCMe$_3$), 45.44 (s, NMe), 64.79 (s, CH_2N), 125.54 (s, Ar), 126.97 (s, Ar), 130.93 (s, Ar), 134.52 (vt, $^3J_{PC} + {}^5J_{PC}$ = 8.2 Hz, Ar), 137.72 (vt, $^2J_{PC} + {}^4J_{PC}$ = 4.8 Hz, Ar), 139.40 (s, Ar). ^{31}P NMR δ (121 MHz, C_6D_6): 75.41 (s, $^1J_{PtP}$ = 4373 Hz). HRMS calcd for $C_{36}H_{65}N_2P_2Pt$ $[M+H]^+$: m/z = 781.4250; found: 781.4246.

[PtH{CH(SO_2CF_3)$_2$}{κ^2*P,S*-*o*-C_6H_4($CH_2PBu^t_2$)(CH_2SBu^t)}] (39)

Complex **34** (23 mg, 0.04 mmol) was dissolved in benzene-d_6 (0.5 mL) in an NMR tube, and a solution of $CH_2(SO_2CF_3)_2$ (10 mg, 0.04 mmol) in benzene-d_6 (0.4 mL) added. Reaction was complete after 15 min (quantitative conversion). ^{1}H NMR δ (500 MHz, C_6D_6): −14.22 (d, J = 16.5 Hz, $^1J_{PtH}$ = 1092.9 Hz, 1H, PtH), 1.12 (d, J = 14.1 Hz, 18H, PBu^t), 1.25 (s, 9H, SBu^t), 3.02 (d, J = 10.5 Hz, $^3J_{PtH}$ = 31.8 Hz, 2H, CH_2P), 3.77 (d, J = 1.7 Hz, $^3J_{PtH}$ = 31.7 Hz, 2H, CH_2S), 5.84 (d, J = 6.1 Hz, $^2J_{PtH}$ = 66.0 Hz, 1H, PtCH), 6.95 (m, 4H, Ar). ^{13}C NMR δ (125 MHz, C_6D_6): 23.93 (d, J = 15.3 Hz, CH_2P), 29.70 (d, J = 3.8 Hz, $^3J_{PtC}$ = 25.0 Hz, PCMe_3), 30.41 (s, SCMe_3), 36.33 (s, CH_2S), 37.26 (d, J = 27.8 Hz, $^2J_{PtC}$ = 60.0 Hz, PCMe$_3$), 52.05 (s, SCMe$_3$), 62.28 (d, J = 63.8 Hz, $^1J_{PtC}$ = 492.5 Hz, PtCH), 120.27 (q, J = 329.2 Hz, CF_3), 131.43 (d, J = 4.8 Hz, Ar), 132.51 (d, J = 2.4 Hz, Ar), 132.91 (d, J = 3.9 Hz, Ar), 135.89 (d, J = 2.4 Hz, Ar), other two Ar obscured by solvent. ^{31}P NMR δ (121 MHz, C_6D_6): 52.28 (s, $^1J_{PtP}$ = 3678 Hz). ^{19}F NMR δ (282 MHz, C_6D_6): −75.57 (s).

[Pt(norbornyl){κ^2*P,S*-*o*-$C_6H_4(CH_2PBu^t_2)(CH_2SBu^t)$}]$BF_4$ (40)

Complex **34** (25 mg, 0.04 mmol) dissolved in dichloromethane (1 mL) was cooled to 0 °C, and tetrafluoroboric acid–diethyl ether complex (8 μL, 85%, 0.04 mmol) added. The solution was stirred at room temperature for 30 min, and removal of solvent under reduced pressure gave desired product **40**. Unstable, off-white solid (>95% conversion). ^{1}H NMR δ (300 MHz, CD_2Cl_2): −1.93 (dd, J = 47.6, 17.1 Hz, $^1J_{PtH}$ = 37.4 Hz, 1H, agostic-CH), 0.90 (m, 3H, norbornyl), 1.42 (d, J = 14.6 Hz, 9H, PBu^t), 1.45 (d, J = 14.6 Hz, 9H, PBu^t), 1.60 (s, 9H, SBu^t), 1.72 (m, 2H, norbornyl), 2.49 (br, $^2J_{PtH}$ = 46.8 Hz, 1H, PtCH), 2.78 (d, J = 2.8 Hz, 1H, norbornyl), 2.98 (s, 1H, norbornyl), 3.83 (dd, J = 15.0, 10.9 Hz, 1H, CH_2P), 3.93 (dd, J = 15.0, 11.5 Hz, 1H, CH_2P), 4.43 (d, J = 12.7 Hz, $^3J_{PtH}$ = 43.3 Hz, 1H, CH_2S), 4.52 (d, J = 12.7 Hz, $^3J_{PtH}$ = 32.2 Hz, 1H, CH_2S), 7.31 (m, 3H, Ar), 7.43 (m, 1H, Ar), other two norbornyl obscured by Bu^t peaks. ^{31}P NMR δ (121 MHz, CD_2Cl_2): 62.46 (s, $^1J_{PtP}$ = 5791 Hz). ^{19}F NMR δ (282 MHz, CD_2Cl_2): −151.63 (s).

[Pt(ethyne){κ^2*P,S*-*o*-$C_6H_4(CH_2PBu^t_2)(CH_2SBu^t)$}] (41)

Complex **34** (25 mg, 0.04 mmol) was dissolved in benzene-d_6 (0.5 mL) in an NMR tube and ethyne gas was bubbled through the solution for 1 min, giving unstable complex **41** (>90% conversion). ^{1}H NMR δ (600 MHz, C_6D_6): 1.27 (d, J = 12.6 Hz, 18H, PBu^t), 1.38 (s, 9H, SBu^t), 3.30 (d, J = 8.4 Hz, $^3J_{PtH}$ = 22.6 Hz, 2H, CH_2P), 4.20 (s, $^3J_{PtH}$ = 35.9 Hz, 2H, CH_2S), 6.74 (d, J = 17.6 Hz, $^2J_{PtH}$ = 33.8 Hz, 1H, ≡CH), 6.98 (t, J = 7.0 Hz, 1H, Ar), 7.03 (d, J = 14.1 Hz, $^2J_{PtH}$ = 90.6 Hz, 1H, ≡CH), 7.03 (m, 1H, Ar), 7.14 (m, 2H, Ar). ^{13}C NMR δ (150 MHz, C_6D_6): 29.00 (d, J = 5.8 Hz, CH_2P), 29.19 (s, $^3J_{PtC}$ = 16.8 Hz, SC*Me*$_3$), 30.03 (d, J = 6.4 Hz, $^3J_{PtC}$ = 17.2 Hz, PC*Me*$_3$), 36.61 (d, J = 16.8 Hz, $^2J_{PtC}$ = 53.0 Hz, P*C*Me$_3$), 40.09 (d, J = 4.0 Hz, $^2J_{PtC}$ = 33.0 Hz, CH_2S), 48.90 (d, J = 3.5 Hz, S*C*Me$_3$), 101.19 (d, J = 8.1 Hz, $^1J_{PtC}$ = 444.5 Hz, ≡CH), 112.27 (d, J = 68.2 Hz, $^1J_{PtC}$ = 258.3 Hz, ≡CH), 126.96 (d, J = 2.3 Hz, Ar), 127.03 (d, J = 1.7 Hz, Ar), 131.70 (d, J = 4.0 Hz, Ar), 132.26 (d, J = 1.7 Hz, Ar), 136.10 (d, J = 2.8 Hz, Ar), 138.92 (s, Ar). ^{31}P NMR δ (121 MHz, C_6D_6): 56.79 (s, $^1J_{PtP}$ = 4018 Hz).

[Pt(O_2){κ^1*P*-*o*-$C_6H_4(CH_2PBu^t_2)(CH_2SBu^t)$}$_2$] (42)

Complex **36** (214 mg, 0.24 mmol) was dissolved in *n*-hexane (25 mL) and O_2 bubbled through the solution until solid began to appear, then cooled to −20 °C overnight. The clear solution was decanted off the resulting crystals and these were dried under a stream of O_2, giving desired complex **42**. Pale brown microcrystals (169 mg, 78%). ^{1}H NMR δ (500 MHz, C_6D_6): 1.18 (s, 18H, SBu^t), 1.48 (d, J = 12.9 Hz, 36H, PBu^t),

3.59 (s, 4H, CH_2S), 3.77 (d, J = 10.5 Hz, $^3J_{PtH}$ = 35.8 Hz, 4H, CH_2P), 6.83 (t, J = 7.5 Hz, 2H, Ar), 6.92 (t, J = 7.4 Hz, 2H, Ar), 7.09 (d, J = 7.5 Hz, 2H, Ar), 8.50 (d, J = 7.5 Hz, 2H, Ar). ^{13}C NMR δ (125 MHz, C_6D_6): 27.02 (m, CH_2P), 30.84 (s, SCMe_3), 31.12 (br s, PCMe_3), 32.41 (s, CH_2S), 38.64 (m, PCMe$_3$), 42.66 (s, SCMe$_3$), 126.57 (s, Ar), 127.18 (s, Ar), 131.31 (s, Ar), 132.29 (m, Ar), 135.52 (m, Ar), 136.70 (m, Ar). ^{31}P NMR δ (121 MHz, C_6D_6): 43.47 (s, $^1J_{PtP}$ = 4112 Hz). HRMS calcd for $C_{40}H_{69}P_2PtS_2$ [M−O_2H]$^+$: m/z = 869.3943; found: 869.3942. Anal. calcd for $C_{40}H_{70}O_2P_2PtS_2$: C, 53.1; H, 7.8; S, 7.1; found: C, 53.4; H, 7.9; S, 7.0.

7.4 Palladium Complexes

[PdCl{κ^2*P*,μ-*S*-*o*-C_6H_4($CH_2PBu^t_2$)(CH_2S)}]$_2$ (43)

Ligand **14a** (30 mg, 0.09 mmol) was dissolved in acetone-d_6 (0.4 mL) in an NMR tube, and a solution of [$PdCl_2$(NCBu^t)$_2$] (31 mg, 0.09 mmol) in acetone-d_6 (0.4 mL) added. After 24 h, the orange solution was heated to 50 °C overnight, resulting in orange crystals of complex **43** (quantitative conversion). ^{1}H NMR δ (500 MHz, CD_2Cl_2): 1.60 (d, J = 13.6 Hz, 36H, PBu^t), 3.32 (br d, J = 8.8 Hz, 4H, CH_2S), 3.80 (br, 4H, CH_2P), 7.06 (m, 2H, Ar), 7.14 (d, J = 7.4 Hz, 2H, Ar), 7.43 (d, J = 7.1 Hz, 2H, Ar), other Ar too broad to be observed. ^{13}C NMR δ (125 MHz, CD_2Cl_2): 25.10 (br d, J = 11.5 Hz, CH_2S), 30.87 (br, PCMe_3), 31.62 (br, CH_2P), 38.76 (d, J = 11.0 Hz, PCMe$_3$), 127.14 (d, J = 1.4 Hz, Ar), 127.86 (d, J = 2.4 Hz, Ar), 130.84 (d, J = 1.9 Hz, Ar), 131.05 (br, Ar), 134.07 (s, Ar), 140.51 (s, Ar). ^{31}P NMR δ (121 MHz, CD_2Cl_2): 51.00 (br). HRMS calcd for $C_{32}H_{54}ClP_2Pd_2S_2$ [M−Cl+2H]$^+$: m/z = 813.0904; found: 813.0895. Anal. calcd for $C_{32}H_{52}Cl_2P_2Pd_2S_2$: C, 45.4; H, 6.2; S, 7.6; found: C, 45.7; H, 6.3; S, 7.5.

[Pd{κ^1*P*-*o*-C_6H_4($CH_2PBu^t_2$)(CH_2SBu^t)}$_2$] (44)

Method 1: Ligand **14a** (34 mg, 0.10 mmol) was dissolved in benzene-d_6 (0.4 mL) in an NMR tube, and a solution of [$PdMe_2$(tmeda)] (13 mg, 0.05 mmol) in benzene-d_6 (0.4 mL) added. Reaction was complete in <24 h (quantitative conversion). Method 2: Ligand **14a** (40 mg, 0.12 mmol) was dissolved in benzene-d_6 (0.4 mL) in an NMR tube, and a solution of [Pd(nb)$_3$] (23 mg, 0.06 mmol) in benzene-d_6 (0.4 mL) added. Reaction was complete in 10 min (quantitative conversion). ^{1}H NMR δ (500 MHz, C_6D_6): 1.29 (s, 18H, SBu^t), 1.41 (vt, $^3J_{PH}$ + $^5J_{PH}$ = 12.2 Hz, 36H, PBu^t), 3.29 (vt, $^2J_{PH}$ + $^4J_{PH}$ = 5.2 Hz, 4H, CH_2P), 4.27 (s, 4H, CH_2S), 7.06 (t, J = 7.2 Hz, 2H, Ar), 7.12 (t, J = 7.7 Hz, 2H, Ar), 7.29 (d, J = 7.3 Hz,

2H, Ar), 8.87 (d, J = 7.6 Hz, 2H, Ar). ^{13}C NMR δ (125 MHz, C_6D_6): 26.34 (vt, $^1J_{PC} + {}^3J_{PC}$ = 4.4 Hz, CH_2P), 31.05 (vt, $^2J_{PC} + {}^4J_{PC}$ = 11.1 Hz, PCMe_3), 31.11 (s, SCMe_3), 33.41 (vt, $^4J_{PC} + {}^6J_{PC}$ = 3.3 Hz, CH_2S), 35.20 (vt, $^1J_{PC} + {}^3J_{PC}$ = 7.2 Hz, PCMe$_3$), 42.64 (s, SCMe$_3$), 126.16 (s, Ar), 126.79 (s, Ar), 131.12 (s, Ar), 133.35 (vt, $^3J_{PC} + {}^5J_{PC}$ = 13.0 Hz, Ar), 137.00 (vt, $^2J_{PC} + {}^4J_{PC}$ = 6.7 Hz, Ar), 138.86 (s, Ar). ^{31}P NMR δ (121 MHz, C_6D_6): 54.40 (s).

Complexes 45 and 46

Ligand **14a** (45 mg, 0.13 mmol) was dissolved in benzene-d_6 (0.4 mL) in an NMR tube, and a solution of [Pd(OAc)$_2$] (30 mg, 0.13 mmol) in benzene-d_6 (0.4 mL) added. Yellow X-ray diffraction quality crystals of complex **45** formed from the solution at room temperature over a few hours. Solvent was removed from the resulting pale yellow solution under reduced pressure to give slightly impure complex **46**. Off-white foam (>90% conversion).

*[Pd$_3$(OAc)$_2$(μ-OAc)$_2${κ^3P,C,S-o-C$_6$H$_3$(CH$_2$PBu$^t{}_2$)(CH$_2$SBu^t)}$_2$]$_2$ (**45**)*
Selected ^{1}H NMR δ (300 MHz, C_6D_6): 1.40 (s, 36H, SBu^t), 1.96 (s, 12H, OAc), 2.30 (s, 12H, OAc), 3.01 (dd, J = 17.8, 8.2 Hz, 4H, CH_2P), 3.73 (dd, J = 17.5, 12.0 Hz, 4H, CH_2P), 4.30 (d, J = 14.4 Hz, 4H, CH_2S), 5.05 (d, J = 14.4 Hz, 4H, CH_2S). ^{31}P NMR δ (121 MHz, C_6D_6): 100.05 (s). IR (KBr disk): 1302 (terminal C−O), 1418 (bridging C−O), 1594 (bridging C=O), 1638 (terminal C=O), 2870–3034 cm^{-1} (CH).

*[Pd(μ-OAc){κ^2P,C-o-C$_6$H$_3$(CH$_2$PBu$^t{}_2$)(CH$_2$SBu^t)}]$_2$ (**46**)*
^{1}H NMR δ (600 MHz, C_6D_6): 1.22 (s, 18H, SBu^t), 1.24 (d, J = 14.4 Hz, 36H, PBu^t), 2.15 (br, 6H, OAc), 3.25 (d, J = 9.7 Hz, 4H, CH_2P), 3.58 (s, 4H, CH_2S), 6.94 (d, J = 7.0 Hz, 2H, Ar), 6.98 (t, J = 7.4 Hz, 2H, Ar), 7.95 (br, 2H, Ar). ^{13}C NMR δ (150 MHz, C_6D_6): 29.22 (br s, PCMe_3), 29.78 (br d, J = 18.5 Hz, CH_2P), 30.85 (s, SCMe_3), 34.45 (br s, CH_2S), 35.36 (d, J = 18.5 Hz, PCMe$_3$), 42.47 (s, SCMe$_3$), 125.95 (br s, Ar), 126.75 (br s, Ar), 131.71 (br, Ar), 135.55 (br, Ar), 148.20 (d, J = 18.0 Hz, Ar), 150.55 (br, Ar), 179.80 (br, CO), acetate Me peak too broad to be observed. ^{31}P NMR δ (121 MHz, C_6D_6): 96.80 (br). IR (film from THF): 1414 (C−O), 1593 (C=O), 2865–3039 cm^{-1} (CH). HRMS calcd for $C_{22}H_{37}NPPdS$ [$\frac{1}{2}$M−OAc+NCMe]$^+$: m/z = 484.1422; found: 484.1424.

[Pd(nb){κ^2*P,S*-*o*-C$_6$H$_4$(CH$_2$PBu$^t{}_2$)(CH$_2$SBu^t)}] (47)

Method 1: Ligand **14a** (33 mg, 0.10 mmol) was dissolved in benzene-d_6 (0.4 mL) in an NMR tube, and a solution of [Pd(nb)$_3$] (39 mg, 0.10 mmol) in benzene-d_6 (0.4 mL)

added. Reaction was complete in 10 min (quantitative conversion). Method 2: Ligand **14a** (33 mg, 0.10 mmol) and norbornene (19 mg, 0.20 mmol) were dissolved in benzene-d_6 (0.4 mL) in an NMR tube, and a solution of [Pd(Cp)(allyl)] (21 mg, 0.10 mmol) in benzene-d_6 (0.4 mL) added. After 3 h, the solution was passed through a plug of celite and the solvent evaporated under reduced pressure. The resulting yellow solid and a crystal of norbornene were dissolved in benzene-d_6 (0.4 mL), giving a reasonably stable solution of complex **47**. ^{1}H NMR δ (500 MHz, C_6D_6): 0.68 (br, 1H, nb), 1.26 (d, J = 11.9 Hz, 18H, PBu^t), 1.37 (br m, 3H, nb), 1.44 (s, 9H, SBu^t), 1.66 (br, 2H, nb), 2.98 (br, 2H, nb), 3.09 (d, J = 5.8 Hz, 2H, CH_2P), 3.21 (br, 2H, nb), 3.88 (s, 2H, CH_2S), 6.95 (t, J = 7.3 Hz, 1H, Ar), 7.00 (t, J = 7.3 Hz, 1H, Ar), 7.12 (d, J = 7.6 Hz, 1H, Ar), 7.20 (d, J = 7.5 Hz, 1H, Ar). ^{13}C NMR δ (125 MHz, C_6D_6): 28.62 (d, J = 5.8 Hz, CH_2P), 29.14 (br, nb), 30.30 (s, SCMe_3), 30.37 (s, PCMe_3), 35.70 (s, PCMe$_3$), 37.24 (br s, CH_2S), 42.52 (br, nb), 44.78 (br, nb), 47.31 (d, J = 4.3 Hz, SCMe$_3$), 66.86 (br, nb C=C), 126.71 (d, J = 1.0 Hz, Ar), 126.79 (s, Ar), 131.65 (s, Ar), 132.73 (s, Ar), 136.98 (d, J = 2.9 Hz, Ar), 139.60 (d, J = 4.3 Hz, Ar). ^{31}P NMR δ (121 MHz, C_6D_6): 56.50 (s).

[Pd(dba){κ^2*P,S*-*o*-C_6H_4($CH_2PBu^t_2$)(CH_2SBu^t)}] (48)

Method 1: Ligand **14a** (22 mg, 0.06 mmol) was dissolved in benzene-d_6 (0.4 mL) in an NMR tube, and a solution of [Pd_2(dba)$_3$] (34 mg, 0.03 mmol) in benzene-d_6 (0.4 mL) added. Reaction was complete in 24 h (>95% conversion). Method 2: Ligand **14a** (44 mg, 0.13 mmol) was dissolved in benzene-d_6 (0.4 mL) in an NMR tube, and a solution of [$PdMe_2$(tmeda)] (33 mg, 0.13 mmol) and dba (30 mg, 0.13 mmol) in benzene-d_6 (0.4 mL) added. Reaction was complete in 5 days (>95% conversion). ^{1}H NMR δ (500 MHz, C_6D_6): 0.91 (br, 9H, PBu^t), 1.27 (br, 9H, PBu^t), 1.45 (s, 9H, SBu^t), 2.92 (m, 2H, CH_2P), 3.49 (br, 1H, CH_2S), 3.71 (br, 1H, CH_2S), 4.80 (br, 1H, coordinated =CH), 4.87 (br, 1H, coordinated =CH), 6.78 (t, J = 7.1 Hz, 1H, Ar), 6.83 (t, J = 7.3 Hz, 1H, Ar), 6.92 (d, J = 7.1 Hz, 1H, Ar), 7.01 (br m, 9H, Ar & dba), 7.30 (br m, 4H, dba). ^{13}C NMR δ (125 MHz, C_6D_6): 27.82 (br s, CH_2P), 29.91 (br, PCMe_3), 30.54 (br, PCMe_3), 30.92 (s, SCMe_3), 32.59 (s, PCMe$_3$), 35.82 (br, CH_2S), 48.52 (s, SCMe$_3$), 64.21 (br, coordinated =CH), 72.90 (br, coordinated =CH), 124.70 (br, dba), 126.92 (s, Ar), 127.04 (s, Ar), 127.14 (br, dba), 128.57 (br, dba), 131.45 (d, J = 3.3 Hz, Ar), 132.55 (s, Ar), 134.89 (br, Ar), 137.56 (br, dba), 138.32 (s, Ar), other PCMe$_3$ peak obscured. ^{31}P NMR δ (121 MHz, C_6D_6): 59.06 (br). HRMS calcd for $C_{37}H_{50}OPPdS$ [M+H]$^+$: m/z = 679.2363; found: 679.2370.

7.5 Sonogashira Catalysis

α-(Di-*t*-butylphosphonium)-α'-(*t*-butylthio)-*o*-xylene tetrafluoroborate (49)

Compound **14a** (0.180 g, 0.53 mmol) was dissolved in dichloromethane (15 mL), 50% aqueous tetrafluoroboric acid (0.7 mL, 5.6 mmol) added and the mixture stirred vigorously for 10 min. Distilled water (3 mL) was added and the layers separated. The organic layer was dried over magnesium sulfate, filtered and the solvent evaporated under reduced pressure leaving a foam. The oil was triturated with *n*-hexane (2 × 3 mL) and the solvent decanted, giving compound **49**. Air-stable white solid (0.195 g, 86%). ^{1}H NMR δ (500 MHz, $(CD_3)_2CO$): 1.42 (s, 9H, SBu^t), 1.56 (d, J = 16.6 Hz, 18H, PBu^t), 4.01 (s, 2H, CH_2S), 4.26 (dd, J = 14.1, 6.1 Hz, 2H, CH_2P), 6.77 (dt, J = 466.3, 6.3 Hz, 1H, PH), 7.35 (m, 2H, Ar), 7.49 (m, 1H, Ar), 7.62 (m, 1H, Ar). ^{13}C NMR δ (125 MHz, $(CD_3)_2CO$): 19.34 (d, J = 39.3 Hz, CH_2P), 27.66 (s, PCMe_3), 30.97 (s, SCMe_3), 31.72 (s, CH_2S), 34.65 (d, J = 34.0 Hz, PCMe$_3$), 44.05 (s, SCMe$_3$), 128.98 (s, Ar), 129.49 (d, J = 1.9 Hz, Ar), 130.41 (d, J = 8.2 Hz, Ar), 131.53 (d, J = 6.7 Hz, Ar), 132.92 (s, Ar), 137.50 (d, J = 6.2 Hz, Ar). ^{31}P NMR δ (121 MHz, $(CD_3)_2CO$): 39.62 (s). ^{19}F NMR δ (282 MHz, $(CD_3)_2CO$): −150.11 (s). HRMS calcd for $C_{20}H_{36}PS$ $[M-BF_4]^+$: m/z = 339.2270; found: 339.2291.

Benzyldi-*t*-butylphosphonium tetrafluoroborate (50)

Benzyldi-*t*-butylphosphine (0.170 g, 0.72 mmol) was dissolved in dichloromethane (10 mL), 50% aqueous tetrafluoroboric acid (0.8 mL, 6.4 mmol) added and the mixture stirred vigorously for 10 min. The aqueous layer was removed, the organic layer dried over magnesium sulfate, filtered and the solvent evaporated under reduced pressure giving compound **50**. Air-stable white solid (0.190 g, 82%). ^{1}H NMR δ (300 MHz, $(CD_3)_2CO$): 1.60 (d, J = 16.4 Hz, 18H, PBu^t), 4.15 (dd, J = 13.5, 5.9 Hz, 2H, CH_2P), 6.39 (dt, J = 466.3, 5.9 Hz, 1H, PH), 7.42 (m, 3H, Ar), 7.57 (m, 2H, Ar). ^{31}P NMR δ (121 MHz, $(CD_3)_2CO$): 48.33 (s). ^{19}F NMR δ (282 MHz, $(CD_3)_2CO$): −150.86 (s).

Sonogashira coupling of 4-bromoanisole and phenylethyne

$[Pd(OAc)_2]$ (6.7 mg, 0.03 mmol), phosphonium salt **49** (12.8 mg, 0.03 mmol) and copper(I) iodide (3.8 mg, 0.02 mmol) were combined in a flask containing a large stir bar. A THF solution (3.0 mL) of 4-bromoanisole (0.13 mL, 1.0 mmol) and di-*i*-propylamine (0.70 mL, 5.0 mmol) was added and the vigorously stirred

(800–1000 rpm) mixture heated to 60 °C for 10 min. Phenylethyne (0.14 mL, 1.3 mmol) was added and the heating continued for 2 h. Samples for GC-MS (0.05 mL) were taken at regular intervals and added to dichloromethane solutions (10.0 mL) containing carbon disulfide (0.01 mL). Samples of these solutions (0.05 mL) were diluted with dichloromethane (1 mL) and GC-MS chromatograms collected using a Restek Rxi-5Sil column (length 30 m, inner diameter 0.25 mm, layer thickness 0.25 μm), helium carrier gas at 83.9 kPa with a 50:1 split, 270 °C injection temperature, and temperature program consisting of 50 °C for 2 min, heating to 100 °C at 10 °C/min, 100 °C for 2 min, heating to 300 °C at 20 °C/min, 300 °C for 5 min. An example of a GC-MS chromatogram from this reaction is shown in Figure 7.1. All reactions were performed in duplicate.

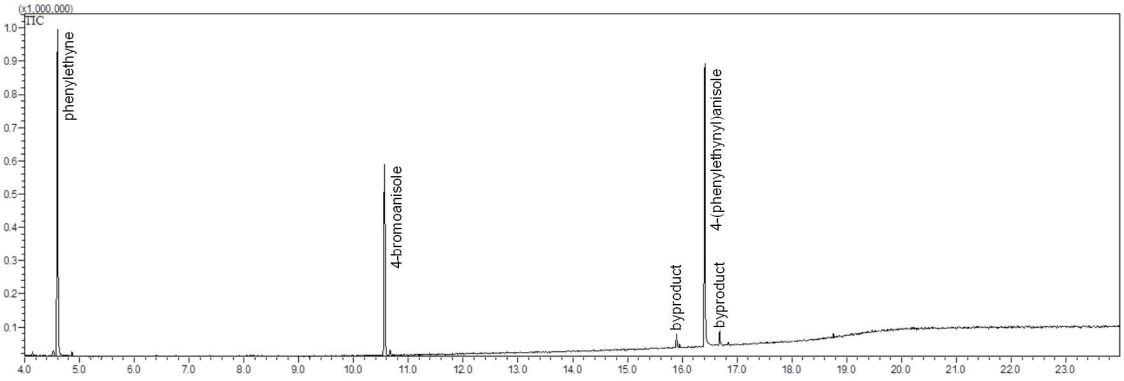

Figure 7.1 Example GC-MS chromatogram from the Sonogashira coupling of 4-bromoanisole and phenylethyne.

For the preparative run, a 2-methylnaphthalene (142 mg, 1.0 mmol) internal standard was included in the reaction. The reaction was followed by NMR spectroscopy, with samples (0.1 mL) taken at 0, 2 and 4 h, solvent evaporated under reduced pressure, and the residue dissolved in chloroform-*d* (0.4 mL). After 4 h, the reaction was quenched with hydrochloric acid solution (20 mL, 2 M) in the air and ethyl acetate (20 mL) added. The resulting layers were separated and the aqueous layer washed with ethyl acetate (10 mL). The combined organic fractions were washed with distilled water (10 mL), dried over magnesium sulfate, filtered, and the solvent removed under reduced pressure giving the crude product as a brown liquid. Elution through a silica gel column with 25:1 petroleum ether/ethyl acetate gave pure 4-(phenylethynyl)anisole (R_f = 0.43). Yellow solid (168 mg, 86%). ^{1}H NMR δ (300 MHz, $CDCl_3$): 3.83 (s, 3H, OMe), 6.88 (d, J = 9.0 Hz, 2H, Ar), 7.33 (m, 3H, Ar), 7.50 (m, 4H, Ar).

Variations to the catalyst mixture were made by using 2 eq. of phosphonium salt **49** (25.6 mg, 0.06 mmol), replacing phosphonium salt **49** with phosphonium salt **50** (9.7 mg, 0.03 mmol), omitting copper(I) iodide, or omitting the phosphonium

salt. A lower catalyst loading was achieved by grinding each of the three catalyst components (6.7 mg of $[Pd(OAc)_2]$, 12.8 mg of phosphonium salt **49** or 9.7 mg of phosphonium salt **50**, 3.8 mg of copper(I) iodide) with an appropriate amount of di-*i*-propylammonium bromide (prepared by combining di-*i*-propylamine and aqueous hydrobromic acid in distilled water at 0 °C and evaporating water under reduced pressure) to produce 50 mg of each mixture. The $[Pd(OAc)_2]$ mixture was freshly prepared as it decomposed over a number of days. For each reaction, 5 mg of each of the three catalyst component mixtures was used. For the mercury poisoning studies, mercury (300 mg, 1.5 mmol) was added to the reaction after 45 or 65 min.

NMR-scale Sonogashira coupling reaction

$[Pd(OAc)_2]$ (6.0 mg, 0.026 mmol), phosphonium salt **49** (11.0 mg, 0.026 mmol) and copper(I) iodide (3.4 mg, 0.017 mmol) were combined in a sealable tube containing a stir bar. A solution composed of 4-bromoanisole (6.5 μL, 0.052 mmol), di-*i*-propylamine (18.0 μL, 0.130 mmol) and THF-d_8 (0.40 mL) was added, the tube sealed, and the mixture heated to 60 °C with rapid stirring for 10 min. The resulting pale yellow solution was transferred to an NMR tube and ^{1}H and ^{31}P NMR spectra collected. Phenylethyne (8.0 μL, 0.070 mmol) was added and ^{1}H and ^{31}P NMR spectra collected again. The pale yellow solution was heated to 60 °C, at which point the solution turned dark brown. After 10, 30 and 60 min, the solution was cooled and ^{1}H and ^{31}P NMR spectra were collected. A number of variations with starting materials omitted were also performed, in order to identify the species formed in the reaction.

*$[Pd(\mu\text{-}OAc)\{\kappa^2 P,C\text{-}o\text{-}C_6H_3(CH_2PBu^t{}_2)(CH_2SBu^t)\}]_2$ (**46**)/di-i-propylamine dynamic system*
Selected ^{1}H NMR δ (300 MHz, THF-d_8): 1.11 (d, J = 6.6 Hz, NCHMe_2), 1.35 (s, SBu^t), 1.36 (br, PBu^t), 1.92 (br, OAc), 3.10 (br, NCHMe$_2$), 3.34 (br, CH$_2$P), 3.71 (s, CH$_2$S), 5.02 (br, NH), 6.71 (br, Ar). ^{31}P NMR δ (121 MHz, THF-d_8): 97.40 (br), 106.65 (br).

*α-(Di-t-butylphosphino)-α'-(t-butylthio)-o-xylene (**14a**)/copper(I) iodide complex*
^{1}H NMR δ (300 MHz, THF-d_8): 1.34 (d, J = 13.2 Hz, PBu^t), 1.63 (s, SBu^t), 3.41 (d, J = 7.9 Hz, CH$_2$P), 4.12 (s, CH$_2$S), 7.14 (t, J = 7.9 Hz, Ar), 7.20 (t, J = 7.3 Hz, Ar), 7.32 (d, J = 6.5 Hz, Ar), 7.35 (d, J = 6.7 Hz, Ar). ^{31}P NMR δ (121 MHz, THF-d_8): 29.06 (br).

[Pd(OAc)$_2$]/di-i-propylamine complex

^{1}H NMR δ (300 MHz, THF-d_8): 1.31 (d, $J = 6.3$ Hz, NCHMe_2), 1.66 (d, $J = 6.6$ Hz, NCHMe_2), 1.68 (s, OAc), 2.79 (oct, $J = 6.3$ Hz, NCHMe$_2$), 7.37 (br, NH).

References

1. C. A. Tolman, *Chem. Rev.*, 1977, **77**, 313–348.

2. H.-U. Blaser, A. Indolese and A. Schnyder, *Curr. Sci.*, 2000, **78**, 1336–1344.

3. P. W. N. M. van Leeuwen, *Homogeneous Catalysis: Understanding the Art*, Kluwer Academic Publishers, Dordrecht, 2004.

4. D. F. Shriver and P. W. Atkins, *Inorganic Chemistry*, Oxford University Press, Oxford, 3rd edn, 1999.

5. C. P. Casey and G. T. Whiteker, *Isr. J. Chem.*, 1990, **30**, 299–304.

6. P. Dierkes and P. W. N. M. van Leeuwen, *J. Chem. Soc., Dalton Trans.*, 1999, 1519–1529.

7. C. P. Casey, G. T. Whiteker, M. G. Melville, L. M. Petrovich, J. A. Gavney Jr and D. R. Powell, *J. Am. Chem. Soc.*, 1992, **114**, 5535–5543.

8. P. C. J. Kamer, P. W. N. M. van Leeuwen and J. N. H. Reek, *Acc. Chem. Res.*, 2001, **34**, 895–904.

9. Z. Freixa and P. W. N. M. van Leeuwen, *Dalton Trans.*, 2003, 1890–1901.

10. M. Kranenburg, P. C. J. Kamer, P. W. N. M. van Leeuwen, D. Vogt and W. Keim, *J. Chem. Soc., Chem. Commun.*, 1995, 2177–2178.

11. T. Fanjul, G. R. Eastham, J. Floure, S. J. K. Forrest, M. F. Haddow, A. Hamilton, P. G. Pringle, A. G. Orpen and M. Waugh, *Dalton Trans.*, 2013, **42**, 100–115.

12. C. J. Moulton and B. L. Shaw, *J. Chem. Soc., Chem. Commun.*, 1976, 365.

13. N. Carr, B. J. Dunne, A. G. Orpen and J. L. Spencer, *J. Chem. Soc., Chem. Commun.*, 1988, 926–928.

14. F. M. Conroy-Lewis, L. Mole, A. D. Redhouse, S. A. Litster and J. L. Spencer, *J. Chem. Soc., Chem. Commun.*, 1991, 1601–1603.

15. N. Carr, B. J. Dunne, L. Mole, A. G. Orpen and J. L. Spencer, *J. Chem. Soc., Dalton Trans.*, 1991, 863–871.

16. N. Carr, L. Mole, A. G. Orpen and J. L. Spencer, *J. Chem. Soc., Dalton Trans.*, 1992, 2653–2662.

17. R. P. Tooze, G. R. Eastham, K. Whiston and X. L. Wang, *Int. Pat.*, WO 9619434, 1996.

18. W. Clegg, G. R. Eastham, M. R. J. Elsegood, R. P. Tooze, X. L. Wang and K. Whiston, *Chem. Commun.*, 1999, 1877–1878.

19. E. Drent and P. H. M. Budzelaar, *Chem. Rev.*, 1996, **96**, 663–681.

20. G. R. Eastham, R. P. Tooze, B. T. Heaton, J. A. Iggo, R. Whyman and S. Zacchini, *Chem. Commun.*, 2000, 609–610.

21. W. Clegg, G. R. Eastham, M. R. J. Elsegood, B. T. Heaton, J. A. Iggo, R. P. Tooze, R. Whyman and S. Zacchini, *Organometallics*, 2002, **21**, 1832–1840.

22. A. Tullo, *Chem. Eng. News*, 2009, **87(42)**, 22–23.

23. Lucite International, 2014, http://www.luciteinternational.com/our-technologies/innovation, accessed 18 April 2014.

24. E. E. Bunel and D. A. Clark, *Int. Pat.*, WO 2002048094, 2002.

25. S. Itsuno, K. Ooka, T. Sagae and T. Inoue, *Jpn. Kokai Tokkyo Koho*, JP 2005247703, 2005.

26. A. K. Keep, S. Collard, M. W. Hooper and T. J. Colacot, *Int. Pat.*, WO 2007029031, 2007.

27. G. R. Eastham, M. Waugh and P. I. Richards, *Int. Pat.*, WO 2008075108, 2008.

28. A. Riisager, R. Fehrmann, J. Xiong and E. J. Garcia Suarez, *US Pat.*, US 20110065950, 2011.

29. B. Sesto and G. Consiglio, *Chem. Commun.*, 2000, 1011–1012.

30. I. D. Gridnev, N. Higashi and T. Imamoto, *Organometallics*, 2001, **20**, 4542–4553.

31. R.-X. Li, X.-J. Li, N.-B. Wong, K.-C. Tin, Z.-Y. Zhou and T. C. W. Mak, *J. Mol. Catal. A: Chem.*, 2002, **178**, 181–190.

32. J. W. Raebiger, A. Miedaner, C. J. Curtis, S. M. Miller, O. P. Anderson and D. L. DuBois, *J. Am. Chem. Soc.*, 2004, **126**, 5502–5514.

33. A. J. Rucklidge, G. E. Morris and D. J. Cole-Hamilton, *Chem. Commun.*, 2005, 1176–1178.

34. H. Ooka, T. Inoue, S. Itsuno and M. Tanaka, *Chem. Commun.*, 2005, 1173–1175.

35. A. J. Rucklidge, G. E. Morris, A. M. Z. Slawin and D. J. Cole-Hamilton, *Helv. Chim. Acta*, 2006, **89**, 1783–1800.

36. T. Fanjul, G. R. Eastham, N. Fey, A. Hamilton, A. G. Orpen, P. G. Pringle and M. Waugh, *Organometallics*, 2010, **29**, 2292–2305.

37. T. Fanjul, G. Eastham, M. F. Haddow, A. Hamilton, P. G. Pringle, A. G. Orpen, T. P. W. Turner and M. Waugh, *Catal. Sci. Technol.*, 2012, **2**, 937–950.

38. G. R. Eastham, *Int. Pat.*, WO 2005118519, 2005.

39. G. R. Eastham and N. Tindale, *Int. Pat.*, WO 2007119079, 2007.

40. G. R. Eastham and N. Tindale, *Int. Pat.*, WO 2007020379, 2007.

41. G. R. Eastham and P. I. Richards, *Int. Pat.*, WO 2009010782, 2009.

42. G. R. Eastham, M. Waugh, P. G. Pringle and T. Fanjul Solares, *Int. Pat.*, WO 2010001174, 2010.

43. G. R. Eastham, M. Waugh, P. G. Pringle and T. P. W. Turner, *Int. Pat.*, WO 2011083305, 2011.

44. N. Tindale and G. R. Eastham, *Int. Pat.*, WO 2013093472, 2013.

45. T. G. Appleton, H. C. Clark and L. E. Manzer, *Coord. Chem. Rev.*, 1973, **10**, 335–422.

46. J. C. Jeffrey and T. B. Rauchfuss, *Inorg. Chem.*, 1979, **18**, 2658–2666.

47. W.-H. Zhang, S. W. Chien and T. S. A. Hor, *Coord. Chem. Rev.*, 2011, **255**, 1991–2024.

48. H. Werner, A. Hampp and B. Windmüller, *J. Organomet. Chem.*, 1992, **435**, 169–183.

49. M. Ito, A. Sakaguchi, C. Kobayashi and T. Ikariya, *J. Am. Chem. Soc.*, 2007, **129**, 290–291.

50. C. S. Slone, D. A. Weinberger and C. A. Mirkin, *Prog. Inorg. Chem.*, 1999, **48**, 233–350.

51. J. R. Farrell, C. A. Mirkin, I. A. Guzei, L. M. Liable-Sands and A. L. Rheingold, *Angew. Chem., Int. Ed.*, 1998, **37**, 465–467.

52. C. G. Oliveri, N. C. Gianneschi, S. T. Nguyen, C. A. Mirkin, C. L. Stern, Z. Wawrzak and M. Pink, *J. Am. Chem. Soc.*, 2006, **128**, 16286–16296.

53. A. M. Spokoyny, C. W. Machan, D. J. Clingerman, M. S. Rosen, M. J. Wiester, R. D. Kennedy, C. L. Stern, A. A. Sarjeant and C. A. Mirkin, *Nat. Chem.*, 2011, **3**, 590–596.

54. C. Pisano, A. Mezzetti and G. Consiglio, *Organometallics*, 1992, **11**, 20–22.

55. K. Hiroi and T. Sone, *Curr. Org. Synth.*, 2008, **5**, 305–320.

56. K. Hiroi, Y. Suzuki, I. Abe and R. Kawagishi, *Tetrahedron*, 2000, **56**, 4701–4710.

57. F. Lang, D. Li, J. Chen, J. Chen, L. Li, L. Cun, J. Zhu, J. Deng and J. Liao, *Adv. Synth. Catal.*, 2010, **352**, 843–846.

58. C. J. Levy and R. J. Puddephatt, *Organometallics*, 1997, **16**, 4115–4120.

59. M. Okazaki, S. Ohshitanai, M. Iwata, H. Tobita and H. Ogino, *Coord. Chem. Rev.*, 2002, **226**, 167–178.

60. R. A. Gossage, G. D. McLennan and S. R. Stobart, *Inorg. Chem.*, 1996, **35**, 1729–1732.

61. M. C. MacInnis, D. F. MacLean, R. J. Lundgren, R. McDonald and L. Turculet, *Organometallics*, 2007, **26**, 6522–6525.

62. S. Wu, X. Li, Z. Xiong, W. Xu, Y. Lu and H. Sun, *Organometallics*, 2013, **32**, 3227–3237.

63. Y. Lee, N. P. Mankad and J. C. Peters, *Nat. Chem.*, 2010, **2**, 558–565.

64. G. S. Mhinzi, S. A. Litster, A. D. Redhouse and J. L. Spencer, *J. Chem. Soc., Dalton Trans.*, 1991, 2769–2776.

65. S. J. Sabounchei and K. Karamei, *Asian J. Chem.*, 2001, **13**, 1581–1585.

66. P. D. Newman, R. A. Campbell, R. P. Tooze, G. R. Eastham, J. M. Thorpe and P. G. Edwards, *Int. Pat.*, WO 9947528, 1999.

67. L. Lochmann, J. Pospíšil and D. Lím, *Tetrahedron Lett.*, 1966, **7**, 257–262.

68. K. Ooka, *Jpn. Kokai Tokkyo Koho*, JP 2004331540, 2004.

69. M. Melaimi, L. Ricard, F. Mathey and P. Le Floch, *Org. Lett.*, 2002, **4**, 1245–1247.

70. D. J. Morris, G. Docherty, G. Woodward and M. Wills, *Tetrahedron Lett.*, 2007, **48**, 949–953.

71. A. Leone and G. Consiglio, *Helv. Chim. Acta*, 2005, **88**, 210–215.

72. K. Tamao and A. Kawachi, *Adv. Organomet. Chem.*, 1995, **38**, 1–58.

73. W. Scherer, V. Herz, A. Brück, C. Hauf, F. Reiner, S. Altmannshofer, D. Leusser and D. Stalke, *Angew. Chem., Int. Ed.*, 2011, **50**, 2845–2849.

74. H. Nagashima, K. Tatebe, T. Ishibashi, A. Nakaoka, J. Sakakibara and K. Itoh, *Organometallics*, 1995, **14**, 2868–2879.

75. H. Gilman and G. L. Schwebke, *J. Org. Chem.*, 1962, **23**, 2044–2045.

76. H. Schmidbaur and A. Mörtl, *J. Organomet. Chem.*, 1983, **250**, 171–182.

77. J. M. Muchowski and M. C. Venuti, *J. Org. Chem.*, 1981, **46**, 459–461.

78. S. E. Cremer, B. C. Trivedi and F. L. Weitl, *J. Org. Chem.*, 1971, **36**, 3226–3231.

79. K. L. Marsi and J. E. Oberlander, *J. Am. Chem. Soc.*, 1973, **95**, 200–204.

80. U. Azzena, S. Carta, G. Melloni and A. Sechi, *Tetrahedron*, 1997, **53**, 16205–16212.

81. O. Dahl, *J. Chem. Soc., Perkin Trans. 1*, 1978, 947–954.

82. X. Yu and T. J. Marks, *Organometallics*, 2007, **26**, 365–376.

83. S. Murahashi, *Sci. Pap. Inst. Phys. Chem. Res. (Jpn.)*, 1936, **30**, 180–194.

84. F. G. Mann and F. H. C. Stewart, *J. Chem. Soc.*, 1954, 2819–2826.

85. K. M. Allan and J. L. Spencer, *Tetrahedron Lett.*, 2009, **50**, 834–835.

86. F. G. Mann, I. T. Millar and H. R. Watson, *J. Chem. Soc.*, 1958, 2516–1519.

87. J. Dogan, J. B. Schulte, G. F. Swiegers and S. B. Wild, *J. Org. Chem.*, 2000, **65**, 951–957.

88. K. M. Allan and J. L. Spencer, *Org. Biomol. Chem.*, 2014, **12**, 956–964.

89. A. Naghipour, S. J. Sabounchei, D. Morales-Morales, S. Hernández-Ortega and C. M. Jensen, *J. Organomet. Chem.*, 2004, **689**, 2494–2502.

90. J. M. Brunel, B. Faure and M. Maffei, *Coord. Chem. Rev.*, 1998, **178-180**, 665–698.

91. A. Staubitz, A. P. M. Robertson, M. E. Sloan and I. Manners, *Chem. Rev.*, 2010, **110**, 4023–4078.

92. B. Hoge, C. Thösen, T. Herrmann and I. Pantenburg, *Inorg. Chem.*, 2002, **41**, 2260–2265.

93. P. A. Chase, M. Gagliardo, M. Lutz, A. L. Spek, G. P. M. van Klink and G. van Koten, *Organometallics*, 2005, **24**, 2016–2019.

94. M. R. Cargill, K. E. Linton, G. Sandford, D. S. Yufit and J. A. K. Howard, *Tetrahedron*, 2010, **66**, 2356–2362.

95. T. Hori and A. Osuka, *Eur. J. Inorg. Chem.*, 2010, 2379–2386.

96. A. Palumbo Piccionello, R. Musumeci, C. Cocuzza, C. G. Fortuna, A. Guarcello, P. Pierro and A. Pace, *Eur. J. Med. Chem.*, 2012, **50**, 441–448.

97. J. Uziel, C. Darcel, D. Moulin, C. Bauduin and S. Jugé, *Tetrahedron: Asymmetry*, 2001, **12**, 1441–1449.

98. P. Hofmann, P. Hanno-Igels, O. Bondarev and C. Jaekel, *Int. Pat.*, WO 2009101162, 2009.

99. I. Mohammadpoor-Baltork, H. R. Memarian and K. Bahrami, *Can. J. Chem.*, 2005, **83**, 115–121.

100. M. K. Syed and M. Casey, *Eur. J. Org. Chem.*, 2011, 7207–7214.

101. M. Majewski and D. M. Gleave, *J. Organomet. Chem.*, 1994, **470**, 1–16.

102. C. J. Collins, M. Lanz, C. T. Goralski and B. Singaram, *J. Org. Chem.*, 1999, **64**, 2574–2576.

103. J. E. Baines and C. Eaborn, *J. Chem. Soc.*, 1956, 1436–1441.

104. J. John, E. Gravel, A. Hagège, H. Li, T. Gacoin and E. Doris, *Angew. Chem., Int. Ed.*, 2011, **50**, 7533–7536.

105. V. C. Gibson, N. J. Long, A. J. P. White, C. K. Williams, D. J. Williams, M. Fontani and P. Zanello, *J. Chem. Soc., Dalton Trans.*, 2002, 3280–3289.

106. R. Malacea, L. Routaboul, E. Manoury, J.-C. Daran and R. Poli, *J. Organomet. Chem.*, 2008, **693**, 1469–1477.

107. F. R. Knight, A. L. Fuller, A. M. Z. Slawin and J. D. Woollins, *Polyhedron*, 2010, **29**, 1956–1963.

108. M. S. Rosen, A. M. Spokoyny, C. W. Machan, C. Stern, A. Sarjeant and C. A. Mirkin, *Inorg. Chem.*, 2011, **50**, 1411–1419.

109. E. W. Abel, R. P. Bush, F. J. Hopton and C. R. Jenkins, *Chem. Commun.*, 1966, 58–59.

110. R. J. Cross, I. G. Dalgleish, G. J. Smith and R. Wardle, *J. Chem. Soc., Dalton Trans.*, 1972, 992–996.

111. S. G. Murray and F. R. Hartley, *Chem. Rev.*, 1981, **81**, 365–414.

112. E. Hauptman, P. J. Fagan and W. Marshall, *Organometallics*, 1999, **18**, 2061–2073.

113. R. J. Cross, G. J. Smith and R. Wardle, *Inorg. Nucl. Chem. Lett.*, 1971, **7**, 191–195.

114. A. De Renzi, R. Palumbo and G. Paiaro, *J. Am. Chem. Soc.*, 1971, **93**, 880–883.

115. C. Pedone and E. Benedetti, *J. Organomet. Chem.*, 1971, **31**, 403–414.

116. I. Zahn, K. Polborn and W. Beck, *J. Organomet. Chem.*, 1991, **412**, 397–405.

117. S. Fallis, G. K. Anderson and N. P. Rath, *Organometallics*, 1991, **10**, 3180–3184.

118. D. L. Oliver and K. Anderson, *Polyhedron*, 1992, **11**, 2415–2420.

119. S. D. Robertson, J. S. Ritch and T. Chivers, *Dalton Trans.*, 2009, 8582–8592.

120. B. B. Macha, J. Boudreau, L. Maron, T. Maris and F.-G. Fontaine, *Organometallics*, 2012, **31**, 6428–6437.

121. J. Chatt, L. M. Vallarino and L. M. Venanzi, *J. Chem. Soc.*, 1957, 2496–2505.

122. W. A. Whitla, H. M. Powell and L. M. Venanzi, *Chem. Commun.*, 1966, 310–311.

123. J. A. Davies, *Adv. Inorg. Chem. Radiochem.*, 1981, **24**, 115–187.

124. R. G. Goel and R. G. Montemayor, *Inorg. Chem.*, 1977, **16**, 2183–2186.

125. R. G. Goel, W. O. Ogini and R. C. Srivastava, *Organometallics*, 1982, **1**, 819–824.

126. R. K. Harris, *Can. J. Chem.*, 1964, **42**, 2275–2281.

127. B. L. Shaw and M. F. Uttley, *J. Chem. Soc., Chem. Commun.*, 1974, 918–919.

128. S. Otto, A. Roodt and J. Smith, *Inorg. Chim. Acta*, 2000, **303**, 295–299.

129. A. Bondi, *J. Phys. Chem.*, 1964, **68**, 441–451.

130. C. A. Tolman, *J. Am. Chem. Soc.*, 1970, **92**, 2956–2965.

131. R. G. Miller, R. D. Stauffer, D. R. Fahey and D. R. Parnell, *J. Am. Chem. Soc.*, 1970, **92**, 1511–1521.

132. A. J. Nielson, *Transition Met. Chem.*, 1981, **6**, 180–184.

133. A. I. Zayya and J. L. Spencer, *Organometallics*, 2012, **31**, 2841–2853.

134. D. G. Gusev, J. U. Notheis, J. R. Rambo, B. E. Hauger, O. Eisenstein and K. G. Caulton, *J. Am. Chem. Soc.*, 1994, **116**, 7409–7410.

135. S. S. Stahl, J. A. Labinger and J. E. Bercaw, *Inorg. Chem.*, 1998, **37**, 2422–2431.

136. R. G. Goel and R. C. Srivastava, *Can. J. Chem.*, 1983, **61**, 1352–1359.

137. M. D. Butts, B. L. Scott and G. J. Kubas, *J. Am. Chem. Soc.*, 1996, **118**, 11831–11843.

138. I. A. Koppel, J. Koppel, V. Pihl, I. Leito, M. Mishima, V. M. Vlasov, L. M. Yagupolskii and R. W. Taft, *J. Chem. Soc., Perkin Trans. 2*, 2000, 1125–1133.

139. R. J. Koshar and R. A. Mitsch, *J. Org. Chem.*, 1973, **38**, 3358–3363.

140. A. R. Siedle, R. A. Newmark and W. B. Gleason, *J. Am. Chem. Soc.*, 1986, **108**, 767–773.

141. T. Miyamoto, *J. Organomet. Chem.*, 1977, **134**, 335–362.

142. L. Vaska, *J. Am. Chem. Soc.*, 1966, **88**, 4100–4101.

143. P. S. Braterman, R. W. Harrill and H. D. Kaesz, *J. Am. Chem. Soc.*, 1967, **89**, 2851–2855.

144. J. R. DeLerno, L. M. Trefonas, M. Y. Darensbourg and R. J. Majeste, *Inorg. Chem.*, 1976, **15**, 816–819.

145. A. M. M. Meij, S. Otto and A. Roodt, *Inorg. Chim. Acta*, 2005, **358**, 1005–1011.

146. D. J. Darensbourg, T. J. Decuir, N. W. Stafford, J. B. Robertson, J. D. Draper, J. H. Reibenspies, A. Katho and F. Joo, *Inorg. Chem.*, 1997, **36**, 4218–4226.

147. S. A. Hoyte, PhD Thesis, Victoria University of Wellington, 2013.

148. L. Canovese, F. Visentin, G. Chessa, C. Santo, P. Uguagliati, L. Maini and M. Polito, *J. Chem. Soc., Dalton Trans.*, 2002, 3696–3704.

149. P. S. Pregosin, *NMR in Organometallic Chemistry*, Wiley-VCH Verlag & Co. KGaA, Weinheim, 2012.

150. M. Camalli and F. Caruso, *Helv. Chim. Acta*, 1990, **73**, 2263–2274.

151. W. Clegg, G. R. Eastham, M. R. J. Elsegood, B. T. Heaton, J. A. Iggo, R. P. Tooze, R. Whyman and S. Zacchini, *J. Chem. Soc., Dalton Trans.*, 2002, 3300–3308.

152. T. Weisheit, D. Escudero, H. Petzold, H. Görls, L. González and W. Weigand, *Dalton Trans.*, 2010, **39**, 9493–9504.

153. H. Petzold, H. Görls, W. Weigand, J. Romanski and G. Mloston, *Heteroat. Chem.*, 2007, **18**, 584–590.

154. T. Weisheit, H. Petzold, H. Görls, G. Mloston and W. Weigand, *Eur. J. Inorg. Chem.*, 2009, 3545–3551.

155. H. Petzold, H. Görls and W. Weigand, *J. Organomet. Chem.*, 2007, **692**, 2736–2742.

156. R. Ugo, F. Cariati and G. La Monica, *Chem. Commun.*, 1966, 868–869.

157. M. Green, J. A. Howard, J. L. Spencer and F. G. A. Stone, *J. Chem. Soc., Chem. Commun.*, 1975, 3–4.

158. S. Otsuka, T. Yoshida, M. Matsumoto and K. Nakatsu, *J. Am. Chem. Soc.*, 1976, **98**, 5850–5858.

159. B. E. Mann and A. Musco, *J. Chem. Soc., Dalton Trans.*, 1980, 776–785.

160. T. F. Vaughan, D. J. Koedyk and J. L. Spencer, *Organometallics*, 2011, **30**, 5170–5180.

161. P. J. Murphy, J. L. Spencer and G. Procter, *Tetrahedron Lett.*, 1990, **31**, 1051–1054.

162. A. D. Batsanov, J. A. K. Howard, J. B. Love and J. L. Spencer, *Organometallics*, 1995, **14**, 5657–5664.

163. R. J. Somerville, unpublished work.

164. S. J. La Placa and J. A. Ibers, *Inorg. Chem.*, 1965, **4**, 778–783.

165. S. Trofimenko, *J. Am. Chem. Soc.*, 1968, **90**, 4754–4755.

166. T. S. Thakur and G. R. Desiraju, *J. Mol. Struct.: THEOCHEM*, 2007, **810**, 143–154.

167. M. P. Mitoraj, A. Michalak and T. Ziegler, *Organometallics*, 2009, **28**, 3727–3733.

168. G. Lange, O. Reimelt, L. Jessen and J. Heck, *Eur. J. Inorg. Chem.*, 2000, 1941–1952.

169. M. Hirano, T. Shibasaki, S. Komiya and M. A. Bennett, *Organometallics*, 2002, **21**, 5738–5745.

170. S. A. Hoyte, unpublished work.

171. A. B. Goel and S. Goel, *Inorg. Chim. Acta*, 1983, **77**, L5–L6.

172. T. Yoshida, K. Tatsumi, M. Matsumoto, K. Nakatsu, A. Nakamura, T. Fueno and S. Otsuka, *Nouv. J. Chim.*, 1979, **3**, 761–774.

173. H. C. Clark, A. B. Goel and C. S. Wong, *J. Organomet. Chem.*, 1978, **152**, C45–C47.

174. T. Yoshida and S. Otsuka, *J. Am. Chem. Soc.*, 1977, **99**, 2134–2140.

175. A. G. Sergeev, H. Neumann, A. Spannenberg and M. Beller, *Organometallics*, 2010, **29**, 3368–3373.

176. G. Wilke, H. Schott and P. Heimbach, *Angew. Chem., Int. Ed. Engl.*, 1967, **6**, 92–93.

177. C. Amatore, S. Aziz, A. Jutand, G. Meyer and P. Cocolios, *New J. Chem.*, 1995, **19**, 1047–1059.

178. C. Adamo, C. Amatore, I. Ciofini, A. Jutand and H. Lakmini, *J. Am. Chem. Soc.*, 2006, **128**, 6829–6836.

179. B. L. Shaw and M. M. Truelock, *J. Organomet. Chem.*, 1975, **102**, 517–525.

180. E. M. Hyde, B. L. Shaw and I. Shepherd, *J. Chem. Soc., Dalton Trans.*, 1978, 1696–1705.

181. L. F. Lindoy, S. E. Livingstone and T. N. Lockyer, *Nature*, 1966, **211**, 519.

182. A. Benefiel, D. M. Roundhill, W. C. Fultz and A. L. Rheingold, *Inorg. Chem.*, 1984, **23**, 3316–3324.

183. S. E. Livingstone and T. N. Lockyer, *Inorg. Nucl. Chem. Lett.*, 1967, **3**, 35–38.

184. A. Albinati, J. Herrmann and P. S. Pregosin, *Inorg. Chim. Acta*, 1997, **264**, 33–42.

185. N. Brugat, A. Polo, Á. Álvarez-Larena, J. F. Piniella and J. Real, *Inorg. Chem.*, 1999, **38**, 4829–4837.

186. A. Dervisi, R. L. Jenkins, K. M. A. Malik, M. B. Hursthouse and S. Coles, *Dalton Trans.*, 2003, 1133–1142.

187. G. Siedle and B. Kersting, *Dalton Trans.*, 2006, 2114–2126.

188. S. Gruschinski, M. Handke and B. Kersting, *Z. Anorg. Allg. Chem.*, 2012, **638**, 1274–1277.

189. M. Capdevila, W. Clegg, P. González-Duarte, A. Jarid and A. Lledós, *Inorg. Chem.*, 1996, **35**, 490–497.

190. I. G. Dance, *Polyhedron*, 1986, **5**, 1037–1104.

191. S. D. Killops and S. A. R. Knox, *J. Chem. Soc., Dalton Trans.*, 1978, 1260–1269.

192. J. Krause, G. Cestaric, K.-J. Haack, K. Seevogel, W. Storm and K.-R. Pörschke, *J. Am. Chem. Soc.*, 1999, **121**, 9807–9823.

193. A. M. Saleem and H. A. Hodali, *Transition Met. Chem.*, 1991, **16**, 458–461.

194. A. M. Saleem and H. A. Hodali, *Inorg. Chim. Acta*, 1990, **174**, 223–229.

195. J. R. Dilworth, C. A. Maresca von Beckh W. and S. I. Pascu, *Dalton Trans.*, 2005, 2151–2161.

196. Y. Fuchita, K. Hiraki, Y. Kamogawa, M. Suenaga, K. Tohgoh and Y. Fujiwara, *Bull. Chem. Soc. Jpn.*, 1989, **62**, 1081–1085.

197. N. N. Lyalina, S. V. Dargina, A. N. Sobolev, T. M. Buslaeva and I. P. Romm, *Koord. Khim.*, 1993, **19**, 57–63.

198. K. Heuzé, D. Méry, D. Gauss, J.-C. Blais and D. Astruc, *Chem. Eur. J.*, 2004, **10**, 3936–3944.

199. T. J. Mooibroek, E. Bouwman, M. Lutz, A. L. Spek and E. Drent, *Eur. J. Inorg. Chem.*, 2010, 298–310.

200. D. Zim and S. L. Buchwald, *Org. Lett.*, 2003, **5**, 2413–2415.

201. G.-C. Ge, D.-L. Mo, C.-H. Ding, L.-X. Dai and X.-L. Hou, *Org. Lett.*, 2012, **14**, 5756–5759.

202. B. L. Shaw, S. D. Perera and E. A. Staley, *Chem. Commun.*, 1998, 1361–1362.

203. C. M. Frech, G. Leitus and D. Milstein, *Organometallics*, 2008, **27**, 894–899.

204. G. D. Frey, C.-P. Reisinger, E. Herdtweck and W. A. Herrmann, *J. Organomet. Chem.*, 2005, **690**, 3193–3201.

205. G. R. Fulmer, A. J. M. Miller, N. H. Sherden, H. E. Gottlieb, A. Nudelman, B. M. Stoltz, J. E. Bercaw and K. I. Goldberg, *Organometallics*, 2010, **29**, 2176–2179.

206. K. Nakamoto, *Infrared and Raman Spectra of Inorganic and Coordination Compounds*, John Wiley & Sons, Inc., New Jersey, 6th edn, 2009.

207. T. A. Stephenson and G. Wilkinson, *J. Inorg. Nucl. Chem.*, 1967, **29**, 2122–2123.

208. W. A. Herrmann, C. Brossmer, C.-P. Reisinger, T. H. Riermeier, K. Öfele and M. Beller, *Chem. Eur. J.*, 1997, **3**, 1357–1364.

209. A. I. Zayya, PhD Thesis, Victoria University of Wellington, 2009.

210. C. Amatore, G. Broeker, A. Jutand and F. Khalil, *J. Am. Chem. Soc.*, 1997, **119**, 5176–5185.

211. L. Canovese, F. Visentin, G. Chessa, P. Uguagliati and A. Dolmella, *J. Organomet. Chem.*, 2000, **601**, 1–15.

212. F. A. Jalón, B. R. Manzano, F. Gómez-de la Torre, A. M. López-Agenjo, A. M. Rodríguez, W. Weissensteiner, T. Sturm, J. Mahía and M. Maestro, *J. Chem. Soc., Dalton Trans.*, 2001, 2417–2424.

213. S. M. Reid, J. T. Mague and M. J. Fink, *J. Organomet. Chem.*, 2000, **616**, 10–18.

214. W. A. Herrmann, W. R. Thiel, C. Broßmer, K. Öfele, T. Priermeier and W. Scherer, *J. Organomet. Chem.*, 1993, **461**, 51–60.

215. H. Tanaka, K. Yamada and H. Kawazura, *J. Chem. Soc., Perkin Trans. 2*, 1978, 231–235.

216. K. Sonogashira, Y. Tohda and N. Hagihara, *Tetrahedron Lett.*, 1975, **16**, 4467–4470.

217. H. Doucet and J.-C. Hierso, *Angew. Chem., Int. Ed.*, 2007, **46**, 834–871.

218. R. Chinchilla and C. Nájera, *Chem. Rev.*, 2007, **107**, 874–922.

219. R. Chinchilla and C. Nájera, *Chem. Soc. Rev.*, 2011, **40**, 5084–5121.

220. D. Mujahidin and S. Doye, *Eur. J. Org. Chem.*, 2005, 2689–2693.

221. L. S. Bleicher, N. D. P. Cosford, A. Herbaut, J. S. Mccallum and I. A. McDonald, *J. Org. Chem.*, 1998, **63**, 1109–1118.

222. B. Babgi, L. Rigamonti, M. P. Cifuentes, T. C. Corkery, M. D. Randles, T. Schwich, S. Petrie, R. Stranger, A. Teshome, I. Asselberghs, K. Clays, M. Samoc and M. G. Humphrey, *J. Am. Chem. Soc.*, 2009, **131**, 10293–10307.

223. L. Xue and Z. Lin, *Chem. Soc. Rev.*, 2010, **39**, 1692–1705.

224. P. Bertus, F. Fécourt, C. Bauder and P. Pale, *New J. Chem.*, 2004, **28**, 12–14.

225. M. Beaupérin, A. Job, H. Cattey, S. Royer, P. Meunier and J.-C. Hierso, *Organometallics*, 2010, **29**, 2815–2822.

226. A. Arques, D. Auñon and P. Molina, *Tetrahedron Lett.*, 2004, **45**, 4337–4340.

227. E. Shirakawa, T. Kitabata, H. Otsuka and T. Tsuchimoto, *Tetrahedron*, 2005, **61**, 9878–9885.

228. H. Liang, S. Ito and M. Yoshifuji, *Org. Lett.*, 2004, **6**, 425–427.

229. K. Nishide, H. Liang, S. Ito and M. Yoshifuji, *J. Organomet. Chem.*, 2005, **690**, 4809–4815.

230. D.-H. Lee, H. Qiu, M.-H. Cho, I.-M. Lee and M.-J. Jin, *Synlett*, 2008, 1657–1660.

231. T. Hundertmark, A. F. Littke, S. L. Buchwald and G. C. Fu, *Org. Lett.*, 2000, **2**, 1729–1731.

232. M. an der Heiden and H. Plenio, *Chem. Commun.*, 2007, 972–974.

233. J. F. Hartwig, *Angew. Chem., Int. Ed.*, 1998, **37**, 2046–2067.

234. A. F. Littke, C. Dai and G. C. Fu, *J. Am. Chem. Soc.*, 2000, **122**, 4020–4028.

235. J. P. Stambuli, M. Bühl and J. F. Hartwig, *J. Am. Chem. Soc.*, 2002, **124**, 9346–9347.

236. M. R. Netherton and G. C. Fu, *Org. Lett.*, 2001, **3**, 4295–4298.

237. E. Ullah, J. McNulty, M. Sliwinski and A. Robertson, *Tetrahedron Lett.*, 2012, **53**, 3990–3993.

238. A. Köllhofer and H. Plenio, *Adv. Synth. Catal.*, 2005, **347**, 1295–1300.

239. H. Kim and P. H. Lee, *Adv. Synth. Catal.*, 2009, **351**, 2827–2832.

240. B. M. Trost, M. T. Sorum, C. Chan, A. E. Harms and G. Rühter, *J. Am. Chem. Soc.*, 1997, **119**, 698–708.

241. C. Yang and S. P. Nolan, *J. Org. Chem.*, 2002, **67**, 591–593.

242. S. Perrone, F. Bona and L. Troisi, *Tetrahedron*, 2011, **67**, 7386–7391.

243. X. Pu, H. Li and T. J. Colacot, *J. Org. Chem.*, 2013, **78**, 568–581.

244. E. Buxaderas, D. A. Alonso and C. Nájera, *Eur. J. Org. Chem.*, 2013, 5864–5870.

245. C. Jahier, O. V. Zatolochnaya, N. V. Zvyagintsev, V. P. Ananikov and V. Gevorgyan, *Org. Lett.*, 2012, **14**, 2846–2849.

246. S. Zhang, X. Liu and T. Wang, *Adv. Synth. Catal.*, 2011, **353**, 1463–1466.

247. A. H. M. de Vries, J. M. C. A. Mulders, J. H. M. Mommers, H. J. W. Henderickx and J. G. de Vries, *Org. Lett.*, 2003, **5**, 3285–3288.

248. J. A. Widegren and R. G. Finke, *J. Mol. Catal. A: Chem.*, 2003, **198**, 317–341.

249. N. T. S. Phan, M. Van Der Sluys and C. W. Jones, *Adv. Synth. Catal.*, 2006, **348**, 609–679.

250. D. Astruc, *Inorg. Chem.*, 2007, **46**, 1884–1894.

251. J. G. de Vries, *Sel. Nanocatal. Nanosci.*, ed. A. Zecchina, S. Bordiga and E. Groppo, Wiley-VCH Verlag GmbH & Co. KGaA, Weinheim, 2011, Chapter 3, 73–103.

252. R. H. Crabtree, *Chem. Rev.*, 2012, **112**, 1536–1554.

253. R. van Asselt and C. J. Elsevier, *J. Mol. Catal.*, 1991, **65**, L13–L19.

254. M. B. Thathagar, P. J. Kooyman, R. Boerleider, E. Jansen, C. J. Elsevier and G. Rothenberg, *Adv. Synth. Catal.*, 2005, **347**, 1965–1968.

255. A. V. Gaikwad, A. Holuigue, M. B. Thathagar, J. E. ten Elshof and G. Rothenberg, *Chem. Eur. J.*, 2007, **13**, 6908–6913.

256. J. Louie and J. F. Hartwig, *Angew. Chem., Int. Ed. Engl.*, 1996, **35**, 2359–2361.

257. F. R. Knight, A. L. Fuller, A. M. Z. Slawin and J. D. Woollins, *Dalton Trans.*, 2009, 8476–8478.

258. O. García Mancheño, R. Gómez Arrayás and J. C. Carretero, *J. Am. Chem. Soc.*, 2004, **126**, 456–457.

259. W. A. Herrmann, K. Öfele, D. v. Preysing and S. K. Schneider, *J. Organomet. Chem.*, 2003, **687**, 229–248.

260. B. L. Shaw, *New J. Chem.*, 1998, **22**, 77–79.

261. V. P. W. Böhm and W. A. Herrmann, *Chem. Eur. J.*, 2001, **7**, 4191–4197.

262. J. Meiners, A. Friedrich, E. Herdtweck and S. Schneider, *Organometallics*, 2009, **28**, 6331–6338.

263. Y. He, R. J. Hinklin, J. Chang and L. L. Kiessling, *Org. Lett.*, 2004, **6**, 4479–4482.

264. E. P. Kündig, C. Dupré, B. Bourdin, A. Cunningham and D. Pons, *Helv. Chim. Acta*, 1994, **77**, 421–428.

265. I. G. Green and B. P. Roberts, *J. Chem. Soc., Perkin Trans. 2*, 1986, 1597–1606.

266. A. E. Leontjev, L. L. Vasiljeva and K. K. Pivnitsky, *Russ. Chem. Bull., Int. Ed.*, 2004, **53**, 703–708.

267. K. A. Jensen, *Acta Chem. Scand.*, 1953, **7**, 866–868.

268. D. Fraccarollo, R. Bertani, M. Mozzon, U. Belluco and R. A. Michelin, *Inorg. Chim. Acta*, 1992, **201**, 15–22.

269. D. J. Daigle, *Inorg. Synth.*, 1998, **32**, 40–45.

270. J. L. Spencer, *Inorg. Synth.*, 1979, **19**, 213–218.

271. L. E. Crascall and J. L. Spencer, *Inorg. Synth.*, 1990, **28**, 126–132.

272. R. D. Cramer and F. N. Jones, *US Pat.*, US 3356748, 1967.

273. P. K. Byers, A. J. Canty, H. Jin, D. Kruis, B. A. Markies, J. Boersma and G. Van Koten, *Inorg. Synth.*, 1998, **32**, 162–172.

274. M. Green, J. A. K. Howard, J. L. Spencer and F. G. A. Stone, *J. Chem. Soc., Dalton Trans.*, 1977, 271–277.

275. V. I. Bakhmutov, J. F. Berry, F. A. Cotton, S. Ibragimov and C. A. Murillo, *Dalton Trans.*, 2005, 1989–1992.

276. Y. Tatsuno, T. Yoshida and S. Otsuka, *Inorg. Synth.*, 1990, **28**, 342–345.

277. T. Ukai, H. Kawazura, Y. Ishii, J. J. Bonnet and J. A. Ibers, *J. Organomet. Chem.*, 1974, **65**, 253–266.

278. H. E. Gottlieb, V. Kotlyar and A. Nudelman, *J. Org. Chem.*, 1997, **62**, 7512–7515.

279. O. V. Dolomanov, L. J. Bourhis, R. J. Gildea, J. A. K. Howard and H. Puschmann, *J. Appl. Crystallogr.*, 2009, **42**, 339–341.

280. G. M. Sheldrick, *Acta Crystallogr., Sect. A: Found. Crystallogr.*, 2008, **64**, 112–122.

281. L. Palatinus and G. Chapuis, *J. Appl. Crystallogr.*, 2007, **40**, 786–790.